MEDICAL UNIVERSITY OF VIENNA

15th VIENNA INTERNATIONAL WORKSHOP ON FUNCTIONAL ELECTRICAL STIMULATION

30 YEARS' IFESS ANNIVERSARY

VIENNA FES

ÖGBMT

IFESS International Functional Electrical Stimulation Society

Vienna, Austria, September 16. - 18. 2025

PROCEEDINGS

ISBN 978-3-900928-14-8

Proceedings

of the

15*th* Vienna International Workshop on Functional Electrical Stimulation

and

30 Years' IFESS Anniversary

Vienna, Austria
September 16th-18th, 2025

Edited by

Manfred Bijak
Martin Schmoll
Winfried Mayr
Melitta Pichler

Published by

Medical University of Vienna,
Center for Medical Physics and Biomedical Engineering
Waehringer Guertel 18-20/4L
A-1090 Vienna
Austria

eMail: office@fesworkshop.org
Tel.: +43-1-40400-19840

http://www.fesworkshop.org
ISBN 978-3-900928-15-5

Cover photo by Julius Silver: © WienTourismus/Christian Stemper

Scientific Committee

Christine Azevedo Coste
Ines Bersch-Porada
Alberto Cliquet Jr
Laura Darabant
Nick Donaldson
Lynsey Duffell
Steffen Franz
Johannes Martinek
Lukas Mitteregger
Gernot Müller-Putz
Kristin Musselman
Theresa Rienmüller
Rüdiger Rupp
Erika G. Spaich

Key Notes

Session 1: Clinical applications of FES

Session 2: Afferent Nerve Stimulation

Session 3: FES-Technology

Session 4: Sensory Restoration

Session 5: Methodological Insights

Session 6: FES-Cycling

Session 7: Movement Restoration

Session 8: Current Challenges and Future Directives of FES 1

Session 9: Current Challenges and Future Directives of FES 2

Authors Index

Keynotes:

Regulatory hurdles for Innovative Medical Devices

Bammer M

Center for Biomedical Research and Translational Surgery, Medical University of Vienna, Austria

Abstract: *In this keynote speech, regulatory hurdles for innovative medical devices will be addressed. Based on more than 30 years of expertise in the research, development, and testing of medical devices across different device classes as well as software and hardware solutions, the presentation highlights the critical interplay between technical and regulatory challenges.*
A particular focus will be placed on the requirements and obstacles introduced by the Medical Device Regulation (MDR) guideline and their impact on the successful transition of novel technologies from research into real-world application.
The keynote will demonstrate how regulatory knowledge and experience are essential in bridging the gap between innovation and market adoption, ensuring that new medical devices meet all necessary standards to fulfil safety and performance requirements as well as highest usability, while also achieving successful commercialization and reimbursement.
Based on practical case studies of the presenter's own experience – including examples that have already reached commercialization and reimbursement stages – the following aspects will be explored in detail.

- *MDR compliance & CE marking.*
- *The role of AI, software, and cybersecurity in regulatory frameworks.*
- *Differences between EU, US (FDA), and global regulatory approaches.*
- *How can small companies and start-ups navigate regulations without excessive costs?*

Author's Address

Manfred Bammer
Center for Biomedical Research and Translational Surgery, Medical University of Vienna, Austria
manfred.bammer@meduniwien.ac.at

"The Success of Nottwil" -Taking a critical look at how "successfully" FES has been integrated into Neurorehabilitation

Bersch-Porada I

International FES Centre®, Swiss Paraplegic Centre Nottwil

Abstract: *The presentation outlines the development and impact of the International FES Centre® in Nottwil, highlighting its integration of electrical stimulation into treatment, research, and education. Since its establishment in 1992, the Centre has steadily expanded treatment numbers and built a reputation for improving body functions, activity, and participation for people with spinal cord injury and related neurological conditions. Its mission is to advance evidence-based strategies in areas such as upper limb function, bowel management, skin integrity, and cardiovascular health, with strong emphasis on transferring research findings into clinical practice. The Centre offers a wide range of services, from acute and chronic care to neuromodulation, strengthening, motor learning, and prevention, supported by diverse stimulation technologies. While clinical effectiveness and patient demand are high, financial reimbursement for stimulation devices remains a challenge. Research projects, international collaborations, and annual courses drive continuous innovation and dissemination of knowledge. Despite limited resources and ongoing struggles with funding, the Centre has established itself as a leader in advancing functional electrical stimulation, underlining both its clinical benefits and the need for larger trials and stronger inter-institutional cooperation.*

Author's Address

Ines Bersch-Porada
International FES Centre®, Swiss Paraplegic Centre Nottwil
ines.bersch@paraplegie.ch

From the Patient's perspective: Vision for the future and current obstacles

Chaloupek B

Dr. Schuhfried Medizintechnik GmbH, Vienna, Austria

Abstract:
The patient's view is becoming an increasingly important aspect of health system assessment.
I first learned about Functional Electrical Stimulation (FES) eight years ago, and have been wondering ever since: ***why is it still not more common?***
Today, I use a variety of devices to reduce the symptoms of Charcot-Marie-Tooth disease, including Stimulette, Cefar Rehab, Lympha-Mat, and HiToP-HTEMS. These make my life much easier: they help me to build muscle, reduce spasms when I ride my trike, replace the function of a lymph pump, slow the progression of polyneuropathy, and relieve pain.
For the future success of FES, it will be important to navigate ***medical device regulations (MDR)*** *and* ***health technology assessments (HTAs)****, and to ensure that devices remain available and reimbursed by healthcare systems. Further progress also requires advances in* ***wearability****, as well as stronger* ***interdisciplinary and interprofessional collaboration****. FES experts and patients alike need time and resources to produce papers, interviews, and publications that bring visibility to these therapies.*
Artificial intelligence offers a unique opportunity to raise awareness, amplify the patient voice, and help establish a future in which FES becomes a standard part of the rehabilitation journey from the very beginning.

Author's Address

Barbara Chaloupek
Dr. Schuhfried Medizintechnik GmbH, Vienna, Austria
chaloupek@schuhfriedmed.at

40 years phrenic nerve pacing: History, Presence, Future

Girsch W

Department of Plastic, Aesthetic and Reconstructive Surgery, Medical University Graz, Austria

Abstract: *In the early 1980s, the Vienna FES group demonstrated the clinical applicability of implanted functional electrical stimulation (FES) systems by enabling active gait in two paraplegic patients. Shortly thereafter, the focus shifted toward phrenic nerve pacing (PNP), in line with pioneering work from William W. L. Glenn et al in the United States. At that time, PNP was the only option for patients with high-level spinal cord injury to leave intensive care, as portable respiratory support systems were not yet available.*

A series of high-level quadriplegic patients was successfully supported with the Vienna PNP system. However, due to the lack of CE certification, the system was no longer available after 2000. Patient care and new implantations continued with the CE-certified Atrotech Phrenic Nerve Stimulation System, which was technically very similar to the Vienna device but up to today in clinical use.

Today, the indication for PNP in patients with intact phrenic nerves and severe respiratory insufficiency remains unchanged. This technology continues to dramatically improve quality of life and long-term independence. Looking ahead, advances in implantable stimulation systems, coupled with developments in personalized respiratory therapy, may further expand the role of PNP in the management of high-level spinal cord injuries and beyond.

Author's Address

Werner Girsch
Department of Plastic, Aesthetic and Reconstructive Surgery, Medical University Graz
werner.girsch@kabsi.at

Human-Machine interfacing for health benefits

Raspopovic S

Center for Medical Physics and Biomedical Engineering, Medical University of Vienna, Austria

Abstract: *Advances in nervous system interfacing present a promising venue for rehabilitation of individuals with different neurological disabilities. Subjects with SCI, pain or diabetes have reduced independence, which can induce a sedentary lifestyle promoting disease development and hindering reinsertion into society, while the neuropathic pain is common and poorly managed with current medications. Despite a wide range of possibilities for human-machine interfacing, the nature of the optimal human-machine interaction remains poorly understood. Knowledge gained from in-silico modelling of targeted neural structures can inform an optimized design of such interfacing, therefore we develop the exact models of different nerves, enabling for AI-based personalized treatments. We have pioneered a human-machine systems that translates artificial sensors' read-outs into "language" understandable by the nervous system. The "smart orthosis" for diabetics "speaks" to their residual healthy nerves while diminishing pain. Combination of neuro-stimulating sleeve and exoskeleton restores the independence to highly disabled SCI and stroke patients. Their effects at the brain level were evaluated, observing important benefits.*

Author's Address

Stanisa Raspopovic
Medical University of Vienna, Center for Medical Physics and Biomedical Engineering
stanisa.raspopovic@meduniwien.ac.at

Paradigm shifts: the foundations of functional electrical stimulation

Salmons S

Center for Medical Physics and Biomedical Engineering, Medical University of Vienna, Austria

Abstract: *In the 1960s it was widely believed that to generate muscle force motor units were activated at random or in rotation, that fully differentiated tissues could not re-express their genome, and that the properties of fast/white and slow/red muscles were determined by chemotrophic substances transported to them via their nerves. The replacement of these ideas by robust, evidence-based theories is worth revisiting, because nearly every mode of functional electrical stimulation depends to some extent on these advances in understanding and practice. It also underlines the value of cross-disciplinary research.*

Author's Address

Stanley Salmons
Professor Emeritus at Liverpool University, UK
ssalmons@liverpool.ac.uk

Session 1:
Clinical applications of FES

Quality of life and patient reported outcome measures following the use of functional electrical stimulation for walking post stroke

Street T[1] and Singleton C[2]

[1]Salisbury NHS Foundation Trust, UK
[2]Birmingham Community Healthcare NHS Foundation Trust

Abstract:
The majority of studies examining the effectiveness of FES for walking following stroke have focused on changes in ten metre walking speed with less examination of whether FES is effective in measures directly relevant to the patient experience such as quality of life, trips, spasticity, joint pain and toe claw. The current observational study explores patient reported outcomes (n=176) for people with chronic stroke who used FES for walking over a period of 10.5 months as well as ten metre walking speed measures.

Keywords: *walking, functional electrical stimulation, stroke, quality of life, patient reported outcome measures*

Introduction

The National Institute for Clinical Excellence (NICE) publishes guidelines and recommendations for further research for treatments offered in the UK National Health Service (NHS). One recommendation for further research into FES for walking in upper motor neuron conditions such as stroke, is the examination of outcome measures directly relevant to the patient experience, such as quality of life and other patient reported outcome measures. The current observational study included measures of quality of life, trips, confidence, effort, spasticity, joint pain and toe claw as well as walking speed to explore whether FES for walking following stroke is effective in improving these patient-reported outcomes.

Material and Methods

A repeated measures within-subjects observational study design was used. Participants (n=176) were assessed and set up over one day using the ODFS Pace FES device (Odstock Medical Ltd, Salisbury, UK). Most devices were fitted by the same physiotherapist (C.S.) at the FES Clinic at Birmingham Community Healthcare NHS Foundation Trust. Written and verbal device education was provided. Patients had access to the service through email and telephone support between appointments. The full clinical procedure is described in a previous study [1]. Data were collected on day one and after 10.5 months follow-up.

Self-reported visual analogue scales (VASs) were used to record joint pain, tripping, confidence, walking effort, quality of life, and spasticity. Individual VAS scores were used as appropriate for each patient. Baseline VAS scores were recorded without FES. Subsequent recordings were with FES. The VAS scores were presented from 0 to 10 as whole numbers on a vertical line with no intervals. People chose whole numbers, including "0." High scores for confidence and quality of life represent improvement, and the inverse is true for joint pain, spasticity, trips, and walking effort. The scoring was presented as such to ensure that people thought about their answers and did not score a particular number across all categories. For further VAS details see Street and Singleton [2] Ten metre walking speed measures with and without FES were also taken. For further details see Street and Singleton [2].

Results

176 stroke (mean age 53 years, time post stroke 4.92 years, 88 left limb, 89 right limb) were referred for assessment of FES for walking. After 10.5 months, 168 patients were still in treatment for walking using FES Two patients continued to use neuromuscular stimulation for exercise rather than walking.
Walking speed data was collected for 113 patients at six months follow up. PROMS data was collected for 99 patients at six months follow up where appropriate.

Table 1 Visual Analogue Scales (0-10) Medians and 25th to 75th percentile (pctl)

Visual Analogue Scales (n)	Day One (25th-75th pctl)	Six months (25th-75th pctl)
Trips (95)	5 (2-7)	1 (0-3)
Confidence (93)	5 (3-7)	8 (7-9)
Effort (93)	8 (6-8)	4 (3-6)
Quality of Life (91)	6 (4-8)	8 (6-9)
Spasticity (86)	7 (4-8)	4 (2-6)
Joint Pain (66)	5 (0-7)	1 (0-5)
Toe Claw (69)	7 (3-8)	2 (0-5.5)

Trips: A Wilcoxon signed rank test found a significant reduction in the number of trips experienced while walking with FES for at follow-up (mdn=1, IQR = 3) compared to day one (mdn=5, IQR =5) (Z =-7.27, p<.001). *Confidence:* A significant improvement in reported levels of confidence while walking with FES at follow up was found (mdn=8, IQR=2) compared to day one (mdn= 5, IQR=4) was also found (Z =-6.20, p <.001). *Effort*: A significant reduction in levels of effort while walking was reported at follow-up of using FES (mdn=4, IQR=3) compared to day one (mdn=8, IQR=2) (Z=-6.86, p <.001). *Quality of Life:* A significant improvement in reported levels of quality of life from using FES at follow-up (mdn=8, IQR=3) was found compared to day one (mdn=6, IQR=4) (Z=-5.30, p <.001). *Spasticity:* A significant reduction in spasticity was reported at follow-

up (mdn=4, IQR=6) compared to day one (mdn=7, IQR=4) (Z =-4.03, p <.001). *Joint Pain:* A significant reduction in pain was reported at follow-up using FES (mdn=1, IQR=5) compared to day one (mdn=5, IQR=7) (Z =-4.42, p<.001). *Toe Claw:* A significant reduction in toe claw was found at follow-up (mdn=2, IQR=5.5) compared to day one (mdn=7, IQR=5) (Z=-5.57, p <.001).

Ten Metre Walking Speed

A main effect was found for time F (1,107) 38.44, p<.001 and condition (no stim vs stim) F (1,107) 72.41, p<.001. No significant interaction was observed. Planned comparisons found an immediate minimal clinically important orthotic difference (MCID) on day one between no FES (.56ms, SD=.26) and walking with FES (.61ms, SD=.28) which was significant (t (107)-6.40, p<.001). An MCID orthotic effect was also found at follow-up between no FES (.61ms, SD=.28) and walking with FES (.67ms, SD=.29) which was significant (t (107)-8.28, p<.001). An MCID therapeutic effect was also found between walking without FES on day one (.56ms, SD=.26) compared to follow-up (.67ms, SD=.29) which was significant (t (107)-5.34, p<.001).

Skin irritation: 10 participants were reported to have experienced skin irritation during study period.

Discussion

An analysis of patient reported outcome measures found a reduction in spasticity, joint pain and effort of walking, toe claw and trips while walking. An improvement in quality of life, confidence while walking was also reported. One limitation of the study is the use of self-reported VAS Scales rather than comprehensive measures. Nevertheless, the use of VAS Scales provided a pragmatic, patient accessible measure for patients to respond and monitor their own progress. This provided the opportunity to explore a wide variety of areas with less burden on the patient and clinician. Walking speed measures were broadly consistent with previous studies for orthotic effects. Interestingly an MCID for therapeutic effect was observed which was not found in a previous large observational stroke study [3]. Potential contributing factors include younger age, level of mobility and residual function. The current study included an ethnically diverse community which is often associated with a younger stroke population and therefore provided representation which is often neglected in FES research.

Conclusions

Further research is required to examine patient reported outcome measures directly relevant to those with stroke over the long-term use of FES. VAS scales provide a pragmatic solution for clinician monitoring of patient progress during treatment as well as a method for exploring new potential lines of research with less burden on patients. Further research is required to examine optimising a therapeutic effect from using FES.

References

[1] T. Street, P. Taylor, and I. Swain, “Effectiveness of Functional Electrical Stimulation on Walking Speed, Functional Walking Category, and Clinically Meaningful Changes for People with Multiple Sclerosis,” *Arch. Phys. Med. Rehabil.*, vol. 96, no. 4, pp. 667–672, Apr. 2015, doi: 10.1016/j.apmr.2014.11.017.

[2] T. Street and C. Singleton, “Five-Year Follow-up of a Longitudinal Cohort Study of the Effectiveness of Functional Electrical Stimulation for People with Multiple Sclerosis,” *Int. J. MS Care*, vol. 20, no. 5, pp. 224–230, Sep. 2018, doi: 10.7224/1537-2073.2016-094.

[3] T. Street, I. Swain, and P. Taylor, “Training and orthotic effects related to functional electrical stimulation of the peroneal nerve in stroke,” *J. Rehabil. Med.*, vol. 49, no. 2, pp. 113–119, Jan. 2017, doi: 10.2340/16501977-2181.

Effect of Electrical Stimulation on the Timing of the Preparatory Phase of Gait Initiation in Parkinson's Disease

Spaich EG[1], Richard MA[1], Andersen OK[1], Bello O[2]

[1]Department of Health Science and Technology, Faculty of Medicine, Aalborg University, Denmark
[2]Departamento de Fisioterapia, Medicina y Ciencias Biomédicas, Grupo de aprendizaje y control del movimiento humano en actividad física y deporte (ACoM), Universidade da Coruña (University of A Coruña), Spain

Abstract: *Gait initiation is usually impaired in people with Parkinson's disease (PD) and improving the spatiotemporal characteristics of gait initiation has been focus of extensive research. Auditory cueing can help reducing the preparatory phase of gait initiation, while sensory electrical stimulation can result in complex synergistic lower limb movements, elicited through spinal reflex responses. The goal of this study was to investigate the effect of combining auditory cueing and painful and non-painful electrical stimulation on the timing of the preparatory phase of gait initiation.*

Twelve people with PD and twelve aged-matched healthy people participated in the study. Auditory cueing to initiate gait was presented alone or concurrently with non-painful (0.7 x pain threshold) or painful (1.3 x pain threshold) electrical stimulation lasting 21 ms (5 pulses, 1 ms long, 200 Hz). Stimulation was delivered on the arch of the foot with a reference electrode placed on the dorsum of the foot.

Painful and non-painful electrical stimulation, concurrent to auditory cueing, resulted in a reduced duration of the preparatory phase ($p<0.001$) as compared to auditory cueing alone. Painful stimulation was more effective than non-painful stimulation to shorten the preparatory phase ($p<0.03$). No differences were detected across groups of participants.

These results may have potential application in developing methods for improving deficiencies in gait initiation in PD.

Keywords: *Gait initiation, Preparatory phase, Parkinson's disease, Electrical stimulation, Withdrawal reflex*

Introduction

The preparatory phase of gait initiation, also known as anticipatory postural adjustment, is a part of the gait initiation process and encompasses a displacement of the center of pressure contributing to the shifting of the center of gravity towards the stance leg. The anticipatory postural adjustment is impaired in people with Parkinson's disease (PD); concretely, people with PD take longer to unload the starting leg, have shorter first step length, and less forward impulse and displacement of the center of pressure at release, as compared to close to age-matched elderly people [1].

Visual and auditory cueing has shown its effectiveness to ameliorate gait initiation impairments in people with PD (for a review see [2]), while somatosensory vibrotactile stimulation did not impact gait initiation [3]. Strong sensory electrical stimulation of the sole of the foot has been successfully used to facilitate swinging of the most affected leg of stroke patients during gait training [4] and could be of interest to facilitate gait initiation.

The goal of this study was therefore to investigate the immediate effect of electrical stimulation delivered during gait initiation in participants with Parkinson's disease and age-matched healthy participants.

Materials and Methods

The effect of electrical stimulation on the timing of the preparatory phase of gait initiation was investigated by delivering an acoustic stimulus for gait initiation concurrent to either non-painful or painful electrical stimulation, or no stimulation (control condition).

Participants: Twelve people with PD and twelve age-matched healthy people participated in this study. Inclusion criteria for participation were (1) diagnosis of levodopa responsive PD and score of at least 2 and at most 3 in the Hoehn and Yahr scale for PD people; and (2) the ability to walk for 10 minutes without stopping, and without walking aids or assistance, for all subjects. Exclusion criteria were (1) dementia (Mini-Mental State Examination score of <24); (2) a past history of neurological conditions other than PD or orthopaedic, cardiovascular and visual disturbances that can affect their walking ability; and (3) inability to tolerate electrical stimulation. Patients participated in the on-medication state. The protocol of the study was approved by the ethics committee of University of A Coruña (CE 08/2013). All volunteers provided written informed consent before participating in the study according to The Declaration of Helsinki.

Electrical and acoustic stimulation: Electric stimulation was delivered by a computer-controlled constant current stimulator on the medial arch of the starting foot (2.63 cm2 surface area electrodes, AMBU, Denmark) with the reference electrode (5 x 9 cm, Pals, Axelgaard Ltd, USA) placed on the dorsal metatarsal aspect of the foot. The stimulus consisted of a constant current pulse burst of five individual 1-ms pulses delivered at 200 Hz [5, 6].

The stimulation intensity was determined as a factor of the pain threshold assessed with the participants in a seated position, using a standard staircase method. The intensity of the non-painful electrical stimulus was 0.7 times the pain threshold and the painful electrical stimulus was 1.3 times the pain threshold.
An acoustic stimulus was used as a cue for gait initiation. The stimulus was a 750 Hz tone burst with a duration of 30 ms and an intensity of ~80 dB. In control trials, the imperative auditory stimulus appeared alone and in stimulation trials it was accompanied by electrical stimulation.

Outcome: Step timing (preparatory phase duration) was measured from signals recorded at 2 kHz from a force resistive resistor (FRS, LuSense, PS3, Standard 174) placed under the heel of the starting foot.

Experimental procedure: Participants were standing with their feet placed 17 cm apart. The foot position was marked to retain consistent foot placement, and visual feedback was provided to maintain equal weight distribution before the gait initiation task. One to six seconds after equal weight distribution was achieved, the auditory cue was delivered. Subjects were asked to initiate walking with their dominant leg as soon as they heard the auditory cue and continue walking until they executed four steps. In some trials the cue was concurrent to non-painful or painful electrical stimulation. The three conditions (no stimulation, non-painful and painful stimulation) were presented randomly in one block. Six blocks were executed; thus, each condition was repeated 6 times.

Data analysis: The preparatory phase duration was computed as the time from the auditory cue (time 0) to the time to heel-off of the stepping leg. Timings under the same condition were averaged for statistical analysis.
2-way repeated measures ANOVA was used to analyse the effect of stimulation type (auditory, auditory and non-painful, auditory and painful) on the timing of the preparatory phase across healthy participants and participants with PD. Post-hoc analysis was performed using the Bonferroni correction. A p value ≤ 0.05 was considered significant.

Results

In the PD group, there were 8 men and 4 women; in the healthy participants group, there were 6 men and 6 women. The average age was 58.91 years (SD = 5.90) for the PD group, and 59.66 years (SD = 7.67) for the healthy participants group. The average weight for the PD group was 75.87 kg (SD = 11.85), and 72.08 kg (SD = 10.73) for the healthy participants group. The average height was 166.75 cm (SD = 7.21) in the PD group, and 165.41 cm (SD = 6.54) in the healthy participants group. The pain threshold was 16.0 mA (SD = 0.51) for the PD group, and 23.4 (SD = 0.79) for the healthy participants group.
Regarding the characteristics of the people with PD, 4 participants were at stage 2 on the Hoehn and Yahr scale, 6 participants at stage 2.5, and 2 participants at stage 3. Four participants experienced freezing of gate in the off-medication state.
No significant differences were found in age, weight, or height between the two groups ($p = 0.790$, $p = 0.420$, and $p = 0.639$, respectively). The pain threshold was significantly lower in the PD group compared to the control group ($p = 0.012$).
The modality of stimulation had a significant effect on the duration of the preparatory phase of gait initiation (RM-ANOVA, $p<0.001$) while no effect of participant type (healthy/PD) was detected (Fig. 1). Non-painful and painful stimulation concurrent with auditory cueing resulted in a shorter preparatory phase than when auditory cueing was delivered alone ($p<0.001$). Additionally, painful stimulation resulted in a shorter preparatory phase than non-painful stimulation, both concurrent to auditory cueing ($P<0.03$).

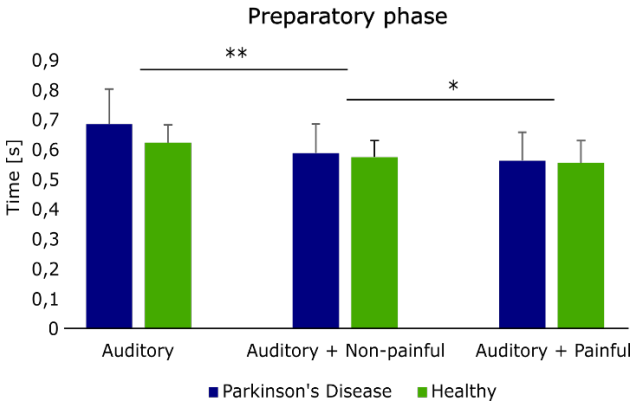

Figure 1: Duration of the preparatory phase of gait initiation for the different stimulation modalities. * indicates $p<0.03$; ** indicates $p<0.001$.

Discussion

In people with PD and aged matched healthy people, a short burst of electrical stimulation (21 ms long) at painful and non-painful stimulation intensities, delivered synchronously with an auditory cue, resulted in a reduced preparatory phase during gait initiation. This effect was more pronounced when the stimulus was painful. On the other hand, no evidence of differences between PD and healthy participants was found.
In the current study, participants with PD were in the on-medication state, which is associated with less impaired anticipatory postural adjustments [7]. This might explain why there was no significant difference in the response of PD and healthy participants.
The stimulation intensities (painful and non-painful) were determined as a factor of the pain threshold (1.3 and 0.7, respectively) but the pain threshold was in average lower in the PD group, which likely affected the size of the response to the electrical stimulation in the PD group. If higher stimulation intensities had been used, a larger effect would be expected in the PD group. Lower pain thresholds across all pain modalities are reported in PD patients when tested in the off-medication state, while

reduced thresholds are not consistently present in the on-medication state (for a review see [8]), which is the case in the current study. This indicates that the cohort of participants showed more pain sensitivity in the on-medication state than other patients in the literature, which in turn might have impacted the amplitude of the outcome [8]. Any influences due to the medication would be associated to the electrical stimulus, since according to the literature, medication state did not influence the effectiveness of auditory cueing in the preparatory phase of gait initiation (for a review see [2]).

Conclusions

This study showed that short lasting, painful and non-painful electrical stimulation concurrent to auditory cueing is effective in reducing the preparatory phase of gait initiation in both healthy and PD people in on-medication state. Furthermore, painful stimulation was more effective that non-painful stimulation. These findings might have application in ameliorating the negative impact of PD in the preparatory phase of gait initiation.

Acknowledgement

The Svend Andersen foundation and Aalborg University financed this study. Thanks to all the participants.
The authors declare that there are no financial or other relationships that might lead to a conflict of interest.

References

[1] S. E. Halliday et al, "The initiation of gait in young, elderly, and Parkinson's disease subjects," Gait Posture, vol. 8, (1), pp. 8–14, 1998.

[2] C. Cosentino et al, "One cue does not fit all: A systematic review with meta-analysis of the effectiveness of cueing on freezing of gait in Parkinson's disease," Neurosci. Biobehav. Rev., vol. 150, pp. 105189, 2023.

[3] C. Schlenstedt, D. S. Peterson and M. Mancini, "The effect of tactile feedback on gait initiation in people with Parkinson's disease: A pilot study," Gait Posture, vol. 80, pp. 240–245, 2020.

[4] E. G. Spaich et al, "Rehabilitation of the hemiparetic gait by nociceptive withdrawal reflex-based functional electrical therapy: A randomized, single-blinded study," J Neuroeng Rehabil, vol. 11, (1), pp. 81, 2014.

[5] O. K. Andersen, F. A. Sonnenborg and L. Arendt-Nielsen, "Reflex receptive fields for human withdrawal reflexes elicited by non-painful and painful electrical stimulation of the foot sole," Clin. Neurophysiol., vol. 112, (4), pp. 641–649, 2001.

[6] E. G. Spaich, L. Arendt-Nielsen and O. K. Andersen, "Modulation of lower limb withdrawal reflexes during gait: a topographical study," J. Neurophysiol., vol. 91, (1), pp. 258–266, 2004.

[7] A. Delval, C. Tard and L. Defebvre, "Why we should study gait initiation in Parkinson's disease," Neurophysiol. Clin., vol. 44, (1), pp. 69–76, 2014.

[8] S. Sung et al, "Pain sensitivity in Parkinson's disease: Systematic review and meta-analysis," Parkinsonism Relat. Disord., vol. 48, pp. 17–27, 2018.

Corresponding author's Address

Erika G. Spaich
Department of Health Science and Technology, Aalborg University
espaich@hst.aau.dk
Homepage: https://vbn.aau.dk/en/persons/espaich

Effectiveness of FES x DDM after twenty years of permanent denervation and degeneration of human muscles

Carraro U[1,2], Casotti A[3], Coraci D[4], Regazzo G[4], Baba A[5], Piccione F[4], Maccarone MC[4], Masiero S[2,4]

[1]Department of Biomedical Sciences, University of Padova, Italy
[2] School of Physical Medicine and Rehabilitation, Department of Neuroscience, University of Padova, Italy
[3]Piacenza, Italy
[4] Rehabilitation Unit of the Department of Neuroscience, University of Padova General Hospital, Italy
[5] Padua Neuroscience Center, Department of Neuroscience, University of Padova, Italy

Abstract: *Chronic denervation of human muscles after spinal cord injury (SCI) is usually considered irreversible, with progressive atrophy and loss of contractility. However, long-term home-based functional electrical stimulation (FES) may offer unexpected effects, even decades after injury. We aim to explore whether intensive, long-term home-based FES, administered as part of the RISE project, can induce lasting improvements in muscle contractility and morphology in a patient with permanent denervation. We describe a single case of a SCI patient treated with home-based FES over several years, who voluntarily discontinued and then resumed stimulation. Mr. AC is an ASIA A patient of the European RISE project. Between 2004 and 2014, he performed daily transcutaneous electrical stimulation for denervated muscles according to the Very High Current Vienna protocol (FES x DDM), using a prototype of the electrical stimulator, later commercialized by Dr. Schuhfried Medizintechnik GmbH of Vienna under the name Schuhfried Den2x RISE, currently the only RISE STIMULATOR available for patients with completely denervated muscles due to permanently lower motor neuron lesions. Mr. AC has been using daily stimulation at home for 10 years but has not practiced it for the last 10 years. On November 30, 2023, he went to the Rehabilitation Unit of Padova (Italy) asking to resume the FES x DDM protocol. By checking his quadriceps muscles with dynamic ultrasound, to the surprise of all the specialists present at the Rehabilitation Unit, the muscle denervated for 20 years responded to the FES x DDM surface electrical stimulation (but not to regular nerve stimulation current) with repetitive contractions, visible even macroscopically. Although this is the only case known to us, it is surprising that his muscles respond to high-current surface electrical stimulation after twenty years of complete and permanent denervation. In our opinion, the only rational explanation is that FES x DDM was very effective during the first 10 years of treatment. Therefore, he has only 10 years of complete rest of his muscles. Mr. AC is now using at home the Schuhfried Den2x stimulator. The follow-up results will be presented at the 15th Vienna International Workshop on Functional Electrical Stimulation to be held from 15 to 18 September 2025 in Vienna, Austria.*

Keywords: *Long-term permanent denervation of skeletal muscles; FES x DDM; Schuhfried Den2x stimulator RISE*

Introduction

Permanent muscle denervation after spinal cord injury (SCI) leads to progressive degeneration traditionally considered irreversible. However, recent evidence suggests that home-based functional electrical stimulation (hbFES) may partially counteract this process, even many years after injury. We here summarize the main concepts pertinent to hbFES as a treatment for SCI patients with permanently denervated muscles in their legs. We hypothesize that intensive, long-term hbFES might not only improve muscle structure and contractility, but that some of these effects could persist even after discontinuing training. Moreover, this intervention may also provide psychological benefits, improving body image and overall quality of life from the patient's perspective. This work introduces a single case report describing an understudied aspect of long-term denervated muscle: specifically, how many years after denervation hbFES can still be effective. We begin by highlighting several key concepts: 1. Upper motor neuron (UMN) and lower motor neuron (LMN) damage to the lower spinal cord; 2. Muscle atrophy/hypertrophy versus processes of degeneration, regeneration, and recovery; 3. Recovery of twitch- and tetanic-contractility by hbFES; 4. Clinical effects of hbFES using the protocol of the "Vienna School"; 5. Limitations and future perspectives. Arguments in favor of using the Vienna protocol include: 1. Increased muscle size in both legs; 2. Improved tetanic force production after 3-5 months of percutaneous stimulation using long stimulus pulses (> 100 msec) of high amplitude (> 80 mAmp), tolerated only in patients with no pain sensibility; 3) Histological and electron microscopic evidence that two years of hbFES return muscle fibers to a state typical of two weeks denervated muscles with respect to atrophy, disrupted myofibrillar structure, and disorganized Excitation-

Contraction Coupling (E-CC) structures; 4. The excitability never recovers to that typical of normal or reinnervated muscles where pulses less than 1 msec in duration and 25 mAmp in intensity excite nerve axons and thereby muscle fibres of the motor units.
It is important to motivate these patients for chronic stimulation throughout life, preferably standing up against the load of the body weight rather than sitting. Only younger and lighter patients might expect to stand and walk a few steps independently. Nonetheless, some patients choose to maintain hbFES training for decades. Finally, the procedure has clear limitations: it requires the use of multiple large surface electrodes and demands significant time commitment from patients willing to engage in regular, long-term muscle training.

Material and Methods

Devices and Vienna Stimulation Strategy for hbFES of large denervated human muscles in SCI: To counteract the progressive changes that transform muscle into an unexcitable tissue unable to generate force with standard commercial stimulators (from six months onward), in the past 30 years Clinicians and Engineers developed in Vienna novel rehabilitation concepts for paraplegic patients with bilateral and complete LMN denervation of the lower extremity due to complete lesion of the Conus Cauda [1,2]. New rehabilitation protocol became possible due to the development and optimization of new stimulation equipments for FES. The devices have been specifically designed to reverse longstanding and severe atrophy of LMN denervated muscles by delivering high-intensity and long-duration impulses that can directly elicit contraction of denervated skeletal fibers in absence of nerve endings. These new stimulators and the large surface electrodes needed to cover the denervated muscles were developed by the Center of Biomedical Engineering and Physics at the Medical University of Vienna, Austria. In parallel, specific clinical assessments and training settings were developed at the Wilhelminenspital Wien, Austria. The rehabilitation progressive training strategy for LMN denervated muscles (Fig 1) are validated by the clinical results, strongly supported by those obtained from light and electron microscopy muscle biopsies' analyses performed in Padua and Chieti Universities (Italy), respectively, as described in longitudinal prospective study [1]. Patients were provided with stimulators and electrodes to perform stimulation at home for five days per week. The large (180 cm2) electrodes (Schuhfried GmbH, Mödling, Austria) made of conductive polyurethane, were placed on the skin surface using a wet sponge cloth (early training) and fixed via elastic textile cuffs. As soon as the skin was accustomed to the necessary high current density, gel was used under the polyurethane electrodes to achieve minimal transition impedance. A special design feature was a nonconductive bulge along the entire edge of the electrode that prevents potential skin burns that presumably can occur where a conductive edge gets in electrical contact with skin surface and causes local current density hot-spots (Mayr W, 2007; Patent -Surface Electrode, EP2021068, WO/2007/131248). The electrodes were flexible enough to maintain evenly distributed pressure to the uneven and moving skin, thus providing homogeneous current distribution throughout the entire contact area. The training strategy consisted of two combined stimulation programs [1,2]. All applicable rules concerning the ethical use of human volunteers were followed during this research (Approval of Ethical Committee, Vienna, Austria: EK- 02-068-0702). At the beginning of the treatment, biphasic stimulation impulses of very long-duration (120-150 ms, 60-75 ms per phase) at high intensity (up to ±80V and up to ±250 mA) were applied (Training Program 1). Then the subjects underwent clinical assessment and stimulated knee torque measurement every 12 weeks by physiatrists, who progressively modified the stimulation. The routine daily training consisted of combined twitch and tetanic stimulation patterns (Training Programs 2, 3 and 4) in consecutive sessions lasting up to 30 min for each group of muscles (gluteus, thigh and lower leg muscles on both sides). After tetanic contractility was achieved and the subject achieved full extension of the leg, the ankle was progressively loaded. Finally, the more compliant patients became able to stand and perform step-in-place and (if young and light) walking exercise (Fig. 1).

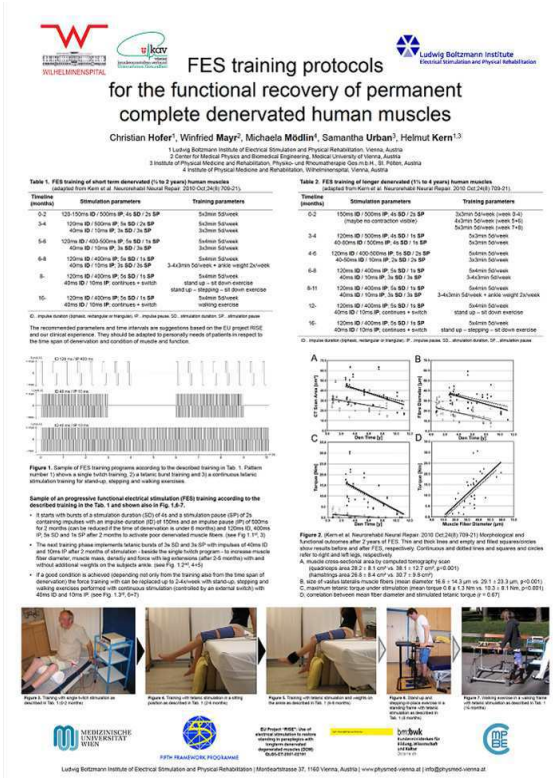

Figure 1: 2017 Spring Padua Muscle Days, Euganean Thermae (Padua), Italy. Poster of Christian Hofer et al. March 14, 2017. Vienna progressive hbFES strategy for long-term complete denervation of quadriceps. Reprinted with permissions from [3].

Results

Mr. AC Case Report

Mr. AC (born 18.01.1965) is a patient of the international RISE project of the 5th EU Framework Programme. In the period between August 2004 and June 2006, he underwent diagnostic analyses and performed daily transcutaneous

electrical stimulation together with a group of patients with complete and permanent lesions of peripheral motor neurons. He has a fracture of the thoracic vertebral bodies 11 and 12, and a fracture at the L 1 level since 10.28.2003 resulting in a complete lesion of the spinal cord (ASIA grade A). He used a prototype of the special electrical stimulator, which was made commercially available by the Schuhfried company after the positive results of the RISE study under the name Schuhfried Den2x which is the successor to the RISE prototypes. As far as we know from the available scientific literature, it is currently the only RISE STIMULATOR available (Dr. Schuhfried Medizintechnik GmbH, Van Swieten-Gasse 10, 1090 Vienna) that provides sufficiently high current pulses for the treatment of the muscles of patients with complete and permanent lesions of the lower motor neurons such as those of Mr. AC. Mr. AC has been using home stimulation of the thighs and other leg muscles for 10 years, but has stopped therapy with FES x DDM in the last 10 years. On November 30, 2023 he went to the Rehabilitation Unit Padua asking to restart the FES x DDM

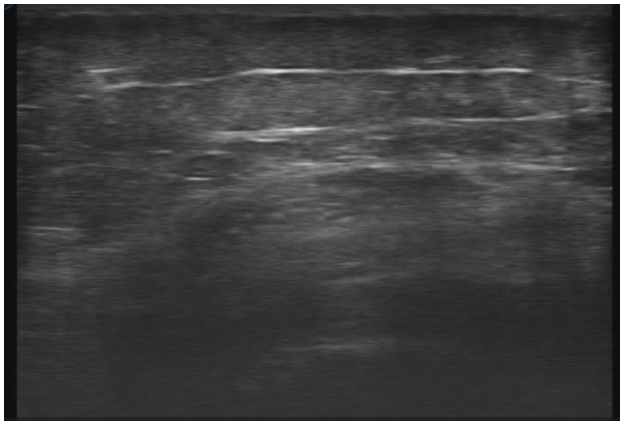

Figure 2: Dynamic ultrasound analysis of thigh muscle of Mr. AC during long-pulse FES x DDM. For the YouTube video link to: https://youtu.be/Gd_f_43GrGg.

With long-pulses (up to 120 millisec long) and high currents (> 80 milliAmp), the new commercial device, because his prototype was no longer usable after years of abandonment. Checking his quadriceps muscles with dynamic ultrasound, to the surprise of all the specialists present at the Rehabilitation Unit of the University Hos pital of Padua, the long-term (20 years) denervated muscle responded to surface FES x DDM with repetitive contraction twitches (see Fig 2). Let us stress again that Mr. AC performed FES x DDM for 10 years after enrolment in the RISE Project, but discontinued it in 2015, ten years ago. Though it is the only case we know, it is astonishing that his muscle responded to surface-high-current-electrical stimulation more than twenty years after permanent complete denervation, but only when stimulation is performed with long pulses at high currents (see Fig. 2) [4]. Even more surprising are the minimal but clear movements of the suspended legs during high-current, long-pulse stimulation. (Fig. 3, personal communication of Mr. AC).

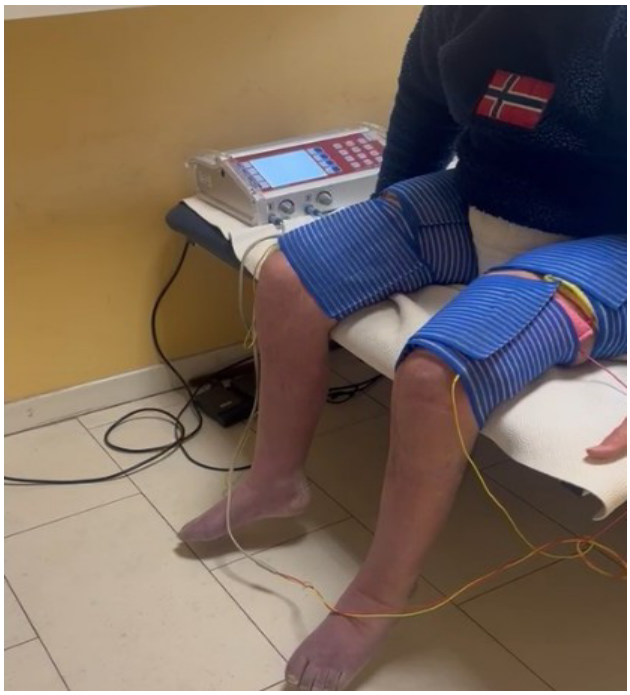

Figure 3: Evidence of macroscopic movements of the legs during long-pulse FES x DDM. (Personal communication of Mr. AC). For the YouTube video link to: https://youtube.com/shorts/p0hvJv0dKPQ.

Discussion

Our findings show that even after two decades of denervation, intensive FES can induce partial recovery of muscle contractility, with some lasting effects. This supports the concept that peripheral electrical stimulation may remodel muscle tissue beyond acute or subacute stages.

By reducing the stimulation to values that elicit motor nerve stimulation (1 millisecond), no muscle contractions were induced. Therefore, skeletal muscles were still denervated and the motor response could not be attributed to local reinnervation events. In our opinion the only rational explanation is that FES x DDM was very effective during the first 10 years of denervation. Thus, Mr. AC can be considered a patient with only 10 years of complete rest of his leg muscles, not more than 20 years. Mr. AC is now using at home the Schuhfried Den2x stimulator. Beyond the physiological effects, the patient's subjective perspective was positive: reporting better self-perception, comfort in daily activities, and motivation to maintain training.

The follow-up results will be presented at the 15th Vienna International Workshop on Functional Electrical Stimulation to be held from 15 to 18 September 2025 in Vienna, Austria.

We acknowledge the lack of a control group as a limitation, making it difficult to quantify the magnitude of FES-specific effects compared to natural history.

In addition to describing the clinical and morphological findings, it should be also important to consider possible biological mechanisms that might underlie the observed effects of long-term hbFES in chronically denervated

muscles. These may include activation of satellite cells, which could contribute to limited muscle regeneration even years after injury; modulation of fibrosis, potentially reducing connective tissue replacement and preserving contractile elements; and increased capillarization, which may enhance local perfusion and metabolic support. Furthermore, repeated stimulation might induce metabolic adaptations that delay degeneration. Although these hypotheses cannot be directly confirmed within a single-case study, future research should explore underlying biological mechanisms and predictors of response in chronic patients.

Conclusions

The clinical case of Mr. AC suggests the possibility of extending FES x DDM to chronically denervated patients, at least those with SCI up to ten years. Our findings highlight the practical importance of adapting long-term hbFES programs to each patient's motivation, lifestyle changes, and psychosocial context, in order to maximize adherence and clinical benefit. Therefore, future research should also focus on developing personalized stimulation protocols and supportive strategies that help patients maintain engagement with FES over the long term. Although such contractions are insufficient for the recovery of functional mobility, they remain critically important for preventing or reducing muscle atrophy, ensuring more physiological functioning of the cardiovascular system (due to improved venous return), and preventing secondary complications such as pressure ulcers and joint deformities. Therefore, stimulation is also crucial in denervated muscles and serves as a key therapeutic strategy to reduce disability and maintain quality of life in patients with long-term denervation

Acknowledgement

The authors thank the A&C M-C Foundation for Translational Myology of Padua, Italy, which provided the Schuhfried Den2x stimulator that Mr. AC uses at home.

References

[1] Kern, H., Carraro, U., et al.: One year of home-based daily FES in complete lower motor neuron paraplegia: recovery of tetanic contractility drives the structural improvements of denervated muscle. *Neurol Res*., vol. 32, pp. 5-12, February 2010

[2] Kern, H., Carraro, U. Home-Based Functional Electrical Stimulation of Human Permanent Denervated Muscles: A Narrative Review on Diagnostics, Managements, Results and Byproducts Revisited 2020. *Diagnostics (Basel)*., vol. 10, 529 July 2020

[3] U Carraro, *How to rejuvenate at 80's.* 2024 pp. 41. Padova, Italy CLEUP sc Coop. Libraria Editrice Università di Padova. ISBN 978 88 5495 727 5

[4] Carraro U, Alberty MS, et al.: Mobility Medicine: A call to unify hyper-fragmented specialties by abstracts sent to 2025Pdm3, and typescripts to Ejtm3, and Diagnostics. *Eur. J. Transl. Myol.,* vol. 34 pp. 13432 December 2024

Author's Address

Ugo Carraro
Department of Biomedical Sciences, University of Padova, Italy
eMail: ugo.carraro@unipd.it

Clinical implications of electrical stimulation in a home-based treatment setting for patients with facial nerve paralysis to stop denervation atrophy

Christina Buchgeher [1], Johannes Krauß [2, 3], Gabriel Meincke [2, 3], Maren Geitner [2, 3, 4,5], Dirk Arnold [2, 3, 4], Jonas Ballmaier [2, 3, 4], Anna Kuttenreich [2, 3, 4], Orlando Guntinas-Lichius [2, 3, 4], Gerd Fabian Volk [2, 3, 4]

[1] MED-EL Medical Electronics, Business Unit STIWELL, Austria
[2]Department of Otorhinolaryngology, Jena University Hospital, Germany
[3]Facial-Nerve-Center, Jena University Hospital, Germany
[4]Center for Rare Diseases, Jena University Hospital, Germany
[5]Interdisciplinary Center for Clinical Research (IZKF), Jena University Hospital, Jena, Germany

Abstract: *With growing evidence on the therapeutic potentialities of electrostimulation treatment in facial paralysis, there is a growing need for standardized guidelines for clinical practice. A recently conducted study with participants with complete unilateral facial paralysis (n = 10) showed significant potential of functional electrical stimulation preventing atrophy of the zygomaticus muscle. Phase durations of 25 to 250 ms showed zygomaticus responses without discomfort. Based on these study results, implications for an implementation into clinical practice can be derived. The stimulation protocol can be transferred onto the treatment of further muscle regions as well as for patients showing signs of reinnervation. Parameter settings such as phase duration, frequency and amplitude should be individualized for each patient and each muscle group and continuously adjusted. Study results show the feasibility of implementing FES in a home-based training, resulting in higher stimulation times, self-efficacy and motivation. Supervision of the home-based training with a continuous adaptation of stimulation parameters is necessary to ensure intervention efficacy.*

Keywords: *surface electrical stimulation, home-based therapy, facial palsy, permanent muscle denervation, electrical stimulation*

Introduction

Increasingly more evidence of the therapeutic potentialities of surface functional electrostimulation (FES) for the treatment of facial paralysis has been published so far [1,2]. Based on the results of the recently conducted prospective "Denervated-Facial-Paralysis Study" (DFP-Study), important implications can be transferred into clinical practice. The main objective of the study was to provide a home-based FES protocol as a therapy supplement for patients with peripheral facial paralysis. In many cases of facial paralysis, reinnervation surgery or even free muscle transfer is the gold standard. However, FES can be an important aid both before and after reconstructive surgery, as well as during the subsequent rehabilitation process. Therein, the aim was to develop a patient set-up to improve facial functionality and symmetry while minimizing discomfort.

Method

Ten patients (24-77 years, median 61 years; 4 female, 6 male, time of denervation: 3-5954 days, median 130 days) were included in the study if they had unilateral complete peripheral facial muscle paralysis as determined via needle electromyography (nEMG). Facial paralysis etiologies were vestibular schwannoma (n = 3), parotid cancer (n = 3), benign parotid tumor (n = 1), chronic otitis media (n = 1), zoster oticus (Ramsey-Hunt syndrome; n =1) and traumatic temporal bone fracture (n = 1). They performed home-based surface electrical stimulation for a maximum of one year according to the protocol until drop-out or exclusion, with a mean study duration of 95 days (range: 35-301). Patients were observed at monthly on-site follow-up visits for clinical and electrophysiological signs of reinnervation.

Surface Electrode Placement and Program Set-up

FES was performed with the STIWELL med4 (STIWELL® med4 device (CE 0297; P/N 9001015; MED−EL Medical Electronics, Innsbruck, Austria), an approved electrostimulation device. Two 6.4x4.0 cm oval surface electrodes (PALS® Neurostimulation electrodes, Axelgaard Manufacturing Co., Ltd., Lystrup, Denmark CE-certified, REF 896230) were placed on the cheek region to mainly stimulate the paralyzed zygomaticus muscle with the patient in an upright position.

Biphasic stimulation was delivered in triangular waveform, with a burst duration of 5 sec and a burst pause of 1 sec. The individual shortest phase duration causing a selective activation of the zygomaticus muscle and without uncomfortable sensation was used to program the device. The amplitude at which a visible contraction of the zygomaticus muscle region could be elicited without the simultaneous unspecific reaction of other facial muscles was determined for each evaluated phase duration, unless the discomfort threshold or an amplitude causing unspecific reactions of other facial muscles was reached before. A metallic taste on the tongue caused by unspecific stimulation of the lingual nerve and/or flash sensations by unspecific stimulation of the retina and/or the optical nerve are typical for long triangular impulses and were not an unexpected side effect or any reason for the withdrawal of

a patient. The chosen phase duration was saved on a close map on the STIWELL med4.

For home training, the patient was instructed and trained to place the electrodes, to switch on the device and to start the saved program. For all patients, monthly study visits were planned, plus a baseline visit, and two remote study visits (after 2 and 6 weeks of home training) conducted via telephone.

Participants were instructed to perform the stimulation twice a day for 20 min, with at least a 6-hours break between sessions. The parameters chosen at baseline were adjusted at the subsequent follow-up visits as necessary to ensure a safe, specific, and effective stimulation of the target region.

Results

A specific response to the stimulation without unspecific activation of other facial muscles and/or discomfort for the patients was observed in all patients with a phase duration ≥ 25 ms (Fig. 1). With shorter phase durations, unspecific responses of the lips, chin, masseter and sometimes eyes could be observed. With such short phase durations, it was impossible to select a parameter combination eliciting a selective zygomaticus muscle stimulation only.

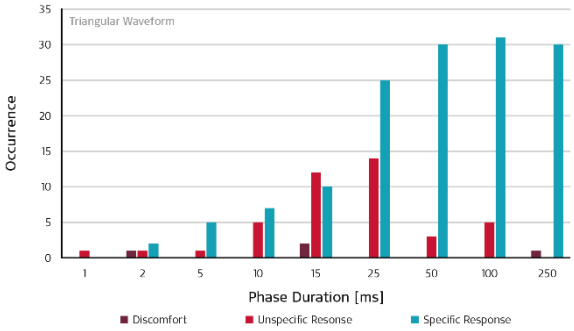

Figure 1: Selective stimulation of the zygomaticus muscle with triangular waveform

During home training, it was observed that the phase duration required to induce a constant visible contraction of the targeted muscles could be reduced over time. The mean phase duration could be reduced from 155.0 ms ± 55.0 to 51.0 ms ± 12.4 over time. The decrease in phase duration from baseline to 12 ± 2 weeks (n = 7, p = 0.003), and the decrease from baseline to 20 ± 2 weeks (n = 4, p = 0.001) were both significant. Consequently, both stimulation amplitude and frequency could be increased throughout the majority of the treatment sessions without causing fatigue in the patients during the 20 minutes home training (Fig. 2) [3].

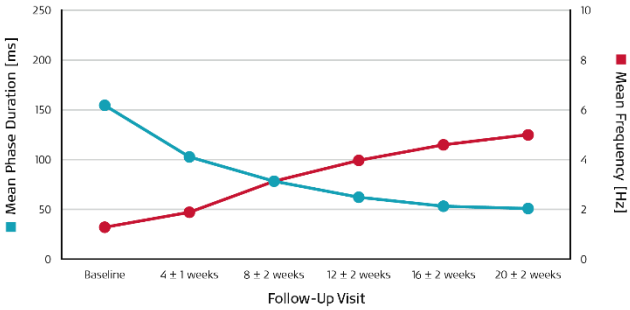

Figure 2: adjustment of phase duration and frequency throughout home training

The mean stimulation frequency could be increased from 1.3 Hz ± 0.5 at baseline to 5.0 Hz ± 1.5 during the observation period of 20 ± 2weeks (Fig. 2). As a consequence of the reduction of the phase duration to generate the same charge of stimulation (following the strength/duration-curve), the mean voltage was increased from 16.2 V ± 2.5 to 27.2 V ± 5.9.

Despite the general trend of reducing the phase duration and increasing the frequency as a result of the home training, in 13 of 41 follow-ups the parameters were not changed because the motor response was weaker. At 3 follow-ups the phase duration had to be increased again, because the patients' denervated muscles did not yet tolerate the higher frequency applied. No harmful side effects of the home-based FES on the facial muscles over the treatment period were observed or reported by patients.

Outcome Measures

The assessment of ultrasound imaging, using an established protocol for facial muscles [4], indicated that the cross-sectional area of the paralytic electro-stimulated zygomaticus muscle increased during the first month of FES, while control muscles outside the focus of FES further decreased. At each baseline and follow up, Sunnybrook facial grading score (SFGS) was assessed by the clinical investigators [5]. While no significant changes were observed in total SFGS scores or sub-scores for resting and voluntary movement across the study period, FDI subscore body functions and FaCE oral function sub-scores improved significantly during FES ($p = 0.031$): FDI subscore body functions increased from 53.0 ± 4.7 to 66.0 ± 6.8 ($p = 0.032$), while FaCE oral function improved from 50.0 ± 9.9 to 69.9 ± 13.9 ($p = 0.097$). The patient related outcome measures (PROMs) [6-10] and the assessment of photographic surface parameters (using automated image analysis with Emotrics [11]), support this positive effect of electrical stimulation.

These results objectify that FES was neither harmful nor unpleasant but appreciated by the patients in individual perception of functional and social improvement. These findings can be further substantiated with an improvement of facial symmetry in automated image assessment. Whereas the stimulated area increased resting mouth symmetry, the non-stimulated ocular region worsened by further dropping of the lower eyelid. Expectedly, voluntary

movement of completely denervated muscles would not improve until reinnervation, as the affected muscles cannot contract voluntarily. No further deterioration of the score was shown. FES could therefore prevent a further deterioration in resting symmetry.

Discussion: Transfer Into Clinical Practice

The results of the study provide a clear indication of FES which can be transferred into clinical practice. Generally, a home-based therapy program should be planned according to a patient's individual condition, goals, priorities and planned surgical treatment.

Target Muscles and Denervation States

The study results show that a suitable combination of phase duration and amplitude allows to elicit a selective response of the targeted zygomaticus muscle without discomfort or the simultaneous unspecific activation of other ipsi- or contralateral facial muscles. The stimulation protocol for the zygomaticus muscle can also be transferred to other denervated muscles in the face. For instance, the stimulation can also be applied to the following main muscle groups: m. frontalis, m. orbicularis oculi, m. orbicularis oris. The principle of a selective stimulation avoiding mass stimulation or activation of neighbouring muscles should be considered. For each muscle (group), an initial testing is necessary. Beginning with long phase durations, the shortest possible duration eliciting visible contractions without discomfort should be determined.

When working with muscles groups of different reinnervation states, it is necessary to find individual settings of parameters for each muscle group. While patients with signs of reinnervation were excluded from the study due to statistical reasons, they can still profit from stimulation treatment in everyday clinical practice.

Continuous Adjustments of Stimulation Parameters

Also, stimulation parameters should be continually readjusted throughout the FES to enhance training intensity. As shown in the DFP-study, there was a general trend towards decreasing phase duration and increasing frequency that led to an increase in training intensity on the denervated facial muscle. According to the stimulation protocol applied in the study, at least monthly adjustments are recommended. In clinical practice, the adjustment intervals should be chosen individually according to clinical development.

Choice of Stimulation Parameters & Stimulation Device

It has been shown that only phase durations of ≥ 25 ms can elicit a zygomaticus response without discomfort or simultaneous non-specific activation of other ipsi- or contralateral facial muscles. Similarly, Arnold et al. [4], demonstrated that a phase duration of ≥ 50 ms resulted in a distinct zygomaticus muscle response following surface stimulation. Many devices that are available on the market can generate only shorter phase durations not allowing specific stimulation of denervated muscles. Hence, the availability of long phase durations has to be considered in the choice of stimulation device.
In response to existing inconsistencies in the literature, we wish to emphasize that the phase durations discussed here are expressed in milliseconds (25 ms equals 25 000 µs which equals 0.025 sec).

Therapy Frequency

The results of the DFP-study are based on a stimulation session frequency of 20 minutes per muscle, twice a day. Considering the number of affected muscles that might even need more stimulation time, this frequency is typically only achievable in a home-based setting. In addition, the feasibility of implementing FES in a home-based setting makes it possible to reduce the number of therapy sessions with a professional, resulting in lower costs for the health care system.

Patient-Related Considerations

Home-based therapy has the potential to enhance self-efficacy and hence motivation, potentially resulting to a better therapy adherence of patients. There were no drop-outs reported in the DFP-study due to unpleasant sensations or impracticability of the stimulation protocol. Rather, patients appreciated the treatment outcomes as indicated in the study report and results.

Conclusions

It has been shown that FES has significant potential to halt and even reverse the atrophy of denervated facial muscles in peripheral facial nerve paralysis patients. A suitable combination of phase duration and amplitude can elicit a selective zygomaticus response without discomfort or simultaneous non-specific activation of other ipsi- or contralateral facial muscles using a phase duration between 25 and 250 ms. Within the scope of the present study, it has been shown that the stimulation of denervated facial muscles is feasible in a home-based setting and offers a promising prospect of being established as an additional therapeutic pillar in the conservative treatment of facial nerve paresis and paralysis. FES may therefore be used as a "bridge technology" to restore facial muscle capacity before undergoing reinnervating surgery treatment. For effective use, stimulation parameters should be individualized to each patient and continually readjusted throughout the FES to enhance training intensity. FES serves to complement existing invasive facial nerve paralysis treatments. Future research requires further investigations with sufficient group sizes and adapted study designs with a control group to meet requirements for establishing standardized guidelines.

Acknowledgement

This paper received research grants, equipment and statistical support from MED-EL Elektromedizinische Geräte GmbH, Innsbruck, Austria.

M. Geitner received financial support for the research, authorship and publication of the article as being a member of IZKJ Jena. Funded by the Deutsche Forschungsgemeinschaft (DFG, German Research Foundation)–(KL 2926/2-1), Clinician Scientist-Program OrganAge, funding number WI 830/12-1.

References

[1] Krauß J, Meincke G, Geitner M, Kuttenreich AM, Beckmann J, Arnold D, Ballmaier J, Lehmann T, Mayr W, Guntinas-Lichius O, Volk GF. Efficacy of electrical stimulation of the zygomaticus muscleomaticus muscle in complete facial paralysis: evidence from facial grading and automated image analysis. Eur J Transl Myol. 2024 Nov 15;34(4):13161. doi: 10.4081/ejtm.2024.13161. PMID: 39555983; PMCID: PMC11726304.

[2] Meincke G, Krauß J, Geitner M, Kuttenreich AM, Arnold D, Ballmaier J, Lehmann T, Mayr W, Guntinas-Lichius O, Volk GF. Deceleration of denervated facial muscle atrophy through functional electrical stimulation: a sonographic quantification in patients with facial nerve paralysis. Eur J Transl Myol. 2024 Nov 13;34(4):13162. doi: 10.4081/ejtm.2024.13162. PMID: 39535548; PMCID: PMC11726303.

[3] Geitner, M., Ballmaier, J., Krauß, J., Meincke, G., Kuttenreich, A.-M., Arnold, D., Mayr, W., Klingner, C., Mastryukova, V., Guntinas-Lichius, O., Volk, G.F. (2025). Selection of electrical stimulation parameters for the treatment of facial nerve paralysis. [Unpublished manuscript]

[4] Volk GF, Wystub N, Pohlmann M, Finkensieper M, Chalmers HJ, Guntinas-Lichius O. Quantitative ultrasonography of facial muscles. Muscle Nerve. 2013 Jun;47(6):878-83. doi: 10.1002/mus.23693. Epub 2013 Mar 21. PMID: 23519888.

[5] Ross BG, Fradet G, Nedzelski JM. Development of a sensitive clinical facial grading system. OtolaryngolHead Neck Surg 1996;114:380-6.

[6] Neumann T, Lorenz A, Volk GF, et al. [Validation of the German Version of the Sunnybrook Facial Grading System]. Laryngo- rhino- otologie 2017;96:168-74.

[7] Kahn JB, Gliklich RE, Boyev KP, et al. Validation of a patient-graded instrument for facial nerve paralysis: the FaCE scale. Laryngoscope 2001;111:387-98.

[8] Ho AL, Scott AM, Klassen AF, et al. Measuring quality of life and patient satisfaction in facial paralysis patients: a systematic review of patient-reported outcome measures. Plast Reconstr Surg 2012;130:91-9.

[9] VanSwearingen JM, Brach JS. The Facial Disability Index: reliability and validity of a disability assessment instrument for disorders of the facial neuromuscular system. Physical therapy 1996;76:1288-98; discussion 1298-300.

[10] Volk GF, Steigerwald F, Vitek P, et al. [Facial Disability Index and Facial Clinimetric Evaluation Scale: validation of the German versions]. Laryngorhinootologie 2015;94:163-168.

[11] Guarin DL, Dusseldorp J, Hadlock TA, et al. A machine learning approach for automated facial measurements in facial palsy. JAMA Facial Plastic Surgery 2018; 20:335-7.

[12] Arnold, D., Thielker, J., Klingner, C. M., Puls, W. C., Misikire, W., Guntinas-Lichius, O., & Volk, G. F. (2021). Selective Surface Electrostimulation of the Denervated Zygomaticus Muscle. Diagnostics (Basel), 11(2), 188. doi: https://doi.org/10.3390/diagnostics11020188

Author's Address

Christina Buchgeher, BSc
MED-EL Medical Electronics
Fürstenweg 77a
A-6020 Innsbruck, Austria
Tel. +43 664 607053146
Email: christina.buchgeher@medel.com
www.medel.com

Gerd Fabian Volk, MD
Department of Otorhinolaryngology
Facial-Nerve-Center Jena
Jena University Hospital
Am Klinikum 1
D-07747 Jena, Germany
Tel. +49 3641 9329396
Email: fabian.volk@med.uni-jena.de
www.fazialis-nerv-zentrum.de

A Randomised, Sham-Controlled, Proof of Principle Study of Abdominal Functional Electrical Stimulation (ABFES) for Bowel Management in Spinal Cord Injury (SCI)

Street T[1], Vinod C[1], Peralta S[1], Strike P[1], Earl R[1]

[1]Salisbury NHS Foundation Trust

Abstract: *A well-managed bowel program is an essential part of daily life for many people living with a spinal cord injury (SCI). Initial observational and small studies suggest abdominal functional electrical stimulation (ABFES) may be useful for decreasing overall bowel management time. The objective was to conduct a proof of principle study to establish reproducibility of previous results using bowel movement duration as a primary outcome measure. Thirty-six participants with a SCI lesion AIS A-D, ≥T12, age ≥18, ≥6 months post SCI, medically stable, with neurogenic bowel were randomized to receive 8 weeks of home- based abdominal electrical stimulation in an intervention or sham control group. The results of the primary outcome measure revealed bowel movement duration was reduced after eight weeks compared to day one for the intervention ABFES intervention group. ABFES may provide a promising new additional treatment option for people experiencing neurogenic bowel due to SCI.*

Keywords: *Neurogenic bowel, spinal cord injury, abdominal functional electrical stimulation,*

Introduction

A well-managed bowel program is an essential part of daily life for many people living with a spinal cord injury (SCI), with between 42-95% of people with SCI experiencing constipation [1], with around 41% requiring 30 minutes or more for a bowel emptying. The prevalence of faecal incontinence is estimated to be present in around 75% of people with a spinal cord injury. Faecal incontinence may or may not be associated with incomplete bowel emptying and is associated with having a profound effect on quality of life and may cause severe restriction on social activities.[1] Neurogenic bowel embraces a spectrum of harms including both physical & psychological distress. Initial studies suggest abdominal functional electrical stimulation (ABFES) may be useful for decreasing overall bowel management time, decreasing colonic transit time and reducing discomfort. [2],[3] Although previous studies have been encouraging, proof of principle for the use of ABFES has not yet been established due to inadequate sample size, brief duration of study and participant inclusion criteria. The objective of the study was to conduct a proof of principle study to establish reproducibility of previous results using bowel movement duration as a primary outcome measure

Material and Methods

The study used a randomised, sham controlled, remotely conducted trial design and was conducted within a community outpatient setting. Thirty-six participants with a SCI lesion AIS A-D, ≥T12, age ≥18, ≥6 months post SCI, medically stable, with neurogenic bowel were randomized to receive 8 weeks of home- based abdominal electrical stimulation in an intervention (40 Hz, 300µs, 30-60 mA) or sham control group using a Microstim 2V2 (*Odstock Medical Ltd*) adapted research stimulator. The primary outcome measure was overall bowel movement duration time measured using an electronic bowel diary. Secondary outcome measures included neurogenic bowel score, bladder function, quality of life, usability of assistive devices and patient reported outcome measures.

Fig. 1 Bowel duration (minutes) for low dose and high dose conditions at baseline and after 8 weeks

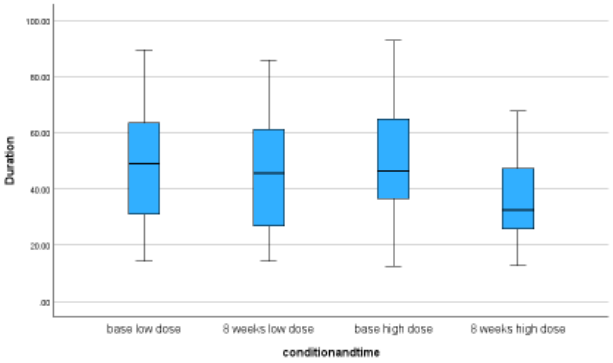

Results

Mixed effects repeated measures linear modelling was used to analyse the data. A significant overall main effect for time was found $F(1,27)=17.37, p<.001$). There was no significant overall main effect for treatment group $F(1,27)=.12, p=.73$) and a significant interaction between time and treatment group was found $F(1,27)=4.73$, p=.04). Post hoc analysis with a Bonferroni adjustment revealed that bowel duration was significantly decreased after 8

weeks of using FES in the high dose group compared to day one (15.13(95% CI: 8.60 to 21.65) mins $p<.001$). There was no significant difference between the low dose group at 8 weeks compared to baseline (4.75 (95% CI:2.54 to 12.05) mins, p =.19). Fig. 1 shows a visual representation of bowel movement duration for the low dose condition compared to the high dose condition at baseline and after 8 weeks.

Further modelling examining lesion level, lesion type, time since injury and participant individual differences were redundant to the model indicating no significant contribution to the findings.

Discussion

As predicted the primary outcome measure of bowel duration was found to be significantly reduced for people in the high dose ABFES group providing proof of principle for using abdominal FES for bowel management for neurogenic bowel following SCI. Interestingly, time since injury, lesion level, lesion type and participant individual differences did not appear to have any influence on the results suggesting that ABFES can be considered for a broad variety of people with neurogenic bowel. This finding is particularly encouraging given several participants had experienced neurogenic bowel for over 40 years.

Conclusions

The results suggest that ABFES may provide a promising new additional treatment option for people experiencing neurogenic bowel due to SCI. Further work is required to examine underlying mechanism and optimisation of stimulation parameters.

Acknowledgements

Participants are acknowledged for giving up their time to take part in the study. The INSPIRE foundation are acknowledged for funding and supporting the study. The Spinal Injuries Association (SIA) are acknowledged for supporting initial patient public involvement on the study and promoting the study to their members. With much thanks to participant identification centres at the Royal Orthopaedic hospital in Stanmore through Dr Sarah Knight; the National Spinal Injuries Centre at Stoke Mandeville hospital through Mr Maurizio Belci; the Princess Royal Spinal Injuries centre through Mr Pradeep Thumbikat; and Torbay and South Devon NHS Trust through RN Angie Folds. With thanks to Odstock Medical for providing Microstim 2V2 research stimulators adapted by Dr Steve Crook. With thanks to Christine Singleton, Dr Anton Emmanuel, Dr Paul Taylor and Prof Michael Craggs for advice.

References

[1] K. Krogh, A. Emmanuel, B. Perrouin-Verbe, M. A. Korsten, M. J. Mulcahey, and F. Biering-Sørensen, "International spinal cord injury bowel function basic data set (Version 2.0).," *Spinal cord*, vol. 55, no. 7, pp. 692–698, Jul. 2017, doi: 10.1038/sc.2016.189.

[2] M. A. Korsten, N. R. Fajardo, A. S. Rosman, G. H. Creasey, A. M. Spungen, and W. A. Bauman, "Difficulty with evacuation after spinal cord injury: colonic motility during sleep and effects of abdominal wall stimulation.," *Journal of rehabilitation research and development*, vol. 41, no. 1, pp. 95–100, 2004, doi: 10.1682/jrrd.2004.01.0095.

[3] R. Hascakova-Bartova, J.-F. Dinant, A. Parent, and M. Ventura, "Neuromuscular electrical stimulation of completely paralyzed abdominal muscles in spinal cord-injured patients: a pilot study.," *Spinal cord*, vol. 46, no. 6, pp. 445–450, Jun. 2008, doi: 10.1038/sj.sc.3102166.

Author's Address

Tamsyn Street
Salisbury NHS Foundation Trust
tamsyn.street@nhs.net

THE EFFECT OF NEUROMUSCULAR ELECTRICAL STIMULATION ON BOWEL MANAGEMENT IN PEOPLE WITH CHRONIC SPINAL CORD INJURY

Ines Bersch* [1,2], Kathrin Schafer[2], Andreas Limacher[2], Marie Alberty[1,2,3]

[1]International FES Centre®, Swiss Paraplegic Centre, Nottwil, Switzerland

[2]Swiss Paraplegic Research, Nottwil, Switzerland

[3]Department of Sport and Sport Science, Neuroscience, University of Freiburg, Germany

*ines.bersch@paraplegie.ch

Abstract: *Spinal cord injury (SCI) disrupts autonomic nervous system function, notably impairing bowel control and significantly impacting quality of life. Non-invasive strategies, such as abdominal massage and neuromuscular electrical stimulation (NMES), are generally preferred over implanted devices for managing bowel dysfunction. This clinical trial evaluated the effects of 16 weeks of home-based NMES on bowel and bladder function in people with chronic SCI. Participants (C5-L3, AIS A-D) applied NMES to abdominal muscles for 30 minutes before defecation. Outcomes included the Neurogenic Bowel Dysfunction Score (NBDS), Qualiveen Short Form, defecation and bowel transit times, and patient satisfaction.*

Twenty participants completed the study. While NBDS scores remained moderate to severe, satisfaction with bowel management improved by two points on a 10-point scale. NMES significantly reduced bowel transit time by 32 hours and defecation time by 8 minutes, though the Qualiveen score was unchanged. The benefits were not sustained after stopping NMES, but many participants continued using it. NMES is a promising, non-invasive method to improve bowel function in chronic SCI; further research should determine optimal dosing.

Keywords: *neurogenic bowel dysfunction; spinal cord injury; bowel management; defecation time*

Introduction

Spinal cord injury (SCI) results in profound physiological changes, notably in autonomic nervous system regulation, which severely impacts gastrointestinal function. Neurogenic bowel dysfunction (NBD) is highly prevalent among individuals with SCI and is characterized by symptoms such as chronic constipation, prolonged evacuation time, fecal incontinence, and incomplete emptying. These symptoms collectively affect physical health, psychological well-being, and social participation. Approximately 14% of individuals with SCI report defecation times exceeding one hour, which can significantly impair their daily routines and limit opportunities for work, leisure, and community engagement.

To manage bowel dysfunction, various strategies are employed, including dietary adjustments, pharmacological agents, manual evacuation techniques, abdominal massage, and transanal irrigation. While some patients benefit from implanted neurostimulation devices targeting sacral or abdominal nerves, many prefer non-invasive solutions due to lower risk, greater ease of use, and better acceptability. Among such strategies, neuromuscular electrical stimulation (NMES) has emerged as a promising technique. By eliciting contractions of the abdominal musculature, NMES can potentially facilitate colonic motility and support defecation through increased intra-abdominal pressure and improved coordination with bowel routines.

Objective

This prospective clinical trial aimed to assess the effect of 16 weeks of structured, home-based NMES of the abdominal muscles on bowel-related outcomes in individuals with chronic SCI. Specific objectives included evaluation of defecation time, bowel transit time, satisfaction with bowel and bladder management, and overall impact on neurogenic bowel and bladder dysfunction.

Material and Methods

Twenty participants with chronic SCI (injury duration >2 years; AIS grades A to D; neurological levels C5–L3) and reported difficulties with bowel function were recruited. Participants applied NMES bilaterally to the abdominal wall using surface electrodes and a portable stimulator. The stimulation protocol was standardized to 30 minutes per session, administered immediately prior to the participants' regular bowel care routines. Stimulation intensity was individually adjusted to achieve a visible, strong, but well-tolerated muscle contraction.

The intervention period lasted 16 weeks, embedded in a 24-week study framework that included five assessment points (baseline, mid-intervention, post-intervention, and two follow-up visits). Outcome measures comprised both objective and subjective domains. Objective outcomes included:

- Defecation time and frequency, recorded by participants in daily logs.
- Bowel transit time, measured using the "corn test" (appearance of sweetcorn kernels in stool after oral ingestion).
- Neurogenic Bowel Dysfunction Score (NBDS), to assess bowel-related symptoms and severity.

Subjective measures included:

- Patient satisfaction with bowel management, rated on a 10-point Likert scale.
- Qualiveen Short Form (SF), assessing bladder-related quality of life.

All data were analyzed using repeated-measures statistics with 95% confidence intervals and significance level set at $p<0.05$.

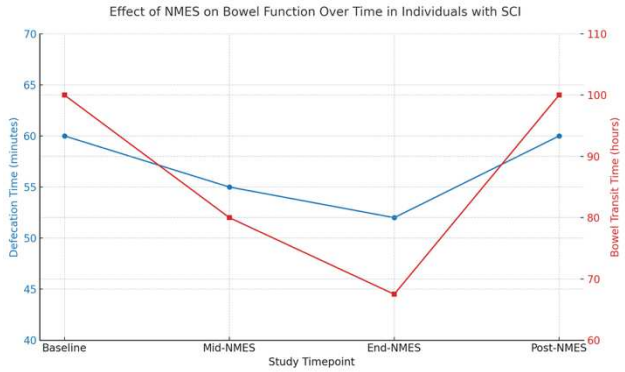

Figure 1: Effect of NMES in terms of defecation time (blue line) expressed in minutes period and bowel transit time (red line) expressed in hours over the 16 weeks stimulation

Results

All 20 participants completed the intervention. During the second half of the stimulation period, defecation time was significantly reduced by an average of 8.0 minutes compared to baseline (95% CI: 4.2–11.9 minutes, $p<0.001$). However, this improvement was not sustained following discontinuation of stimulation, and defecation times returned to near-baseline levels in the post-intervention phase.

Bowel transit time demonstrated a significant reduction of 32.5 hours after 16 weeks of NMES (95% CI: 4.0–61.1, $p=0.031$), indicating an accelerated passage through the gastrointestinal tract. Despite improvements in transit time and defecation duration, the NBDS remained in the moderate to severe range (≥14) throughout the study, reflecting the complexity and chronicity of bowel dysfunction in this population.

Participants reported a statistically significant increase in satisfaction with their bowel routine, with a mean improvement of 1.5 points on the Likert scale during the stimulation phase (95% CI: 0.4–2.6, $p=0.011$). This subjective improvement did not correlate with changes in bladder function, as assessed by the SF-Qualiveen, which remained unchanged across all timepoints.

Importantly, no adverse events were reported related to NMES use, and adherence to the home-based protocol was high. Several participants opted to continue NMES independently after study completion, indicating a high degree of acceptance and perceived benefit.

Discussion

This study demonstrates that NMES applied to the abdominal wall significantly improves bowel transit and defecation times in individuals with chronic SCI. Although the effects diminished once the stimulation ceased, the clinical relevance and patient-reported satisfaction underscore the potential of NMES as an effective, non-invasive adjunct to conventional bowel management strategies. The absence of impact on bladder function suggests a targeted effect on gastrointestinal motility, rather than generalized autonomic modulation.

Given the chronic burden of bowel dysfunction in SCI and the limitations of pharmacological or surgical interventions, NMES offers a practical and user-driven alternative. Further studies are warranted to determine optimal stimulation parameters, identify subgroups most likely to benefit, and explore combined strategies that include dietary, behavioral, and neurostimulation-based approaches. Incorporating NMES into standard bowel care protocols may enhance autonomy, reduce caregiving demands, and improve quality of life for people living with SCI.

Conclusions

NMES applied to the abdominal wall significantly reduced defecation and bowel transit times in individuals with chronic SCI, with effects observed during the stimulation phase but not sustained post-intervention. These findings lend support to the notion that NMES is a feasible, non-invasive adjunct to bowel management, offering meaningful functional and subjective benefits.

Acknowledgement

We would like to express our sincere gratitude to all the patients who generously participated in this study. Their willingness to share their time and experiences was invaluable to our research. Without their contribution, this work would not have been possible.

References

[1] Coggrave, M., Norton, C. et al.: Management of neurogenic bowel dysfunction in the community after spinal cord injury: A postal survey in the United Kingdom, Spinal Cord, vol. 47, pp.323-333, April 2009.

[2] Anderson, K.: Targeting Recovery: Priorities of the Spinal Cord-Injured Population, J. Neurotrauma, vol. 21, pp. 1371-1383, October 2004.

[3] Ayaş S, Leblebici B, Sözay S, Bayramoğlu M, Niron EA. The effect of abdominal massage on bowel function in patients with spinal cord

injury. Am J Phys Med Rehabil. 2006 Dec;85(12):951-5. doi: 10.1097/01.phm.0000247649.00219.c0. PMID: 17117000.

[4] Bochkezanian V, Henricksen KJ, Lineburg BJ, Myers-Macdonnell LA, Bourbeau D, Anderson KD. Priorities, needs and willingness of use of nerve stimulation devices for bladder and bowel function in people with spinal cord injury (SCI): an Australian survey. Spinal Cord Ser Cases. 2024 Mar 21;10(1):15. doi: 10.1038/s41394-024-00628-3. PMID: 38514608; PMCID: PMC10957911.

[5] Bourbeau D, Bolon A, Creasey G, Dai W, Fertig B, French J, Jeji T, Kaiser A, Kouznetsov R, Rabchevsky A, Santacruz BG, Sun J, Thor KB, Wheeler T, Wierbicky J. Needs, priorities, and attitudes of individuals with spinal cord injury toward nerve stimulation devices for bladder and bowel function: a survey. Spinal Cord. 2020 Nov;58(11):1216-1226. doi: 10.1038/s41393-020-00545-w. Epub 2020 Sep 7. PMID: 32895475; PMCID: PMC7642195.

[6] Hascakova-Bartova R., Dinant JF., et al.: Neuromuscular electrical stimulation of completely paralyzed abdominal muscles in spinal cord-injured patients: a pilot study, Spinal Cord, vol. 46, pp. 445-450, January 2008.

Author's Address

Ines Bersch
International FES Centre®
ines.bersch@paraplegie.ch
https://www.paraplegie.ch/spz/en/medical-services/outpatient-acute-rehabilitation/international-fes-centre/

A retrospective analysis of ABFES in treating and managing constipation in individuals with neurological impairment

Forrest B[1], Singleton C[2], Peace C[2], Maycock L[2], Nightingale T[1]

[1] University of Birmingham, England
[2] West Midlands Rehabilitation Centre, England

***Abstract**: Introduction: Constipation is common in multiple sclerosis (MS) and spinal cord injury populations, leading to increased risk of hospital admission and poor psychosocial quality of life. However, current conventional management is ineffective. Novel alternatives, including abdominal functional electrical stimulation (ABFES), have previously improved constipation in patients with neurological conditions. Methods: This single-centre, retrospective, longitudinal study used data from 51 clinically constipated patients (43 with MS and 8 with other neurological conditions). ABFES was administered over an 18-week intervention. The primary outcome measure used was the Patient Assessment of Constipation Quality of Life Questionnaire (PACQoL), which was assessed at baseline, 6 weeks, and 18 weeks. One-way repeated measures ANOVAs were run to analyse the data. Secondary outcome measures included laxative medication changes, time spent on the toilet, and changes in the urge to pass faeces. Results: ABFES significantly improved each PACQoL domain at 6-week and 18-week timepoints compared to baseline ($P<0.01$), with between 54% and 88% of patients achieving a clinically meaningful change. Patients reported reductions in laxative medication and the time spent on the toilet, while improvements in the urge to pass faeces were also observed. Conclusion: ABFES appears to be a safe, non-invasive technique to treat and manage constipation across an array of neurological conditions. However, more controlled trials are needed to provide clinicians with robust evidence on the longitudinal efficacy of ABFES.*

***Keywords**: Neurological Conditions, Constipation, ABFES, PAC-QoL.*

Introduction

Constipation is common in Multiple Sclerosis (MS) and Spinal Cord Injury (SCI) populations [1,2]. Constipation can lead to severe secondary complications, including megacolon, bowel perforations, and pseudo-obstruction [3]. This increases the risk of hospital admission and can lead to a poor psychosocial quality of life (QoL). Conventional constipation management involves generalised advice regarding improving diet and physical activity levels, alongside prescriptions for laxatives, suppositories, or enemas. Current management is not effective at treating constipation in those with neurological impairment, and recommendations are based on small sample sizes that are uniformly low in methodological quality [4]. Therefore, research has turned to finding novel alternatives to manage constipation more effectively.

One novel alternative is functional electrical stimulation (FES). Early pilot studies, involving 4 MS participants, demonstrated that 30 minutes a day of abdominal functional electrical stimulation (ABFES) for 6 weeks, alongside conventional management, found improvements in the Patient Assessment of Constipation Quality of Life Questionnaire (PACQoL) [5]. These improvements in the PACQoL were later replicated in larger sample-sized studies involving ~20 MS participants, with some of them reporting improvements in bowel opening frequency, reduced straining, and a preference for using ABFES over laxatives [6,7]. Early ABFES studies used in SCI populations also recorded improvements in bowel opening frequency, defecation desire, and reduced defecation effort [8]. Despite ABFES appearing to be a safe, non-invasive solution for treating constipation in neurologically impaired populations, current evidence is based on small sample sizes that are mainly restricted to MS populations and fail to provide longitudinal data beyond a 6-week intervention. Therefore, the current study aimed to evaluate the effectiveness of ABFES in treating and managing constipation over an 18-week intervention across a neurologically diverse population.

Materials and Methods

This single-centre retrospective longitudinal study collected data on patients attending the West Midlands Rehabilitation Centre in Birmingham. Patients' data were included if they met the Rome IV criteria, had been diagnosed with any neurological condition, and were 18 years of age or older. Patients' data were excluded if they were not considered clinically constipated or had any FES contraindications. Adhesive, carbon surface electrodes were placed on participants' external obliques and rectus abdominus muscles. FES, set at 40 Hz, 330 μ pulse width, and 40–50 mA, was delivered via the Microstim 2 device, a portable, battery-powered stimulator unit (**Fig. 1**). The protocol for the first 6 weeks included 30 minutes of ABFES twice daily. No set time of day was given to administer the treatment each day. Following the 6 weeks, an ad-hoc approach was taken, allowing for dosage alterations at the participant's discretion. No control over medication or lifestyle changes was applied.

All outcome measures were taken at baseline, 6-week, and 18-week timepoints. The primary outcome measure was the PAC-QoL, a reliable and valid constipation-related QoL questionnaire, in which a decrease of $\geq$0.5 suggests a minimal clinically important difference (MCID) [9]. Secondary outcome measures included patient-reported changes in time spent on the toilet, urge to pass faeces, and laxative medication use. One-way repeated measure

ANOVAs and Bonferroni post-hoc tests were run to determine ABFES effects on each PAC-QoL domain. Significance levels were set at p>0.05. No statistical analysis was performed on any secondary outcome measures.

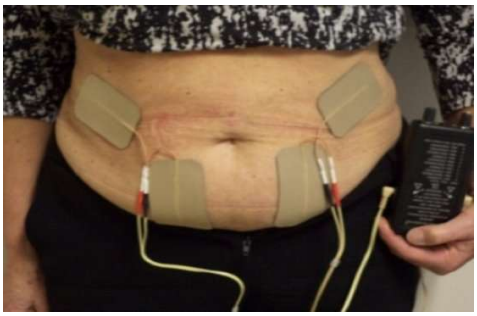

Figure 1: Electrode positioning over the transverse and rectus abdominal muscles using the Microstim 2 device to deliver the ABFES intervention.

Results

Table 1 illustrates the characteristics of the 51 patients included in the present study. Data is presented in means and standard deviations. In total, 43 MS patients were included, while 8 patients had other neurological conditions including SCI, Stiff Person Syndrome, Cerebral Palsy, Spastic Paraplegia, Charcot Marie-Tooth, Functional Neurological Disorder, and C3/4 Cervical Myelopathy.

Table 1: Patient characteristics of the whole cohort. Abbreviations. M: Male, F: Female, EDSS: Expanded Disability Status Scale

Characteristics	Combined Cohort
Age (years)	55.26 ± 10.18
Sex (M/F)	19/32
Years of Constipation	12.89 ± 14.75
EDSS	6.19 ± 1.04

A one-way repeated measures ANOVA demonstrated that ABFES results in significant improvements (P>0.01) across all domains of the PAC-QoL at 6 and 18-week timepoints (**Fig. 2**). This included a 43-62% mean decrease between baseline and 6-week scores and a 38-62% mean decrease between baseline and 18-week scores. However, no statistical difference was found between 6 and 18-week time points across all domains (P>0.05). The current study also found ABFES results in minimal clinically meaningful change across all domains. **Figure 3** demonstrates that between 54% and 88% achieved MCID between baseline and 6 weeks across each domain. The percentage of participants who achieved MCID between baseline and the 18-week timepoint remained similar (**Fig. 3**).

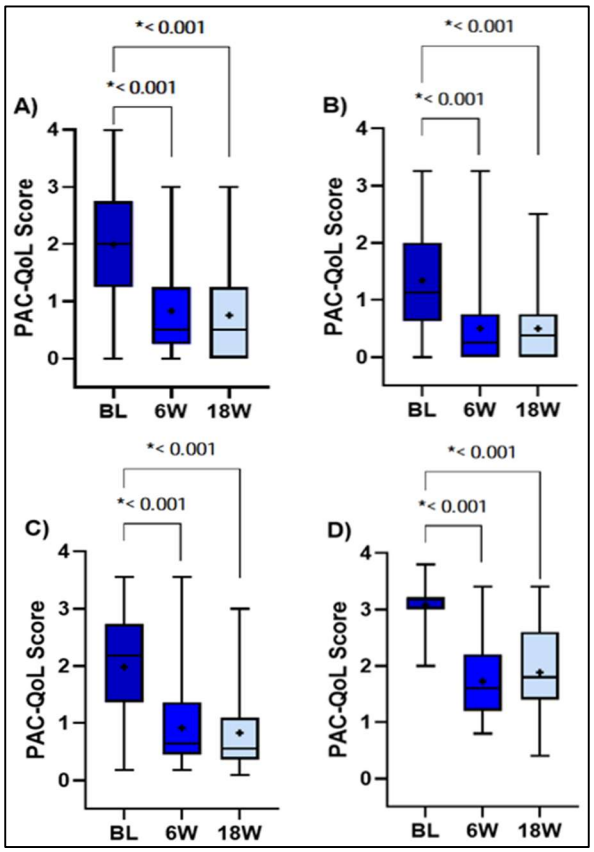

Figure 2: Box and whisker plots (median, interquartile range, and range) illustrating individual PAC-QoL domain scores across baseline (BL), 6-week (6W), and 18-week (18W) time points for all 51 patients. + indicates mean score. Physical Discomfort (A), Psychological Discomfort (B), Worries and Concerns (C), and Satisfaction (D). Satisfaction scores are reversed: a lower score indicates higher satisfaction.

To establish the broader impact ABFES has on other parameters, secondary outcome measures were collected. These parameters included recording patients' changes in urge to pass faeces, time spent on the toilet, and laxative medication alterations. **Figure 4** illustrates that 6 of 22 patients did not have the urge to defecate at baseline, but by the 6-week mark, all of them had the urge at least some of the time, which was also sustained at 18 weeks. **Figure 5** shows the time spent on the toilet by 28 patients. At baseline, 11 participants (~40%) spent <15 minutes on the toilet each sitting. By 6 weeks, this number had increased to 26 patients (~93%). No patient spent >30 minutes on the toilet at each sitting by 6 weeks. 38 patients reported their laxative medication use. **Figure 6** demonstrates the percentage change of patients either increasing, maintaining, or decreasing their daily laxative medication dose. Furthermore, 6 out of 27 patients (~22%) who

reported taking laxative medication at baseline had stopped taking them altogether by the 18-week timepoint.

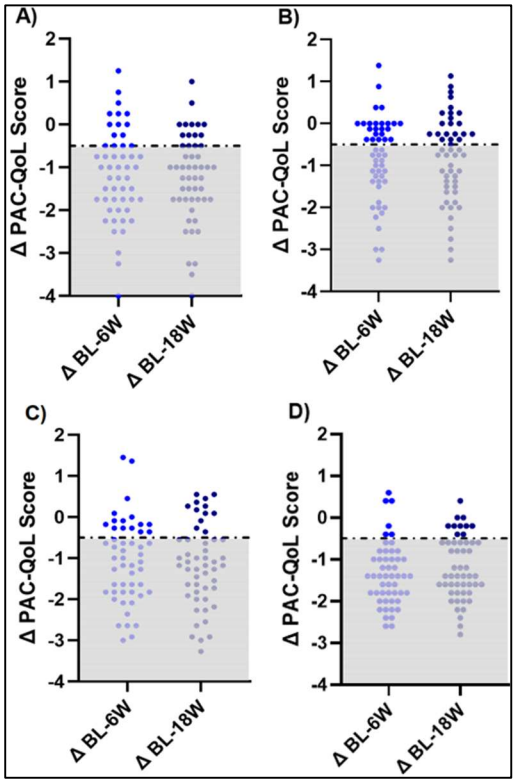

Figure 3: Scatter plots illustrating the number of patients who achieved MCID for each PAC-QoL domain. MCID for PACQoL set at ≥0.5 (defined as the gray shaded area). Data points represent the change (Δ) in individual patient scores comparing baseline (BL) vs. 6 weeks (6W) and BL vs. 18 weeks (18W) for each domain. Physical Discomfort (**A**), Psychological Discomfort (**B**), Worries and Concerns (**C**), and Satisfaction (**D**). Satisfaction scores are reversed: a decreased score indicates improved satisfaction.

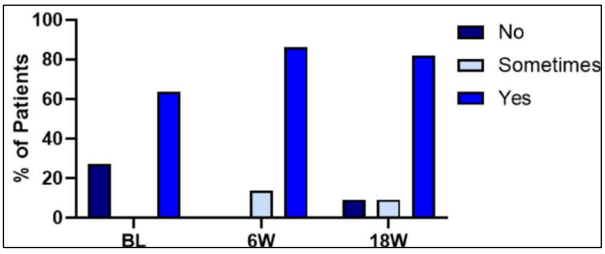

Figure 4: A bar chart showing the percentage of 22 patients' changes in urge at baseline (BL), 6 weeks (6W), and 18 weeks (18W) when using ABFES.

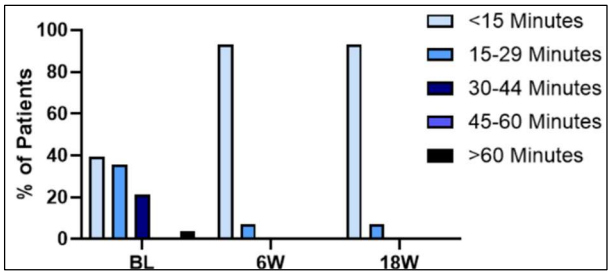

Figure 5: A bar chart showing the percentage of 28 patients' time spent on the toilet at baseline (BL), 6 weeks (6W), and 18 weeks (18W) when using ABFES.

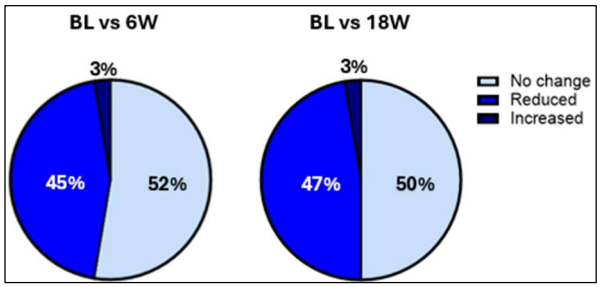

Figure 6: Pie charts showing the percentage of 38 patients' changes in laxative medication at baseline (BL) vs. 6 weeks (6W), and BL vs. 18 weeks (18W) when using ABFES.

Discussion

This single-centre, retrospective, longitudinal study is the first to demonstrate the significantly positive effects ABFES has on constipation-related QoL beyond a 6-week timeframe. Furthermore, the current study also provides evidence that the ABFES intervention can have positive outcomes in a wider number of neurological conditions.

Early ABFES studies, involving ~20 MS patients, reported an average median decrease of ~70% across all domains of the PAC-QoL [6], a result which aligns nicely with the current study, which found an average mean decrease of ~55% (**Fig. 2**). Despite significant changes observed across all domains of the PAC-QoL, the efficacy of using ABFES in a healthcare setting will be questioned if it cannot demonstrate a clinically meaningful change [10]. In the current study, analysis revealed that after a 6-week ABFES intervention, between 54 and 88% of patients achieved MCID for each domain of the PAC-QoL. Again, these results align nicely with Street and colleagues' findings, in which between 65% and 95% of their MS patients had achieved MCID [6]. However, what the present study also provides is evidence that these significant and MCID changes are sustained at 18-week timepoints when patients have continued with the ABFES intervention ad libitum. This may suggest that ABFES could be used to manage constipation longitudinally in individuals with neurological conditions. Previous reports have suggested that ABFES results in increased defecation frequency [6,8],

but the current study did not report findings on this. However, changes in the urge to pass faeces have been previously reported. Santos and colleagues suggested that 50% of their 10 SCI participants reported improvements in the urge to defecate [8]. The current study found that 6 out of 8 patients who did not have an urge at baseline reported having it at least some of the time by 6 weeks (**Fig. 4**). Furthermore, ~45% of patients reported reductions in laxative medication use (**Fig**. **6**). Considering the adverse side effects associated with laxative medications, combined with the ineffectiveness of current constipation management guidelines [4], may suggest why patient treatment satisfaction scores had a large percentage improvement (**Fig. 2**).

Despite the positive effects of ABFES on constipation-related outcomes, there remains no conclusive evidence of the underpinning mechanisms driving these changes. One hypothesis suggests that individuals with a central neurological condition are likely to have reduced motor unit recruitment, leading to weakened trunk muscles [11]. ABFES can elicit abdominal muscle contraction, which can increase intrabdominal pressure, aiding in straining and faeces expulsion. A second hypothesis postulates that neurological disease or injury can compromise the function of the enteric nervous system (ENS). Electrical stimulation may directly engage excitable cells of the myenteric musculature surrounding the intestinal organs, potentially increasing peristaltic action, reducing faecal transit time, and decreasing the risk of constipation [12]. If either hypothesis holds, it may indicate that an optimal time for patients to use ABFES would be within a couple of hours after food consumption or during attempts to open their bowels. Despite these theories explaining why bowel function improves when using ABFES regularly, they fail to explain why improvements in bladder and sexual function have previously been reported [6, 13] or why some patients can stop using ABFES and still maintain their bowel improvements. Therefore, the changes are more likely driven by improved neuronal function rather than direct stimulation causing myogenic contraction. In theory, ABFES would increase the electrical stimulus received by the ENS, which could promote neuroplastic changes within its intrinsic structures and synapses [12].

Study limitations and future direction. Given the current study's retrospective design, no sham ABFES group was included, and patients' lifestyle and medication changes were not controlled for. Therefore, it is hard to determine whether ABFES was the primary driver of the improvements observed in this study's outcome measures. To make the evidence more definitive and robust, future research may want to analyse an ABFES intervention in a more controlled setting. This might include using a placebo or sham stimulation experimental group while controlling for parameters such as lifestyle and medication factors.

Conclusion: ABFES appears to be a safe, non-invasive technique to treat and manage constipation across an array of neurological conditions, as evidenced in this retrospective analysis. To provide more robust efficacy data, a randomised controlled trial including a shame intervention group is needed with patients who have chronic constipation and neurological conditions.

References

[1] Mackenzie I, et al. Incidence and prevalence of multiple sclerosis in the UK 1990–2010: a descriptive study in the General Practice Research Database. J Neurol Neurosurg Psychiatry 2014; 85(1): 76-84.

[2] Glickman S, Kamm MA. Bowel dysfunction in spinal-cord-injury patients. Lancet 1996; 347(9016): 1651-1653.

[3] Serra J, et al. Clinical practice guidelines for the management of constipation in adults. Part 2: Diagnosis and treatment. Gastroenterol Hepatol 2017; 40(4): 303-316.

[4] Coggrave M, et al. Management of faecal incontinence and constipation in adults with central neurological diseases. Cochrane Database Syst Rev 2014; (1): CD002115.

[5] Singleton C, et al. The Efficacy of Functional Electrical Stimulation of the Abdominal Muscles in the Treatment of Chronic Constipation in Patients with Multiple Sclerosis: A Pilot Study. Mult Scler Int 2016; (1): 33-36.

[6] Street T, et al. Abdominal functional electrical stimulation for bowel management in multiple sclerosis. Neurodegener Dis Manag 2019; 9(2): 83-89.

[7] Lin SD, et al. The effect of abdominal functional electrical stimulation on bowel function in multiple sclerosis: a cohort study. Mult Scler J Exp Transl Clin 2020; (3): 2055217320941530.

[8] Santos LT, et al. Effect of transcutaneous abdominal electrical stimulation in people with constipation due to spinal cord injuries: a pilot study. Rev Esc Enferm USP. 2022; 56: e20210449.

[9] Marquis P, et al. Development and validation of the Patient Assessment of Constipation Quality of Life questionnaire. Scand J Gastroenterol 2005; 40(5): 540-551.

[10] Page P. Beyond statistical significance: clinical interpretation of rehabilitation research literature. Int J Sports Phys Ther 2014; 9(5): 726.

[11] Enoka RM, et al. Electrical stimulation of muscle: electrophysiology and rehabilitation. Physiol 2019; 35(1): 40-56.

[12] Moore JS, et al. Neuromodulation via interferential electrical stimulation as a novel therapy in gastrointestinal motility disorders. J Neurogastroenterol Motil 2018; 24(1): 19.

[13]Parittotokkaporn S, et al. Non-invasive neuromodulation for bowel, bladder, and sexual restoration following spinal cord injury: a systematic review. Clin Neurol Neurosurg 2020; 194: 105822

Stimulation of Neurovascular Bundles during Robot-Assisted Radical Prostatectomy

Rozman J[1,2], Bizjak J[3], Hawlina S[2,3]

[1]Center for Implantable Technology and Sensors, ITIS d. o. o. Ljubljana, Republic of Slovenia
[2]Faculty of Medicine, University of Ljubljana, Republic of Slovenia
[3]Department of Urology, University Medical Centre Ljubljana, Republic of Slovenia

Abstract: *The primary objective of this study was to develop a system for neurovascular bundle (NVB) stimulation during robot-assisted radical prostatectomy (RARP) and to assess its potential to estimate the recovery rate of erectile function (EF) after RARP. One specific objective was to evaluate the effects of NVB stimulation on the induction of penile erection using two different stimulating pulse protocols in a group of five men with prostate cancer who underwent RARP. In this context, the paper presents a paradigm for assessing erection-related parameters, wherein both stimulation and assessment were conducted on a single NVB at three different sites using different stimulating pulses applied via a custom-developed stimulating probe. One specific aim was to determine which stimulation pattern might be more effective for selective NVB stimulation. To assess the clinical feasibility of the paradigm, a multi-sensorial probe was developed to measure the penile axial rigidity, glans penis temperature, and galvanic skin response (GSR). In addition to these parameters, spontaneous corpus cavernosum electromyography (CC-EMG), CC-EMG triggered by two NVB stimulation protocols and toe photoplethysmography (TPCG) were assessed during RARP under total intravenous anaesthesia. Preliminary results provide evidence that the stimulating probe can effectively deliver electrical stimuli to neural tissue when applied to the NVB during RARP. In two of the five enrolled patients, NVB stimulation elicited measurable CC-EMG waveforms. However, in none of the patients was a measurable increase in penile axial rigidity observed in response to NVB stimulation*

Keywords: *robot-assisted radical prostatectomy, neurovascular bundles, electrical stimulation, physiological measurements, corpus cavernosum electromyography*

Introduction

Radical prostatectomy (RP) is currently considered the standard treatment for localized prostate cancer, with relatively favourable long-term oncological outcomes. However, following radical prostatectomy, the majority of men lose the ability to achieve an erection. Erectile dysfunction (ED) is a side effect of prostate surgery and significantly impacts the quality of life in a substantial portion of men following RP. The nerve-sparing technique used during RP plays a critical role in both oncological and functional outcomes. Guidelines on ED rehabilitation after RP remain non-uniform and inconsistent [1]. Accordingly, the preservation of potency after RP is considered as important as cancer control itself from a surgical standpoint [2]. The main reason for ED is injury to the NVBs during radical prostatectomy [3]. NVBs are tubular structures composed of interwoven autonomic fibres that innervate the corpus cavernosum and blood vessels within the connective tissue. They run posterolaterally between the lateral pelvic fascia and prostatic fascia along the surface of each side of the prostate and give off branches to the prostate at the apex and base [4]. To optimize these outcomes, various nerve sparing techniques have been developed [5]. However, an optimal nervesparing strategy involves more than merely preserving the anatomical integrity of the NVBs. In this regard, analyses conducted in large centres have suggested that post-prostatectomy potency rates have not significantly improved in the past two decades, despite the adoption of robotic surgical technology. The precise location and course of the NVBs during RP, when identified using appropriate nerve-tracing techniques, may facilitate their preservation. One important technique of nerve tracing involves the use of electrical nerve stimulators to elicit an erection that can be evaluated either indirectly via physiological measurements or directly through corpus cavernosum electromyography (CC-EMG). CC-EMG is a non-invasive method for measuring the electrical activity of the smooth muscle of the corpus cavernosum in the penis, which is a prerequisite for erection. To utilize CC-EMG recording, monopolar needle electrodes and/or non-invasive surface electrodes placed on the penis can be used [6].

The primary goal of the study was therefore to improve nerve-sparing control during RARP with the aim of increasing the preservation rate of sexual potency following surgery and minimising urinary incontinence.

Material and Methods

The study was approved by the National Medical Ethics Committee, Ministry of Health, Republic of Slovenia (Unique Identifier No. 0120-138/2024-2711-6). Five subjects with a mean age of 57 years, all scheduled for RARP, were enrolled in the study. All participants were confirmed to have clinically localized prostate cancer (stage T1 or T2). After being informed about the purpose and procedures of the study, they provided written informed consent.

Stimulating electrodes were designed based on published findings of studies modelling the selective stimulation of

peripheral nerves [7], realistic structural topography of the NVBs [8], and the model developed by the authors. For the encapsulation of the electrodes, a self-curing denture material (ProBase Cold Professional PMMA denture base material, Ivoclar, Schaan, Liechtenstein) was used.
For sterilisation of the stimulating probe, low-temperature hydrogen peroxide gas plasma sterilization was selected.

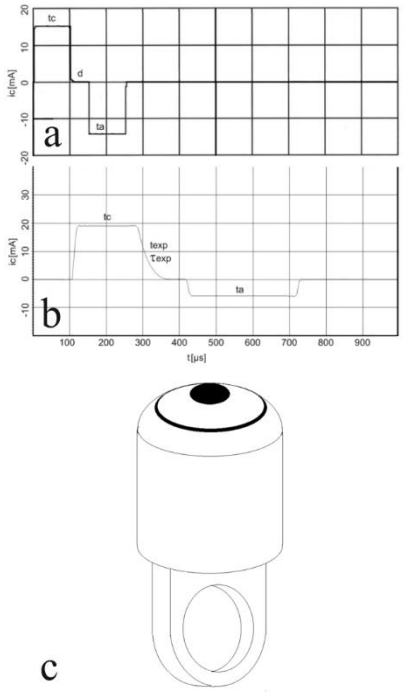

Figure 1: (a) Waveform of the rectangular stimulating pulse, (b) waveform of quasi-trapezoidal stimulating pulse, (c) schematic diagram showing the arrangement and shape of the stimulating electrodes

The stimulating probe (Fig. 1c) was introduced into the operating field through the lateral right port. NVB stimulation was delivered via stimulating electrodes through lead wires placed within the port and connected to the custom-designed nerve stimulator.

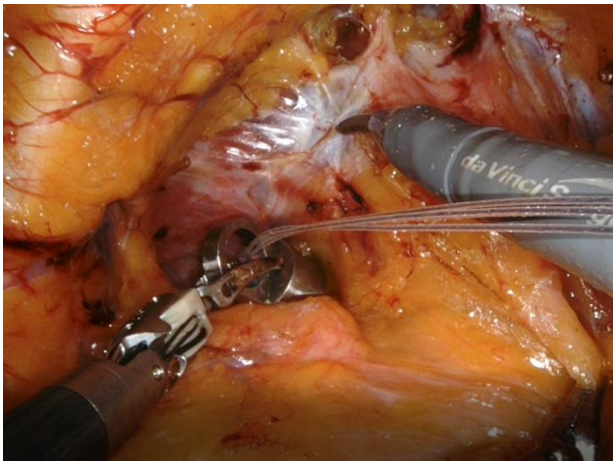

Figure 2: Stimulating probe placed on the left NVB prior to RARP.

NVB stimulation was applied prior to (Fig. 2) and after RARP using a stimulating probe placed at the top, middle, and base of the NVB once on the left side and once on the right. NVB stimulation was administered for 30 seconds once using either rectangular or quasi-trapezoidal waveforms and biphasic pulse pairs. The intensity of cathodic phase (i_c) ranged from 10 to 30 mA, and the pulse width of the cathodic phase (t_c) was 160 μs (Fig. 1a, b). If no increase in axial rigidity was observed, the assessment was considered unsuccessful and was terminated. However, in the case of erection, a multi-sensorial probe would be placed onto the glans penis and pressed to measure axial rigidity, galvanic skin response (GSR), and glans penis temperature.
We developed a multi-sensorial probe that combined both commercial and custom-built sensors capable of monitoring and evaluating penile erectile responses. It consisted of a sensor for axial rigidity, an infrared (IR) sensor for glans penis skin temperature, and GSR recording electrodes (Fig. 3).

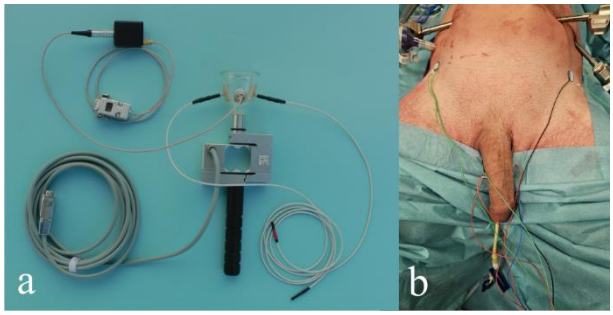

Figure 3: (a) Multi-sensorial probe, infrared (IR) thermometer for glans penis skin temperature, non-contact IR chip sensor, electrodes for sensing GSR within a bell-shaped probe, and a force transducer, (b) Arrangement of CC-EMG electrodes

To study activity within the penile shaft, dual-channel CC-EMG measurements were performed using a high performance general-purpose amplifier (ETH-256 2-Channel Bridge/ECG/EMG/EEG/Bio-Amplifier, iWorx/CB Sciences, Dover, U. S. A.) and a 3-lead isolated biopotential recording preamplifier (C-ISO-256, iWorx/CB Sciences, Dover, U. S. A.). CC-EMG was recorded using a combination of surface and intracavernous subdermal needle electrodes so CC-EMG, with signals measured between the base and the tip region of the penis [9].
To monitor glans penis skin activity potentially influenced by NVB stimulation, a GSR device (GSR BI GSR BIOFEEDBACK, Prasad Psycho Private Limited, Gautam Budh Nagar, India) (Biofeedback), was used.
To capture TPCG, a pulse oximeter (Nellcor N-600, Tyco Healthcare Group LP, Nellcor Puritan Bennett Division, Pleasanton, CA, U.S.A.) and a custom-crafted sensor were employed. Recordings of TPCG were intended to highlight potential erectile events during specific periods of cardiac activity.
All signals were conditioned and recorded at 5 kHz with 24-bit resolution using a USB 2.0 interface I/O data acquisition system(DEWE-43A, DEWESOFT d. o. o., Republic of Slovenia). The data were subsequently stored on a hard drive for offline analysis using DEWESoft 7.0.2 software.

Results

Figure 4 shows the results obtained from one of the five enrolled patients. The figure presents CC-EMGr, CC-EMGl, and TPCG signals recorded during at different sites of the left (L) and right (R) NVBs . The label "U" denotes the upper part of the NVB, while "L" denotes the lower part.

Specifically, Figure 4a shows the results recorded during stimulation of the upper part of the left NVB prior to RARP (1UL): the top trace shows the stimulating current (i_c), the first trace below displays CC-EMGr, the second CC-EMGl and the bottom trace represents TPCG. Figure 4b presents results recorded during stimulation of the upper part of the left NVB after RARP (2UL): the top trace represents the stimulating current (i_c), followed by CC-EMGr, CC-EMGl, and TPCG, in descending order

Figure 4c displays results from stimulation of the lower part of the left NVB after RARP (2LL): the top trace shows the stimulating current (i_c), followed by CC-EMGr, CC-EMGl, and at the bottom, TPCG.Figure 4d presents results recorded during stimulation of the upper part of the right NVB prior to RARP (1UR): the top trace shows the stimulating current (i_c), the first trace below displays CC-EMGr, the second trace CC-EMGl and the bottom trace represents TPCG. Figure 4e shows results recorded during stimulation of the upper part of the right NVB after RARP (2UR): the top trace shows the results recorded during the stimulating current (i_c), followed by CC-EMGr, CC-EMGl, and TPCG in descending order. Finally, Figure 4f presents results recorded during stimulation of the lower part of the right NVB after RARP (2LR): the top trace shows the stimulating current (i_c), the first trace below displays CC-EMGr, the second trace CC-EMGl, and the bottom trace represents TPCG.

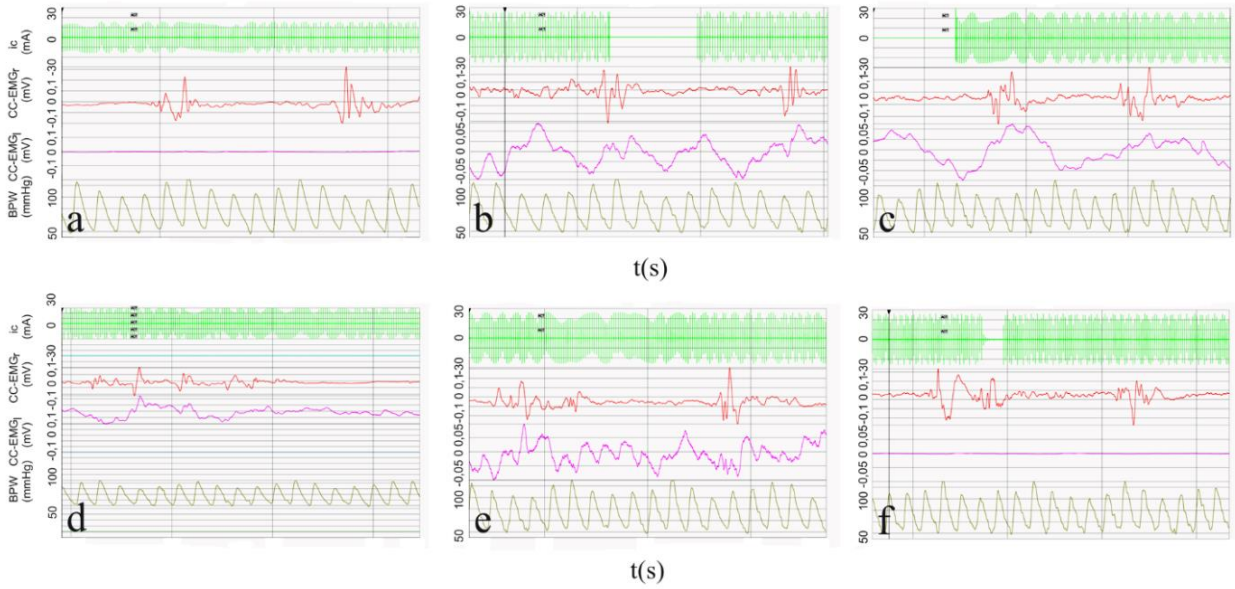

Figure 4: CC-EMGr and CC-EMGl signals recorded during stimulation at different sites of the left and right NVBs. The label l refers to the left CC-EMG, and r refers to the right CC-EMG. Panels (a) to (f) show the following signal traces: the top trace represents the stimulating current (ic), the first trace below shows CC-EMGr, the second shows CC-EMGl, and the bottom trace shows TPCG. Stimulated NVB sites are: a) 1UL, b) 2UL, c) 2LL, d) 1UR, e) 2UR and f) 2LR.
The label L denotes the left NVB and R the right NVB of the patient. The label U refers to the upper part of the NVB, while L (in this context) refers to the lower part of the NVB

Discussion

This paper describes the design, development, and feasibility testing of a system intended for NVB stimulation during RARP to induce erectile responses and help determine whether the NVBs have been preserved during nerve-sparing RARP. The multi-sensorial probe was developed to explore the utility of NVB stimulation for the preservation of NVBs during nerve-sparing procedures [8]. Specifically, to assess which stimulating conditions were most likely to contribute to an erection during NVB stimulation, the multi-sensorial probe sensing - capable of sensing axial rigidity (ARIG), GSR, and glans penis temperature - could be used. The probe could be deployed simply by axially placing it onto the penis while NVBs were being stimulated. The results of the study showed that NVB stimulation did not result in measurable erections, and the multi-sensorial probe failed to provide any quantitative data. Possible reasons for the lack of erectile responses may include the limited time allocated

for NVB stimulation and measurement during the standard surgical procedures, and the small surface area of the stimulating cathode, which may not have been able to establish effective electrical contact with a sufficient number of NVB neural fibres.
It was observed that the peak-to-peak amplitudes of CC-EMGr and CC-EMGl varied depending on the site of the NVB exposed to NVB stimulation [9]. The CC-EMG recordings exhibited a gently sloping waveform, presumably due to sharp filtering within a frequency band between 0.05 and 5 Hz.

Conclusions

This report provides evidence that the stimulating probe can effectively activate nerve fibres within the NVB under the delivered stimuli during RARP. Notably, concomitant CC-EMG measurements in two patients clearly demonstrated the occurrence of CC-EMG activity in both CCs even after nerve-sparing procedures. However, none of the patients demonstrated a measurable increase in penile axial rigidity in response to NVB stimulation. In order to elicit ARIG during RARP, further improvement in the NVB and a prolonged stimulation period are anticipated. It may be concluded that the proposed technique could assist surgeons in more accurately predicting erectile function recovery following RARP. We know that the number of patients is limited, which reflects the complexity and relatively infrequent nature of the procedure. However, our primary aim was to assess the feasibility and safety of the technique. In this regard, the results are encouraging, as the procedure was successfully completed in all cases without major complications. While larger studies are needed to confirm the findings, we believe our data provide important preliminary evidence supporting the clinical applicability of this approach.

Acknowledgement

This work was financed by research grant P3-0171 from the Slovenian Research and Innovation Agency (ARIS), Ministry of Education, Science and Sport, Ljubljana, Republic of Slovenia.

References

[1] Tal, R., Teloken, P., Mulhall, J. P.: Erectile function rehabilitation after radical prostatectomy: Practice patterns among AUA members, J. Sex. Med., vol. 8(8), pp. 2370-2376, June 2011

[2] Kyriazis, I., Spinos, T. et al.: Different Nerve-Sparing Techniques during Radical Prostatectomy and Their Impact on Functional Outcomes, Cancers (Basel), vol. 14(7), pp. 1601, March 2022

[3] UFHealth: Robotic Nerve-Sparing Radical Prostatectomy, https://urology.ufl.edu/patient-care/robotic-laparoscopic-urologic-surgery/procedures/robotic-nerve-sparing-radical-prostatectomy/

[4] Villeirs, G. M., Verstraete, K. L. et al.: Magnetic Resonance Imaging Anatomy of the Prostate and Periprostatic Area: A Guide for Radiotherapists, Radiother, Oncol., vol. 76(1), pp. 99-106, July 2005

[5] Tzelves, L., Protogerou, V., Varkarakis, I.: Denonvilliers' Fascia: The Prostate Border to the Outside World, Cancers (Basel), vol. 14(3), pp. 688, January 2022

[6] Ponseti, J., Bosinski H.A.: Brain potentials related to corpus cavernosum electromyography, Int. J. Impot Res., vol. 22(3), pp. 171–178, May-June 2010

[7] Goodall, E. V., Kosterman, L. M. et al.: Modeling study of activation and propagation delays during stimulation of peripheral nerve fibers with a tripolar cuff electrode. IEEE Trans. Rehab. Eng., vol. 3(3), pp. 272-282, January 1995

[8] A. Takenaka, H. Soga et al.: Classification of the distribution of cavernous nerve fibers around the prostate by intraoperative electrical stimulation during laparoscopic radical prostatectomy, Int. J. Impot. Res., 23(2), pp. 56-61, March-April 2011

[9] Song, W. H., Park, J. H. et al.: Establishment of novel intraoperative monitoring and mapping method for the cavernous nerve during robot-assisted radical prostatectomy: results of the phase I/II, first-in-human, feasibility study, Eur. Urol., 78(2), 221-228, August 2020

Author's Address

Janez Rozman
Center for Implantable Technology and Sensors, ITIS d. o. o. Ljubljana, Lepi pot 11, 1000 Ljubljana, Republic of Slovenia
jnzrzmn6@gmail.com

Session 2:
Afferent Nerve Stimulation

Treatment of Chronic Neuropathic Pain with Peripheral Nerve Stimulation

Girsch W, Geissler J, Girsch M, Smolle C, Weigel G
Institute, Department of Plastic, Aesthetic and Reconstructive Surgery, Medical University Graz

Abstract:

Introduction:
Central nerve stimulation (CNS) already has proved its efficacy for treatment of chronic severe pain. The aim of our clinical study was to prove the effectiveness of Peripheral Nerve Stimulation (PNS)with implanted systems for treatment of chronic neuropathic pain syndrome (CRPS2) of the extremities.

Material and Methods:
We selected two patient cohorts, 31 patients in a retrospective and 10 patients in a prospective setup. According to the inclusion criterias all patients suffered from CRPS2, each patient had a history of microsurgical interventions to the nerves and every conservative treatment which was possible, but without any effect on the problem of neuropathic pain. None of the patients was able to use the extremity functionally. In all patients the VAS was in mean >7, even at rest. Stimulation leads were implanted close to the peripheral nerves (fascicles of the brachial plexus or sciatic or femoral nerve) and connected with percutaneous leads for temporary testing. Pain reduction of more than 4 points on the VAS scale gave indication for implantation of a pulse generator for permanent PNS.

Results:
A total number of 41 patients had implanted elevtrodes and underwent testing. 38 out of these 41 patients were supported with the whole system. PNS was effective to reduce pain from VAS mean >7 to VAS mean 3 and to regain functional use of the extremity in most of the cases in both cohorts. In the every first patients technical complications, mostly electrode dislocation had to be noted. Later, no complications were observed due to modifications of the electrode implantation. Relief from pain occurred immediately after onset of stimulation. The positive effect was directly correlated with PNS, and stable over years. On a scale from -5 to +5 patients rated + > 4. in answering the question if they would undergo the procedure again.

Discussion:
PNS reduced pain deriving from peripheral nerves reliable and effective. PNS produced a stable, nearby pain free interval over many years (min 2 years, max >20 years) in all patients. Positioning of the electrodes direct to the fascicles of the brachial plexus and close to the sciatic nerve at mid-thigh allowed movement of shoulder and hip at a nearby normal ROM. PNS seems to represent an important technology for treatment of chronic neuropathic pain in selected cases.

Keywords: *Chronic Pain, Peripheral Nerve Stimulation, Patient study*

Author's Address

Werner Girsch
Medical University Graz
Department of Plastic, Aesthetic and Reconstructive Surgery
werner.girsch@kabsi.at

Clinical advances in full body neuromodulation to treat spastic motor disorder and chronic pain: A Systematic literature review

Mileusnic M, Hahn A

Ottobock Healthcare Products GmbH, Vienna, Austria

Abstract: *A full body garment as concomitant treatment for spasticity and chronic pain was presented in 2012. Early research and anecdotal clinical practice showed potential and promising case results. However, overall clinical evidence remained exploratory and heterogeneous. Recently more focused studies have become available on a more matured technical basis. A systematic literature review was conducted to assess the most recent literature. The studies show consistent effects on pain and impact reduction in fibromyalgia. Also, focus on spastic movement disorder and the description of benefits in terms of functional assessments help to better assess the clinical impact.*

Keywords: *neuromodulation, full body garment, fibromyalgia, spastic motor disorder, Exopulse*

Introduction

The full body neuromodulation garment Exopulse Mollii Suit was first presented by Fredrik Lundqvist in 2012.
The suit includes 58 embedded electrodes in its version 9.3. A control unit attached to the suit via a belt and connected via magnetic pads provides the stimulation pulses and allows the application of preprogrammed stimulation pattern. Relaxation of spastic muscles and spastic motor disfunction is addressed via targeted stimulation of the spastic antagonist. The underlying mechanisms utilize reciprocal inhibition and post-activation depression. Pain reduction is applied by additional full body stimulation.

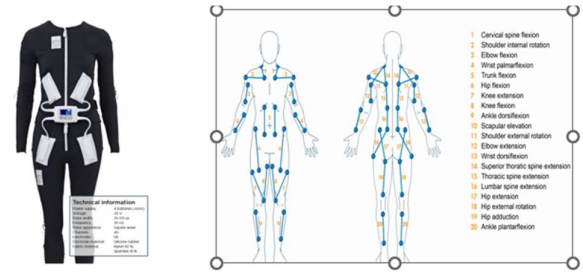

Figure 1: Exopulse Mollii Suit and electrode schematics

Early clinical research was performed with earlier versions of the suit and included a large variety of outcomes, mixed cohorts (e.g. the evaluation of walkers and non-walkers in the same study). Since the early prototypes, the suit undergoes continuous improvement and industrialization. The documentation of the clinical application increased significantly and so did the quality of clinical evidence. We give an update on the current state of evidence.

Material and Methods

We conducted a systematic literature review on major literature databases including Cochrane, Embase, Pubmed and Google scholar. Search terms included “exopulse AND spasticity”, “exopulse AND spastic syndrome”, “exopulse AND spastic motor disorder”, “exopulse AND chronic pain”, “exopulse AND fibromyalgia”. The search period was from 01/01/2023 until 28/02/2025 and only articles in English language were included. Excluded were technical reports, articles involving different patient populations, general overview articles not containing clinical data. The authors received in addition non-systematically information on upcoming literature. The review was not registered (e.g. PROSPERO).
Relevant articles were extracted, analysed and summarized. We present the latest studies published since 2023. While initial research was heterogenous, the overall potential of this therapy to improve motor functions of neurological patients in clinical practice could be extracted from a systematic review of the literature prior to 2023 [1] which is also included in this review.

Results

Fígure 2 summarizes the literature search which identified 9 relevant articles. One of those articles is the systematic review addressing the literature prior to 2023 which included 12 published studies having different patient populations (cerebral palsy, stroke, fibromyalgia) and designs: 9 studies with before-and-after-design,
2 studies with inactive/placebo stimulation as control,
1 study with parallel control group with conventional therapy [1].

Fibromyalgia:
From twelve studies used in the systematic literature of studies prior to 2023, two involved patients suffering from fibromyalgia and report of significant reduction in pain [1].
Since the systematic review of older literature in 2023, six additional papers have been published.
Riachi et al. [2] published a short term uncontrolled longitudinal observation on 50 female subjects. They reported a 62% decrease in the VAS pain score immediately after one 60 min session of stimulation and 25% decrease in the VAS pain score 24 hours after the stimulation ($p<0.001$).
Mattar et al. [3] published the results of a randomized sham-controlled crossover trial with 14 days intervention period, followed by a four-week longitudinal open label observation (Figure 3). They report on 14% decrease in

VAS pain after 2 weeks and 25% after four weeks of daily stimulation. Furthermore, they report on 18% reduction in total Fibromyalgia Impact Questionnaire (FIQ) after 2 and 25% after four weeks of stimulation as well as significant and clinically improvements in Quality of Life (SF-36) and Global Clinical Impression.

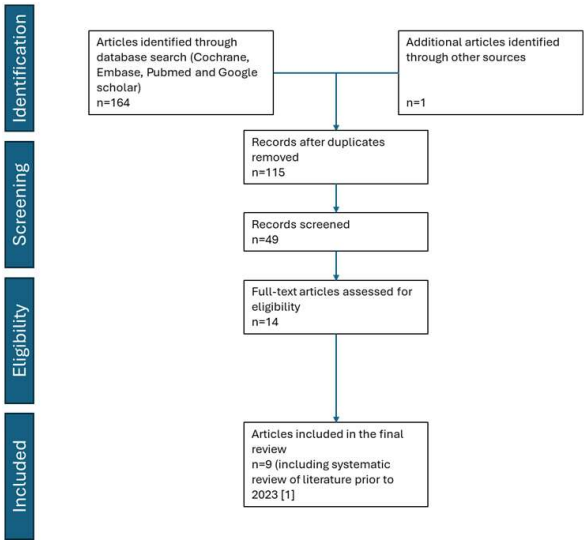

Figure 2. Literature search and selection.

Rubio-Zarapus et al. report their results in a series of four papers. Rubio-Zarapus et al 2023 [4] refers to a single case report showing functional improvement in a FM subject with respect to one-legged balance. 2024 a [5] and 2024 b [6] refer to a randomized controlled crossover trial with 10 female subjects and comparison to High Intensity Interval Training (HIIT) with Exopulse Mollii suit. Both groups improve significantly, and results are comparable. Findings on Heart Rate Variability are interpreted as hints towards the involvement of the autonomic nervous system (ANS). An RCT with 89 female subjects [7] suggests a superiority of Exopulse Mollii Suit when combined with VR technology (2024c).

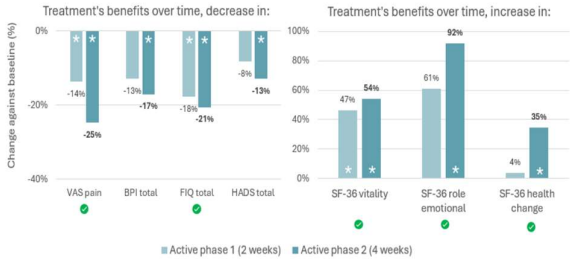

Figure 3: Results of Mattar et al., * indicating $p<0.05$ and the green checkmark relating effects better than the minimally important clinical difference (MCID).

Spasticity

From twelve studies used in the systematic literature of studies prior to 2023, ten involved patients having spasticity [1]. They report of reduction in spasticity and pain, as well as increase in mobility, activity, range of motion and function in patients with cerebral palsy and stroke. Since systematic review of older literature, two studies were published providing insights with respect to spasticity.

Hahn et al. [8] report on improvements in functional outcomes related to the treatment of spasticity induced motor disorder. Real-world trial fitting data was analyzed from 72 subjects with cerebral palsy, (CP) multiple sclerosis (MS) and stroke. Increase of the Berg Balance Scale score suggests significant reduction in fall risk in many patients. Further improvements include reduction of spasticity-related pain, increase in quality of life, etc.

All cohort (n=72)	CP		MS		Stroke	
Outcome	ΔT0–T2	Cohen's d	ΔT0–T2	Cohen's d	ΔT0–T2	Cohen's d
BBS	5.92*** (n=25)	1.161	8.24*** (n=21)	1.377	5.6*** (n=20)	1.184
TUG	−3.2*** (n=27)	0.369	−5.93*** (n=21)	0.67	−8.55** (n=20)	0.572
FGA	4.86*** (n=22)	1.543	6.25*** (n=12)	1.349	3.86** (n=14)	0.783
10mWT	0.11* (n=26)	0.562	0.166*** (n=18)	0.991	0.16** (n=19)	0.721
WMFT	5.72*** (n=18)	0.795	4.6* (n=10)	0.647	7.19* (n=16)	0.727
EQ 5D 5L	0.11** (n=27)	0.538	0.08 (t) (n=21)	0.337	0.13* (n=17)	0.776

Table 1: Changes in functional outcomes after four-week stimulation. BBS: Berg Balance Scale, TUG: Timed up and go, FGA: Functional Gait Assessment, 10mWT: 10-meter walk test, WMFT: Wolf Motor Function Test, EQ 5D 5L: Euroquol questionnaire, *:$p<0.05$, **:$p<0.01$, ***:$p<0.001$.

Perpetuini et al. [9] report on 28 children with CP (gross motor functional classification score (GMFCS) ranging from I to V) experiencing significant increase in trunk control and good initial acceptance of the suit. They emphasize these assessments being insights in an initial stage investigation.

Mattar et al. [10] have reported the finalisation of the first randomized sham-controlled crossover trial with multiple sclerosis. The results will be available at the conference and included in the analysis.

Discussion

Research regarding the effects of full body neuromodulation increased in quantity and quality. Studies focussing on more heterogeneous populations give insight into potential therapeutic benefits. Targeted sham controlled randomized trials seem to confirm these findings.

Conclusions

Evidence of full body neuromodulation as effective concomitant therapy to address symptoms related to fibromyalgia and spastic motor disorder is increasing. The reviewed literature suggests that Exopulse Mollii Suit appears promising in the context of debilitating and difficult-to-manage diseases such as fibromyalgia. Furthermore, the studies show that stimulation resulted in the increase of ambulation-related skills in subjects with upper motor neuron syndrome stemming from infantile cerebral palsy, multiple sclerosis and stroke.

References

[1] Perpetuini D et al. (2023): Use and Effectiveness of Electrosuit in Neurological Disorders: A Systematic Review with Clinical Implications. *Bioengineering* 10 (6) DOI: 10.3390 / bioengineering 10060680.

[2] Riachi N et al. (2023): Effects of the TENS device, Exopulse Mollii Suit, on pain related to fibromyalgia: An open-label study. *Neurophysiologie clinique* 53 (4), S. 102863. DOI: 10.1016/j.neucli.2023.102863.
[3] Mattar J et al. (2024): The effect of the EXOPULSE Mollii Suit on pain and fibromyalgia-related symptoms-A randomized sham-controlled crossover trial. *European journal of pain*. DOI: 10.1002/ejp.4729.
[4] Rubio-Zarapuz A et al. (2023): Acute Effects of a Session with The EXOPULSE Mollii Suit in a Fibromyalgia Patient: A Case Report. *International journal of environmental research and public health* 20 (3). DOI: 10.3390/ijerph20032209.
[5] Rubio-Zarapuz A et al. (2024): Comparative Efficacy of Neuromodulation and Structured Exercise Program on Autonomic Modulation in Fibromyalgia Patients: Pilot Study. *JCM* 13 (15), S. 4288. DOI: 10.3390/jcm13154288.
[6] Rubio-Zarapuz A et al. (2024): Comparative efficacy of neuromodulation and structured exercise program on pain and muscle oxygenation in fibromyalgia patients: a randomized crossover study. *Front. Physiol.* 15, Artikel 1414100. DOI: 10.3389/fphys.2024.1414100.
[7] Rubio-Zarapuz A et al.; (2024): Comparative Analysis of Psychophysiological Responses in Fibromyalgia Patients: Evaluating Neuromodulation Alone, Neuromodulation Combined with Virtual Reality, and Exercise Interventions. In: *Medicina (Kaunas, Lithuania)* 60 (3).
[8] Hahn, A et al. (2023): Effects of a full-body electrostimulation garment application in a cohort of subjects with cerebral palsy, multiple sclerosis, and stroke on upper motor neuron syndrome symptoms. *Biomedical Engineering / Biomedizinische Technik* 0 (0). DOI: 10.1515/bmt-2023-0271.
[9] Perpetuini, et al. (2023): Assessing the Impact of Electrosuit Therapy on Cerebral Palsy: A Study on the Users' Satisfaction and Potential Efficacy. *Brain sciences* 13 (10). DOI: 10.3390/brainsci13101491.
[10] Mattar et al. (2025): The Effects of EXOPULSE Mollii Suit on Motor Functions in Patients With Multiple Sclerosis (EXOSEP Study): A Randomized Sham-Controlled Crossover Study, presented at ISPO 2025, Stockholm

Conflict of Interest

Both authors are full-time employees of the Ottobock Health Care Products GmbH who acquired ExoNeural Network (ENN) - the manufacturer of Exopulse Mollii Suit.

Author's Address

Name: Milana Mileusnic, PhD
Affiliation: Ottobock Healthcare Products GmbH
e-Mail: milana.mileusnic@ottobock.com

Functional Impact of the Exopulse Mollii Suit in SPG4 Hereditary Spastic Paraplegia: A Single-Subject AB Case Study

Grenfell R.[1]
[1]NeuroRehab Allied Health Network, Melbourne, Australia

Abstract: *This AB case study investigates the effects of the Exopulse Mollii Suit (EMS) in a 25-year-old male with SPG4 Hereditary Spastic Paraplegia (HSP). The intervention aimed to reduce lower limb spasticity and improve functional mobility over a 5-week trial. Assessments included the TUGT, 10MWT, 6MWT, SCATS, Modified Tardieu, and TCMS, conducted at baseline, midpoint, endpoint, and two weeks post-trial. Significant improvements were observed across all functional and spasticity-related outcomes during the intervention phase, with minimal overlap and high visual and statistical effect sizes. These findings support the integration of EMS into home-based management for individuals with HSP.*

Keywords: *Hereditary Spastic Paraplegia, Exopulse Mollii Suit, AB design, spasticity management, single-case study*

Introduction

SPG4 Hereditary Spastic Paraplegia (HSP) is a progressive neurodegenerative disorder that impairs gait, balance, and trunk control due to bilateral corticospinal tract degeneration. Existing treatments offer limited efficacy in managing chronic spasticity and maintaining function. The Exopulse Mollii Suit (EMS), delivering low-frequency transcutaneous electrical stimulation, aims to reduce spasticity through reciprocal inhibition. This study evaluates its impact on function and tone in an adult with SPG4.

Materials and Methods

Participant: A 25-year-old male with SPG4-HSP, primarily a manual wheelchair user, limited indoor ambulation using AFOs and a posterior walker with reported pain, high degrees of effort and fatigue with standing and walking activities.
No AFOs were used during testing.
Design: An AB single-subject design:
- Phase A: Baseline assessments over 2.5 weeks
- Phase B: EMS intervention for 5 weeks, used 60 minutes/day, 5x/week.
- Assessments occurred at baseline (week 0), midpoint (week 2.5), endpoint (week 5), and post-trial (week 7).

Outcome Measures
- Functional: TUGT, 10MWT, 6MWT, Modified 5xSTS, Modified Step Test, Modified FRT, TCMS
- Spasticity: SCATS, Modified Tardieu Scale, Modified Ashworth Scale (key lower limb joints)
- Subjective: LegA, CP QoL-Teen, QUEST, Trial Feedback form, and Pain & Effort Ratings (VAS) collected for major mobility tasks.

Results

Functional

The table below presents the key outcome data:

Measure	Baseline	Midpoint (No Stim / Stim)	End (Stim)	Post (No Stim)
TUGT (s)	92.1s	85.3 / 39.97	49.8	41
10MWT (s, steps)	96s, 76	52.28s, 64 / 35.28s, 47	48.61s, 51	59.8s, 61
Speed (m/s)	0.11	0.19 / 0.28	0.21	0.17
Cadence (steps/min)	47.5	73.5 / 79.9	62.9	61.2
6MWT (m)	68	78 / 95	92	85
m5x STS (s)	53.58	36.63 / 22.91	19.4	19.4
mStep Test R/L	5 / 5	5 / 6 ; 8 / 8	9.5 / 9.5	9.5 /10.5
TCMS (/58)	27	27 / 48	49	48
mFRT R/L (cm)	14 / 12	26 / 30	27 / 34	27/29

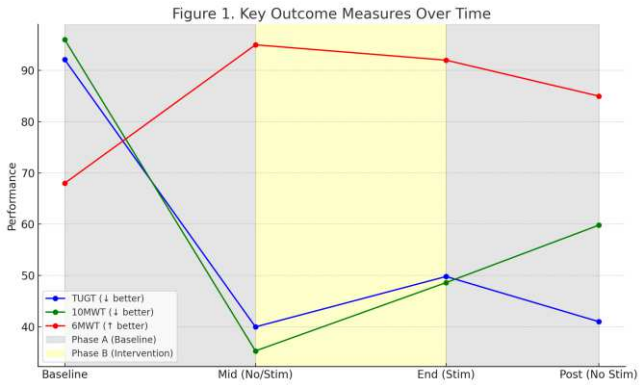

Figure 1. Key Outcome Measures Over Time
(TUGT, 10MWT, and 6MWT) across the AB timeline: Grey zones represent Phase A (Baseline and Post-Trial). Yellow zone represents Phase B (Intervention with EMS use). TUGT and 10MWT show immediate and sustained reductions (improvements) during Phase B. 6MWT shows a clear increase (improvement) during stimulation, with partial retention post-intervention.

Spasticity (SCATS, Modified Tardieu Scale, Modified Ashworth Scale):
Improvements in clonus and extensor spasms observed (R/L: from 4/3 to 1/1 and 4/3 to 0/1, respectively). Modified Tardieu measures showed increased R2-R1 angle, indicating improved muscle length and reduced hyperreflexia. These measures are not easily reduced to a single numerical effect size but align qualitatively with functional improvements.

The full table of SCATS, MTS & MAS can be found in supplementary data here: Case Study Outcome Measures - Exopulse Mollii Suit

Subjective:
Changes from to 70 to 61 on the LegA and from 57 to 68 CP-QOL, indicating significant positive changes in activity and QOL. The trial feedback from which assessed spasms using the Penn spasm scale, stiffness, sleep quality, pain, stiffness, and effort & fatigue with activity (VAS) showed a mean change of 3 points on the VAS in the positive direction for spasms, pain & effort and 2 points for fatigue, stiffness & sleep quality. Improvements in all categories were not sustained post trial. The QUEST showed the AT was easy to use, well tolerated and integrate into lifestyle.

Analysis
Visual Analysis
A visual analysis of the outcome measures between the baseline (Phase A) and intervention (Phase B) phases reveals clinically meaningful changes in functional mobility, spasticity, and dynamic balance by showing immediate, stable improvements post-intervention across functional outcomes; minimal overlap between phases supporting a strong phase effect with separation between A and B; and a consistent downward trends in effort and time required for movement tasks,
Statistical Analysis
PND: 100% for all primary measures. A PND of ≥90% is considered highly effective.
Tau-U: TUGT = 1.0, 10MWT = 1.0, 5xSTS = 0.83.
Tau-U values >0.8 reflect a large effect size, supporting the strong observed effects across functional tests.

Discussion
The EMS intervention phase demonstrated meaningful improvements in dynamic balance, step length, gait speed, trunk control, spasticity and muscle tone. The reduced effort required for walking and transitions highlights a clinically significant change in functional independence. Notably, some benefits persisted post-intervention, though slight regressions were observed, suggesting ongoing use may be necessary for long-term benefit. The combination of SCATS and Tardieu measures with functional mobility outcomes provided a comprehensive profile of EMS effects in HSP. The greatest clinical value appeared in trunk control (TCMS), forward reach, and reduced extensor spasms; areas often less responsive to traditional spasticity management. The suit was well tolerated, with positive subjective feedback on reduced pain, fatigue and improved confidence.

The results support the EMS as a low-risk adjunct in managing HSP, warranting further trials in larger cohorts with long-term follow-up. Limitations include the single-subject design, limited generalizability, and variability in effort-based self-report measures. Future work should consider a multi-subject longitudinal design and include neurophysiological assessments (e.g., EMG, H-reflex).

Summary of Findings
Statistically and visually significant improvements occurred across all tested domains. The intervention produced an immediate and sustained functional benefit. There was minimal phase overlap and high effect magnitude across mobility and spasticity indices. These findings satisfy quality criteria for single-case AB design research and support clinical effectiveness of the Exopulse Mollii Suit in the management of SPG4 Hereditary Spastic Paraplegia.

Conclusion
This AB case study provides strong visual and statistical evidence for the functional benefits of EMS in SPG4. The intervention is feasible, impactful, and relevant for community-based HSP management strategies.

The Exopulse Mollii Suit may provide a non-invasive, low-risk intervention to reduce spasticity and improve function in individuals with SPG4-HSP. For this participant, improvements in gait quality, balance, and trunk control suggest potential utility in home-based management programs. Integration into existing neurorehabilitation pathways is recommended pending further controlled trials.

Acknowledgements
We acknowledge the participant & NeuroRehab Allied Health Network for their contributions to this trial.

Author's Address
Name: Rebecca Grenfell
Profession: Senior Neurological Physiotherapist
Affiliation: NeuroRehab Allied Health Network
Email: rebecca@nrah.com.au
Linkedin: https://www.linkedin.com/in/rebecca-grenfell

Optimal parameters for lower limb afferent nerve root activation using transcutaneous spinal cord stimulation in healthy adults.

Massey S[1,2], Halpern L[2], Lopez-Belmonte Deza E[1], Suganthan S[1], Duffell L[1,2]

[1]Department of Medical Physics & Biomedical Engineering, University College London, United Kingdom
[2]Aspire Centre for Rehabilitation Engineering & Assistive Technologies, Royal National Orthopaedic Hospital, University College London, United Kingdom

l.duffell@ucl.ac.uk

Abstract: *Transcutaneous spinal cord stimulation (tSCS) is a promising rehabilitation technology following spinal cord injury. However, stimulation parameters across research groups are inconsistent and the effects of changing parameters such as frequency and pulse width remain largely unknown. This study consisted of two experiments: i) to compare the optimal pulse width for recruiting afferent fibres using peripheral nerve stimulation (PNS) versus tSCS, and; ii) to assess the effects of short sub-motor threshold bursts of tSCS at varying frequency on spinal and corticospinal excitability. Experiments were conducted on healthy human participants and outcomes were measured by electromyography at the soleus muscle. In experiment 1, recruitment curves were performed with PNS and tSCS at pulse widths ranging from 0.2-2ms and strength-duration curves were generated. In experiment 2, sub-motor threshold 1-sec bursts of tSCS were applied at varying frequency (1-100Hz) immediately followed by corticospinally or spinally evoked potentials. Results showed that the optimal pulse width for recruiting afferent fibres with tSCS is lower than PNS (0.3 versus 1.3ms) and higher frequency tSCS is optimal both for corticospinal facilitation.*

Keywords: *Transcutaneous spinal cord stimulation, posterior-root reflex, motor-evoked potential, H-reflex*

Introduction

Spinal cord injury (SCI) is a neurological disorder which affects sensory and motor function below the level of injury. Transcutaneous spinal cord stimulation (tSCS) involves usually continuous, sub-motor threshold stimulation of the posterior (afferent) nerve roots at the lumbosacral enlargement [1] has been used as a tool to facilitate functional rehabilitation [2]–[4] and to manage spasticity [5]–[7]. However, for both applications, stimulation parameters including pulse width, frequency, stimulation intensity and use of a kilohertz carrier frequency remain inconsistent across research studies [8], [9].

Previous studies applying tSCS as a rehabilitation intervention after SCI have used relatively long pulse widths, based on previous work that suggested a greater H-reflex (afferent) contribution when stimulating mixed peripheral nerves with longer duration pulses (0.5-1ms) [10], [11]. However, the afferent and efferent fibres are separated at the nerve roots and therefore the optimal pulse width cannot be assumed to be the same as with a mixed peripheral nerve. To our knowledge the optimal pulse width, to efficiently activate afferent neurons at the posterior roots, has not yet been investigated using tSCS.

It has previously been reported that electrical stimulation of a mixed peripheral nerve can enhance afferent-induced facilitation of cortical motor networks [12], which may benefit motor rehabilitation after neurological injury. We have reported similar or greater afferent-induced facilitation using tSCS compared with PNS, both with single pulses and short 30 Hz trains of stimulation [13]. However, the effects of modifying stimulation frequency on afferent-induced facilitation using tSCS has not yet been investigated.

The aims of this study were 1) to determine the optimal pulse width for recruiting afferent nerve fibres at the posterior roots using tSCS, and 2) to determine the effects of tSCS frequency on afferent-induced changes in spinal and corticospinal excitability in the lower limb.

Material and Methods

Adult participants (> 18 years old) with an intact neurological nervous system were recruited to take part in experiments described below. Exclusion criteria: those with neurological or musculoskeletal problems relating to their back or lower limbs, those with implanted devices close to the stimulation device, pregnancy. Ethical approval was obtained from the UCL Research Ethics Committee (6864/014). All participants provided written informed consent prior to taking part. The two experiments took place on separate days.

Experimental set-up

In both experiments, participants were lying supine on a plinth and a wedge was positioned under the kneed to maintain approximately 30°of flexion. Electromyography was measured using bipolar surface electrodes (Ø2.4 cm) over the soleus (SOL) and tibialis anterior (TA) muscles. EMG signals were amplified (x1000) and filtered (2-10 000 Hz, with a 50 Hz notch) using a D360 patient preamplifier/amplifier system (Digitimer, UK), digitised at

5000 Hz and sampled into data acquisition software (Signal v7.07, CED, UK).

tSCS was delivered via a Digitimer DS8R electrical stimulator via a cathode (Ø5 cm) placed over the T12 vertebrae, and two anodes (5 x 9 cm) placed over the iliac crests. Peripheral nerve stimulation (PNS) was used to trigger Hoffman (H)-reflexes in the SOL muscle via stimulation of the tibial nerve using a Digitimer DS7A electrical stimulator. The cathode (Ø2.5 cm) was placed in the popliteal fossa, and the anode (Ø2.5 cm) placed laterally on the patella.

Experiment I: pulse width

Posterior-root reflexes (PRRs) were triggered via the tSCS electrodes and H-reflexes were triggered via PNS and measured in the SOL muscle.

Experimental protocol

A total of six recruitment curves were performed via both tSCS and PNS using monophasic pulses at pulse widths of 0.2, 0.5, 1 and 2ms. For H-Reflexes, single pulses of PNS were applied, whereas for PRRs, pairs of pulses were applied with a 50ms interstimulus interval (ISI). The order of pulse width used, and electrical stimulation modality were randomised. Pulses of tSCS or PNS were delivered every 7s. Stimulation intensity began below threshold (determined as the minimum stimulation intensity required to elicit a peak-to-peak response of >0.05mV) and was progressively increased until the peak-to-peak amplitude of PRRs (tSCS) or the M-wave (PNS) plateaued, with three pulses applied at each stimulation intensity.

Data analysis

Data analyses were conducted using Signal v7.07 software and SPSS statistics software (v26, IBM, USA). Peak-to-peak amplitudes of PRRs and H-reflexes were measured at each stimulation intensity. Charge (Q) required to reach motor threshold (p-p amplitude >0.05mV) was calculated for PNS and tSCS (Eq. 1). Data were tested for normality using the Shapiro-Wilk's test. Repeated measured ANOVAs were performed to compare across pule widths, with a Bonferroni correction for post-hoc pairwise comparisons. Statistical significance was considered for $p < 0.05$.

$$Q\ (\mu C) = current\ (mA) \times pulse\ witdh\ (ms) \qquad (1)$$

Average current required to reach motor threshold at each pulse width was used to generate strength-duration curves (Eq. 2) for PNS and tSCS [14].

$$I = b \times (1 + \frac{c}{d}) \qquad (2)$$

Where, I=current; b=rheobase; c=chronaxie; d=stimulus duration.

Experiment II: frequency

Experimental protocol

To measure the effects of varying frequency on spinal and corticospinal excitability, a 1 s burst of tSCS was followed by either PRR, H-reflex or a motor-evoked potential (MEP) in three separate blocks, which occurred in a random order. Within each block, the relevant outcome measure was preceded by the 1 s burst of tSCS was randomly delivered at 1, 10, 50 and 100 Hz (Fig. 1), as well as a control condition where no burst of tSCS was delivered. There were five repeats for each frequency condition and the control condition. The 1 s burst of tSCS was delivered using a 1 ms pulse width at 80 % of PRR threshold, or at the participant's maximum tolerance, whichever was lower.

Outcome measures

For the PRR block, threshold was determined as above, using a 1ms pulse width. PRRs were elicited at 1.2x threshold via the same tSCS electrodes, using the Digitimer DS7A electrical stimulator.

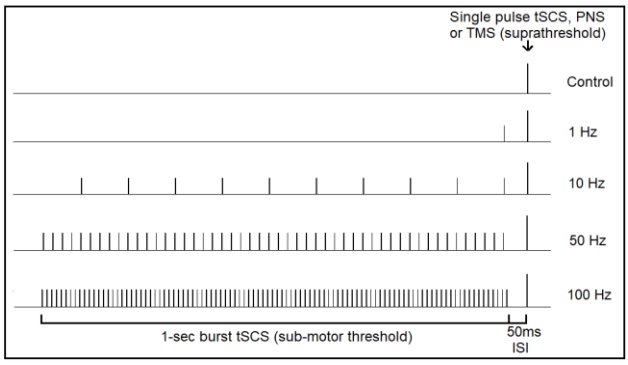

Figure 1. Experiment II stimulation protocol. 1-sec sub-motor threshold (80% MT) trains of tSCS were applied at 0 (control), 1, 10, 50 or 100 Hz followed by a single suprathreshold pulse of tSCS, peripheral nerve stimulation (PNS) or Transcranial Magnetic Stimulation (TMS).

An H-reflex recruitment curve was performed as described above, using a 1 ms pulse width. For the outcome measure, H-reflexes were elicited at the current intensity which correlated to the peak-to-peak amplitude of the H-wave on the rising edge of the recruitment curve.

Transcranial magnetic stimulation (TMS) was delivered via a Magstim 200^2 to elicit MEPs in the SOL muscle. A double-cone coil (Ø7 cm) was placed over the leg area of the primary motor cortex and stimulation was delivered in a posterior-anterior direction. A recruitment curve was performed to determine threshold (peak-to-peak MEP response >0.05 mV). For the outcome measure, MEPs were elicited at 1.4x threshold.

Data analysis

Average peak-to-peak amplitudes of H-reflexes, PRRs and MEPs at each frequency condition were normalised to the corresponding control condition, then averaged across participants.

All data were tested for normality using the Shapiro-Wilk's test. Repeated measured ANOVAs were performed on each outcome measure, with a Bonferroni or LSD correction for post-hoc pairwise comparisons. Statistical significance was considered for $p < 0.05$.

Results

Experiment I: pulse width

Ten healthy people (8 female) with a mean ± SD age, height and weight of 23.7 ± 7.1 years, 1.70 ± 0.08m and 61.6 ± 5.5kg, respectively, were recruited.

Charge required to reach motor threshold was an order of magnitude higher for tSCS compared with PNS across all pulse widths tested. For both PNS and tSCS, significantly greater charge was required to reach motor threshold with a 2ms pulse width compared with all other pulse widths tested ($p<0.05$). For PNS, there was no significant difference between the other pulse widths tested (0.2-1ms; $p>0.05$) whereas, for tSCS, significantly less charge was required to reach motor threshold at 0.2ms compared to both 0.5 and 1ms ($p<0.05$). Charge required to reach motor threshold was also significantly greater with a 1ms pulse width compared to 0.5ms for tSCS only ($p<0.05$). Strength-duration curves revealed rheobase values of 3mA for PNS and 31mA for tSCS, and chronaxie values of 1.3ms for PNS and 0.3ms for tSCS (Fig. 2).

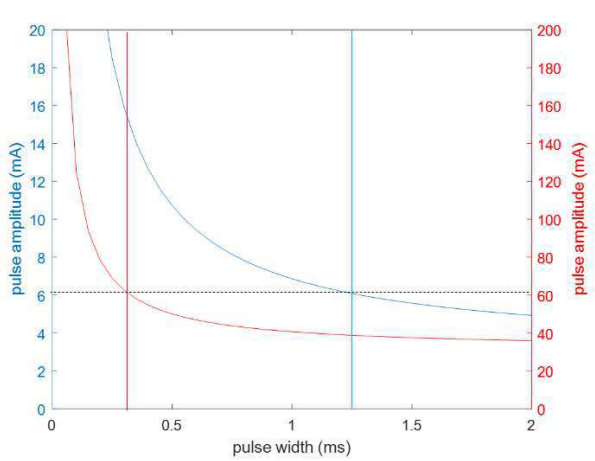

Figure 2. Strength-duration curves for PNS (blue) and tSCS (red). Twice rheobase for both PNS and tSCS is shown by the black dashed line and chronaxie is indicated by the vertical lines for PNS (blue) and tSCS (red).

Experiment II: frequency

Ten healthy people (5 female) with a mean ± SD age, height and weight of 23.7 ± 7.1 years, 1.73 ± 0.08m and 66.5 ± 12.0kg, respectively, were recruited.

Spinal excitability was assessed by PRRs and H-Reflexes elicited at 1.2 x motor threshold 50 ms after a 1-sec train of sub-motor threshold tSCS. Peak-peak amplitudes of PRRs were significantly reduced compared to the control condition following a 1-sec burst of tSCS delivered at 50 and 100Hz ($p<0.05$; Fig. 3). H-Reflex peak-peak amplitude was significantly reduced compared to the control and 1 Hz conditions following a 1-sec burst of tSCS delivered at 10Hz ($p<0.05$; Fig. 3). H-Reflex amplitudes were equally reduced following the 50 and 100Hz tSCS burst, although these did not reach statistical significance ($p=0.083$, $p=0.078$ respectively). Corticospinal excitability was assessed by MEPs elicited at 1.4 x motor threshold 50 ms after a 1-sec train of sub-motor threshold tSCS. Peak-peak amplitudes of MEPs were significantly increased compared to the control condition following a 1-sec burst of tSCS delivered at 50 and 100Hz ($p<0.05$; Fig. 3).

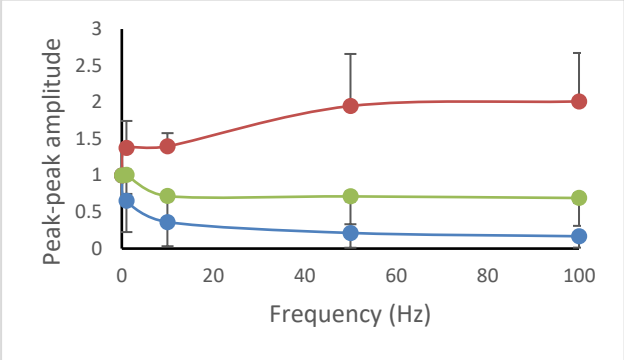

Figure 3. Average (SD) normalised peak-peak amplitude of motor evoked potentials (red), posterior root reflexes (blue) and H-Reflexes (green) following a 1-sec burst of tSCS at 1, 10, 50 and 100Hz.

Discussion

This study has shown that tSCS activates the afferent nerve roots more efficiently when narrower pulse widths are applied (~0.3ms). In addition, higher frequency stimulation (50-100Hz) appears to decrease spinal excitability and facilitate corticospinal excitability, which may benefit rehabilitation in people with SCI.

Previous research has suggested that wider pulse widths (~0.5-1ms) are optimal for recruiting afferent fibres when stimulating a mixed peripheral nerve with transcutaneous electrodes placed over the nerve [10], [11]. Here, we have confirmed that result for tibial nerve stimulation but also found that much shorter pulse widths (~0.3ms) should be used to efficiently recruit afferent nerve fibres at the posterior roots using transcutaneous SCS. It is unclear exactly why such different pulse widths are optimal between PNS and tSCS, given that the same neurons are being targeted only in different locations. The separation of afferent and efferent fibres at the nerve roots, as well as the bone and muscular tissue between the electrode and targeted nerve roots are likely to be contributing factors. Indeed, the charge required to recruit the nerve roots was an order of magnitude greater with tSCS than PNS.

In terms of frequency, we have found that a short burst of tSCS at sub-motor threshold intensity and at relatively high frequency (50-100Hz) can inhibit spinal excitability, which may be due to modulation of spinal inhibitory circuits at the dorsal horn [16]. This supports the beneficial effects of tSCS for lower limb spasticity in people with SCI [17]. The inhibition of H-Reflex amplitude following tSCS at 10Hz suggests that an alternative mechanism may affect this purely spinal reflex, compared to PRRs, which have heteronymous influences [15]. It was surprising that, despite the reduction in spinal excitability, a simultaneous facilitation in corticospinal excitability was found at 50-100Hz, indicating supraspinal facilitation that more than

compensated for the spinal inhibition. Most likely, this was due to afferent-induced facilitation of cortical motor networks [12], due to the substantial afferent input from tSCS, where many lower limb afferent nerve roots are targeted simultaneously.

Conclusions

This study has shown for the first time that tSCS activates the afferent nerve roots more efficiently when narrower pulse widths are applied (~0.3ms). We have also shown that higher frequency stimulation (50-100Hz) inhibits spinal excitability, whilst simultaneously facilitating corticospinal excitability, which may benefit rehabilitation in people with SCI.

References

[1] K. Minassian, I. Persy, F. Rattay, M. R. Dimitrijevic, C. Hofer, and H. Kern, "Posterior root-muscle reflexes elicited by transcutaneous stimulation of the human lumbosacral cord," *Muscle and Nerve*, vol. 35, no. 3, pp. 327–336, 2007, doi: 10.1002/mus.20700.

[2] F. Inanici, S. Samejima, P. Gad, V. R. Edgerton, C. P. Hofstetter, and C. T. Moritz, "Transcutaneous electrical spinal stimulation promotes long-term recovery of upper extremity function in chronic tetraplegia," *IEEE Trans. Neural Syst. Rehabil. Eng.*, vol. 26, no. 6, pp. 1272–1278, 2018, doi: 10.1109/TNSRE.2018.2834339.

[3] C. Moritz *et al.*, "Non-invasive spinal cord electrical stimulation for arm and hand function in chronic tetraplegia: a safety and efficacy trial," *Nat. Med. 2024*, vol. 17, no. May, pp. 1–8, 2024, doi: 10.1038/s41591-024-02940-9.

[4] Y. Al'joboori, S. J. Massey, S. L. Knight, N. de N. Donaldson, and L. D. Duffell, "The effects of adding transcutaneous spinal cord stimulation (TSCS) to sit-to-stand training in people with spinal cord injury: A pilot study," *J. Clin. Med.*, vol. 9, no. 9, pp. 1–22, 2020, doi: 10.3390/jcm9092765.

[5] U. Hofstoetter, W. B. McKay, K. E. Tansey, W. Mayr, H. Kern, and K. Minassian, "Modification of spasticity by transcutaneous spinal cord stimulation in individuals with incomplete spinal cord injury," *J. Spinal Cord Med.*, vol. 37, no. 2, pp. 202–211, 2014, doi: 10.1179/2045772313Y.0000000149.

[6] J. L. Vargas Luna *et al.*, "Effects of sustained electrical stimulation on spasticity assessed by the pendulum test," *Curr. Dir. Biomed. Eng.*, vol. 2, no. 1, pp. 405–407, 2016, doi: 10.1515/cdbme-2016-0090.

[7] U. S. Hofstoetter *et al.*, "Transcutaneous Spinal Cord Stimulation Induces Temporary Attenuation of Spasticity in Individuals with Spinal Cord Injury," *J. Neurotrauma*, vol. 37, no. 3, pp. 481–493, 2020, doi: 10.1089/neu.2019.6588.

[8] M. U. Rehman, D. Sneed, T. W. Sutor, H. Hoenig, and A. S. Gorgey, "Optimization of Transspinal Stimulation Applications for Motor Recovery after Spinal Cord Injury: Scoping Review," *J. Clin. Med.*, vol. 12, no. 3, 2023, doi: 10.3390/jcm12030854.

[9] S. Massey, A. Vanhoestenberghe, and L. Duffell, "Neurophysiological and clinical outcome measures of the impact of electrical stimulation on spasticity in spinal cord injury: Systematic review and meta-analysis," *Front. Rehabil. Sci.*, vol. 3, no. December, pp. 1–15, 2022, doi: 10.3389/fresc.2022.1058663.

[10] O. Lagerquist and D. F. Collins, "Stimulus pulse-width influences H-reflex recruitment but not H max/Mmax ratio," *Muscle and Nerve*, vol. 37, no. 4, pp. 483–489, 2008, doi: 10.1002/mus.20957.

[11] M. Panizza, J. Nilsson, and M. Hallett, "Optimal stimulus duration for the H reflex," *Muscle Nerve*, vol. 12, no. 7, pp. 576–579, 1989, doi: 10.1002/mus.880120708.

[12] F. D. Roy and M. A. Gorassini, "Peripheral sensory activation of cortical circuits in the leg motor cortex of man," *J. Physiol.*, vol. 586, no. 17, pp. 4091–4105, 2008, doi: 10.1113/jphysiol.2008.153726.

[13] Y. Al'joboori *et al.*, "The Immediate and Short-Term Effects of Transcutaneous Spinal Cord Stimulation and Peripheral Nerve Stimulation on Corticospinal Excitability," *Front. Neurosci.*, vol. 15, no. October, pp. 1–17, 2021, doi: 10.3389/fnins.2021.749042.

[14] L. Geddes and J. Bourland, "The strength-duration curve," *IEEE Trans. Biomed. Eng.*, vol. 32, no. 6, pp. 458–459, 1985.

[15] U. S. Hofstoetter, B. Freundl, H. Binder, and K. Minassian, "Recovery cycles of posterior root-muscle reflexes evoked by transcutaneous spinal cord stimulation and of the H reflex in individuals with intact and injured spinal cord," *PLoS One*, vol. 14, no. 12, p. e0227057, 2019, doi: 10.1371/journal.pone.0227057.

[16] K. Minassian, B. Freundl, P. Lackner, and U. S. Hofstoetter, "Transcutaneous spinal cord stimulation normalizes glycinergic and GABAergic inhibition in the control of spinal spasticity," *Under Rev.*, vol. 5, no. 11, p. 101805, 2024, doi: 10.1016/j.xcrm.2024.101805.

[17] Hofstoetter *et al.*, "Modification of spasticity by transcutaneous spinal cord stimulation in individuals with incomplete spinal cord injury," *J. Spinal Cord Med.*, vol. 37, no. 2, pp. 202–211, 2014, doi: 10.1179/2045772313Y.0000000149.

Author's Address

Name: Lynsey Duffell
Affiliation: Department of Medical Physics & Biomedical Engineering, University College London, United Kingdom
eMail: l.duffell@ucl.ac.uk

Home-Based Transcutaneous Electrical Nerve Stimulation for Idiopathic Sensory Polyneuropathy: A Personalized Approach

Pataraia A[1,2], Mayr W [1,3], Gesslbauer C[1,2], Crevenna R[1,2]

[1]Department of Physical Medicine, Rehabilitation and Occupational Medicine, Medical University of Vienna, Austria
[2]Comprehensive Center for Musculoskeletal Disorders, Medical University of Vienna, Austria
[3]Center for Medical Physics and Biomedical Engineering, Medical University of Vienna, Austria

Abstract: *Idiopathic sensory polyneuropathy (PNP) presents with symmetrical sensory disturbances such as numbness, tingling, and gait instability, with limited effective non-pharmacological treatment options. This case report describes a 77-year-old male with PNP who underwent a personalized, home-based Transcutaneous Electrical Nerve Stimulation (TENS) protocol targeting the peroneal nerve. Over a 15-month period, the patient experienced significant clinical improvement, including reduced sensory thresholds, improved balance, and near normalization of vibration sensation. The case highlights the potential of individualized afferent stimulation combined with high adherence and physical therapy to address sensory dysfunction in idiopathic polyneuropathy. These findings support the feasibility and therapeutic promise of home-based neuromodulation in managing chronic sensory neuropathies.*

Keywords: *Idiopathic sensory polyneuropathy, TENS, afferent stimulation, home-based therapy, neuromodulation, peripheral neuropathy, PNP*

Introduction

Idiopathic sensory polyneuropathy is characterized by symmetrical sensory disturbances, often manifesting as numbness, tingling, and balance difficulties in the lower extremities.
Although various treatment options are available, Transcutaneous Electrical Nerve Stimulation (TENS) has emerged as a promising non-invasive modality for symptom relief. Traditionally employed for pain management, emerging evidence now suggests that TENS may also alleviate sensory dysfunction associated with peripheral neuropathies.

Case Presentation

A 77-year-old male presented in April 2024 to the Department of Physical Medicine, Rehabilitation, and Occupational Medicine at the Medical University of Vienna with complaints of dizziness and unsteady gait. Neurological examination revealed normal skin sensory function but significantly reduced vibration sensation in the lower limbs (2/8). Nerve conduction studies confirmed sensory polyneuropathy of the lower extremities. His symptoms had started approximately five months before presentation. The patient was otherwise healthy and remained physically active.

Intervention:

We initiated subthreshold afferent stimulation of the peroneal nerve using a Cefar Rehab X2 stimulator (DJÖ France, Mouguerre, France). Electrode placement was as shown in Figure 1: bilateral hydrogel electrodes (Axion GmbH, Leonberg, Germany) were used - one 4×4 cm electrode (anode) positioned proximally to the lateral fibular head over the peroneal nerve, and a 5×5 cm counter electrode placed at the proximal third of the tibialis anterior muscle. Initial stimulation parameters were set at 30 Hz, 400 µs (per phase, symmetric biphasic rectangular pulse), with subthreshold intensity adjusted to a slightly subsensory level (initially 8.5 mA right, 6 mA left). The patient applied stimulation almost daily for up to 2 hours during overground walking, both indoors and in outdoor settings. He also engaged in regular physiotherapy with an emphasis on balance training.

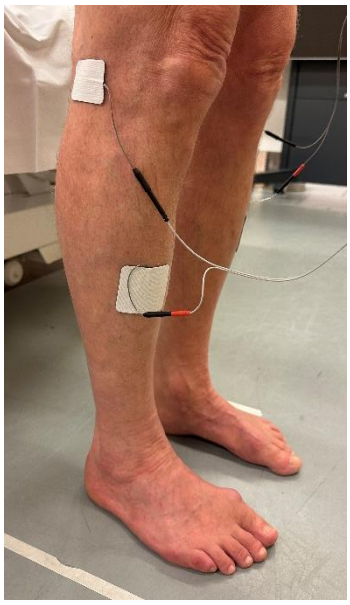

Figure 1: electrode placement

Progress and Outcomes

After 10 months, therapy transitioned to sock-based electrical stimulation (Figure 2) to improve compliance and coverage. Follow-up assessments revealed improved sensory thresholds, decreasing from 8.5 mA (right) and 6 mA (left) to 5 mA (right) and 5.5 mA (left). Reflex thresholds remained unchanged (18 mA left, 19 mA right), likely due to differing devices and methods between measurements. Subjectively, the patient reported complete resolution of dizziness, enhanced balance, and markedly reduced sensory disturbances. Neurological re-examination showed near-normal vibration sensation (6/8). Gait was steady, with the patient able to perform single-leg stance and tandem walking without difficulty. Nerve conduction studies on July 15, 2025 demonstrated normal results. Comparison with previous examination on February 23, 2024: Right peroneal nerve: Increase in the maximum compound muscle action potential (CMAP) amplitude from 4,800 µV to 7,400 µV. Left peroneal nerve: Increase in the maximum CMAP amplitude from 5,700 µV to 7,800 µV. Increase in motor conduction velocity from 41 m/s to 46 m/s. Right tibial nerve: Increase in the maximum CMAP amplitude from 5,200 µV to 7,900 µV. Left tibial nerve: Increase in the maximum CMAP amplitude from 3,900 µV to 6,600 µV. Right sural nerve: Increase in sensory antidromic conduction velocity from 42 m/s to 44.5 m/s.

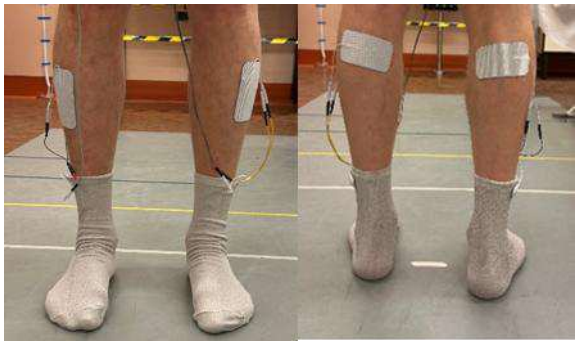

Fugure 2: Sensory Stimulation Socks

Discussion

This case highlights the potential of an individualized, home-based TENS program in the treatment of idiopathic sensory polyneuropathy. While TENS is conventionally used for analgesia, growing evidence supports its broader neuromodulatory role in sensory rehabilitation. In this case, personalized electrode placement and parameter adjustment, combined with high adherence and physical therapy, led to clinically meaningful improvements.

The home-based design enables patients to perform the program independently, offering a convenient and cost-effective alternative that minimizes reliance on healthcare infrastructure.

Limitations include the single-patient design, lack of neurophysiological follow-up, and the potential influence of placebo effects. Nonetheless, the patient's consistent improvements support further exploration of individualized TENS protocols.

Controlled trials incorporating objective sensory assessments and long-term follow-up are needed to validate these findings.

Conclusions

TENS therapy, when combined with physical therapy, may represent a viable non-pharmacological approach for managing idiopathic sensory polyneuropathy in elderly patients. This case supports the feasibility of personalized, home-based stimulation protocols and highlights the importance of patient engagement in achieving therapeutic success.

References

[1] Gwathmey KG, Pearson KT. Diagnosis and management of sensory polyneuropathy. BMJ. 2019 May 8;365:l1108. doi: 10.1136/bmj.l1108. PMID: 31068323.

[2] Jin DM, Xu Y, Geng DF, Yan TB. Effect of transcutaneous electrical nerve stimulation on symptomatic diabetic peripheral neuropathy: a meta-analysis of randomized controlled trials. *Diabetes Res Clin Pract*. 2010;89(1):10-15. doi:10.1016/j.diabres.2010.04.018pubmed.ncbi.nlm.nih.gov+2ncbi.nlm.nih.gov+2cybermedlife.eu+2

[3] Püsküllüoğlu M, Tomaszewski KA, Grela-Wojewoda A, Pacholczak-Madej R, Ebner F. Effects of Transcutaneous Electrical Nerve Stimulation on Pain and Chemotherapy-Induced Peripheral Neuropathy in Cancer Patients: A Systematic Review. *Medicina (Kaunas)*. 2022;58(2):284. doi:10.3390/medicina58020284pubmed.ncbi.nlm.nih.gov+2pubmed.ncbi.nlm.nih.gov+2pmc.ncbi.nlm.nih.gov+2

[4] Kılınç M, Livanelioğlu A, Yıldırım SA, Tan E. Effects of transcutaneous electrical nerve stimulation in patients with peripheral and central neuropathic pain. *J Rehabil Med*. 2014;46(5):454-460. doi:10.2340/16501977-1271

Author's Address

Anna Pataraia
Department of Physical Medicine, Rehabilitation and Occupational Medicine, Medical University of Vienna, Austria
anna.pataraia@meduniwien.ac.at
www.meduniwien.ac.at/physmedrehab

Real-Time R -Peak Prediction in ECG for cardiac-gated Auricular Vagus Nerve Stimulation

Chowdhury D[1], Schuh K[1], Kaniusas E[1]

[1]Institute of Biomedical Electronics, TU Wien, Austria

Abstract: *Auricular vagus nerve stimulation (aVNS), a pivotal aspect of bioelectronic medicine, offers an accessible therapeutic approach by targeting the vagus nerve in the ear region for treating a wide array of pathological conditions. Continuous aVNS modulates sympathovagal balance and offers therapy, yet its effects vary significantly among individuals for specific disorders. To overcome this challenge, utilising relevant biomarkers and tailoring stimulation to the individual's physiological state is highly effective and desirable. Predictive modelling of the biomarkers could enhance the therapeutic outcomes. In this study, we predict the timing of electrocardiogram (ECG) R-peaks in real-time to enable closed-loop cardiac-synchronised aVNS. We continuously detect ECG R-peaks in real time, compute beat-to-beat intervals, implement computational models to average RR intervals, predict the occurrence of future R peaks of the ECG signal, and deliver aVNS synchronised with the predicted R peaks. In a 5-minute ECG recording under relaxed breathing conditions, we accurately predicted future R-peaks and delivered stimulation with standard deviations of 58 ms and 85 ms for 1-point and 2-point averaging, respectively. Thus, the preliminary test shows promising accuracy in the prediction of cardiac effects. It would allow optimal stimulation along with the enhancement of neuromodulation effects.*

Keywords: *Auricular Vagus Nerve Stimulation, Biomarkers, ECG R-Peaks Prediction*

Introduction

Auricular vagus nerve stimulation (aVNS) delivered to a branch of the vagus nerve located in the ear is a valuable neuromodulation technique for reestablishing the sympathovagal balance and providing therapy for various neurological, psychological, and pathological conditions [1]. Existing commercial aVNS devices are using the open-loop approach, resulting in suboptimal therapeutic efficacy for a significant proportion of individuals [2]. Cardiac, neural, other physiological, and biochemical biomarkers from the body are responsive to aVNS, which leads to the development of closed-loop systems that incorporate biomarker feedback, with the aim to enhance stimulation effects [3]. In conjunction with closed-loop, the prediction of a physiological state could be impactful for early detection of various pathological conditions, preventing alarming situations and providing effective therapy. Researchers developed an in-silico nonlinear predictive control model of cardiac biomarkers to calculate multiple control actions over future time windows. Although this model is computationally efficient, implementing it in real-time remains challenging [4].

In this study, we utilise the electrocardiogram (ECG) as a biomarker due to its significant responsiveness to aVNS, safety and cost-effectiveness [5]. We aim to develop real-time cardiac-synchronised aVNS by predicting future ECG R-peaks based on prior RR intervals and triggering stimulation accordingly Fig. 1. This is achieved by a

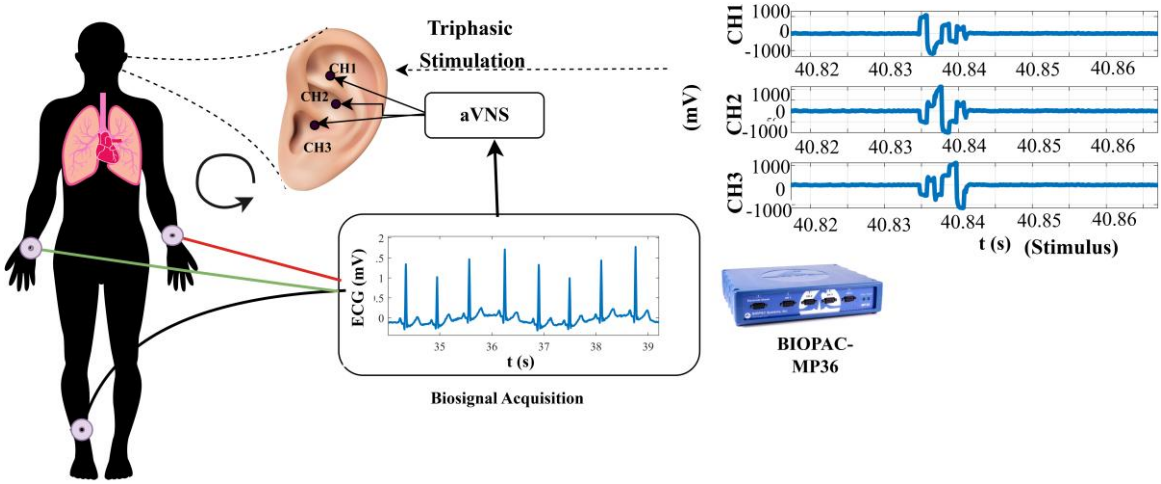

Figure 1: Schematic representation of predictive closed loop aVNS with channels (CH1, CH2, CH3) with ECG RR interval used as a biomarker.

stimulator board developed in the institute, a BIOPAC system for ECG signal, and stimulus signal acquisition and delivery of the ECG signal to the stimulator.

Proposed Methodology

The setup to achieve personalized aVNS consisted of a customized printed circuit board (PCB) that was programmed to provide triphasic stimulus [6] and receive and analyze external analog bio-signal in real time. The BIOPAC-MP36 system was used to record ECG data and transfer the ECG signal to the developed PCB instantaneously.

In this work, we carried out an initial test and functional evaluation of the system where the R-peaks detected from the ECG signal, in real-time, are utilized to compute RR intervals. An averaging algorithm, as given in Eq. 1, was used to predict the future RR intervals and the time instant of subsequent R-peaks.

$$RR_{\mathrm{P,n}} = \frac{\sum_{\mathrm{i=n}}^{\mathrm{n-N+1}} RR_{\mathrm{i}}}{N} \qquad (1)$$

Where n is the current instance and $RR_{\mathrm{P,n}}$ is the future RR interval to be predicted. Here RR_{i} represents the RR interval at the i^{th} past time point within the window of size *N*.

The stimulus is a tripolar waveform of peak magnitude 1 V, and burst length: 1 [6], was delivered in sync with the anticipated R-peaks; specifically, a triphasic stimulation was applied 200 ms before the predicted R peak. The entire test was conducted on a single individual over a duration of five minutes. During this time, the stimulus, along with the ECG, was recorded in real time and stored in the BIOPAC system. The recorded data was used for further analysis in MATLAB-2023A. The individual remained in a seated position and exhibited eupnea throughout the procedure.

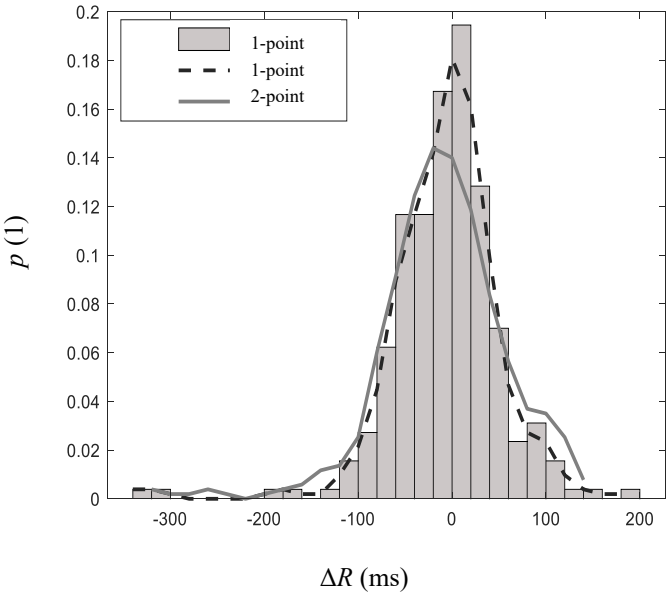

Figure 2: Histogram of one-point and two-point averaging between Real R-peaks and Predicted R peaks.

Additional analysis is performed to identify the window length that maximizes the prediction accuracy of the averaging algorithm. To achieve this, RR intervals are calculated from the recorded ECG data using MATLAB in a post-acquisition process. The averaging algorithm (Eq. 1) is then applied for various window lengths (*N*). For each case, the prediction error (ΔRR), defined as the difference between the true RR interval and the predicted value, is computed. These errors are visualised and analysed using histograms. The spread of each histogram, quantified by its width at 50% of the peak of its envelope ($\Delta RR_{50\%}$) is used as a metric for variability. Finally, $\Delta RR_{50\%}$ is plotted as a function of window length '*N*' to assess the relationship between the averaging window size and predictive accuracy.

Results

The developed hardware is equipped with prediction algorithms (from Eq. 1) for *n*=1 and *n*=2, referred to as 1-point and 2-point averaging, respectively. These algorithms use Eq. 1 to determine future RR intervals and are configured to generate a stimulation spike 200 ms before the upcoming R-peak. Post recording the data is loaded in MATLAB, and how accurately the hardware is predicting the R-peaks and simultaneously act by supplying stimulus is presented with a histogram in Fig. 2. This evaluation is described through a distribution of the error (ΔR) between the true R-peaks from the ECG of the individual (denoted by R_{T}), and the predicted R-peaks, as calculated instantaneously from the stimulator (denoted by R_{P}), as shown in Eq. 2, validating the effectiveness of the proposed method.

$$\Delta R = R_{\mathrm{T}} - R_{\mathrm{P}} \qquad (2)$$

The mean and standard deviation of error for the 1-point averaging were 41 ms and 58 ms, respectively, and those of the 2-point averaging were 59 ms and 85 ms, respectively. Hence, alignment of stimulation with the cardiac rhythm for effective delivery of treatment can be achieved with the proposed method. Further, Fig. 3 provides an example for *N*=1, displaying ΔRR together with $\Delta RR_{50\%}$. The range of $\Delta RR_{50\%}$ values across different window lengths are presented in Fig. 4.

Discussion

The ECG-gated aVNS enables stimulus delivery during either systole or diastole in afferent aVNS, allowing the effects of efferent nerves to be analysed and better understood. Thus, time series prediction of the ECG data, mainly the future R peak, is important for optimal aVNS therapy [7]. It provides flexibility for desirable stimulation aligned with the cardiac rhythm to personalize aVNS, reduce side effects, and avoid overstimulation. This pilot evaluates the system and prediction algorithm performance in real time. The heart rate continuously changes with respect to respiration, known as respiratory sinus arrhythmia, thus leading to a continuous variation of the RR interval. As a result, predicting future RR intervals becomes challenging,

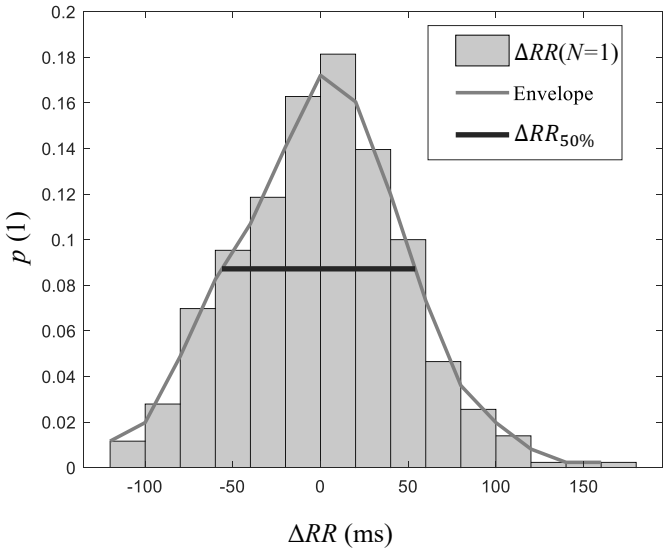

Figure 3: Histogram of the variance between true RR interval and predicted RR interval for averaging (N=1), with a spread of 50%.

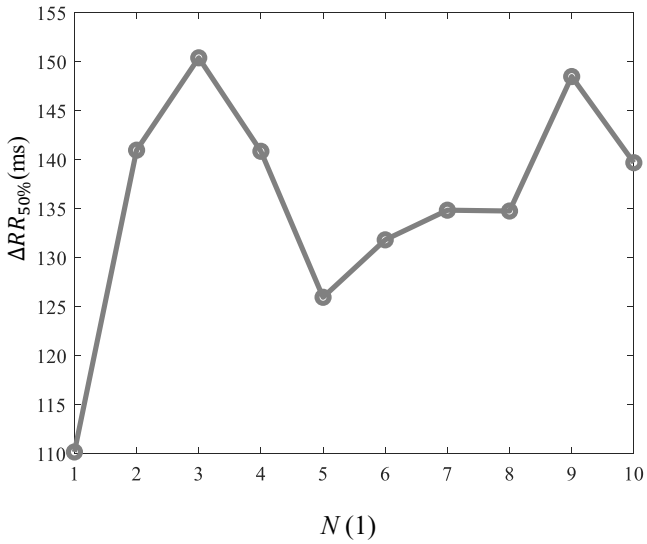

Figure 4: $\Delta RR_{50\%}$ as a function of varying averaging window size (N).

which limits the overall accuracy. The results of the averaging technique, shown in Fig. 2, illustrate that the comparatively higher error in the 2-point method could be because the averaging method tends to obscure the effects of respiratory cycles on the RR intervals. An important observation in Fig. 4 indicates that the accuracy for predicting future RR intervals improves when N approximates the number of RR intervals within a single respiratory cycle. However, due to the variability in the number of RR intervals in different respiration cycles, it is not possible to define a fixed optimal value for N. This leads to the need for a more sophisticated method that considers the respiration cycle.

Thus, future work will involve introducing more complex algorithms like extrapolation from the time course of previous RR interval values, which would include the respiratory effects on the heart rate and, accordingly, predict the RR interval. Testing the different algorithms under different breathing conditions like diaphragmatic breathing and optimization of the algorithm for different positions, be it a supine or sitting position, follows. While achieving optimal performance with complex algorithms may require more powerful and costly hardware, future efforts will focus on balancing prediction accuracy with resource and power constraints to ensure feasibility for real-time applications in the stimulator system.

Conclusion

Real-time cardiac-gated aVNS offers significant challenges due to its variability in the physiological responses. To address this, we propose a method using averaging algorithms (1-point, 2-point) for RR intervals to accurately forecast R-peaks, enabling precise control over beat-to-beat intervals and tailored delivery of aVNS, with a motivation to enhance therapeutic efficacy.

Acknowledgement

The authors express gratitude for funding by TU Wien, Austria, the Institute of Biomedical Electronics.

References

[1] E. Kaniusas et. al.: Current Directions in the Auricular Vagus Nerve Stimulation II – An Engineering Perspective, Frontiers in Neuroscience, vol.13, July 2019.

[2] Hajo M. Hamer, Sebastian Bauer: Lessons learned from transcutaneous vagus nerve stimulation (tVNS), Epilepsy Research, vol. 153, 2019, page: 83-84.

[3] Yuan H, Silberstein SD. Vagus Nerve and Vagus Nerve Stimulation, a Comprehensive Review: Part I. Headache. 2016 Jan;56(1):71-8.

[4] Yao Y, Kothare MV. Nonlinear Closed-Loop Predictive Control of Heart Rate and Blood Pressure Using Vagus Nerve Stimulation: An In Silico Study. IEEE Trans Biomed Eng. 2023 Oct;70(10):2764-2775.

[5] Capilupi MJ, Kerath SM, Becker LB. Vagus Nerve Stimulation and the Cardiovascular System. Cold Spring Harb Perspect Med. 2020 Feb 3;10(2): a034173.

[6] Kaniusas et al.: Stimulation Pattern Efficiency in Percutaneous Auricular Vagus Nerve Stimulation: Experimental Versus Numerical Data. IEEE Trans Biomed Eng. 2020 Jul;67(7):1921-1935.

[7] Tischer Johannes, Szeles Jozsef Constantin, Kaniusas Eugenijus. Personalized auricular vagus nerve stimulation: beat-to-beat deceleration dominates in systole-gated stimulation during inspiration - a pilot study. Frontiers in Physiology, vol 15, 2025 Jan.

Author's Address

Dibya Chowdhury
Institute of Biomedical Electronics, TU Wien, Austria
dibya.chowdhury@tuwien.ac.at
https://www.tuwien.at/etit/bme

Session 3: FES-Technology

Design Parameters of Concentric Electrodes: A Simulation Study to Optimise Non-invasive Functional Electrical Stimulation

Sáez J[1], Saavedra F[2], Osorio R[1], Andrews B[3,4], Aqueveque P[1]

[1]Department of Electrical Engineering, Universidad de Concepción, Chile.
[2]Department of Electrical and Electronical Engineering, Universidad del Bío-Bío, Chile.
[3]Nuffield Department of Surgical Sciences, University of Oxford, UK.
[4]School of Engineering, University of Warwick, UK.

Abstract: *Concentric ring electrodes offer a promising alternative for non-invasive functional electrical stimulation (FES), with the potential to improve stimulation selectivity and reduce off-target effects compared to traditional geometries. This study investigates how electrode geometry—specifically size and inter-electrode distance—influences current density distribution and axonal activation, using finite element method (FEM) simulations coupled with the MRG axon model. Five concentric electrode designs were evaluated on a simplified forearm model. Results indicate that medium-sized electrodes with reduced inter-electrode spacing achieve a favourable trade-off between selectivity and minimised current density peaks. In contrast, designs with thin outer rings exhibited increased edge effects and reduced selectivity. These findings provide critical insights into the biophysical performance of concentric electrodes, guiding the design of more precise and comfortable FES systems and supporting future clinical translation.*

Keywords: *Concentric Electrodes, Computational Modelling, Electrode Design, Functional Electrical Stimulation.*

Introduction

Functional electrical stimulation (FES) is increasingly used in neurorehabilitation to restore movement and assist activities of daily living (ADLs) in individuals with stroke or spinal cord injuries (SCI) [1]. Among its various modalities, surface FES stands out for being non-invasive, low-cost, and clinically accessible, particularly when compared to implanted FES. It has been shown to promote neuroplasticity and improve motor learning outcomes [2]. A key challenge—particularly in upper-limb applications—is achieving selective nerve stimulation that is both effective and comfortable, without triggering unintended muscles. Here, selectivity refers to the ability of an electrode to activate the target nerve while limiting activation of neighbouring nerves. This balance remains a major limitation of non-invasive FES. Striking this balance is crucial for enabling fine motor control, such as hand grasping [3], and for improving patient adherence to long-term therapy [4].

Traditional square side-by-side electrodes are limited by broad current dispersion and poor field focality, which can reduce stimulation selectivity and increase the risk of activating unintended muscles. Concentric ring electrodes, by contrast, allow greater control over the spatial distribution of the electric field, offering the potential to improve targeting of specific nerve structures in non-invasive FES. From a biophysical perspective, two key mechanisms limit the performance of surface FES: edge effects, which create localised peaks in current density and are often associated with discomfort [5], and broad current distribution, which can lead to the unintended activation of off-target neural or muscular structures. Previous studies using square side-by-side electrodes have shown that geometric modifications—such as adjusting electrode size, inter-electrode distance, and geometry—can reshape the electric field, thereby enhancing stimulation selectivity and reducing adverse effects [5], [6]. Concentric electrode configurations have been explored to investigate their potential to enhance stimulation performance in FES applications. Computational and experimental analyses have shown that concentric serpentine designs, can improve selectivity and facilitate effective motor activation in wearable systems [6]. Additionally, analytical modelling approaches indicate that optimising the geometric parameters of concentric electrodes can reduce peak current densities at the electrode–skin interface while increasing the focality of the generated electric field [7]. While these findings highlight the potential of concentric designs, the influence of key geometric parameters—such as ring thickness and inter-electrode spacing—has not yet been systematically assessed in anatomical-inspired models. To address this, the present study combines FEM modelling with axon-level simulations to evaluate how concentric electrode geometry shapes current density and neural activation in the context of non-invasive FES.

Material and Methods

The impact of concentric ring electrode geometry on current density distribution and axonal activation was assessed by varying two key design parameters: electrode size and inter-electrode distance, while keeping the anode–cathode surface area constant across designs (Fig. 1). The study followed a two-stage simulation approach comprising finite element modelling (FEM) and axon-level simulations using the MRG model [8].

In the first stage, FEM simulations were performed using COMSOL Multiphysics 6.1 (Burlington, MA, USA) to compute the extracellular electric field generated by each electrode configuration. A simplified cylindrical anatomical model of the human forearm was constructed, consisting of three tissue layers (skin, fat, and muscle), three peripheral nerves (ulnar, median, and radial), and two bones (ulna and radius), as previously described [9].

The median nerve was positioned centrally, with the radial and ulnar nerves placed at −1.1 cm and +1.6 cm from the centre, respectively. Tissue dielectric properties were assigned based on literature values at 50 Hz [10]. A stationary 5 mA simulation solved the quasi-static field equations using von Neumann, Dirichlet, and insulating boundary conditions, with the external ring as the anode and the central electrode as the cathode [6]. Current density was measured along a longitudinal line beneath the electrode surface. To assess current density non-uniformity, we used the normalised peak-to-average ratio, this value is represented by the maximum, minimum and average values of current density (J)(1) [6]. Higher values of k indicate greater spatial variability and potential for localised discomfort. Two concentric designs differing in size (Designs 1 and 2) were also compared to a square electrode of equivalent surface area and inter-electrode spacing to assess differences in current distribution.

$$k = \frac{J_{max} - J_{min}}{J_{avg}} \quad (1)$$

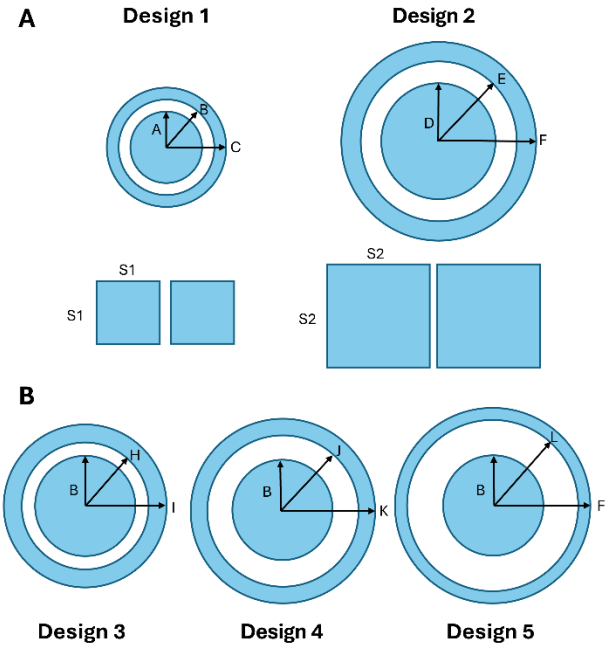

Figure 1: To-scale representation of the concentric ring electrode designs utilized in this study. A) Designs 1 and 2 illustrate variations in electrode size with a comparison of square electrode of equal areas, while B) Designs 3 to 5 adjust the inter-electrode distance maintaining the same area of anode and cathode and between designs. Dimensions in mm: A=7.5, B=10, C=12.5, D=12, E=16, F=20, H=12.2, I =15.75, J=15, K=18, L=17.32 S1=13.4 and S2=21.3.

The MRG model was implemented in MATLAB using the AxonSim framework, which was adapted to incorporate extracellular potentials extracted from the FEM simulations [11], [12]. A single myelinated fibre with a diameter of 16 µm was used to represent a large Aα motor axon and was positioned at the centre of the nerve [12]. The external voltage was interpolated to the axon structures and applied as external stimulus. The fibre model included 134 Ranvier nodes along its length, and a monophasic pulse with a duration of 150 µs was used for stimulation. Transmembrane potentials were computed over time at each node to assess axonal activation. A three-level selectivity scale was applied based on the activation pattern of the target and off-target axons: *poor selectivity* (activation of all nerves), *partial selectivity* (target and off-target activation), and *high selectivity* (only target activation).

Results

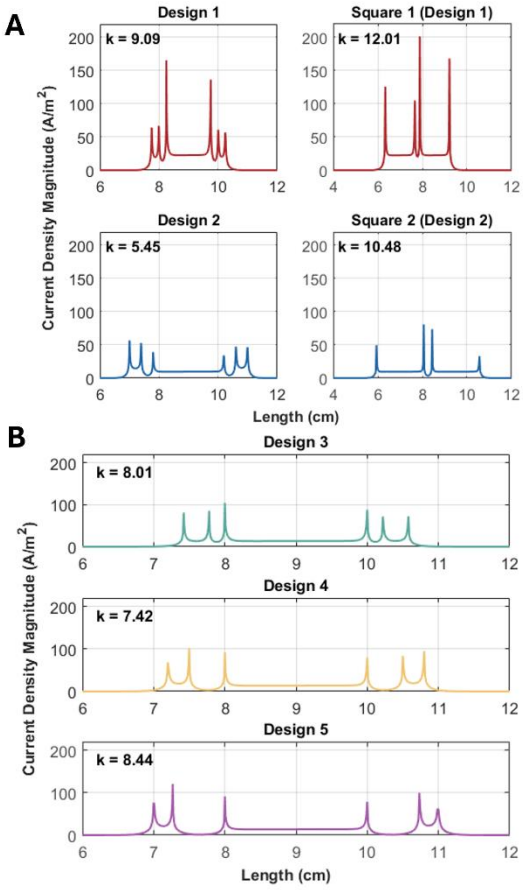

Figure 2: Current density magnitude profiles and k values for different designs of concentric electrodes. A) Shows the influence of electrode size compared to a square electrode with same dimensions. B) Shows the effect of varying inter-electrode distance.

The current density distributions for the five concentric electrode designs are shown in Fig. 2. Higher current density peaks were observed at the electrode edges, particularly in smaller configurations such as Design 1, which reached values near 160 A/m². In contrast, Design 2 exhibited a lower peak (~60 A/m²) and improved uniformity, reflected by a reduced k value. Comparisons with equivalent square geometries showed consistently higher k values, indicating greater non-uniformity. In Designs 3-5, where inter-electrode distance was varied, central current density remained relatively stable, but decreasing the thickness of the external electrode led to elevated peripheral peaks and increased k values. Axonal responses to each design are presented in Fig. 3. Action potential propagation occurred in the median nerve for all designs, while activation of off-target nerves varied. Designs 1 and 3 demonstrated high selectivity, whereas Designs 2 and 5 activated all three nerves.

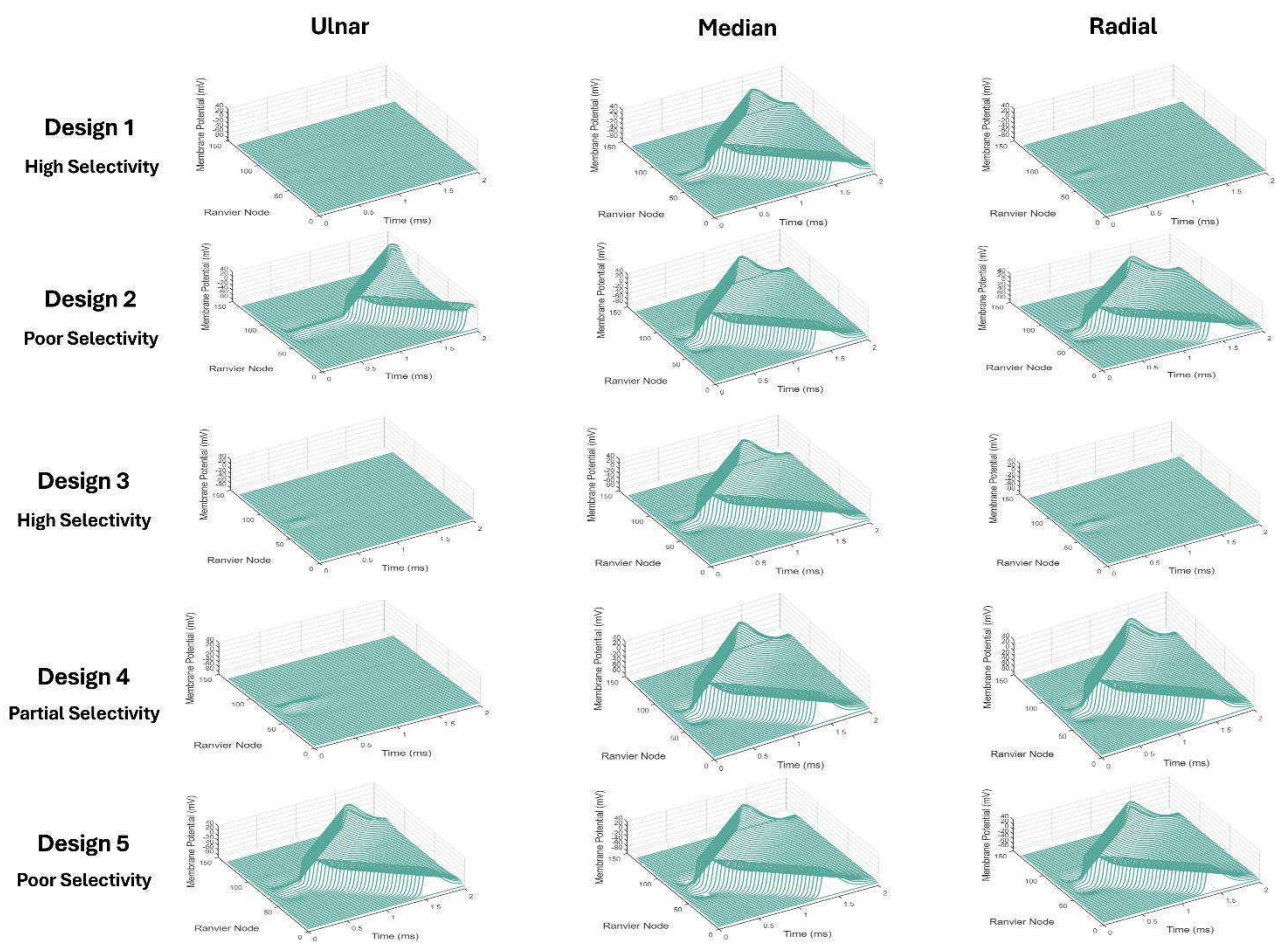

Figure 3: Membrane potential (mV) over time and along Ranvier nodes in the ulnar, median, and radial nerves for each electrode design. Propagating action potentials indicate nerve activation and reflect differences in stimulation selectivity across configurations.

Design 4 resulted in partial selectivity, activating both target and one off-target nerve. Square electrode 1 showed a propagation of the action potential in the median and radial nerve but not in the ulnar (partial selectivity), in contrast, the Square 2 triggered action potential in the three nerves (poor selectivity).

Discussion

This study systematically evaluated how geometric parameters of concentric electrodes—specifically electrode size and inter-electrode distance—influence current density distribution and axonal activation using a combined FEM and axon modelling approach.

The results show that medium-sized concentric configurations with reduced inter-electrode spacing can preserve selective activation while limiting current concentration at the electrode edges. Building on earlier analytical studies of concentric electrode configurations [7], this work incorporates anatomically inspired volume conductors and active fibre models to analyse design parameters effects on stimulation selectivity and comfort. Concentric electrodes with smaller surface areas exhibited higher stimulation selectivity, effectively activating the target nerve while avoiding off-target responses [6]. However, these same configurations also generated greater peak current densities and more pronounced edge effects, as reflected in elevated k values. Compared to square electrodes of equivalent area and spacing, concentric designs demonstrated lower k values and greater selectivity, emphasising the relevance of geometry in optimising stimulation performance. Medium-sized concentric rings with reduced inter-electrode distance preserved selective activation while lowering peak current density at the skin surface. Conversely, increasing the inter-electrode spacing—resulting in a thinner outer ring—led to elevated edge current densities and higher k values. While reducing this spacing improved selectivity, it may also limit activation depth, underscoring the importance of managing skin impedance. This could be addressed using high-performance hydrogels [13] or medium-frequency stimulation to enhance current penetration. While this study offers detailed insights into the effects of concentric electrode geometry, it is based on a simplified anatomical model and a simulation-only approach. Although effective for controlled analysis, these models do not fully capture in vivo complexity.

A detailed understanding of how concentric ring geometry influences both current distribution and axon activation is essential for the rational design of electrodes tailored to specific functional applications. The results of this study highlight that design parameters—particularly outer ring thickness and inter-electrode spacing—play a critical role in balancing stimulation selectivity, field

uniformity, and potential discomfort. Fine-tuning these parameters enables the customisation of electrode configurations to meet the distinct requirements of different FES applications, whether prioritising focal activation or improved comfort. Future work will focus on conducting in vivo experiments to validate the proposed electrode designs under physiological conditions. Additionally, task-specific evaluations will be assessed to tailor concentric configurations to different clinical objectives, enabling the optimisation of stimulation strategies for neurorehabilitation applications.
This work provides a systematic and anatomically grounded evaluation of concentric ring electrode geometry, demonstrating how specific design parameters influence current distribution and axons electivity in non-invasive FES. By identifying configurations that optimise both stimulation precision and field uniformity, the findings offer practical guidance for electrode design across diverse clinical applications. These results lay the foundation for translating concentric electrode systems into more targeted, comfortable, and effective neurorehabilitation interventions.

Conclusions

This study provides a systematic, simulation-based analysis of concentric ring electrode design for non-invasive FES, demonstrating how geometric parameters influence stimulation selectivity and current distribution. The results offer practical guidance for optimising electrode configurations to improve comfort and targeting precision and establish a foundation for future in-vivo validation and clinical translation.

Acknowledgement

The authors would like to thank ANID-Subdirección de Investigación Aplicada for their financial support under grant FONDEF ID24i10422, which made this research possible. Javier Sáez would like to thank ANID for its support through the scholarship ANID-Subdirección de Capital Humano/Magíster Nacional/22250256.

References

[1] A. S. P. Sousa *et al.*, 'Usability of Functional Electrical Stimulation in Upper Limb Rehabilitation in Post-Stroke Patients: A Narrative Review', *Sensors*, vol. 22, no. 4, Art. no. 4, Jan. 2022, doi: 10.3390/s22041409.

[2] M. Gandolla, L. Niero, F. Molteni, E. Guanziroli, N. S. Ward, and A. Pedrocchi, 'Brain Plasticity Mechanisms Underlying Motor Control Reorganization: Pilot Longitudinal Study on Post-Stroke Subjects', *Brain Sci*, vol. 11, no. 3, p. 329, Mar. 2021, doi: 10.3390/brainsci11030329.

[3] A. Martín-Odriozola *et al.*, 'Analysis of the movements generated by a multi-field functional electrical stimulation device for upper extremity rehabilitation', *Artificial Organs*, vol. 46, no. 10, pp. 2027–2033, 2022, doi: 10.1111/aor.14346.

[4] M. G. Garcia-Garcia, L. I. Jovanovic, and M. R. Popovic, 'Comparing preference related to comfort in torque-matched muscle contractions between two different types of functional electrical stimulation pulses in able-bodied participants', *The Journal of Spinal Cord Medicine*, vol. 44, no. sup1, pp. S215–S224, Sep. 2021, doi: 10.1080/10790268.2021.1970882.

[5] A. Kuhn, T. Keller, M. Lawrence, and M. Morari, 'The Influence of Electrode Size on Selectivity and Comfort in Transcutaneous Electrical Stimulation of the Forearm', *IEEE Transactions on Neural Systems and Rehabilitation Engineering*, vol. 18, no. 3, pp. 255–262, Jun. 2010, doi: 10.1109/TNSRE.2009.2039807.

[6] N. RaviChandran, M. Y. Teo, K. Aw, and A. McDaid, 'Design of Transcutaneous Stimulation Electrodes for Wearable Neuroprostheses', *IEEE Trans. Neural Syst. Rehabil. Eng.*, vol. 28, no. 7, pp. 1651–1660, Jul. 2020, doi: 10.1109/TNSRE.2020.2994900.

[7] M. G. Cassar, C. Sebu, M. Pidcock, S. Chandak, and B. Andrews, 'Optimal design of electrodes for functional electrical stimulation applications to single layer isotropic tissues', *COMPEL*, vol. 42, no. 3, pp. 695–707, May 2023, doi: 10.1108/COMPEL-08-2022-0293.

[8] M. Stefano, F. Cordella, A. Loppini, S. Filippi, and L. Zollo, 'A Multiscale Approach to Axon and Nerve Stimulation Modeling: A Review', *IEEE Transactions on Neural Systems and Rehabilitation Engineering*, vol. 29, pp. 397–407, 2021, doi: 10.1109/TNSRE.2021.3054551.

[9] J. Sáez *et al.*, '3D-Printed Electrode Fabrication for Functional Electrical Stimulation (FES): Prototyping Concentric Electrodes', in *2024 46th Annual International Conference of the IEEE Engineering in Medicine and Biology Society (EMBC)*, Jul. 2024, pp. 1–4. doi: 10.1109/EMBC53108.2024.10782379.

[10] IT'IS Foundation, 'Dielectric Properties'. [Online]. Available: https://itis.swiss

[11] S. Danner, C. Wenger, and F. Rattay, *Electrical stimulation of myelinated axons: An interactive tutorial supported by computer simulation*. 2011.

[12] C. C. McIntyre, A. G. Richardson, and W. M. Grill, 'Modeling the Excitability of Mammalian Nerve Fibers: Influence of Afterpotentials on the Recovery Cycle', *Journal of Neurophysiology*, vol. 87, no. 2, pp. 995–1006, Feb. 2002, doi: 10.1152/jn.00353.2001.

Author's Address

Pablo Aqueveque.
Department of Electrical Engineering, Universidad de Concepción.
E-mail: paaqueve@udec.cl
https://sites.google.com/biomedica.udec.cl/pabloaqueveque/home?authuser=0

Low-Resistance Cost-Efficient Interfacing for Neurostimulation Needles based on Printed Circuit Board Technology

Schuh K[1], Scholz M[1], Chowdhury D[1], Kaniusas E[1]

[1]Institute of Biomedical Electronics, TU Wien, Austria

Abstract:
Neurostimulation is progressively coming into focus as a treatment for chronic diseases. Percutaneous neurostimulation typically involves connecting electrodes to wires via electrode holders. Common needle holders are proprietary, which results in reduced flexibility and high costs, posing significant barriers to experimental and research purposes. This work presents a cost-efficient, low-resistance connector interface design for neurostimulation needles, based on a two-layer Printed Circuit Board. The mechanical and electrical characteristics of two geometric designs, with inner hole diameters of 1.95 mm, 2.05 mm, and 2.15 mm, were investigated. The electrical properties of the produced needle holders were analysed through systematic resistance measurements using a precision milliohm meter and a four-wire technique. The v*alidation results indicate an average contact resistance in the milliohm range of 62 mΩ to 70 mΩ, representing a reduction in resistance by a factor of at least 658 compared to conventional commercial adapters with a resistance in the range of 46 Ω to 90 Ω. The proposed solution has high potential for rapid prototyping and small-batch production in biomedical neurostimulation research.*

Keywords:
Percutaneous Neurostimulation, Printed Circuit Board, Needle Holder, Four-Wire Technique, Milliohm Meter

Introduction

The treatment of chronic pain and injuries still mainly consists of administering various types of drugs. Two promising concepts for improving success rates and the overall healing period are functional muscle stimulation and neurostimulation [1]. Different electrical stimulation devices have been developed, with electrical neurostimulation representing one branch of the evolution of acupuncture [2].
Regardless of the application area, the initial problem with neurostimulation using percutaneous needles is establishing an electrical connection between the stimulator device and the specific microneedle. While modern commercial stimulators have custom-made electrical connectors for their neurostimulation needles, prototypes or stimulator units intended for research purposes often lack flexible options for connecting commercially available and self-designed neurostimulation needles.
This research therefore focuses on developing low-resistance, cost-efficient connectors for neurostimulation needles that are designed for small-batch production using common Printed Circuit Board (PCB) technology. A PCB panel featuring two designs of needle holder was created for percutaneous auricular Vagus Nerve Stimulation. The panel featured the two designs of needle holders with three different hole sizes, to evaluate the most suitable hole size and geometry for connecting the neurostimulation needles.

Material and Methods

The PCB design software Altium Designer was used to generate the necessary PCB design files. The individual components of this PCB were designed as a panel design.

To automate the generation of the design files, a custom output job file was created to generate the necessary Gerber X2 files for the specific PCB manufacturer. A process called edge plating is used to establish a connection through the hole in the PCB, connecting the traces on the top and bottom sides with the cable connection side. To remove a single connector from the batch, so-called 'mouse bits' need to be used to enable a cut-out via wire cutters. To reduce production costs, the manufacture of these connectors was outsourced to the Chinese company JLCPCB.
The geometric design of the needle holders was based on a design produced by a company that will be referred to as 'reference design' in this publication. Due to the unknown manufacturing tolerances for the hole diameters, PCB needle holders with hole diameters of 1.95 mm, 2.05 mm and 2.15 mm were chosen, since the reference design of the needle holders has a hole diameter of 2.10 mm.
To evaluate the resistance of the custom-made needle holders, a DC Milliohm Meter (RS PRO RM-805) was used. This device uses a four-clamp measurement technique to compensate for the resistance added by the source connection lines to the Device Under Test (DUT), enabling more precise measurement of the connector's resistance. The DUT was connected to the milliohm meter using 4-wire terminals (GW Instek, 1100MTL308001). In this case, the DUT is the entire needle holder. Five needle holders were prepared for each design, and the resistance was measured from the tip of the neurostimulation needle to the end of the 10 cm long connection cable (Alpha Wire, 2840/7 BK005) using the described milliohm meter. To determine the resistance of each individual needle holder, each design was measured 100 times in succession.
The measurements were performed at a mostly constant temperature ranging from +22 °C to +28 °C. To ensure that the temperature remained constant throughout the

measurement period, the entire setup was enclosed in an acrylic housing containing a temperature probe to monitor the temperature during the measurement (Fig. 1). A PT-100 temperature sensor (Pico Technology, SE011) was used to record the temperature development.

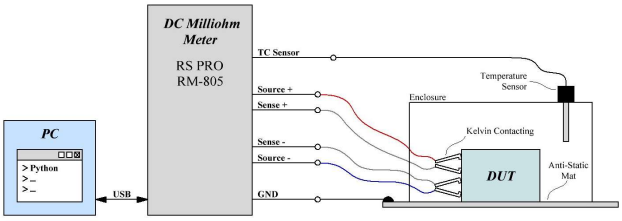

Figure 1: Illustration of the schematic test procedure for determining the resistance of the needle holders, including co-measurement of the ambient temperature.

To measure the DUT's resistance, the milliohm meter was set to 'pulse' operation to compensate for the thermoelectric electromotive force (EMF) formed at the contact point between the test lead and the DUT. The devices therefore switch their output voltage on the source channels of the measuring device every 50 ms between +6.25 V and -6.25 V [3, p. 32-33]. To achieve the best measurement resolution, the measuring device was set to auto range, which allows it to adapt smoothly to the best measurement range. The characteristics of the measurement ranges used can be found in Tab. 1. To ensure that the measuring range characteristics specified in Tab. 1 are valid, special measurement conditions must be observed. Therefore, the measuring device must operate within a temperature range of +18 °C to +28 °C, with a relative humidity no greater than 80%. These limitations were set during the measurement process. Additionally, the data acquisition rate must be set to 'slow', resulting in a rate of 10 readings per second. Finally, the device was switched on for at least 30 minutes before the acquisition of data started to ensure the thermal stability of the device. To also ensure the thermal stability of the DUT, each measurement was carried out one minute after the DUT had been connected [3, p. 156-157].

Table 1: Accuracy of the milliohm meter at different measurement ranges [3, p. 156].

		Accuracy	
Range (Ω)	**Resolution (mΩ)**	**Reading (%)**	**Range (%)**
0.5	0.01	0.05	0.02
50	1	0.05	0.02
500	10	0.05	0.08

The mean measurement error resulting from the overall accuracy of the measuring device can be calculated for all measured needle holders using Eq. 1 from the mean values. Where ΔR_{sys} represents the systematic measurement error, γ represents the total accuracy found in Tab. 1, R_{meas} represents the measured mean value of the DUT's resistance, and δ represents the resolution of the device's specific range found in Tab. 1.

$$\Delta R_{sys} = \sqrt{(\gamma \cdot R_{meas})^2 + \delta^2} \quad (1)$$

Data acquisition and milliohm meter control were carried out via a universal serial bus (USB) interface connected to a notebook on which a self-written Python program was being executed. This program was responsible for establishing the connection with the measurement device, performing all the initial settings, triggering the measurements, and storing the generated data in an Excel file. The data has been analysed and evaluated via Matlab R2024a, using box plots to represent the distribution of resistance in the individual measurements. Any measured value above 1.5 times the Interquartile Range (IQR) or below 1.5 times the IQR is considered an outlier.

Results

Two different designs of needle holders were realised, which are shown in Fig. 2. Design 2 is completely round, while design 1 has a small solder pad attached to one side. Each of these two designs was executed twice on the panel in the hole sizes 1.95 mm, 2.05 mm, or 2.15 mm to determine the optimal size for connection with the neurostimulation needles. Each connector style, with each hole size is executed 16 times on the PCB, resulting in 96 individual needle holders on one panel. Each needle holder is connected to the panel using mouse bites, which allow the individual needle holders to be cut out with a wire cutter. This PCB design uses panel design and mouse bites due to manufacturing limitations, as the geometry of a needle holder is smaller than the PCB's minimum design size.

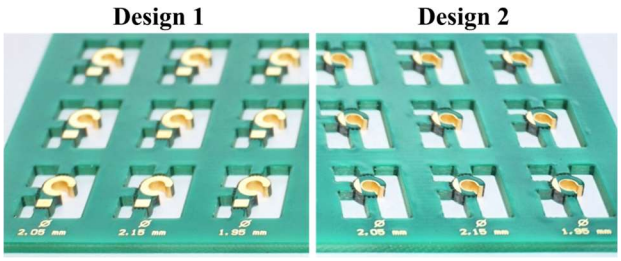

Figure 2: Layout of the PCB needle holder panel. Two different geometric designs are shown, with three different hole sizes.

The final design of the needle holders consists of a custom-made 2-layer PCB with a thickness of 1.6 mm. FR4 was used as the base material for the PCB, which was coated with a 35 µm (1 oz) thick copper layer. To prevent direct skin, contact with the copper, an ENIG layer with a thickness of 0.0508 µm (2 u") was applied, and all non-essential surfaces were coated with solder resist. To ensure stable, low-resistance electrical connection with the neuron needle, a copper layer was first applied to the through-hole using edge plating and then coated with an ENIG layer.
A comparison of the different needle holders can be seen in Fig. 3. The Computer-Aided Design (CAD) models of the custom-made needle holders (Fig. 3a and 3b) are shown alongside the manufactured ones (Fig. 3c and 3d).

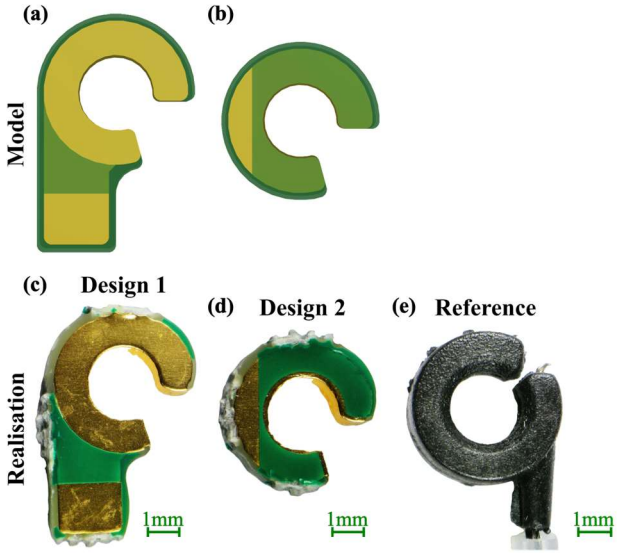

Figure 3: Illustration of the three different needle holders for connecting percutaneous neurostimulation needles. a) Model design 1, b) Model design 2, c) Realised design 1, d) Realised design 2, e) Company reference design.

The mechanical removal process from the PCB panel caused damage to the connectors in the form of dents in the metal layers, cracks in the solder resist and uneven edges. A comparison of the dimensions shows that design 1 (Fig. 3c) has the largest dimensions, resulting in a length of 6.8 mm and a width of 4.5 mm. Design 2, seen in Fig. 3d, on the other hand, has the smallest geometrical dimensions, with a diameter of 4.5 mm. Finally, the reference design, seen in Fig. 3e, has a length of 5.48 mm and a width of 4.36 mm.
Although two designs of needle holder with three different hole sizes were developed, only the adapters from both designs with a 2.15 mm hole size were measured. The average results for each needle holder design can be found in Tab. 2 and are essential for feasibility considerations if the measurements were carried out correctly. According to the measurement data found in Table 2, 2, designs 1 and 2 perform similarly, with mean resistances between 62.6234 mΩ and 70.9053 mΩ. The reference design, on the other hand, have resistance values ranging from 46.6603 Ω to 90.5832 Ω, which is at least a factor of 658 higher.

Table 2: Display of the averaged measured values (mean value ±standard deviation) of the tested needle holders. Each sample n = 5 was subjected to 100 consecutive individual measurements.

n (1)	Design 1 (mΩ)	Design 2 (mΩ)	Reference Design (Ω)
1	67.9846 (±0.0351)	64.3472 (±0.0263)	90.5832 (±1.2063)
2	70.9053 (±0.1431)	64.7648 (±0.4895)	77.0519 (±0.0390)
3	67.3189 (±0.0432)	68.7143 (±0.0531)	46.6603 (±0.1468)
4	62.6234 (±0.0212)	63.5070 (±0.0052)	85.7503 (±0.6015)
5	67.1361 (±0.0925)	68.2485 (±0.0094)	79.6098 (±0.7326)

The measured resistance distribution of the five needle holders, measured per design group, is displayed in boxplots shown in Fig. 4. Classified outliers are represented by red circles in the figure shown. The higher number of outliers for the self-made needle holders is due to the low resistance values that were measured. Even minor environmental influences can have a significant impact on the measurement. As can be seen from the data displayed in Fig. 4, the resistance of the custom-made needle holders varies from 0.01% to 0.76% when compared to the reference design, which varies from 0.05% to 1.33%. Conversely, there is a significant difference in the resistance of the reference design. The displayed data also shows that the resistance values of the custom-made and company-produced needle holders differ by a factor of at least 658.

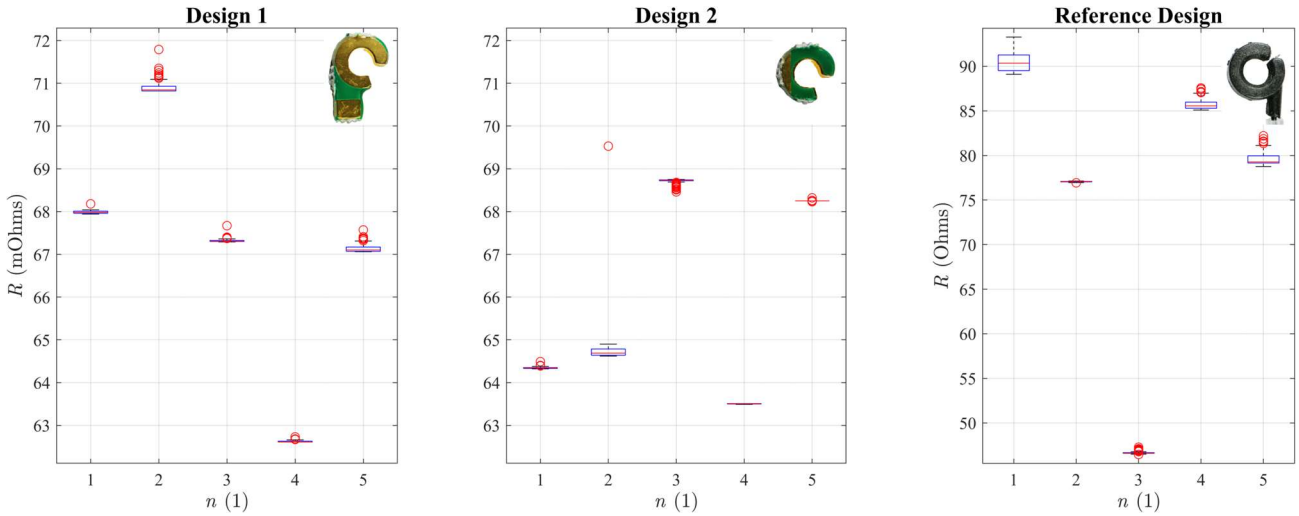

Figure 4: Boxplots of measured resistance values for investigated needle holders (n = 5 samples for each design, with 100 consecutive individual measurements, outliers in red).

Discussion

Considering that the main goal of electrical neurostimulation is to transmit power from the stimulation device to the targeted nerve, it is important that most of the emitted power reaches its intended destination. To minimise power loss during stimulation, the resistance of the connection between the stimulation device and the neurostimulation needle must be as low as possible. Otherwise, the stimulation device would need to compensate for the voltage drop across the interface by increasing the output voltage. Currently, many different approaches are available on the market, but they are mostly restricted to specific customers. Therefore, a solution must be found to create an easily produced, cost-efficient connector that provides excellent resistance characteristics. Based on these requirements, PCB technology was chosen, as it has proven its worth in electronics development over many years.

In our research, we developed two designs of needle holder with hole sizes of 1.95 mm, 2.05 mm and 2.15 mm that use PCB technology to test the connection of a specific, commercially available neurostimulation needle. Although designs with three different hole sizes were developed for the needle holders, only the adapters with a 2.15 mm hole size from both designs were measured, as only these fit the neurostimulation needles used in our research group. The PCB needle holders exhibited resistance values ranging from 62.6234 mΩ to 70.9053 mΩ, whereas the reference design exhibited values ranging from 46.6603 Ω to 90.5832 Ω.

In accordance with the requirements for the needle holder, the fit must be as accurate as possible and reproducible. While achieving the required accuracy of fit for the needle geometry used in the PCB design programme is not challenging in principle, implementing the design in PCB production certainly is.

One particular limitation of this technology is that full reproducibility cannot be guaranteed due to contact between the layers and the through-hole, as the copper layer applied is highly dependent on the electroplating process used. Irregularities in this process can result in uneven layer thicknesses and altered hole diameters.

As the chosen production approach for the needle adapters is novel and their long-term skin compatibility is largely unknown, further investigations into their cytotoxicity for this application are necessary.

In this context, it should be noted that cracks or splintering of the solder resist may occur due to the structure of the PCB panel, which could result in uncoated copper encountering the skin. This is due to the resistance of the FR4 base material. The needle holders can only be removed from the contact points of the mouse bites using wire cutters with increased force. To counteract this problem in future developments, the distance between the mouse bites and the required copper plane for connection can be increased. Alternatively, a V-cutting process could be employed during PCB production. Reducing the PCB thickness from 1.6 mm to 0.8 mm to 1 mm could also reduce the occurrence of these problems, as this would reduce the base material's resistance. The outlook for future PCB designs should focus on structural modifications that minimise mechanical stress concentrations during the cutting process.

Conclusions

The proposed PCB needle holders are a cost-effective solution for small-batch production and prototyping. Their low resistance also makes them an ideal interface between neurostimulation needles and stimulator units for percutaneous applications.

Acknowledgement

The authors acknowledge funding by the TU Wien and its Institute of Biomedical Electronics.

References

[1] Y. Zheng et al., Neurostimulation for Chronic Pain: A Systematic Review of High-Quality Randomized Controlled Trials With Long-Term Follow-Up, Neuromodulation: Technology at the Neural Interface, vol. 26, no. 7, pp. 1276–1294, 2023, doi: 10.1016/j.neurom.2023.05.003.

[2] M.-H. Jun, Y.-M. Kim, and J. U. Kim, Modern acupuncture-like stimulation methods: A literature review, Integrative Medicine Research, vol. 4, no. 4, pp. 195–219, 2015, doi: 10.1016/j.imr.2015.09.005.

[3] Good Will Instrument, D.C. Milli-Ohm Meter: GOM-804 & GOM-805, [Datasheet], URL: https://www.gwinstek.com/en-global/products/downloadSeriesDownNew/11052/862, June 2025.

Author's Address

Kevin Schuh
Institute of Biomedical Electronics
TU Wien
kevin.schuh@tuwien.ac.at
https://www.tuwien.at/etit/bme

AI electrode and stimulus design for FES research: a pilot study

Hall SM[1], Sáez J[2], Tsakonas P[3], Osorio R[2], Saavedra F[4], Aqueveque P[2], FitzGerald J[1], Andrews B[1,3]

[1]University of Oxford, Oxford, United Kingdom
[2]Universidad de Concepción, Concepción, Chile
[3]University of Warwick, Coventry, United Kingdom.
[4]Universidad del Bio Bio, Concepción, Chile

Abstract: *We present a pilot study to explore the potential for AI surrogate modelling to support state-of-the-art numerical methods for iterative electrode design for transcutaneous peripheral nerve stimulation. The numerical methods are computationally intensive, slowing down the initial exploratory phase. We demonstrate a data collection pipeline, which comprises generation of simulation data using numerical methods, followed by training of a three layered feed-forward artificial neural network (ANN). We present results demonstrating proof of concept, that an ANN can be trained to predict whether or not an axon within a femoral nerve bundle at a specific depth below the surface will activate under a range of applied geometries and stimuli. This is achieved with a significantly reduced computational cost. We speculate on future uses, specifically the potential for the electrode design process to be accessible to multiple disciplines, in low resource environments (e.g. a computer in a clinical department), as well as to be used by clinicians and physiotherapists in real-time to determine parameters suitable for a specific patient.*

Keywords: *transcutaneous electrodes, functional electrical stimulation, finite element modelling, surrogate modelling*

Introduction

The therapeutic uses for transcutaneous peripheral nerve stimulation, such as FES, are widely adopted, given its advantages over invasive techniques such as reduced cost and risk of surgical complications. The effects of stimulation are determined by a combination of the shape of the electrode (which may be optimised to increase selectivity by modifying the stimulating potential field distribution), its anatomical placement and the applied stimulus parameters. Since the advent of low-cost microcontrollers it has been possible to synthesise a wide variety of stimulus waveforms, but in therapeutic settings the applications are still limited by the selection of commercially available electrode shapes that have not changed significantly for more than 100 years. However, the development of more effective combinations of electrodes and stimulus waveforms for research is progressing. This is due to recent advancements in computational methods and printed electrode technology. These techniques have been used to better target nerves using both traditional round, rectangular or square electrodes [1,2]; as well as customisable and optimised shapes. In the latter case, these shapes may provide a more effective solution but are not available commercially. However, they can be printed in the lab, in small series, using low cost 3D printers [3]. Specialist companies exist that can print larger numbers of customised electrodes commercially.

The typical pipeline for modelling peripheral nerve stimulation involves the coupling of a finite element model to a compartmental model (in our case, the McIntyre-Richardson-Grill (MRG) axon). These involve two physical systems: the first physical system is the finite element model (FEM), which solves for the quasi-static field equation which approximates the potential field. The second physical system is the MRG axon which is coupled to the potential field to approximate the response of an axon to the stimulation. The combined physical systems allow us to approximate whether an axon will activate or not given a proposed electrode configuration and stimulation protocol.

Despite numerical methods being considered state-of-the-art (SOTA) in this domain, there are significant computational constraints that limit our ability to rapidly explore the parameter space in models of transcutaneous electrical nerve stimulations. The growing field of AI surrogate modelling aims to address this problem. Surrogate modelling is an engineering method to develop an approximation of a mathematical model, such as the combined physical system we describe above. Essentially, we aim to develop a "model of a model" using an artificial neural network (ANN). The idea being that once sufficiently trained, we can use the surrogate model to determine whether an axon will activate or not, more rapidly and with a lower computational cost than with the primary model. Surrogate models, particularly those making use of ANNs, typically follow one of two core methodologies: data-driven (where the ANN is treated as a black box and trained to learn an input-output mapping) [4] and physics-inspired (where we constrain the learning process and parameter space using physics principles) [5]. While the latter of these solutions is typically more interpretable, in this exploratory study we have focussed exclusively on a data-driven approach. Related works have shown initial proof of concept using ANNs to demonstrate surrogates of implanted electrodes in the peripheral [6] and the central nervous systems [7], as well as to train a neural network to approximate the MRG axon [8]. We look to expand upon this, specifically within the field of transcutaneous stimulation of the femoral nerve. We will explore two electrode configurations, a square and a concentric electrode, to determine if an ANN can learn to predict if an axon activates or not, under a range of applied geometries and

stimuli. The training and testing data are based on simulation data we run.

This work is predicted to impact the field of electrode design by supporting iterative and fast exploratory phases that complement the SOTA numerical methods. We also foresee these being used in low resource settings (e.g. a computer in a clinical department) to be used by clinicians and physiotherapists in real-time to determine parameters suitable for a specific patient. We also hope to facilitate wider participation from multiple disciplines in the electrode design process (see Figures 1 and 2).

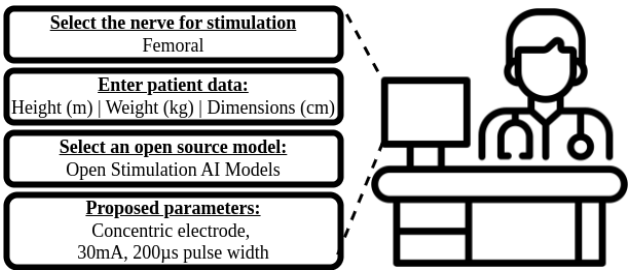

Figure 1: Imagining a future of customisable electrode design and stimulation protocols.

Material and Methods

Our hypothesis is that a neural network can be trained to predict whether or not an axon within a femoral nerve bundle will activate under a range of applied geometries and stimuli. Parameters include the axon depth below the skin surface, the electrode shape and configuration, and the specific stimulation protocol. We present the methods employed to investigate this. All code and simulated data is available on Github: https://github.com/idslabudec/fes-ai-surrogate-modelling.

Data preparation: In order to train the ANN, we prepared multiple simulations coupling the potential field to an MRG axon and recorded parameters and output. The data preparation was two-fold: *1) Finite element model:* We started with a baseline template 3D model of the thigh, femoral nerve and electrodes, set up manually in the COMSOL GUI, using the methods described in [9,10]. Electrode geometries (a square and concentric electrode, see Figure 3) were systematically varied by altering both the inter-electrode distance and electrode size to explore a wide stimulation parameter space. Additionally, we iterated parameters creating permutations of all the following variables. The axon depths below the surface ranged between 1.4 - 3.4 cm (step 0.4 cm). For the square electrode, the inter-electrode distance and length of the side ranged between 0.1 to 3.7 cm (step 0.4 cm), and 2-4 cm (step 0.2 cm) respectively. For the concentric ring, the inter-electrode distance range is 0.1-1 cm (step 0.25 cm); with the central electrode diameter ranging between 1-5 cm (step 1 cm) ringer inner radius 0.6-3.5 (step 0.5 cm) and ring outer radius 0.78-4.3 cm (step 0.7 cm). Current was varied between 0 - 60 mA (step 3 mA) and the pulse duration ranged between 0 - 250 µs (step 50 µs). The mesh was built, and the model solved using the stationary solver. The potential field was exported as a 1D array of extracellular potential values (V) to be coupled to the MRG axon. *2) MRG axon:* Each stimulus was modelled as a monophasic pulse with a varied pulse duration. The axonal response was computed across time to determine action potential initiation and propagation, with activation defined as a membrane potential deflection crossing a threshold of 0 mV in the nodes of Ranvier (see Figure 4).

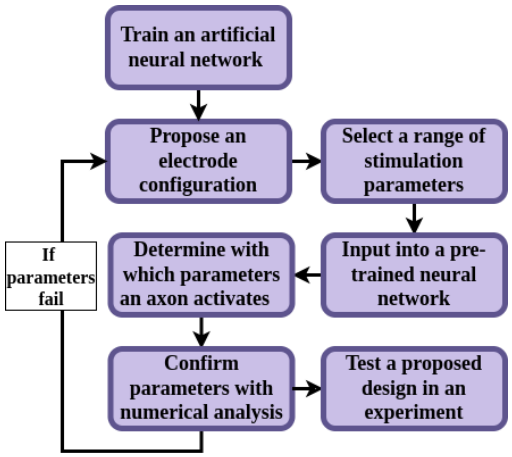

Figure 2: Proposed computational pipeline to support iterative electrode design

Model architecture: The neural network is set up using PyTorch and comprises a three layer feedforward neural network, with tanh and ReLU non-linearity and a sigmoid activation function. We use a binary cross entropy loss.

Model training: We split the data (total number of simulations per electrode is detailed in Table 3) into a training set (70%), as well as validation and test sets (15% each) for the final inference test. Distribution checks of the training, validation and test sets were done to ensure similar proportions across all sets. A separate ANN is trained for each electrode configuration.

Computational requirements: A core motivation of this work is to reduce computational demands, and therefore we detail all the computations required to prepare the simulation data, as well as to train and test the ANN. All simulations were run using COMSOL Multiphysics® 6.1 in conjunction with LiveLink™ for MATLAB® R2023a on a computer with an Intel core i7-10700 and 32 GB RAM. For the ANN, training and inference is run on a CPU, using 16 GB RAM.

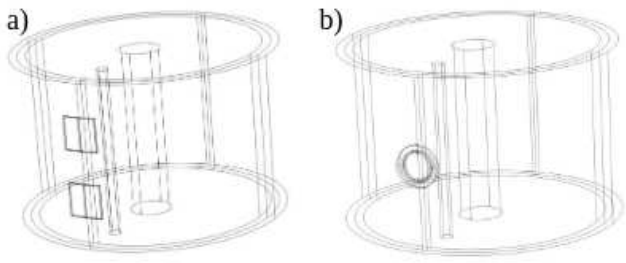

Figure 3: Template of the square (a) and concentric (b) electrode configurations

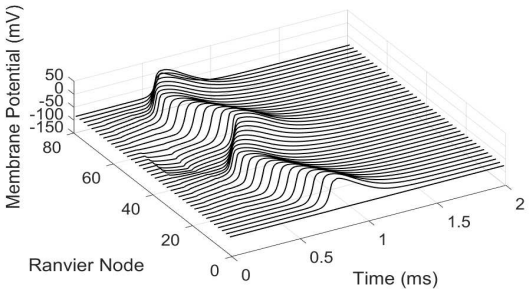

Figure 4: Example simulation of a MRG axon activation: the membrane potential crosses the threshold

Table 2: Average compute times (s) for a MRG axon simulation as well the requirements for the ANN training and for inference, per electrode configuration

		Square electrodes	Concentric electrode
MRG	**Average time per simulation**	25.48	28.80
ANN	**No. of simulations**	15876	18990
	Training (s)	196.77	307.15
	Inference (s)	0.042	0.045

Results

Computational demands: For each iteration, we recorded the total computational time and number of degrees of freedom (DOFs) in the FEM (see Figure 5), as well as the computational time required to simulate the MRG axon model in MATLAB (see Table 2). In addition to the above, there is an initial setup time of 2 hours for both templates and the code. As shown in Table 2, there is a significant reduction in the computation time, with the entire training process taking less than 2 minutes in both cases, as compared to approximately 25-28 seconds *per simulation run* of the MRG axon.

ANN training: We trained a neural network using 70% of the data, and validated on 15% of the data. Figure 6 demonstrates both the ANNs for both electrode configurations are learning, as the accuracy increases, while the validation and training loss decreases. This indicates the model is making fewer mistakes as training progresses across the epochs.

ANN testing: We tested the model on a held out test set comprising 15% of the data. Results are presented in Table 3. The ANNs for both the square and the concentric electrodes yield accurate predictions of activation on unseen data and require negligible time for inference.

Table 3: Test accuracy per ANN

	Square electrodes	Concentric electrode
Test accuracy (%)	98.27	97.90

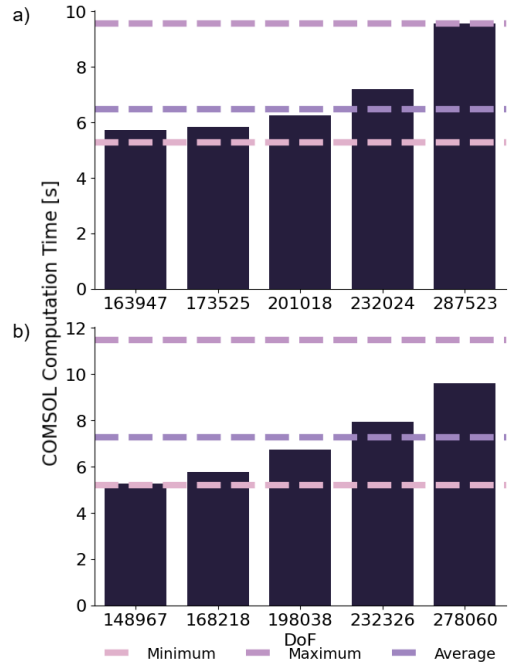

Figure 5: Compute times per increasing degrees of freedom (DoF) in a FEM with a square (a) and a concentric (b) electrode configuration. The bars represent a subsample of the DoF, with the average, minimum, and maximum being for the entire set.

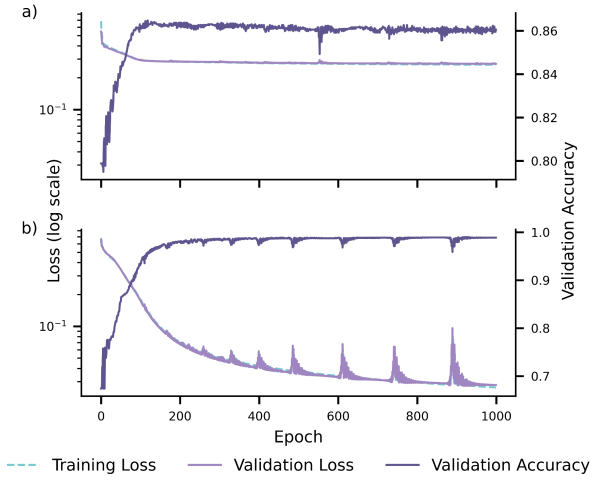

Figure 6: Training loss, and validation loss and accuracy for the square (a) and concentric (b) electrode configurations

Discussion

We have demonstrated proof of concept that a data driven ANN can be trained to predict the activation of an axon, given input parameters. We envisage this pipeline will accelerate research in FES, particularly in transcutaneous electrical nerve stimulations. Importantly, this was done for multiple electrode configurations, which is important for future work to support exploratory and iterative electrode design. However, while we are able to predict the output of the ANN accurately, we currently have limited interpretability. As such, additional outputs from the ANN are required to validate whether this model has

captured the full dynamics of the MRG axon. In future work, we intend to explore a physics inspired approach to increase interpretability by constraining the ANN's learning space.

Using simulation data to train the model, we essentially create a "model of a model". This is important, as the primary model is already a reduced approximation of reality. We implicitly assume that these simulations are reasonable "ground truth" sources to understand axonal activation. This is supported by the extensive body of literature in functional electrical stimulation that compares the output of the types of numerical methods we have used FEM and the MRG axon) to experimental results [11-12]. This validates the in silica models with reasonable certainty to support their basis in surrogate modelling. However, in the long term, these results can in turn be vetted by experiments as well.

We close by speculating on the future use of these surrogate models. With reduced computational requirements, and a library of sufficiently verified models, we can distribute access to a broader spectrum of disciplines. Of special interest would be in empowering clinicians, particularly physio- and occupational therapists in the electrode design process and to support customisable, patient specific electrode design. This will support translation from research to practice. With the computational gains shown, software can be run on devices with modest computational capacity and this can support education and intuition building by providing a platform where electrode configurations and stimulation protocols can be tested in real-time. Transcutaneous nerve stimulation is often promoted with insufficient evidence, and the in-silico method presented here may offer a degree of verification to augment and support clinical use. We refer the reader back to Figure 1 where we envision this future. Perhaps this can be developed by the FES community based on open-source principles.

Conclusions

We demonstrate proof of concept in that a small feed-forward ANN can be trained to predict whether or not an axon within a femoral nerve bundle will activate under a range of applied geometries and stimuli.. This is the first step to improving the SOTA modelling pipeline for in silico experiments, with the vision to support iterative electrode design and to develop computationally efficient methods to support clinicians and physiotherapists in making real time decisions about stimulation parameters.

Acknowledgements

We acknowledge the following funding sources: CONICYT (scholarship CONICYT-PFCHA/Doctorado Nacional/2020—21202217) (RO); ANID-Scholarships Subdirección de Capital Humano/Magíster Nacional/22250256 (JS) and Subdirección de Investigación Aplicada FONDEF ID24i10422 (PA)); and the National Institute for Health Research Oxford Biomedical Research Centre (JF).

References

[1] C. Keogh et al., "Non‐invasive phrenic nerve stimulation to avoid ventilator‐induced diaphragm dysfunction in critical care," *Artif. Organs*, vol. 46, no. 10, pp. 1988-1997, 2022.

[2] R. Osorio et al., "Characterization and Evaluation of Interferential Current Stimulation for Functional Electrical Stimulation," *Artif. Organs*, 2025, doi: 10.1111/aor.15027.

[3] J. Sáez et al., "3D-Printed Electrode Fabrication for Functional Electrical Stimulation (FES): Prototyping Concentric Electrodes," in *2024 46th Annual International Conference of the IEEE Engineering in Medicine and Biology Society* (EMBC), Orlando, FL, USA, 2024, pp. 1-4, doi: 10.1109/EMBC53108.2024.10782379.

[4] M. Davids et al., "Optimizing selective stimulation of peripheral nerves with arrays of coils or surface electrodes using a linear peripheral nerve stimulation metric," *J. Neural Eng.*, vol. 17, no. 1, p. 016029, 2020.

[5] A. K. Sahoo, S. Kumar, and S. Chakraverty, "Application of Physics-Informed Neural Networks for Simulating Mass-Spring-Damper Systems," 2024.

[6] L. Toni et al., "Characterization of Machine Learning‐Based Surrogate Models of Neural Activation Under Electrical Stimulation," *Bioelectromagnetics*, vol. 46, no. 1, p. e22535, 2025.

[7] J. Golabek et al., "Artificial neural network-based rapid predictor of biological nerve fiber activation for DBS applications," *J. Neural Eng.*, vol. 20, no. 1, p. 016001, 2023.

[8] M. A. Hussain, W. M. Grill, and N. A. Pelot, "Highly efficient modeling and optimization of neural fiber responses to electrical stimulation," *Nature Commun.*, vol. 15, no. 1, p. 7597, 2024.

[9] E. Losanno et al., "Neurotechnologies to restore hand functions," *Nature Rev. Bioeng.*, vol. 1, no. 6, pp. 390-407, 2023.

[10] L. R. Osorio et al., "Finite Element Modelling for Biophysical Models of Nervous System Stimulation: Best Practices for Multiscale Adaptive Meshing," *IEEE Trans. Neural Syst. Rehabil. Eng.,* 2025.

[11] N. RaviChandran et al., "Modeling the excitation of nerve axons under transcutaneous stimulation," *Comput. Biol. Med.*, vol. 165, p. 107463, 2023.

[12] B. Howell, S. P. Lad, and W. M. Grill, "Evaluation of intradural stimulation efficiency and selectivity in a computational model of spinal cord stimulation," *PloS One*, vol. 9, no. 12, p. e114938, 2014.

Cost-Effective Remotely Fully-Controlled Electrical Stimulator for Skeletal Muscles Rehabilitation

Shaker H[1], Tammam A[1], Khail K[1,2], Yousof K[1], Mahran S[3], Khedr E[3], Abbas M[1]
[1]Electrical Engineering Dept., Assiut University, Egypt
[2]Electrical and Computer Engineering Dept, Mississippi University, USA
[3]Rhematology, Neurology Depts., Faculty of Medicine , Assiut University, Egypt

Abstract: *This paper presents a programmable, portable, low-cost, non-invasive electric muscle stimulator. The device is designed utilizing readily available components generating a biphasic stimulation signal with adjustable parameters. It operates using 9V lithium-ion battery and can deliver a stimulation current of up to 50 mA with wide range of timing parameters, which makes it suitable for fully-denervated and partially innervated skeletal muscle rehabilitation. The device allows users to set the stimulation signal amplitude and timing parameters, including burst on and off times, as well as pulse frequency and stimulation current through a mobile app and GSM network. The proposed device is interfaced with a GSM module which enables not only the remote control capabilities but also remote monitoring the status of the stimulated muscle. The preliminary measurement results show the effectiveness of the proposed design.*

.

Keywords: *Electric stimulation, Muscle rehabilitation, Remotely controlled, Portable muscle stimulator.*

Introduction

The individuals with spinal cord injuries (SCI) in developing countries experience high mortality rates within 1 to 5 years post-injury. This is primarily due to a lack of proper information regarding the injury, its complications, and appropriate management strategies [1]. Epidemiological studies from the Middle East and North Africa (MENA) region reveal that traumatic SCI is significantly more prevalent in males (71%), with complete paraplegia being the most common injury type. Most affected individuals are aged between 20 and 39 years [2–3].

The consequences of SCI can be devastating. One of the most debilitating effects is the immediate loss of voluntary movement and contractile force, leading to rapid and severe muscle atrophy in the first few months post-injury. This is accompanied by increased intramuscular fat and changes in body composition, including decreased lean mass and increased fat mass [4–6]. These physiological alterations reduce basal metabolic rate and promote obesity, which in turn is associated with cardio-metabolic disorders, diminished aerobic fitness, glucose intolerance, insulin resistance, and impaired mitochondrial function [6–7]. Ultimately, these outcomes contribute to reduced productivity and a lower quality of life.

Lower motor neuron (LMN) injuries often affect the sensory, motor, autonomic, and terminal branches of the peripheral nervous system. Peripheral nerve injuries are typically classified into three types, namely neurapraxia, axonotmesis and neurotmesis [8–9]: The last is the most severe type, involving complete disruption of nerve and axonal continuity. It is often caused by compression or tension injuries, leading to total loss of motor, sensory, and autonomic function [10].

In Functional Electrical Stimulation (FES), stimulation is delivered as a waveform composed of electrical biphasic current pulses. A biphasic signal means it alternates between negative and positive amplitudes. These pulses are characterized by three key parameters [11]: pulse duration (width), pulse frequency and amplitude. In addition to the application and pause times which are referred to as burst on and burst-off times. These parameters are illustrated in Fig. 1. The strength of muscle contraction is regulated by adjusting these parameters. The status of the injured muscle, either fully denervated or partially innervated, determines the stimulation signal parameters. In general, at low pulse frequencies, the muscle responds with a series of twitches. As the stimulation frequency increases beyond a certain threshold, the muscle exhibits smooth contractions. However, higher frequencies, while generating stronger contractions, also lead to faster muscle fatigue.

Various devices have been developed to address muscle denervation. For partial denervation, systems such as the H200 are employed [12]. In cases of full denervation, home-based functional electrical stimulation (hbFES) of permanently denervated muscles via surface electrical stimulation has been explored [13]. In [14] the authors describe a locally wireless and modular device that enables programmable electrical stimulation and supports a closed-loop FES Cycling setup. Traditionally, neuroprosthetic systems are built around a single multi-use device, which often limits the number of stimulation and sensor channels that can be effectively implemented. To address this limitation, the authors of [15] introduced a modular system which is adaptable for various applications, including hand grasp, reach, trunk support, transfer assistance, bladder control, standing, and stepping. In response to these concerns, [16] proposes a biphasic stimulator for wearable functional electrical stimulation systems based on FPGA and off-the-shelf components to build a 24-channel biphasic stimulator, offering enhanced control over stimulation parameters. The cost, portability, power

consumption and remote control and/monitoring are common issues in some of the previous works.

In this paper, the authors present the design and preliminary measurements of a single-channel stimulation device. The proposed stimulation system is intended to work as a remotely controlled muscle pacemaker. The device allows precise control over key stimulation parameters and is built using a low-cost microcontroller along with readily available components. The system has the feature of remote control via GSM connectivity. Additionally, the architecture supports future expansion to multiple channels with controllable timing sequences. Furthermore, the interface through GSM gives the ability to not only controllability of the system but also the observability of the muscle response. The developed device can be utilized in various muscle conditions ranging from fully denervated to partially innervated muscles.

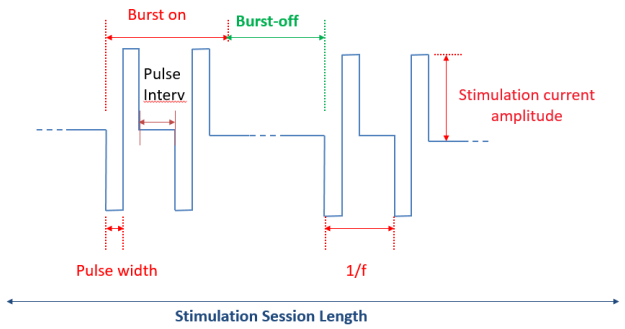

Figure 1. The biphasic signal along with its important parameters

Proposed Stimulation System

The system block diagram is shown in Fig. 2. It is composed of the following blocks. First; the power supply generates the necessary DC voltage levels to operate the stimulation circuitry along with the microcontroller and interfacing circuits using rechargeable batteries. Second; stimulation signal generator produces the output waveform with tuneable parameters. Third: the muscle response sensing circuitry enables feedback of the muscle status to the physician (this part is beyond the scope of this paper). Fourth; the control application and communication device, which is called Stim-App, is used to identify the stimulation parameters and interface with the muscle pacemaker through GSM network. The system gives controllability for five parameters, which are pulse width, pulse period (1/f), burst-on time, burst-off time, and stimulation current amplitude. Though the systems is easily scalable for multiple channels with minimal additional hardware, this paper focuses on a single-channel stimulation system. The stimulation signal used in this system is typically biphasic, with equal negative and positive charges to achieve the charge balance. This balance is essential to prevent tissue damage caused by residual charge accumulation. Based on the muscle status, either fully denervated or partially innervated, the stimulation signal parameters including the pulse width, pulse frequency, burst-on and burst-off timing in addition to stimulation current amplitude are selected. The system is primarily designed for upper limb forearm muscles, however, it can be tweaked to suit any other skeletal muscle. The proposed portable stimulation system, illustrated in Fig. 2, operates using 9V lithium-ion rechargeable batteries and allows the adjustment of all stimulation parameters via a mobile app. The design prioritizes adjustability and practical usability under the full supervision of physicians at the Rheumatology and Rehabilitation Unit, Assiut University Hospital.

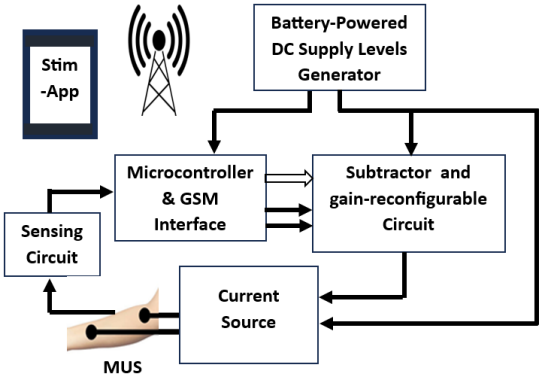

Figure 2. Block diagram of the stimulation signal generator

A. The stimulation signal generator

The stimulation signal generator circuit is based on an Arduino microcontroller (µC) (ATmega328p). As illustrated in Fig. 3, the µC is programmed to produce two trains of monophasic pulses that are fully out phased. Using a dedicated mobile app , these pulses are generated by programming the µC remotely to adjust the pulse width, frequency, burst-on time, burst-off time and the stimulation amplitude. The two pulse trains are then passed to two separate voltage-controlled amplifiers as illustrated in Fig. 4 to control the amplitude of the stimulation signal. A message is sent to the microcontroller to generate a pulse width modulated (PWM) signal. The PWM output is then derived to an integrator to produce a proportional DC voltage V_{con} as shown in Fig. 3. V_{con} is used to control the on-resistance of a P-channel JFET as illustrated in Fig. 4. Therefore, the feedback resistance of the amplifier changes and the gain is adjusted accordingly. The outputs of the voltage-controlled amplifiers are applied to the subtractor circuit to produce the needed biphasic signal as shown in Fig. 4. To accommodate the high compliance voltage needed by the tissue load, the subtractor stage along with the Holland current source are designed using high voltage OP AMP IC like OPA455. The stimulation by current is much better than stimulation by voltage because it guarantees fixed charge arriving the tissue despite the variations in the impedance of the electrode-electrolyte interface. [17]

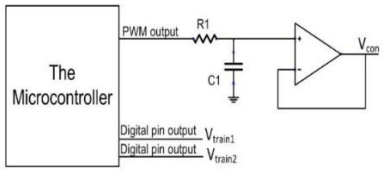

Figure 3. the schematic of the microcontroller along with the integrator

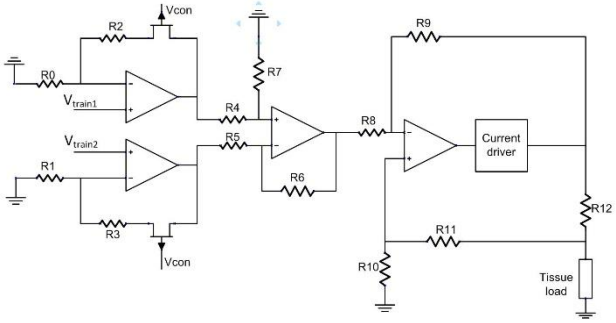

Figure 4. The schematic of the voltage-controlled amplifiers, the subtractor stage along with the Holland current source

The biphasic voltage is converted to current using the Holland constant current source. To ensure adequate current supply—potentially up to 50 mA—to the load muscle, the limited drivability of the OPA455 operational amplifier is augmented with a Darlington transistor pair, enhancing the current driving capability.

B. DC Power Source

For the stimulation signal, both positive and negative voltages of up to ±60V are required with a supply current of up to 1A. Additionally, a+5V to power supply is needed to supply the microcontroller. The DC power system consists of three circuits: a boost converter and buck-boost converter to elevate the 9V from the battery to ±60V. In addition to a regulator circuit to convert the battery voltage to +5V, as illustrated in Fig. 5.

In both the boost and buck-boost converters, power electronic components with suitable ratings are utilized. The main components include a 47µH, 20A toroidal inductor that stores energy during switching; a IRFP250 N-channel power MOSFET switch; a MBR20100CT Schottky diode to ensure unidirectional current flow; and a TL494 PWM controller to generate high-frequency switching pulses with an adjustable duty cycle.

Results and Discussion

To verify the correct operation of the proposed system, a PCB (printed circuit board) was fabricated, and the entire system was assembled on it. The output is measured at various settings. Sample measurement results are presented in Fig. 6 and Fig. 7. The figures demonstrate the full controllability of the proposed system over the stimulation signal parameters.

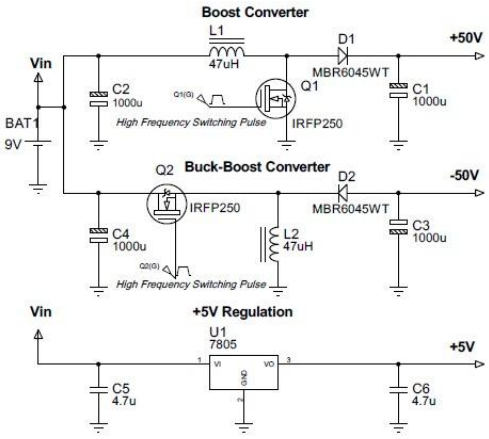

Figure 5. The schematic of the DC Power Supply

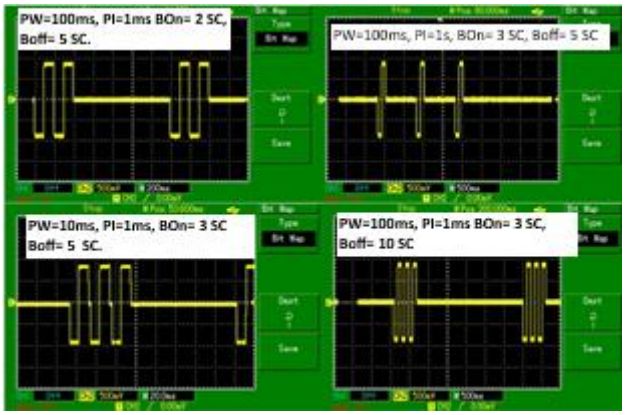

Figure 6. Samples results of stimulation signals for fully denervated muscles.

Fig. 6 shows sample results of stimulation signals for fully denervated muscle. The upper right signal has the following timing parameters: pulse width (PW) of 100ms and pulse interval (PI) of 1s with burst-on (BOn) time taking 3 stimulation cycles (SC) and burst-off (Boff) time taking 5 stimulation cycles. The upper left signal has the following timing parameters: pulse width of 100ms and pulse interval of 1ms with burst-on period taking 2 stimulation cycles and burst-off period taking 5 stimulation cycles. The lower left signal has the following timing parameters: pulse width of 10ms and pulse interval of 1ms with burst-on period taking 3 stimulation cycles and burst-off period taking 5 stimulation cycles. The lower right signal has the following timing parameters: pulse width of 100ms and pulse interval of 1ms with burst-on period taking 3 stimulation cycles and burst-off period taking 10 stimulation cycles.

Fig. 7 shows sample results of stimulation signals for partially innervated muscle. The upper left signal has the following timing parameters: pulse width of 500µs and frequency 20Hz. The upper right signal has the following timing parameters: pulse width of 500µs and frequency

50Hz. The lower left signal has pulse width of 200µs. The lower right signal has the following timing parameters: pulse width of 500µs and frequency 50Hz captured during the transition from burst-on period of 5s to burst-off period of 10s.

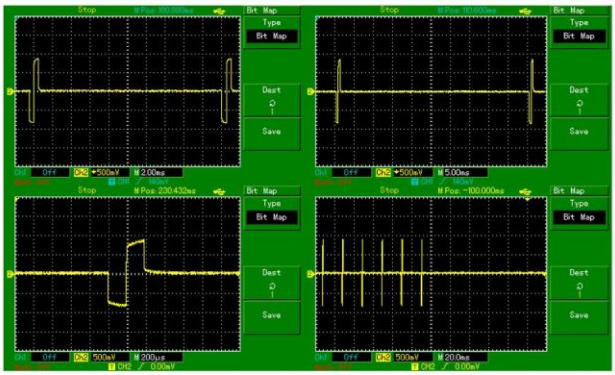

Figure 7. Samples results of stimulation signals for partially innervated muscles.

Conclusions

In this work, a low-cost electrical stimulator has been presented, the stimulator was fabricated using low-cost and available off-shelf components. The proposed design gives controllability over a wide range of stimulation parameters via a simple mobile app and GSM network. The design is power-efficient, and the only energy source of stimulator is a 9V lithium-ion battery. The measurement results of proposed device show its ability to generate stimulation signal with wide range of timing parameters. The focus of this work is the development and evaluation of the single channel. stimulator, however, designing a multi-channel-based stimulator is one of future works.

Acknowledgement

The authors gratefully acknowledge the financial support provided by the Science, Technology & Innovation Funding Authority (STDF) under grant number 45959. Their funding and resources were instrumental in facilitating this research. We deeply appreciate STDF's commitment to advancing scientific research and innovation in Egypt.

References

[1] https://www.who.int/news/

[2] Mohamed H Elshahidi et al "Epidemiological Characteristics of Traumatic Spinal Cord Injury (TSCI) in the Middle-East and North-Africa (MENA) Region: A Systematic Review and Meta-Analysis", Apr;6(2):75-89, 2018.

[3] Heba G. Sayed et al , " Prevalence and Characteristics of Traumatic Spinal Cord Injuries for Educational Hospitals in Cairo", Med. J. Cairo Univ., Vol. 87, No. 6, September: 3687-3690, 2019

[4] Kern H et al, "Home-based functional electrical stimulation rescues permanently denervated muscles in paraplegic patients with complete lower motor neuron lesion", Neurorehabil Neural Repair (2010) 24:709-721

[5] Gorgey A. , et al, "Prevalence of obesity after spinal cord injury" Top Spinal Cord Inj Rehabil, 12:1-7, 2007.

[6] Gorgey A. Et al , "Effects of spinal cord injury on body composition and metabolic profile" – Part I. J Spinal Cord Med 37: 693-702, 2014.

[7] Sumrell RM et al, "Anthropometric cutoffs and associations with visceral adiposity and metabolic biomarkers after spinal cord injury", PLoS One 13 (8) 2018.

[8] Seddon H , "Advances in nerve repair". Triangle 8:252-259, 1968.

[9] Chandrasekaran S et al "Electrical stimulation and denervated muscles after spinal cord injury". Neural Regen Res 15(8):1397-1407, 2020.

[10] Carp SJ, "Peripheral nerve injury: an anatomical and physiological approach for physical therapy intervention. 2015, Philadelphia: F. A. Davis Company

[11] Peckham P. et al , "Functional electrical stimulation for neuromuscular applications." Annu. Rev. Biomed. Eng. 7, no. 1 (2005): 327-360.

[12] https://www.bionessinc.com/Products/H200_for_Hand_Paralysis/What_is_It.php

[13] http://schuhfriedmed.at/stimuletteen/stimulette-den2x

[14] Giacinto C. et al. "Design of a Wireless, Modular and Programmable Neuromuscular Electrical Stimulator", Annual International Conference IEEE Eng Med Biol Soc.. 9:3815-3818 Jul 2019

[15] Nathaniel S et al "Design and Testing of Stimulation and Myoelectric Recording Modules in an Implanted Distributed Neuroprosthetic System", IEEE Transactions on Biomdical Circuits and Syatems Vol. 15, No. 2, April 2021.

[16]Tyler W. Et al, "Multichannel Biphasic Muscle Stimulation System for Post Stroke Rehabilitation", Electronics 2020, 9, 1156; doi:10.3390/electronics9071156.

[17] Jin-Young Son, Hyouk-Kyu Cha "An Implantable Neural Stimulator IC With Anodic Current Pulse Modulation Based Active Charge Balancing", IEEE Access, July 27, 2020, Digital Object Identifier 10.1109/ACCESS.2020.3012028

Author's Address

Name: Mohamed Abbas
Affiliation: Professor, EE Dept. Assiut University
eMail: m-abbas@aun.edu.eg

Increasing the reliability of an implantable pulse generator for small and large animals

Lanmüller H[1], Schmoll M[1], Jarvis J[2], Unger E[1] and Bijak M[1]

[1] Center of Medical Physics and Biomedical Engineering, Medical University of Vienna, Austria
[2] School of Sport and Exercise Science, Liverpool John Moores University, United Kingdom

Abstract: Reliability and user-friendliness are the most important attributes for an implantable pacemaker. This applies to both human and animal use. Our stimulator, called MiniVstim 18B, was primarily developed for direct stimulation of nerves and denervated muscles in small laboratory animals. MiniVstim 18B is an implantable, battery-powered, transcutaneous programmable, single-channel stimulator that delivers either monophasic or biphasic pulses. The implant has a simple design, consisting of a circular circuit multilayer printed circuit board (PCB) with a diameter of 18 mm and a battery, both components being encapsulated in synthetic resin.
In an initial series of 33 implantations (rats, sheep, implantation duration 12 – 14 weeks), we had an unexpectedly high failure rate of 36 %, prompting us to conduct a detailed analysis of the causes. The analysis showed that two implants had failed due to an electronic fault, five implants due to self-discharge of the battery (defect of the battery manufacturer), and five implants due to moisture entering the synthetic resin coating.
To fix the causes of failure, we implemented a detailed semi-automatic testing procedure of the circuits, changed the battery type, and modified the circuit layout. The minimum distances between the contacts and conductor tracks on the PCB surface are now 200 µm, resulting in a maximum field strength of 18 kV/m. As a further measure, we added a parylene coating onto the PCB after production.
The measures proved to be extremely successful. In the following 77 implantations of the MiniVstim 18B implant (rats, sheep, pigs, implantation duration 8 - 12 weeks), we did not observe any additional failures. For other developments, it can be concluded that a parylene-coated PCB with additional synthetic resin encapsulation is stable in the long term if the field strengths on the PCB surface remain below 18 kV/m

Keywords: *Implantable pulse generator, animal study, reliability*

Introduction

Basic research in the fields of muscle physiology, muscle training, electrode testing, and related areas is primarily conducted on small animals. For this purpose, we have developed a stimulation system called MiniVstim. Its functionality and range of applications have been gradually expanded. In the first development stage of the MiniVstim A variant [1], the stimulation parameters (i.e., amplitude, frequency, phase width, burst duration, and pauses) were pre-programmed during the manufacturing prozess. The implant could be switched on via an external magnet and one of the pre-programmed patterns could be selected. In the next stage of development of the MiniVstim B variant, a bidirectional communication link was implemented, allowing the stimulation parameters to be freely selected and changed at any time during the experiment via an external programming device. In the MiniVstim 18B1 variant, either monophasic or biphasic pulses with an amplitude of up to 8mA with up to 5ms long pulses could be delivered, making the implant suitable also for direct muscle stimulation of small denervated muscles.
The choice of power supply and the design of the housing are the most obvious distinguishing features for implants used in animal experiments. MiniVstim implants are powered by a battery, as is the case with most implant systems [2,3,4], because this makes them easiest to handle in animal experiments. External radio frequency transmitter coils [5] or ultrasound transmitters [6] are also used. To protect the implant electronics, silicone [4] or synthetic resin [1] are mainly used in animal experiments. We are not aware of any use of titanium housings as in human applications.
Compared to implants used in humans, the attributes for successful use in animal experiments are comparable. In terms of user-friendliness, the requirements are higher in animal experiments, as the test animal wants to escape any manipulation, which makes operation even more difficult. In terms of reliability, the implantation period in animal experiments is usually shorter (often 12 to 18 weeks). Within this time frame, the most important development objective is to avoid failures for ethical and financial reasons. This paper presents the measures we have taken, our findings, and the results we have achieved in increasing the reliability of the MiniVstim.

Material and Methods

We used a standard Android tablet for data entry, which communicates via Bluetooth Low Energy with a programmer with an integrated transmitter/receiver unit. Bidirectional data exchange from the programmer to the implant is done via amplitude shift keying, and from the implant to the programmer via pulse code modulation, both with a carrier frequency of 400 kHz. A MiniVstim 18B implant consists of an electronic circuit (round 4-layer printed circuit board (PCB) with a diameter of 18 mm) and a lithium-ion battery in a metal housing with glass feedthroughs (see Figure 1). The battery and PCB are encapsulated in medical-grade epoxy resin (EP 601,

Polytec, Karlsbad, Germany). The implant is controlled by a PIC16LF1783 microcontroller (Microchip, Chandler, AZ, USA). The implant enables the delivery of monophasic pulses with an amplitude of 0,05-8 mA, a pulse width of 32-5000 µs, and a frequency of 1 to 500 Hz. For biphasic pulses, an amplitude of 0-8 mA, a pulse width of 258-5000 µs, and a frequency of 1 to 100 Hz can be selected. Burst duration and pauses can be freely selected throughout the day.
In the first series, we used the ER1860 lithium battery (EVE, Lewis Center, OH, USA), which was encapsulated in medical-grade synthetic resin without additional coating of the PCB. During the manufacturing process, 24 criteria based on manual measurements were used for quality assurance.
Implants with a functional failure in an animal study were stored in saline solution immediately after removal. To determine the cause of the failure, the synthetic resin coating was partially milled away and the battery and PCB were examined separately.
In the follow-up series, we used the ER22G68 lithium battery (EVE, Lewis Center, OH, USA) and the PCB was coated with Parylene (PPS, Rosenheim, Germany) before encapsulation in epoxy resin. To simplify the coating process, the PCB was slightly adapted. The minimum distance between two solder joints is 200 µm, resulting in a maximum electric field strength of 18 kV/m on the surface of the PCB. An additional automatic test was used to add a further 31 criteria for quality assurance.

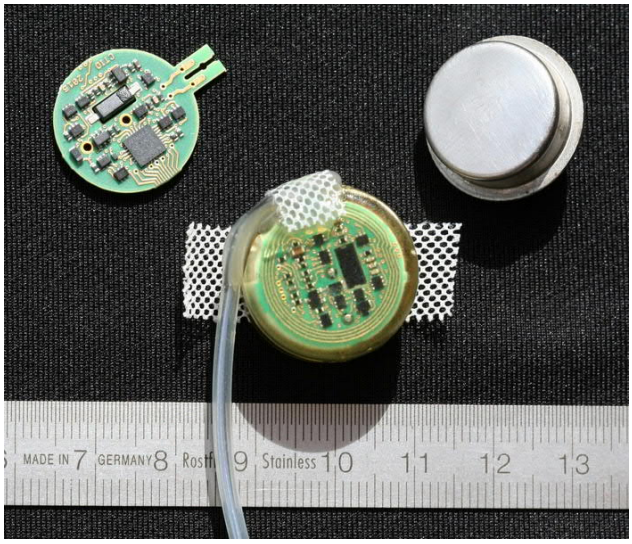

Figure 1: MiniVstim 18B implant from the follow-up series; top left: PCB; top right: battery; center: encapsulated implant with electrode lead.

Results

Implants from the first series (33 units) were implanted in sheep for a planned implantation period of 12 weeks and in rats for a period of 14 weeks. A total of 12 implants failed to function. Analysis of the failed implants revealed the cause to be an electronic fault (2 implants), a battery fault due to self-discharge (5 implants – manufacturing fault by the battery manufacturer) and moisture ingress into the synthetic resin coating (5 implants – battery discharge due to increased power consumption by the PCB). Self-discharge of the battery was also observed in unused batteries that we had stored.
The follow-up series of MiniVstim 18B implants was used in sheep (35 units for 12 weeks and 24 units for 8 weeks), rats (12 units for 12 weeks), and pigs (6 units for 8 weeks) without a single failure of the pulse generator. Of these 77 implants, 36 were stored in saline solution and tested for functionality. The shortest functional life of an implant was an additional 36 weeks after explantation.

Discussion

It is evident that strict quality assurance leads to improved product quality, and this does not need to be discussed. The problem lies in the fact that the weak points of the product are not yet known and quality control can only be adjusted after an initial series has been produced. One example in our case of this is the incoming inspection of batteries. A one-time measurement of the battery characteristics was not sufficient to detect the manufacturing defect. As a result, we carried out an incoming inspection, stored the batteries for at least 6 months, and repeated the measurements. Only if the measurement data was approximately the same in both cases, we used the batteries for our implants.
Encapsulating an electronic circuit with synthetic resin or silicone always carries the risk of moisture ingress, which can cause creepage on the PCB, increase power consumption, or cause the circuit to malfunction. For this reason, implants used in humans are primarily protected by tightly welded metal housings (titanium). The financial cost of a titanium case for an animal study is generally too high, especially since the implantation period is much shorter than in human use. The two-layer coating with parylene and synthetic resin that we now used offers a good compromise between cost and long-term stability.

Conclusions

By combining detailed testing with strict quality criteria and the use of a two-layer coating of parylene and synthetic resin on the electronic circuit, reliability has been significantly increased. In 77 cases with an implantation period of 8-12 weeks, there were no failures of the Minivstim 18B implant. In general, for all implants, it can be said that an electronic circuit with field strengths below 18kV/m between the solder pins of the PCB with the presented 2-layer coating remains stable for a period of 12 weeks.

References

[1] Bijak M, Schmoll M, Jarvis JC, Unger E, Lanmüller H. MiniVStimA: A miniaturized easy to use implantable electrical stimulator for small laboratory animals. PLOS ONE. 2020 Oct 30;15(10):e0241638.
[2] de Haas R, Struikmans R, van der Plasse G, van Kerkhof L, Brakkee JH, Kas MJH, et al. Wireless implantable micro-stimulation device for high frequency bilateral

deep brain stimulation in freely moving mice. J Neurosci Methods. 2012 Jul 30;209(1):113–9.
[3] Dennis RG, Dow DE, Faulkner JA. An implantable device for stimulation of denervated muscles in rats. Med Eng Phys. 2003 Apr 1;25(3):239–53.
[4] Russold M, Jarvis JC. Implantable stimulator featuring multiple programs, adjustable stimulation amplitude and bi-directional communication for implantation in mice. Med Biol Eng Comput. 2007 Jul;45(7):695–9.
[5] Kane MJ, Breen PP, Quondamatteo F, ÓLaighin G. BION microstimulators: a case study in the engineering of an electronic implantable medical device. Med Eng Phys. 2011 Jan;33(1):7–16.
[6] Piech DK, Johnson BC, Shen K, Ghanbari MM, Li KY, Neely RM, et al. A wireless millimetre-scale implantable neural stimulator with ultrasonically powered bidirectional communication. Nat Biomed Eng. 2020 Feb;4(2):207–22.

Author's Address

Hermann Lanmüller
Center of Medical Physics and Biomedical Engineering
Hermann.Lanmueller@meduniwien.ac.at
https://mpbmt.meduniwien.ac.at/

Towards a Safe Long-Term Implantable Electrical Stimulation: A High-Efficiency Charge Balancer Design

Shaker H[1], Tammam A[1], Yousef K[1], Khalil K[1], Mahran S[2], Khedr E[2], Abbas M[3]

[1]Electrical Engineering Dept., Faculty of Engineering, Assiut University, Assiut 71718, Egypt
[2]Rhematology, Neurology Depts., Faculty of Medicine, Assiut University, Assiut 71715, Egypt

Abstract: *Electrical stimulation of neuromuscular tissues has been proven effective in treating many clinical disorders due to spinal cord injuries, including motor function restoration and epilepsy, as well as in other biomedical applications. Implantable electrical stimulators have emerged as promising techniques for long-term therapeutic and scientific use. However, the design of such stimulators faces numerous challenges, including efficiency, miniaturization, and power constraints. This paper presents an integrated circuit for an implantable electrical stimulator that offers high stimulation efficiency within a compact silicon area. The proposed device can provide a programmable stimulation current of up to 800 μA - a range suitable for neuro-electrical stimulation applications such as epidural spinal cord stimulation - to a tissue load impedance of 2.5 kΩ while ensuring proper charge balancing.*

Keywords: *Spinal Cord Injuries, Functional Electric Muscle Stimulator, Wireless Power Transfer, Charge Balancing.*

Introduction

Electrical stimulation of the neuromuscular system has significant potential in both scientific research and therapeutic biomedical applications. By delivering the needed electrical activity to the target nerve or muscle, it can directly deliver therapy to the targeted regions. Electrical stimulation can enhance treatment efficacy while minimizing the systemic side effects often associated with conventionally surgical or pharmaceutical interventions [1]. Both central and peripheral nerve stimulation have been employed to address a wide range of clinical conditions. For instance, vagus nerve stimulation is used in the treatment of epilepsy [2], while ethmoid nerve stimulation is promising treatment for dry eye disease [3]. Deep brain stimulation is an established approach for alleviating symptoms of Parkinson's disease [5], and spinal cord stimulation is applied for pain relief and motor function recovery [6][7]. Additionally, phrenic nerve pacing is utilized to restore respiratory function [4], and electrical stimulation has been instrumental in the restoration of various sensory functions such as hearing [8]. Besides, functional electrical stimulation (FES) is particularly noteworthy for its ability to restore the function of denervated muscles [4]. In practice, electrical stimulation is typically delivered in the form of biphasic current pulses with positive and negative phases while its key parameters include pulse frequency, amplitude, and duration (or width) [4]. An increase in pulse frequency generates stronger contractions [4]. But too high pulse frequencies can cause muscle fatigue, thus this must be avoidable. In addition, increasing the stimulation pulse width or amplitude increases the number of activated motor units, leading to stronger contractions as well [4]. One of the main challenges in electrical stimulation is charge balancing [15]. Charge imbalance often arises due to process variations, device mismatches, circuit noise, and other unpredictable factors. When left unaddressed, this imbalance leads to the accumulation of residual net charge on tissues, potentially causing irreversible faradaic reactions, toxic byproducts, shifts in pH, and electrode corrosion [14]. To mitigate these effects, charge balancing schemes are employed to eliminate or minimize the residual voltage. Charge balancing techniques can be passive or active. Passive techniques do not monitor continuously the residual charges such as insertion of blocking capacitors and electrodes' shorting. Blocking capacitors' insertion typically ranging from 1 μF to 100 μF [15]-[16] is a straightforward effective solution. But this occupies considerable silicon area and limit the stimulator's output voltage compliance [17]. Passive charge balancing circuits cannot be effective with varying conditions as stimulation frequency and changes in the electrode-electrolyte interface impedance [18]. Conversely, active charge balancing incorporates periodic monitoring of the residual charge voltage, offering enhanced control, precision, and reliability in maintaining safe stimulation conditions. The focus of the work presented in this paper is introducing a power-efficient, actively charge-balanced, and small-area neuromuscular stimulator with a DC power supply generator that powers the stimulator through the near field RF power. The rest of this paper is organized as follows; section II illustrates the design details of the DC power supply circuit. Details of the neuromuscular stimulator and the charge balancing circuits. Section III lists and discusses the simulation results of the proposed system while section IV concludes this work.

Material and Methods

A. DC Power Supply Circuit

Power delivery to an implantable device is challenging. Traditionally, bulky batteries require invasive surgical treatment for replacement or recharging. Wireless Power Transfer (WPT) has been adopted to overcome this issue. WPT allows energy to be transferred wirelessly to an implanted device. This ensures patient comfort and safety while supporting long-lifetime of pacemakers, neurostimulators, and drug delivery pumps. WPT helps introduce smaller and lighter implants, which reduces the physical burden on patients and minimizes the risk of

infection associated with wired connections or repeated surgeries [9]. The supply voltage for the stimulation circuit is generated by a Wireless Power Transfer (WPT) system, which consists of three main stages as shown in Fig. 1.

i- RF-to-DC Rectifier

The first stage of WPT system is the RF-DC rectifier. This stage converts the RF signal, which is transmitted from the near-field transmitter (located outside the body), into a DC voltage. There are various CMOS rectifier topologies designed to convert RF signals to DC while maximizing power conversion efficiency (PCE) and voltage conversion ratio (VCR) [10],[11]. In this paper, we use a fully bootstrapped rectifier shown in Fig. 2. This topology employs a bootstrapped circuit, also known as a clamper circuit, to apply a positive DC voltage to the gate of the NMOS transistor and a negative DC voltage to the gate of the PMOS transistor, thus facilitating fast conduction of the MOS transistors and compensating for threshold voltage variations. This approach results in an improved PCE with a peak value of 81% and a peak VCR of 87% at an RF input power of -12.4 dBm [12].

ii- DC-DC Boost Converter

Due to the weak RF power, the rectified voltage is quite low. Therefore, we need to increase this voltage using a DC-DC converter. In our system, we employ a cross-coupled charge pump topology. A cross-coupled charge pump DC-DC boost converter is a switched-capacitor circuit that efficiently steps up the input voltage without using inductors, shown in Fig. 3. It operates by alternately charging and discharging capacitors within a cross-coupled switching network, typically controlled by non-overlapping clock signals. During the first phase, the flying capacitors charge to the input voltage. In the second phase, these capacitors are reconfigured in series with the input, thereby boosting the output voltage. This architecture is especially beneficial for low-power applications.

To generate non-overlapping clock signals, we employ a ring oscillator consisting of three inverter stages, operating at a frequency of 11 MHz A driving buffer is used to isolate the oscillator from external loads, such as charge pump capacitors. This setup enhances signal integrity and ensures reliable clock distribution.

To generate our supply voltages of 2.4V and 1.3V, we utilized three stages of a cross-coupled charge pump boost converter, as shown in Fig. 3. The output of the first stage was regulated to 1.3V, with a transient current of up to 70µA, while the output of the third stage was regulated to 2.4V, with a transient current of up to 1mA. This regulation was achieved using two Low Dropout Regulators (LDOs).

B. Neuromuscular Stimulator

The block diagram of the proposed neuromuscular stimulator system is shown in Fig. 4. A digital input word, generated by the finite state machine (FSM), is first fed into a digital-to-analog converter (DAC). The DAC converts this input into an analog voltage proportional to the digital word. Since stimulation requires current rather than voltage, the DAC output is then passed to a voltage-to-current (V-I) converter, which generates a proportional current signal. However, the output current from the V-I converter is too low to effectively stimulate biological tissue. Then, a current mirror—specifically, a wide-swing cascode current mirror —is employed in the third stage of the system. This current mirror amplifies the current to a suitable level and isolates the low-power circuitry from the high-power stimulation output. The current mirror is configured with a mirroring ratio of 1:40. The wide swing cascode topology has also the advantage of high output impedance and improved voltage headroom, which allows higher stimulation current. The output current of the current mirror is unidirectional. For biphasic stimulation, H-bridge circuit is employed. Two-transistor stacked H-bridge is used to accommodate high-compliance voltage and as a result, more currents can be pushed to the loads.

Fig. 5 illustrates the two-transistor stacked H-bridge introduced in this work. Control signals—Anode 1, Anode 2-, Cathode 1, and Cathode 2—are generated by a finite state machine (FSM) programmed to match the required pulse width and frequency.

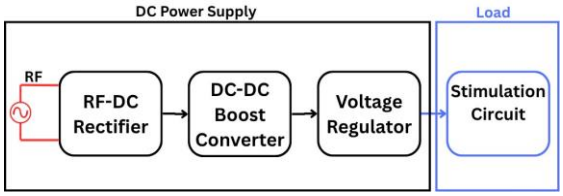

Figure 1: DC Power Supply Block Diagram

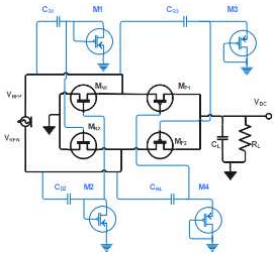

Figure 2: Fully Bootstrapped RF-DC Rectifier [12]

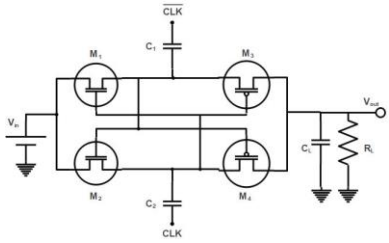

Figure 3: Cross-coupled charge pump [13]

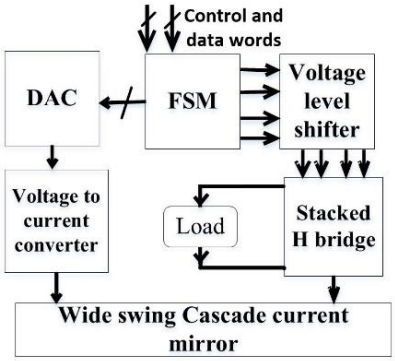

Figure 4: Block diagram of neuromuscular stimulator

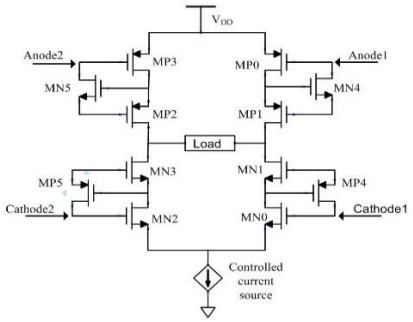

Figure 5: The schematic of the Stacked H-bridge

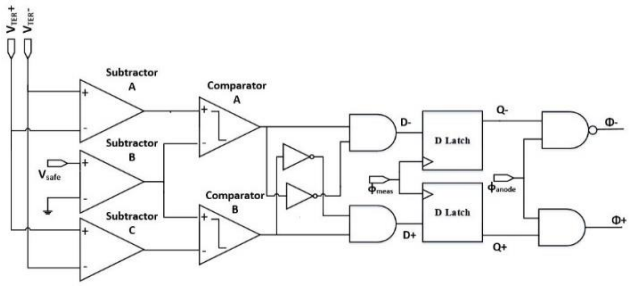

Figure 6: Block diagram of the charge balancing system

These signals directly control the main H-bridge transistors (MN0, MN2, MP0, and MP3). The auxiliary transistors (MP4, MP5, MN4, and MN5) ensure safe and complete switching. For example, when Cathode 1 activates MN0, no current initially flows since MN1 is still off. However, turning on MN0 pulls its drain voltage low, which activates MP4. MP4 then connects the gate of MN1 to the Cathode 1 signal, turning MN1 on as well. This allows both transistors in one branch to act as a single switch. The same principle applies to MP5, MN4, and MN5.

C. Charge Balancing Circuit

Fig. 6 illustrates the active charge balancing system. Initially, load terminals represent the input of a subtractor stage. If $VTER_- > VTER_+$, the output of Subtractor A is HIGH, while the output of Subtractor C is LOW and vice versa. These outputs are then fed into Comparators A and B, respectively. The comparators are designed with preamplification gain provided by the subtractor stages to reduce the risk of metastability. Subtractor B is configured to provide the same gain as Subtractors A and C. A small reference voltage, V_{safe} (e.g., 5 mV), is used to ensure effective charge balancing. This reference is configurable via the finite state machine and is amplified by Subtractor B for comparison with the outputs of Subtractors A and C. Comparator A produces a HIGH output only when $(VTER_- - VTER_+) > V_{safe}$. Similarly, Comparator B provides a HIGH only when $(VTER_+ - VTER_-) > V_{safe}$. To improve the reliability of the decision-making, the output of Comparator A output is ANDed with the inverted output of Comparator B. This results in signal D_-, which is HIGH only when Comparator A output is HIGH and Comparator B output is LOW. A similar operation produces signal D_+, which is HIGH only when Comparator B output is HIGH and Comparator A output is LOW. Next, D latches are employed to capture variations in D_- and D_+ during a brief measurement window, ϕ_{meas}. This window occurs during the non-stimulation phase and is typically very short (e.g., 15 µs). The latched version of D_- is Q_- and the latched version of D_+ is Q_+. In the final stage, logic gates (AND and NAND) are used to ensure that Q_- and Q_+ are only activated during the anodic stimulation phase. This control is achieved using ϕ_{anode}, a timing signal indicating the start of the anodic phase. For this reason, the technique is referred to as Anodic Current Pulse Modulation-Based Active Charge Balancing [19]. The final system outputs are ϕ_+ and ϕ_-, which are applied to current mirror switches to modulate the anodic current accordingly.

Results and Discussion

Fig. 7 displays the output from the DC power supply circuit. It shows the RF input voltage, the output from the RF-DC rectifier circuit. Fig. 8 displays the output from the first stage of the DC-DC boost converter, the output of the first regulator (1.3V), the output from the third stage of the DC-DC boost converter, and the output of the second regulator (2.4V). Fig. 9 shows the output biphasic current of the stimulator versus the digital DAC input word. Both pre-layout and post-layout results are illustrated showing monotonic behaviour and acceptable level of linearity. The charge balancing circuit post-layout simulations were also obtained. Fig. 10 shows the post-layout simulation results in case of 10µs pulse width, 10 KHz frequency and current amplitude of 820µA, the effect of the anodic modulation charge balancing appears at the second stimulation pulse, the anodic current phase reduces to 785 µA instead of 820 µA. The reduction in current happens because of the high value of the measured residual voltage 42mv. Fig. 11 illustrates the residual voltage corresponding to Fig. 10. It shows the high value of the residual voltage at region 1 (42 mv) entailing the charge balancing of the next anodic phase. However, in regions 2,3 and 4, the residual voltage values are 23.6 mV, 19.5 mV, and 13.9 mV respectively which are less than critical residuals. So, there is no need of anodic current modulation in the third, fourth and fifth anodic phase of stimulation. The design could keep the residual voltage within a window of ±35 mV that is much less the needed safe window of the residual charge [19]. Fig. 12 displays the post-layout simulation for a pulse width of 50 µs, a frequency of 4 kHz, and an amplitude of 450 µA. Electrode shorting and anodic modulation (reducing the second anodic pulse to 425 µA) are also demonstrated. The layout of both the stimulator and the charge balancing circuit has silicon area of 0.1375 mm^2. The power efficiency of the two parts is 66.3% with a maximum stimulation current of 800µA introducing a suitable current range for epidural spinal cord stimulation [17]. The value of power efficiency is the best among the prior work [19].

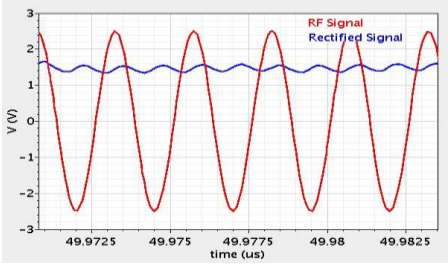

Figure 7: The input and outputs of RF-DC Rectifier.

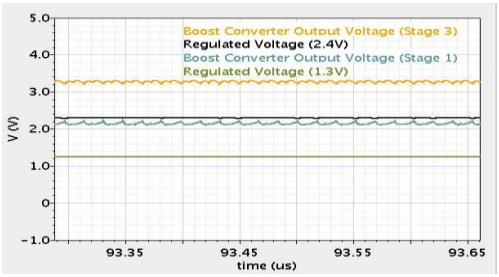

Figure 8: The output of DC-DC and Regulators Circuits

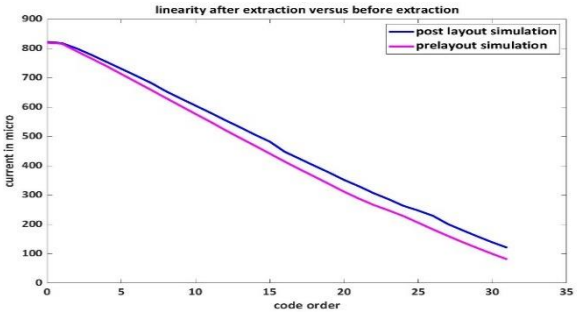

Figure 9: Output stimulation current of the neuromuscular stimulator vs. the digital code increment.

Figure 10: Output biphasic current for 10µs pulse width, 10KHz frequency and 820µA amplitude.

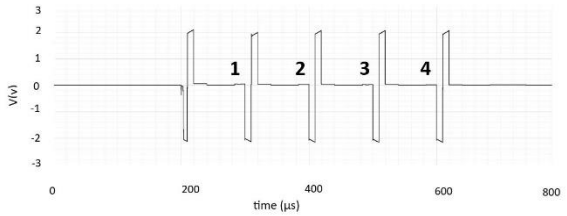

Figure 11: Residual voltage of biphasic signal of 100µs, 1KHz frequency and 820µA amplitude.

Conclusions

The paper develops a design for an implantable electrical stimulator including a DC power supply circuit that harvests energy from the RF with high efficiency and a charge balancing circuit that maintains residual voltage within safe limits. The stimulator delivers programmable stimulation currents up to 800 µA. Both the stimulator and the charge balancing circuit have very small silicon area of 0.1375 mm^2 and high-power efficiency of 66.3% that is higher than prior work.

Acknowledgement

The authors gratefully acknowledge the financial support provided by the **Science, Technology & Innovation Funding Authority (STDF)** under grant number 45959.

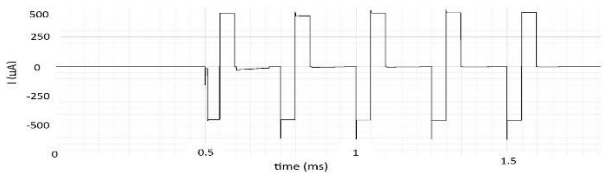

Figure 12: Output biphasic current of biphasic signal with 50µs pulse width, 4KHz frequency and 450 µA amplitude.

References

[1] Mishra, S.: Electroceuticals in medicine–The brave new future, *Indian heart journal* 69, no. 5 (2017): 685-686.

[2] Ben-Menachem, E.: Vagus-nerve stimulation for the treatment of epilepsy, *The Lancet Neurology* 1, no. 8 (2002): 477-482.

[3] Brinton, M. et. al.: Electronic enhancement of tear secretion, *Journal of neural eng.* 13, no. 1 (2015):016006.

[4] Peckham, P. et. al.: Functional electrical stimulation for neuromuscular applications, *Annu. Rev. Biomed. Eng.* 7, no. 1 (2005): 327-360.

[5] Benabid, A.: Deep brain stimulation for Parkinson's disease, *Current opinion neur.* 13, no. 6 (2003): 696-706.

[6] MayfieldClinic.com spinal cord stimulation.

[7] Wang, S. et. al.: Epidural electrical stimulation effectively restores locomotion function in rats with complete spinal cord injury, *Neur. Reg. Resear.* 16, no. 3 (2021): 573-579.

[8] Kan, A. et. al.: "Binaural hearing with electrical stimulation, *Hearing Research* 322 (2015): 127-137.

[9] Zhang, J. et. al.: Battery-Free and Wireless Technologies for Cardiovascular Implantable Medical Devices, *Adv Mater Technol*, vol. 7, no. 6, p. 2101086, 2022

[10] Sidhu, R., et. al.: CMOS Rectifier Topologies for RF Energy Harvesting: A Review, Aug. 2020.

[11] Akram M. A. et. al.: A 434-MHz Bootstrap Rectifier with Dynamic Compensation for Wireless Biomedical Implants, *IEEE Trans Power Electron* 38.2:1423–1428.

[12]Tammam, A. et. al.: An Efficient Fully Bootstrapped RF-to-DC Rectifier for Implantable Biomedical Applications in CMOS Technology, *Journal of Engineering Sciences (JES)* 52.6 (2024):88-102.

[13] Jung et. al.: A Capacitive DC-DC Boost Converter with Gate Bias Boosting and Dynamic Body Biasing for an RF Energy Harvesting System, *Sensors* 23, no. 1: 395.

[14] Merrill, R. et. al.: Electrical stimulation of excitable tissue: design of efficacious and safe protocols, *Journal of neuroscience methods* 141, no. 2 (2005): 171-198.

[15] Hageman, N. et. al.: A CMOS neural interface for a multichannel vestibular prosthesis, *IEEE Trans Biomed Cir. Syst.* 10, no. 2 (2015): 269-279.

[16] Liu, X. et. al.: Five valuable functions of blocking capacitors in stimulators, *Biomed Techn* 53, no. 1 (2008): 322-324.

[17] Capogrosso, M. et al.: Configuration of electrical spinal cord stimulation through real-time processing of gait kinematics, *Nature Protocols* 13, no. 9 (2018): 2031–2061.

[18] Reza, R. et. al.: Polarity detection base pulse insertion for active charge balancing in electrical stimulation, *In 2014 IEEE Conference on Bio Eng. and Sci. (IECBES): 38-41.*

[19] Son, J. et. al.: An implantable neural stimulator IC with anodic current pulse modulation based active charge balancing, *IEEE Access* 8 (2020): 136449-136458.

Session 4:
Sensory Restoration

Computer Simulation of Combined Vestibular/Cochlear Implant Stimulation for the Analysis of Cross-Talk and Neuronal Responses

Handler M[1,2], Vey B[1], Glueckert T[3,4], Saba R[5], Garnham C[5], Baumgartner D[1]

[1]Department of Mechatronics, University of Innsbruck
[2] Institute of Electrical and Biomedical Engineering, UMIT TIROL
[3]Department of Otolaryngology, Medical University of Innsbruck
[4]Tirol Kliniken, University Clinics Innsbruck
[5]MED-EL GmbH

Abstract: *Combined vestibular/cochlear implants (VCIs) facilitate simultaneous stimulation of nerves of the vestibular and auditory system for combined rehabilitation of severe hearing loss and bilateral vestibular loss. In addition to in-vivo experiments and clinical studies, computer models are used to investigate effects of different stimulation scenarios on stimulation outcome considering amongst others varying inner ear anatomy, electrode designs, electrode contact positions, stimulation protocols and neural parameters. Several computer models for simulating the stimulation of only a single system (either the auditory or vestibular system) exist. Our group developed a modular simulation framework, enabling the simulation of combined vestibular and cochlear nerve fiber stimulation by VCIs. Electrical fields originating from electrical stimuli of VCIs are computed by the finite element method based on volume conductor models of segmented human inner ear anatomy. Neural stimulation is simulated using these electrical fields in combination with neuronal cable models considering realistic nerve fiber properties and pathways. Based on the presented framework, selective stimulation of vestibular nerve branches and sections of the cochlear nerve can be evaluated, enabling the analysis of potential stimulation cross-talk and optimization of implant and stimulation design in adjustable conditions. In addition, electrically evoked compound action potentials (eCAPs) can be simulated, allowing for the analysis of recorded neuronal responses down to the single fiber level. The presented framework thereby contributes to the continuous improvement of treatment and potentially also diagnosis options of VCIs.*

Keywords: *In vitro, ex vivo and in silico models, Sensory neuroprostheses (hearing, vision)*

Author's Address

Michael Handler
Department of Mechatronics, University of Innsbruck
michael.handler@uibk.ac.at

Focal stimulation of retinal ganglion cells by pulse duration modulation and current steering

Koppenwallner L.X.[1], Zeck G[1], Werginz P[1]

[1]Institute of Biomedical Electronics, TU Wien, Austria

Abstract: *Electrical stimulation of the retina by retinal implants is a promising technology to restore vision to blind people suffering from degenerative retinal diseases. However, these implants are severely limited due to the lack of spatial resolution afforded by electrical stimulation, which is heavily influenced by the undesired co-activation of distal neurons due to their axons passing close to targeted cells. In our recent work, we demonstrated that short pulse stimulation in the range of 10µs pulse duration is a promising method to avoid such co-activation. Here, we expand this idea by combing short pulse stimulation with current steering in a model of the electrically stimulated retina. Our results demonstrate that vertical electric fields strengthen the effect of short pulse stimulation thereby potentially allowing more sophisticated stimulating paradigms in future retinal implants.*

Keywords: *electrical stimulation, retinal ganglion cells, retinal implant, short pulse stimulation*

Introduction

Millions of people worldwide have sustained a severe loss of vision due to degenerative retinal illnesses, such as retinitis pigmentosa or age-related macular degeneration, both of which cause photoreceptors in the retina to permanently and irreversibly lose their function. In the recent past, multiple avenues have been explored to find viable treatment methods for these debilitating diseases. One particularly promising approach, having resulted in products which have received regulatory approval, is the restoration of vision via retinal implants which use electrical stimulation to excite the remaining nervous tissue of the retina [1].

A key reason for this low spatial resolution, particularly affecting epiretinal implants which target retinal ganglion cells (RGCs), is the co-activation of axons of passage. Ideally, stimulation with a specific electrode would elicit circular visual percepts in the region surrounding the electrode by exciting RGC somas only within the electrode's receptive field. However, due to similarities in somatic and axonal thresholds, the axons of distal RGCs, which travel from the periphery towards the center of the retina where they bundle to form the optic nerve are excited as well. This gives the impression that light was perceived at the location of these radially distant RGC somas, resulting in percepts that are radially elongated [2].

In this work, we aim to develop more focal stimulation protocols for epiretinal implants. Based on our recent work showing that short pulse stimulation increases the difference between somatic and axonal thresholds [3], here we expand this idea and combine it with current steering in a computational model.

Material and Methods

Spiking activity of RGCs in response to electrical microstimulation in the *ex-vivo* retina was recorded by patch-clamp electrophysiology [3]. Models were developed to replicate experimental results, the response of RGCs to electrical stimulation was computed in a two-step process: First, the electric field generated by a stimulating electrode was computed by finite element modeling. Second, computed electric fields were used as input for multicompartment models of RGCs which were evaluated based on spiking responses.

FEM models were realized in the *electric currents (ec)* module of COMSOL Multiphysics. The geometry of the surrounding system, e.g., a petri dish, was reproduced according to the electrophysiological setup in the lab. Stimulating (active) and ground electrodes were modeled to optimize electric fields with principal directions across the retina (vertical).

Multi-compartment models of RGCs were based on a previously published model by our group [4]. 37 model RGCs with different dendritic and axonal morphologies were used in this study. The NEURON simulation environment version 8.0 controlled via Python was used to solve the arising system of differential equations of the multi-compartment model. Spatial discretization of dendrites, soma, proximal and distal axon was set to 5, 1, 2 and 10µm, respectively; simulation time step was set to 0.5µs. Ion channel dynamics were based on the RGC membrane model from Fohlmeister et al. [5].

Results

As demonstrated in our recent publication [3], short pulse stimulation is promising strategy to avoid the problem of axonal co-activation in epiretinal implants. Here, we sought to improve focal RGC stimulation by the addition of current steering.

Short pulse stimulation with pulses in the range of 10us results in an increased soma-to-axon threshold ratio (Fig. 1A-B), i.e., axonal thresholds increase more strongly for short pulses than somatic thresholds. The arising difference in threshold amplitude between the soma and the axon can potentially be used as a window of opportunity for focal RGC stimulation in retinal implants.

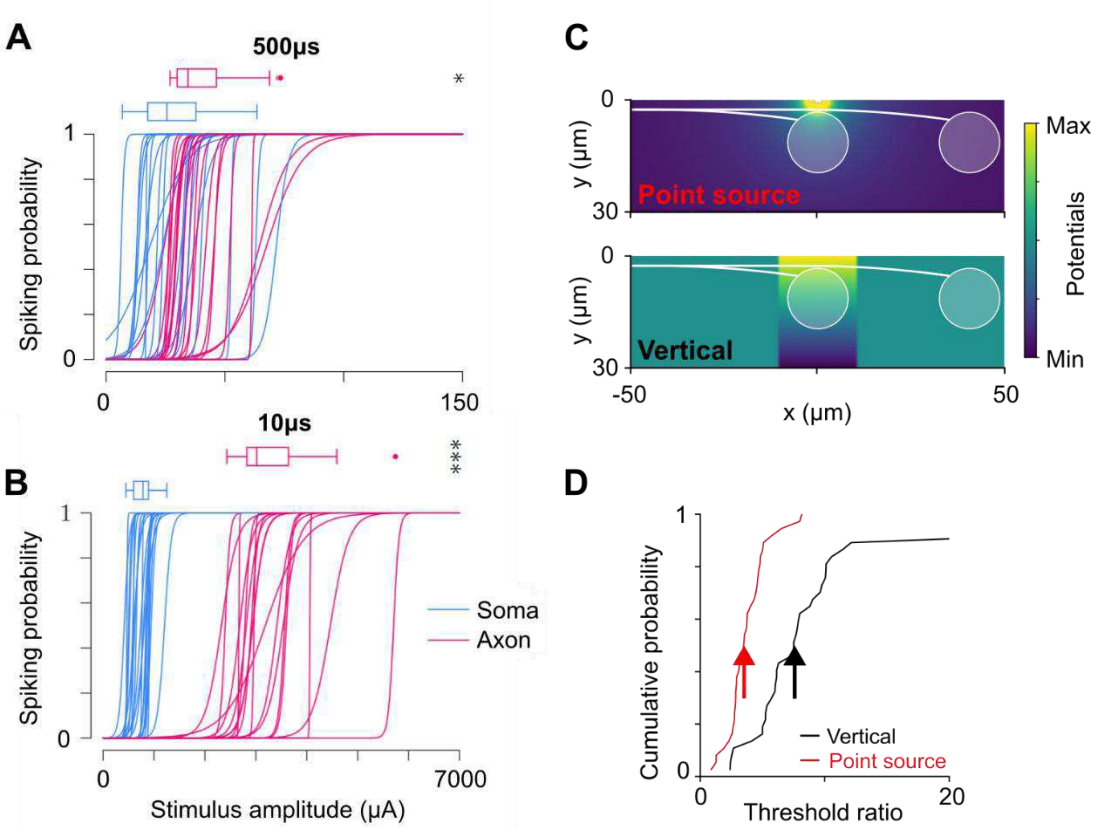

Figure 1: (**A**) Estimated spiking probabilities for somatic (blue) and axonal (red) stimulation for biphasic rectangular pulses with durations of 500µs. (**B**) Estimated spiking probabilities for somatic (blue) and axonal (red) stimulation for biphasic rectangular pulses with durations of 10µs. Data from panels A and B were obtained by patch-clamp electrophysiology [3].(**C**) Electric potentials with schematics of somatic and axonal stimulation for a point source electrode (top) and an artificial vertically oriented electric field (bottom). (**D**) Threshold ratio for all model neurons (n=37) is plotted as cumulative probability for the point source electrode (red) and the artificial vertical field (black). Arrows indicate median threshold ratios.

We showed that the proximity of the stimulating electrode and the targeted RGC structures in combination with the polarization across the soma is the leading cause for increasing threshold ratios with shorter pulse duration; therefore, our modeling approach aimed to create vertical electric fields to maximize the observed effect (Fig. 1C). Model activity in response to stimulation with a point source electrode resulted in median threshold ratios in the range of 4-5 similar to experimentally determined values with a microelectrode (Fig. 1D, red). However, by creating a perfect vertically directed electric field across the retina increased the effect by approximately 2-fold with median threshold ratios of 8-9 (Fig. 1D, black).

Discussion

Axonal co-activation is one of the main limiting factors of current epiretinal implants. Patients report elongated phosphenes, making it impossible to restore a higher quality of vision. While many technological advances in the fields of engineering, medicine and neuroscience improved implant performance, current retinal implants are still operating with pulses in the classical range of milliseconds. Our recent work and results shown here indicate that, at least for epiretinal implants targeting RGCs directly, short pulses are a promising approach to create focal activation without stimulation of passing axons.

Conclusions

In this work, we show that a combination of short pulse stimulation and current steering is a potential strategy to avoid the long-standing problem of axonal co-activation in retinal implant patients. The underlying mechanism, i.e., vertical electric field polarizing RGC somata, is not only limited to electrical stimulation of the retina but also applies to other systems employing electrical microstimulation.

Acknowledgement

Research was supported by the Austrian Science Fund (FWF; 10.55776/P35488).

References

[1] Ayton L.N. et al.: An update on retinal prostheses, *Clin. Neurophysiol.*, vol. 131, no. 6, pp. 1383–1398, Jun. 2020

[2] Nanduri D. et al.: Frequency and amplitude modulation have different effects on the percepts elicited by retinal stimulation, *Invest. Ophthalmol. Vis. Sci.*, vol. 53, no. 1, pp. 205–214, Jan. 2012

[3] Koppenwallner L.X. et al.: Short pulse epiretinal stimulation allows focal activation of retinal ganglion cells, *IEEE TNSRE*, vol. 33, pp. 542–553, Jan. 2025
[4] Werginz P. et al.: Avoidance of axonal activation in epiretinal implants using short biphasic pulses, *CDBME*, vol. 8, pp. 5–8, Sep. 2022
[5] Fohlmeister J.F. et al.: Mechanisms and distribution of ion channels in retinal ganglion cells: using temperature as an independent variable, *J Neurophysiol.*, vol. 103, no. 3, pp. 1357–1374, Mar. 2010

Author's Address

Paul Werginz
Institute of Biomedical Electronics, TU Wien
paul.werginz@tuwien.ac.at
https://www.tuwien.at/etit/bme

A first approach to phase-modulated interference stimulation for generating moving tactile perception

Koch Klaus Peter[1,2], Pinnecker Jana[1], Merz Simon[2,3]

[1]Trier Univeristy of Applied Sciences, Germany

[2]Institute for Cognitive and Affective Neuroscience, University of Trier, Germany;

[3]Department of Psychology, University of Trier, Germany

Abstract: *This study explores a novel approach to generating directional tactile feedback using phase-modulated interference stimulation combined with amplitude modulation. Two electrode pairs generate 2 kHz sinusoidal bursts with controlled phase shifts and dynamically modulated amplitudes, creating a moving interference focus perceived as tactile motion. In tests with 14 participants, this novel stimulation led to a significant perception of movement. Directional recognition was clearer along the distal–proximal axis than radial–ulnar. No significant correlation was found between current intensity and perception quality. The results highlight the potential of this method for non-invasive, focus controlled tactile feedback, with applications in prosthetics and haptic systems.*

Keywords: *Tactile feedback, Interference stimulation, Amplitude modulation, Sensory prosthetics*

Introduction

Tactile perception is one of the central senses of humans. A loss or impairment of this sense, such as when wearing prostheses, represents a significant functional impairment. One way to return sensory information from prostheses to the body is through electrical stimulation of the skin [1].
A special form of this method is burst stimulation with sinusoidal bursts, which, similar to classic electrical impulses, generates focused stimulation in the area of the electrodes [2]. Temporal interference stimulation is used to control the focus of stimulation spatially. Both concepts, the application of burst interference and temporal interference, have already been investigated in the context of stimulating deeper neural structures [3, 4].
The use of temporal interference stimulation to generate sensory perception was recently described in a publication [5]. Building on these foundations, the present work investigates the combination of burst-shaped interference stimulation and targeted spatial modulation to generate tactile motion sensations. The aim is to evaluate the potential of this method for generating direction-dependent, moving tactile perceptions.

Material and Methods

Stimulation Signal:
Two independent pairs of electrodes are used to deliver phase-modulated interference stimulation, in which the spatial pattern of interference is controlled by adjusting the phase and amplitude of the signals. Each electrode pair delivers sinusoidal, current-controlled stimulation signals. Both stimulation signals share the same carrier frequency of 2 kHz. This high frequency lies outside the bandwidth of neural excitability, in the sense of classical temporal interference stimulation, which means that no direct action potentials are triggered. In the resting state, there is a phase shift of 180° between the two signals, which leads to destructive interference when their local amplitudes are equal, thus cancelling out the resulting field strength in the target tissue. To generate a targeted stimulation pulse, one of the signals is briefly switched (for 250 µs) to twice the frequency (4 kHz). This induces a phase shift that temporarily aligns both signals in phase, enabling constructive interference. Subsequently, this generates an effective stimulation pulse in the tissue. After the desired pulse duration (1 ms) has elapsed, the same channel is switched back to 4 kHz for 250 µs to restore the original phase shift of 180° and thus re-establish destructive interference (Figure 1). Across all condition, 10 targeted stimulation pulses were presented per second (stimulation frequency: 10 Hz).

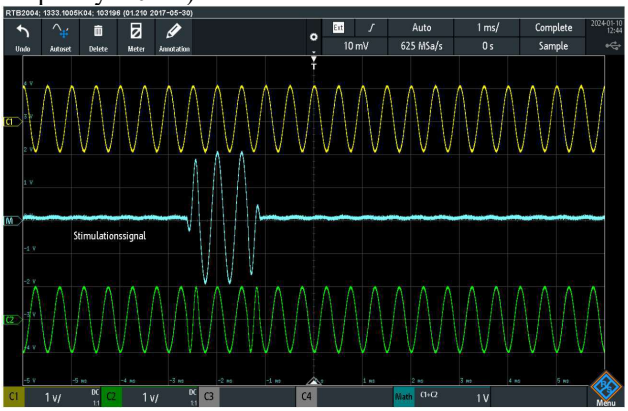

Figure 1: Measurement (zoom) of the two output channels and representation of the superposition with equal weighting of the two channels. C1 channel with constant phase, C2 channel with modulated phase, M **superposition of C1 and C2**.

The stimulation site results from the superposition of the two stimulation signals in the tissue and is located in the area of strongest interference, i.e., where the fields

constructively overlap. In order to specifically shift the location of maximum interference within the tissue area between the electrode pairs, the amplitude ratio of the two signal channels is modulated (75 % modulation factor). This modulation takes the form of a linear triangular pattern in which the amplitude of one channel is successively increased while that of the other is correspondingly decreased – and vice versa. This continuous, opposite amplitude distribution dynamically shifts the interference focus back and forth between the two electrode pairs, enabling directional, oscillating stimulation of the target tissue.

In the area of negative (destructive) interference—typically in the middle between the two pairs of electrodes—the superposition of the signals results in a sinusoidal curve whose amplitude varies depending on the modulation of the amplitude ratio of the two channels. This manifests itself in the fact that the amplitude of the resulting sine wave periodically becomes larger or smaller. In the areas of constructive interference, on the other hand, the signals from both sources add up almost completely, regardless of the current amplitude ratio. If the amplitude of one channel is reduced, this reduction is compensated by a corresponding increase in the amplitude of the second channel, so that the total amplitude in the area of constructive interference remains almost constant (Figure 2).

This dynamic configuration primarily changes the amplitude difference ("jump height") between the continuously present, sinusoidal basic excitation and the short-term stimulation pulses caused by constructive interference. This difference is crucial for the effectiveness of phase-modulated stimulation and can be specifically controlled via the amplitude distribution.

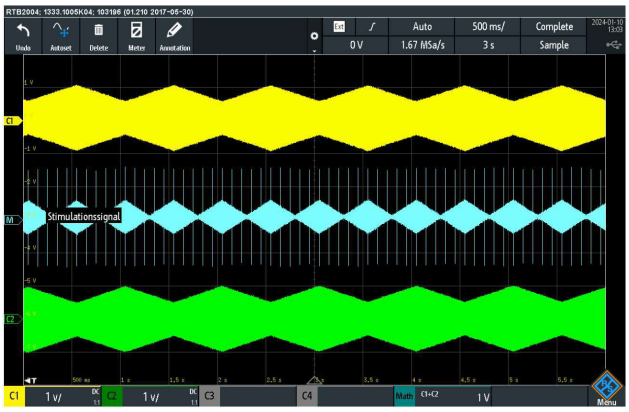

Figure 2: Measurement of the two output channels and representation of the superposition with equal weighting of the two channels with **modulation of amplitude ratio**. C1 channel with constant phase, C2 channel with modulated phase, M superposition of C1 and C2.

Technical setup:

The stimulation signal was generated using a standard PC in combination with an NI-PCI-6723 analog output card (National Instruments, USA). The sampling rate was set to 45 kS/s (kilosamples per second) per channel to ensure a sufficiently accurate representation of the high-frequency stimulation signals. Signal control and generation were performed using specially developed software programmed in MATLAB (MathWorks, USA).

A linearly isolated stimulator (model STMISOLA, Biopac Systems Inc., USA) was used to convert the generated voltage signal into a controlled current signal. The stimulator was operated in current output mode, with the load setting $Z\text{out} = 1\ \text{k}\Omega$. To rule out potential hazards from direct current components—for example, as a result of programming errors, device malfunctions, or incomplete skin contact—an additional protective circuit was integrated between the stimulator output and the electrode. Among other things, this circuit limits the maximum possible output voltage, for example, in the event of a sudden loss of skin contact.

A specially manufactured flexible printed circuit board served as the electrode (gold), which was integrated into an ergonomically designed mouse housing for better handling. This design ensures both stable skin contact and user-friendly application during stimulation (Figure 3).

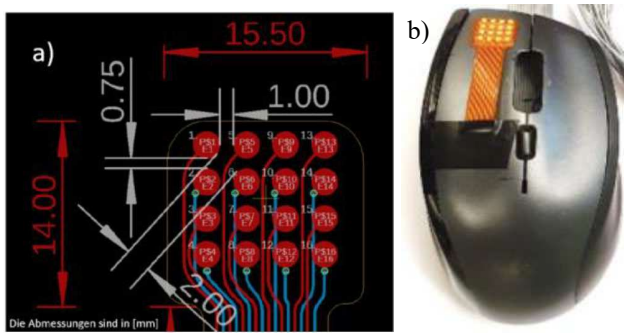

Figure 3: Electrode configuration: a) dimensions of the electrode in mm, b) mounting the electrode

Experiment

Overall, three different stimulation conditions were designed: One phase-modulated burst stimulation without any amplitude modulation, intended to create a focal stimulation percept without directional movement, and two phase modulated bust stimulations with amplitude manipulation with the goal to induce the percept of a moving stimulation, either in the distal / proximal direction or in the the radial / ulnar direction. In all conditions, only the four outer electrodes were used, each positioned at the corners of the stimulation array. The current sources were connected to two opposite electrodes. Variant 1: distal and proximal sides. This is intended to enable movement along the longitudinal axis of the thumb. Variant 2: radial and ulnar sides. This is intended to enable movement orthogonal to the longitudinal axis of the thumb (Figure 4, 5). Variant 3: Static phase-modulated burst stimulation without amplitude modulation, using the same electrode configuration as in Variant 2 and the stimulation signal as shown in Figure 1. This condition is intended to create a focal, non-moving stimulation percept (Figure 5)

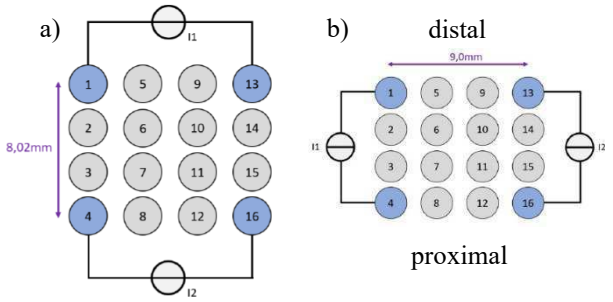

Figure 4: Electrode configuration for stimulation applied in Variant 1 (a) and Variants 2 and 3 (b)

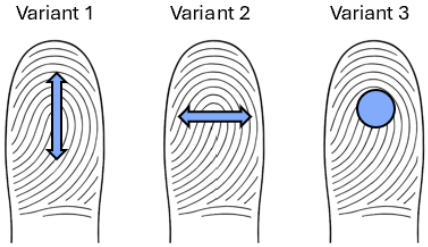

Figure 5: Intended movement directions of stimulation pulses

The experiment was approved by the Ethics Committee of Trier University of Applied Sciences. All participating subjects were fully informed about the aim, procedure, and potential risks of the experiment before the study began. Written consent to participate was obtained from all subjects.

The stimulation amplitude was determined individually for each subject. For this purpose, the current strength was gradually increased from a starting value of 1 mA as part of dynamic stimulation along the proximal direction of movement. The adjustment was made until the stimulation was clearly perceived by the test subjects but was not perceived as unpleasant or painful. This stimulus intensity, which was subjectively perceived as clear but tolerable, was then used to carry out the actual experiments.

A total of 14 test subjects between the ages of 21 and 51 participated in the study, allowing for the observation of the any effect given the generally high sensitivity of human direction perception ($dz > 1$ [6]. Each test subject was exposed to 30 stimuli, divided into five blocks of six stimuli each, in which each of the three stimulations was presented twice. Within each block, the order of the stimuli was randomized to minimize order effects. To assess subjective perception, a standardized questionnaire with three items was used after each stimulus:

Perception of stimulation: Was the stimulus perceived?
Response Options: Yes or no.

Perception of movement: Was a movement perceived?
Response Options: Yes or no.

Direction recognition: In which direction was the movement perceived?
Response Options: Horizontal (right-left) movement / Vertical (up-down) movement

Data analysis

Four hypotheses addressing different aspects of phase-modulated interference stimulation were formulated as part of the experimental study.

Hypothesis 1 assumes that pure phase-modulated burst stimulation, i.e., without additional amplitude modulation (Variant 3), is perceived by the test subjects as a focal, static sensation rather than as movement The aim of this hypothesis is to differentiate between punctual and movement-perceived stimulation and thus to examine the necessity of additional modulations to evoke the perception of moving stimulation.

Hypothesis 2 examines whether the combination of phase-modulated burst stimulation and inverted amplitude oscillation of two superimposed sinusoidal signals actually produces a tactile motion percept. The aim is to analyse whether directional stimulation can be simulated by targeted modulation of the signal amplitudes.

Hypothesis 3 refers to the ability of the test subjects to correctly recognize different directions of movement generated by targeted control of different pairs of electrodes. Two directions of movement were tested: distal-proximal (along the thumb) and radial-ulnar (across the surface of the thumb). The evaluation was carried out in two ways:

A) regardless of whether a movement was subjectively perceived, and

B) exclusively taking into account the stimuli in which the test subjects actually recognized a movement.

Hypothesis 4 examines whether there is a correlation between the individually adjusted current strength and the recognition rate of the stimulation. The aim of this hypothesis is to clarify whether higher current strengths are associated with more reliable perception or improved direction identification.

Results

The evaluation shows that phase-modulated interference stimulation was reliably perceived by the test subjects in the vast majority of cases. Electrical stimulation was detected in 96.4% of all stimuli.

Hypothesis 1: The analysis was performed using a one-sided t-test against the random value of 0.5. The mean value determined was 0.569, with a p-value of 0.487, which does not represent a statistically significant deviation from the random level. This indicates that selective stimulation without additional amplitude modulation was not successful to be perceived as no movement in our sample.

Hypothesis 2 examined the effect of contrary amplitude oscillation on the perception of movement. Here, too, a t-test was performed against the test value 0.5. The mean value was 0.727 with a p-value of 0.002, which represents a significant deviation from the random level. This confirms the hypothesis that the contrary amplitude modulation of the two sinusoidal signals leads to a clear perception of movement.

Hypothesis 3 investigated the directional differentiation of the perceived movement generated by different electrode combinations.

In consideration A, which includes all stimuli regardless of whether the movement was perceived, a significant mean value of 0.526 ($p = 0.007$) was found for the distal-proximal movement. For radial-ulnar movement, the mean value was 0.431 ($p = 0.110$) and was therefore not

significantly recognized. A rate probability of 0.33 was used in both tests.
In consideration B, which only took into account those stimuli that were perceived as movement by the test subjects, the mean values for distal-proximal movement were a significant mean value of 0.672 ($p = 0.006$) and for radial-ulnar movement a significant mean value of 0.345 ($p = 0.016$). Here, 1 stood for distal-proximal movement and 0 for radial-ulnar movement. These results suggest that direction perception is more reliable when the movement was consciously recognized, especially for the distal-proximal orientation.
Hypothesis 4 analyzed the relationship between the individually set current intensity (6.5–10 mA) and the recognition rate of the stimulation. The calculated Pearson correlation coefficients ranged between -0.191 and 0.338 and showed no significant correlations in the p-value analysis.
It can therefore be concluded that the selected current intensity had no systematic influence on the quality of perception or direction differentiation. However, it should be noted that only one stimulation intensity was used for all test subjects.

Discussion

Hypothesis 1 – Perception without amplitude modulation
The results show no clear perception of motionless stimulation. This may be related to the fact that the stimulation was performed at a relatively low stimulation frequency of 10 Hz. This can lead to the perception of pulsating stimulation, which can also be interpreted as motion [7].
Hypothesis 2 – Perception with inverted amplitude modulation
Stimulation with inverted amplitude modulation led to a significantly increased sensation of movement, which clearly confirmed the hypothesis. This is considered a success of the methodological implementation: the configuration generates a shiftable interference zone that apparently triggers a kinesthetically interpretable stimulus perception. This shows that the spatial-dynamic control of the interference field works in principle.
Hypothesis 3 – Directional perception
The different movement directions were successfully differentiated:
In the distal-proximal direction, the stimuli could be recognized significantly better than in the radial-ulnar direction. Awareness of the movement (part B) increased the hit rate in both directions, which suggests that unconsciously perceived stimuli are less distinguishable. The poorer performance in the radial-ulnar direction could be due to anatomy (e.g., finger structure), electrode placement, or signal overlap and aligns with findings from previous studies on tactile perception at the fingers, such as motion direction discrimination tasks, which also reported lower performance in the radial–ulnar direction compared to the distal–proximal axis [8]. These results suggest that directional tactile perception is possible but varies in quality depending on the direction.
Hypothesis 4 – Influence of current strength
The analysis of the correlation between current intensity and perception quality did not reveal any significant relationships. It is therefore concluded that the individually adjusted stimulus intensity is not decisive for the ability to perceive direction as long as it is within a comfortable and clearly perceptible range. Such findings align with recent studies on interference haptic stimulation, which demonstrated that effective and consistent tactile perception can be achieved at relatively low current densities without the need for high intensities [5]. This suggests robust perception efficiency, regardless of slightly varying individual thresholds.

Conclusions

The present study successfully demonstrates that phase-modulated interference stimulation with dynamically modulated amplitude distribution can evoke a clear and directed tactile perception in human subjects. While pure burst stimulation without amplitude modulation did not reliably elicit the perception of motion, the application of inverted amplitude oscillation between two high-frequency sinusoidal stimulation sources resulted in a statistically significant sensation of movement. This validates the underlying principle that spatially controllable interference stimulation can be used to simulate tactile motion on the skin.
The ability to differentiate movement direction was found to be direction-dependent: stimuli aligned along the distal-proximal axis were perceived more reliably than those along the radial-ulnar axis. The poorer performance in lateral directions may reflect anatomical constraints, suboptimal electrode positioning, or overlapping field effects that should be addressed in future optimizations.
Importantly, the individually adjusted stimulation intensities, though calibrated for subjective comfort did not correlate with performance measures. This suggests that the method is robust across a range of current levels and does not require high intensities to achieve effective sensory stimulation.
Overall, the results support the feasibility of using phase-modulated interference combined with amplitude modulation to generate non-invasive, directionally controlled tactile feedback. This approach offers promising applications for future sensory feedback systems in neuroprosthetics, human-computer interaction, and haptic interfaces. Further research should focus on improving spatial resolution, optimizing electrode configuration and stimulation patterns, and expanding the dimensions of perception beyond direction to include, for example, speed or type of perception.

References

[1] E. D. Papaleo et al., "Integration of proprioception in upper limb prostheses through non-invasive strategies: a review," Journal of neuroengineering and rehabilitation, vol. 20, no. 1, p. 118, 2023, doi: 10.1186/s12984-023-01242-4.

[2] B. Bromm and H. Lullies, "Über den Mechanismus der Reizwirkung mittelfrequenter Wechselströme auf die Nervenmembran," *Pflgers Archiv*, vol. 289, no. 4, pp. 215–226, 1966, doi: 10.1007/BF00363808.

[3] R. B. Budde, M. T. Williams, and P. P. Irazoqui, "Temporal interference current stimulation in peripheral nerves is not driven by envelope extraction," *Journal of neural engineering*, vol. 20, no. 2, 2023, doi: 10.1088/1741-2552/acc6f1.

[4] Y. Terasawa, H. Tashiro, T. Ueno, and J. Ohta, "Precise Temporal Control of Interferential Neural Stimulation via Phase Modulation," *IEEE transactions on bio-medical engineering*, vol. 69, no. 1, pp. 220–228, 2022, doi: 10.1109/TBME.2021.3091689.

[5] K. Lim *et al.,* "Interference haptic stimulation and consistent quantitative tactility in transparent electrotactile screen with pressure-sensitive transistors," *Nature communications*, vol. 15, no. 1, p. 7147, 2024, doi: 10.1038/s41467-024-51593-2.

[6] G. K. Essick, K. R. Bredehoeft, D. F. McLaughlin, and J. A. Szaniszlo, "Directional sensitivity along the upper limb in humans," *Somatosensory & motor research*, vol. 8, no. 1, pp. 13–22, 1991, doi: 10.3109/08990229109144725.

[7] S. J. Bolanowski, G. A. Gescheider, R. T. Verrillo, and C. M. Checkosky, "Four channels mediate the mechanical aspects of touch," *The Journal of the Acoustical Society of America*, vol. 84, no. 5, pp. 1680–1694, 1988, doi: 10.1121/1.397184.

[8] S. Kuroki and S. Nishida, "Motion Direction Discrimination with Tactile Random-Dot Kinematograms," *i-Perception*, vol. 12, no. 2, 20416695211004620, 2021, doi: 10.1177/20416695211004620.

Author's Address

Klaus Peter Koch: Trier Univeristy of Applied Sciences, Schneidershof, Trier, Germany, Koch@hochschule-trier.de, https://www.hochschule-trier.de/hauptcampus/technik/persoenliche-webseiten/klaus-peter-koch;
Jana Pinnecker: Trier Univeristy of Applied Sciences, Trier, Germany, pinneckerjana@gmail.com;
Simon Merz: Institute for Cognitive and Affective Neuroscience, Department of Psychology, University of Trier, Germany, merzs@uni-trier.de, https://www.uni-trier.de/universitaet/fachbereiche-faecher/fachbereich-i/faecher-und-institute/psychologie/professuren/cognitive-psychology/team-alt/simon-merz

Session 1: Methodological Insights

Ultrasound Assessment of Forearm Muscle Changes Following FES in Sarcopenic Elderly: Preliminary Results of a Feasibility Study

Hashim HAS[1], Hamzaid NA[1]

[1]Department of Biomedical Engineering, Faculty of Engineering, Universiti Malaya, Malaysia

Abstract: This pilot feasibility study explores the ultrasound imaging to assess changes in forearm muscle size following Functional Electrical Stimulation (FES) training in elderly individuals diagnosed with sarcopenia, compared with healthy young adults. Muscle thickness was measured using B-mode ultrasound imaging in sagittal and axial planes at baseline (W0) and after 2 weeks (W2) of FES training. Preliminary results show a consistent increase in muscle thickness in elderly participants, while young adults exhibited minimal change. The findings suggest that ultrasound imaging is a sensitive tool to monitor FES-induced muscle changes. The study is ongoing, and results through week 4 will be presented at the workshop.

Keywords: sarcopenia, ultrasound imaging, functional electrical stimulation, muscle morphology, aging

Introduction

Sarcopenia, the age-related loss of muscle mass and function, poses significant risk to elderly individuals, particularly in Malaysia's aging population [1,8]. Early detection is critical, yet conventional methods like DXA and MRI are impractical for large-scale or routine use. Ultrasound imaging has emerged as a portable, non-invasive alternative capable of visualizing muscle morphology in real-time [4,7]. Functional Electrical Stimulation (FES), meanwhile, offers potential to activate and restore muscle contractility in aging populations. Despite their individual utility, limited research has evaluated their combined application for monitoring muscle changes in sarcopenic elderly. This study investigates whether ultrasound can detect FES-induced changes in forearm muscle size, comparing sarcopenic elderly to healthy young controls.

Material and Methods

Participants

This feasibility study involved two elderly participants diagnosed with sarcopenia (1 M 60+ years old, 1 F 60+ years old) and two healthy young adult controls (2 F, 20+ & 30+ years old). The elderly participants met the diagnostic criteria for sarcopenia based on clinical screening and muscle function tests.

Equipment

Ultrasound imaging was conducted using the Xinsight DC-60 Exp system (Mindray) to assess forearm muscle thickness in sagittal and axial views. Functional Electrical Stimulation (FES) was administered using the Techcare Wireless TENS device, and muscle function was evaluated using a digital hand dynamometer to measure grip strength before each stimulation session.

Study Protocol

The study protocol spanned four weeks. At the beginning of each week, ultrasound imaging was performed to establish a baseline measurement before initiating FES sessions. Participants underwent FES training three times per week on non-consecutive days (e.g., Monday, Wednesday, and Friday). Prior to each session, grip strength was assessed and recorded to monitor potential functional improvements. During each session, the FES device was set to maximum intensity (level 16), and stimulation was applied for a total of 30 minutes, split into two consecutive 15-minute periods to accommodate the device's session limit. Electrodes were positioned over the same anatomical locations used in the ultrasound scans to ensure consistency across sessions. At the end of each week, ultrasound imaging was repeated to evaluate any morphological changes resulting from the cumulative FES sessions.

Data was collected from Week 0 to Week 2. Study continues to Week 4.

Figure 1: (left) Transverse Probe Position, (right) Longitudinal Probe Position

Results

Muscle thickness increased in both elderly participants between Week 0 and Week 2. Young adult participants showed minimal or no changes.

Table 2: Muscle Thickness Measured via Ultrasound

Subject	View	Side	W0 (cm)	W2 (cm)
	Sagittal	R	2.0	2.2
Elderly		L	1.8	2.0
1	Axial	R	1.7	1.9
		L	1.6	1.7
	Sagittal	R	2.2	2.3
Elderly		L	2.0	2.2
2	Axial	R	1.9	2.0
		L	1.8	1.9
			1.88±0.19	**2.02±0.20**
	Sagittal	R	2.9	2.9
Young 1		L	2.8	2.8
	Axial	R	2.6	2.7
		L	2.5	2.6
	Sagittal	R	3.0	3.0
Young 2		L	2.9	2.9
	Axial	R	2.7	2.8
		L	2.6	2.7
			2.75±0.18	**2.80±0.13**

Discussion

The preliminary results of this study, covering the first two weeks of FES training, demonstrate a positive trend in muscle adaptation in the elderly sarcopenic group. Both participants in this group showed measurable increases in forearm muscle thickness across all measured sites (sagittal and axial views), indicating early hypertrophic response to the electrical stimulation.

This finding aligns with existing literature suggesting that aging skeletal muscles, although atrophied, retain the ability to respond to appropriate stimulation when delivered consistently and at a sufficient intensity [3,6]. The use of FES, particularly at the highest tolerated level (level 16 – maximum level of the FES device), appears to have effectively triggered muscle contractions sufficient to stimulate growth. This supports the therapeutic potential of FES in counteracting sarcopenia, especially in populations where voluntary physical activity is limited due to frailty or mobility impairments [3,6].

In contrast, the young adult participants showed little to no change in muscle size over the same period. This is an expected outcome, as their muscle tissues are already at or near optimal baseline levels [3]. The lack of hypertrophy suggests that FES, at least in short-term protocols, primarily benefits muscles that are under-conditioned or affected by age-related degeneration. Interestingly, slight increases observed in axial thickness in young adults may reflect measurement variability or temporary fluid shifts, rather than structural adaptation [4].

Furthermore, the consistency in data collection (e.g., using the same time slots for stimulation, repeatable ultrasound measurement sites, and pre-session grip testing) helped ensure reliable week-over-week comparisons. The methodology also demonstrated feasibility and ease of integration into a clinical or community health setting, especially given the portable and user-friendly nature of the equipment used.

The integration of grip strength measurement offers functional insight into muscle performance, though its full analysis will be more meaningful with data from all four weeks. Grip strength trends will be essential in determining whether morphological gains also translate into functional improvements which a critical outcome in sarcopenia management [2].

Additionally, this study contributes methodologically by demonstrating that ultrasound, when combined with FES protocols, is a practical, non-invasive, and cost-effective monitoring tool that can be used outside of specialized imaging centers [4]. The ability to visualize subtle muscle adaptations over short periods reinforces its value as both a diagnostic and progress-tracking modality [4,7].

While the findings are promising, limitations should be acknowledged. The sample size is small, and the short duration may not capture the full extent of muscle remodelling. Participant variability (e.g., baseline health, nutrition, and hydration) could also influence the results. However, the ongoing data collection through Week 4 will help validate these early trends and provide a stronger basis for clinical recommendations.

Conclusions

Ultrasound imaging is a feasible and reliable method to monitor FES-induced changes in elderly muscle tissue. The Week 2 findings confirm muscle adaptation following regular FES application in the sarcopenic group. Data collection through Week 4 will further clarify the intervention's efficacy and optimal stimulation parameters.

Acknowledgement

The author wishes to thank the study participants and all clinical and technical staff involved in the study. Special thanks to the sonographers for consistent and accurate imaging throughout the intervention.

References

[1] Rosenberg, I.H. Sarcopenia: origins and clinical relevance. J Nutr. 1989.
[2] Cruz-Jentoft, A.J. et al. Sarcopenia: revised European consensus on definition and diagnosis. Age Ageing. 2019.
[3] Maffiuletti, N.A. et al. Neuromuscular electrical stimulation for preserving muscle function after surgery. Phys Ther. 2018.

[4] Pillen, S. et al. Skeletal muscle ultrasound: correlation between fibrous tissue and echo intensity. Ultrasound Med Biol. 2009.
[5] De Lorenzo, A. et al. Normal weight obese: new insight in metabolic syndrome. Acta Diabetol. 2016.
[6] Gondin, J., et al. Neuromuscular electrical stimulation training: neurophysiological and functional effects. Eur J Appl Physiol. 2005;94(4): 395–401.
[7] Arts, I.M.P., et al. Normal values for quantitative muscle ultrasonography in adults. Muscle Nerve. 2010;41(1):32–41.
[8] Ministry of Women, Family and Community Development (Malaysia), Aged Population Statistics, 2011.

Author's Address

Nur Azah Hamzaid
Department of Biomedical Engineering, Faculty of Engineering, Universiti Malaya, 50603, Kuala Lumpur, Malaysia
azah.hamzaid@um.edu.my
umexpert.um.edu.my/azah-hamzaid

Muscle Oxygenation-based Classification of Spinal Cord Injury During FES using NIRS and Machine Learning

Hamzaid NA[1], Saw SN[2], Cheong GKX[1], Lim HQ[1], Li JX[2], Hasnan N[3], Davis GM[4]
[1]Department of Biomedical Engineering, Faculty of Engineering, Universiti Malaya, Malaysia
[2]Department of Artificial Intelligence, Faculty of Computer Science and Information Technology, Universiti Malaya, Malaysia, [3]Department of Rehabilitation Medicine, Faculty of Medicine, Universiti Malaya, Malaysia, [4]Discipline of Exercise and Sports Science, Sydney School of Health Sciences, Faculty of Medicine and Health, The University of Sydney, Camperdown, NSW, Australia

Abstract: *This study proposes a signal-based classification method to differentiate tetraplegia (SCI) patients from able-bodied (AB) individuals using near-infrared spectroscopy (NIRS) data. Thirty-three AB and seven SCI subjects underwent FES-induced wrist extension exercises until fatigue. The signals analysed included oxyhaemoglobin (O_2Hb), deoxyhaemoglobin (HHb), total haemoglobin (tHb), and tissue saturation index (%TSI). These parameters served as input features for classification models. Due to the class imbalance between AB and SCI samples, three modelling strategies were adopted: default modelling, SMOTE-based oversampling, and SMOTE combined with GridSearchCV for hyperparameter optimization. Six machine learning algorithms—Decision Tree, K-Nearest Neighbors, Logistic Regression, Random Forest, Support Vector Classifier, and Extreme Gradient Boosting—were evaluated. Performance was measured across multiple metrics, with emphasis on recall to ensure correct identification of SCI patients. Results demonstrated that SMOTE and SMOTE+GridSearchCV notably improved classification accuracy and recall. The study highlights the potential of combining blood oxygenation signals and machine learning to assist in SCI diagnosis and rehabilitation planning.*

Keywords: *Blood oxygenation, tetraplegia, near-infrared spectroscopy, classification, machine learning*

Introduction

Spinal cord injury (SCI) is a multidimensional disorder resulting from direct or indirect damage to the spinal cord, which disrupts communication between the brain and the rest of the body. This disruption often leads to severe motor and sensory impairments, profoundly affecting an individual's functional abilities and quality of life (Bennett et al., 2024). Rehabilitation techniques such as Functional Electrical Stimulation (FES) have been widely adopted to induce muscle contractions in SCI patients to restore partial movement and delay muscle atrophy. Functional electrical stimulation has increasingly been used to elicit rhythmic muscle contractions and purposeful movements in the paralyzed lower limbs of persons with SCI (Hasnan et al., 2018). It has been used as a rehabilitation tool that enables localized exercise benefits to denervated muscles, resulting in greater strength, enhanced circulation, and blood flow, with concomitant adaptations in skeletal muscle mitochondrial function. However, FES also leads to rapid muscle fatigue, and the underlying physiological responses, especially in muscle oxygenation and haemodynamics, differ greatly between SCI patients and able-bodied individuals. Following prolonged training with FES, the muscle adaptation to fatigue responses may improve and this could be used as an index of recovery. A relevant tool for this could be post-fatigue recovery via non-invasive spectroscopic imaging devices such as near-infrared spectroscopy (NIRS).

Recent advances in non-invasive technologies like NIRS enable real-time assessment of muscle oxygenation by detecting changes in light absorption of oxygen-sensitive molecules in tissue. NIRS is a versatile and powerful optical technique that provides continuous monitoring of muscle haemodynamics and oxygenation by measuring parameters such as oxyhaemoglobin (O_2Hb), deoxyhaemoglobin (HHb), total haemoglobin (tHb), and tissue saturation index (%TSI). These signals are chosen because they collectively offer detailed insights into oxygen delivery, extraction, and blood volume within the muscle. Since arterial oxygen saturation remains relatively stable, changes in these NIRS-derived signals—especially those unrelated to cardiac pulsations or muscle contractions—often reflect venous blood volume dynamics and vascular compliance (Jones et al., 2016). Due to its non-invasive nature and ability to capture dynamic physiological changes, NIRS has seen increasing application across laboratory research, sports science, and clinical practice (Barstow, 2019). This widespread use underscores its value in elucidating the mechanisms of oxygen transport and utilization in both healthy and pathological conditions.

Machine learning (ML) techniques have shown promise in extracting meaningful patterns from biomedical signals for diagnostic and classification tasks. In this study, we aim to distinguish tetraplegia patients from healthy individuals based on their muscle oxygenation responses during FES-induced wrist extension exercises. By leveraging NIRS-derived signal data and applying various ML algorithms—including Decision Tree, K-Nearest Neighbours, Logistic Regression, Random Forest, Support Vector Classifier, and Extreme Gradient Boosting—we investigate the classification potential of these features. Furthermore, to

address the inherent class imbalance in our dataset (33 AB vs. 7 SCI), we implemented the Synthetic Minority Over-sampling Technique (SMOTE) and GridSearchCV to optimize model performance.

This research explores the integration of physiological signal monitoring with machine learning to provide accurate and automated approach for identifying and understanding neuromuscular response in tetraplegia and potentially comparing these to exercise responses of healthy muscles, ultimately contributing to more personalized rehabilitation strategies.

Material and Methods

Equipment:

- Functional Electrical Stimulation (FES) system
- Near-Infrared Spectroscopy (NIRS) device
- Muscle Mechanomyogram (MMG) system
- Blood pressure cuff (for arterial occlusion)

This study proposes a signal-based classification method to differentiate tetraplegia (SCI) patients from able-bodied (AB) individuals using near-infrared spectroscopy (NIRS) data collected during functional electrical stimulation (FES)-evoked exercise.

Participants:
Forty subjects were recruited, including 33 able-bodied individuals age 21-24 years, and 7 tetraplegic SCI patients. Inclusion criteria of the SCIs were age 18–80 years, SCI at level C5 or above, ability to understand and follow instructions, willingness to use the FES device, and medical stability confirmed by a physician. Both traumatic and non-traumatic SCI cases were included. Exclusion criteria included pre-existing bone conditions, skin allergies to electrodes, autonomic dysreflexia or neurological/psychiatric disorders, implanted electronic devices (e.g., pacemakers), prior botulinum toxin injections, orthopaedic conditions affecting limb function, and morbid obesity (BMI > 40).

Experimental Protocol:
All subjects underwent a 4-session experimental protocol targeting the wrist extensor muscle group due to its preserved function and importance in upper limb activity among SCI patients. Each session involved sustained, FES-evoked exercise-mode-only contractions designed to induce muscle fatigue. The stimulation parameters were adjusted to evoke strong yet tolerable wrist extension contractions lasting approximately 30 minutes per session. Immediately following each exercise session, a super-systolic arterial occlusion was applied at 260 mmHg for 3 minutes using a blood pressure cuff to evaluate post-exercise oxygen kinetics and recovery.

Muscle Oxygenation Monitoring (NIRS):
Muscle oxygenation and hemodynamic responses were monitored in real-time using near-infrared spectroscopy (NIRS), a noninvasive technique measuring key parameters:

- Oxyhaemoglobin (O_2Hb): Represents oxygenated haemoglobin concentration, reflecting oxygen delivery.
- Deoxyhaemoglobin (HHb): Reflects oxygen extraction by muscle tissue.
- Total Haemoglobin (TtO_2): Sum of O_2Hb and HHb, indicating local blood volume and perfusion.

The NIRS probe was placed longitudinally on the muscle belly and secured with optically neutral double-sided waterproof adhesive tape (Shimadzu, Kyoto, Japan). To minimize ambient light interference, limbs were wrapped in light-blocking fabric during measurements. Data collection occurred continuously throughout the FES-evoked exercise sessions.

Data Acquisition and Signal Processing:
NIRS signals were recorded exclusively during the FES exercise mode. Signal preprocessing included artifact removal and normalization relative to baseline. Extracted parameters (O_2Hb, HHb, and TtO_2) served as input features for classification models.

Classification Modelling:
Given the class imbalance between AB and SCI groups, three modelling strategies were employed: default modelling without data balancing, SMOTE (Synthetic Minority Over-sampling Technique) for oversampling the minority class, and SMOTE combined with GridSearchCV for hyperparameter optimization. Six machine learning algorithms were evaluated: Decision Tree, K-Nearest Neighbours, Logistic Regression, Random Forest, Support Vector Classifier, and Extreme Gradient Boosting. Model performance was assessed using multiple metrics, with an emphasis on recall to prioritize accurate identification of SCI patients.

The study initially compared muscle oxygenation signals—oxygenated haemoglobin (O_2Hb), deoxygenated haemoglobin (HHb), and total haemoglobin (TtHb)—between seven able-bodied (AB) male participants and seven individuals with tetraplegia (SCI). Independent t-tests revealed no significant difference in O_2Hb levels, suggesting similar oxygen delivery in both groups. However, HHb and TtHb were significantly lower in the SCI group, indicating reduced oxygen extraction and blood volume, likely due to decreased muscle activation, autonomic dysfunction, or anemia-related factors common in SCI.

The dataset was then expanded to include 33 AB and 7 SCI participants. NIRS-derived features (O_2Hb, HHb, TtHb, and %TSI) were input into six classification algorithms: Decision Tree (DT), K-Nearest Neighbours (KNN), Logistic Regression (LR), Random Forest (RF), Support Vector Classifier (SVC), and Extreme Gradient Boosting (XGB). Three modeling strategies were applied: default (no class balancing), SMOTE (Synthetic Minority Over-sampling Technique), and SMOTE combined with GridSearchCV for hyperparameter tuning. Performance

was evaluated across five key metrics: accuracy, precision, recall, ROC AUC, and F1-score.

Results

Among the strategies, SMOTE and SMOTE+GridSearchCV consistently improved recall and F1 scores, particularly for the SCI group. Notably, Logistic Regression under SMOTE+GridSearchCV demonstrated the best recall and balanced performance across all metrics, indicating it as the most suitable classifier for this dataset. In contrast, other algorithms such as Random Forest and Decision Tree performed well in accuracy but lagged in recall, especially when class imbalance was not addressed.

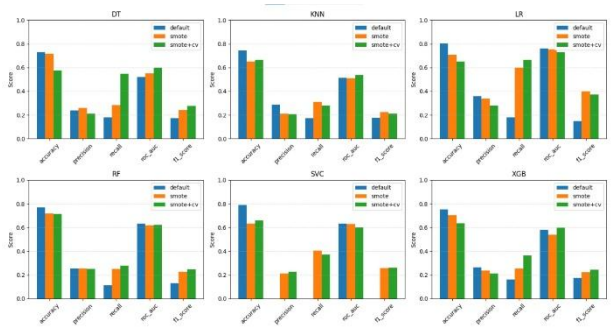

Figure 1: Comparison of Classification Metrics Across Models and Sampling Strategies

Figure 1 presents the classification performance of six commonly used machine learning models—Decision Tree (DT), K-Nearest Neighbours (KNN), Logistic Regression (LR), Random Forest (RF), Support Vector Classifier (SVC), and XGBoost (XGB)—under three different data processing strategies: default (original imbalanced data), SMOTE (Synthetic Minority Over-sampling Technique), and SMOTE combined with cross-validation (SMOTE+CV). The evaluation metrics are accuracy, precision, recall, ROC AUC, and F1 score. Using SMOTE usually helps models detect classes better, shown by higher recall and F1-scores. The SMOTE+CV strategy makes models more stable, often gives more balanced results, especially in ROC-AUC and F1 score. However, different models react differently to each strategy, but Logistic Regression and Decision Tree perform best with SMOTE+CV. They are good choices for classifying imbalanced datasets.

Discussion

The findings from this study highlight key physiological and computational insights in the context of SCI muscle physiology during exercise. Statistically, the lower HHb and TtHb levels observed in SCI subjects reflect reduced oxygen extraction and local perfusion, aligning with clinical expectations of altered haemodynamics in non-innervated muscles. These trends support the use of NIRS as a standalone, non-invasive modality to monitor muscular responses during FES-evoked exercise.

On the computational side, the machine learning results demonstrate the importance of both model selection and data preprocessing strategies. Logistic Regression outperformed other algorithms in detecting SCI profiles, particularly when SMOTE and GridSearchCV were applied. This aligns with logistic regression's strength in small and imbalanced biomedical datasets, offering stable generalisation when combined with oversampling.

The observed improvements in recall—an essential metric for identifying minority class samples (i.e., SCI)—confirm that balancing techniques like SMOTE are critical in enhancing model fairness and clinical reliability. Moreover, the effectiveness of Logistic Regression with minimal complexity reinforces its practical value for real-world integration into FES rehabilitation systems. Together, these results suggest that NIRS signals can not only capture physiological fatigue but also serve as viable input for real-time classification in adaptive rehabilitation platforms.

Conclusion

This study demonstrated that NIRS-derived muscle oxygenation signals, when processed through appropriate machine learning models, can effectively distinguish between able-bodied and spinal cord injury participants during FES-induced fatigue. Statistical analysis confirmed key physiological differences in oxygen extraction and blood volume, while classification models, particularly logistic regression, successfully identified SCI-specific patterns with high recall. The combined use of SMOTE and hyperparameter tuning significantly enhanced model sensitivity to SCI cases, addressing the imbalance challenge inherent in clinical datasets. These findings support the feasibility of developing AI-driven, NIRS-based feedback systems that could eventually inform therapy adjustments in real time.

Future work will expand subject recruitment, refine the classification pipeline, and explore integration into closed-loop FES rehabilitation tools that are both personalised and physiologically aware.

Acknowledgement

This study was conducted with support from Universiti Malaya's internal research funding. The authors would like to thank all volunteers and patients who participated in the study.

References

[1] Hasnan, N., Saadon, N. S. M., Hamzaid, N. A., Teoh, M. X., Ahmadi, S., Davis, G. M.: Muscle oxygenation during hybrid arm and functional electrical stimulation–evoked leg cycling after spinal cord injury, Medicine, vol. 97, no. 43, p. e12922, 2018.

[2] Bennett, J., Das, J. M., Emmady, P. D.: Spinal cord injuries, StatPearls, NCBI Bookshelf, 2024.
[3] Jones, S., Chiesa, S. T., Chaturvedi, N., & Hughes, A. D.: Recent developments in near-infrared spectroscopy (NIRS) for the assessment of local skeletal muscle microvascular function and capacity to utilise oxygen, Artery Res., vol. 16, no. C, p. 25, 2016.
[4] Barstow, T. J.: Understanding near infrared spectroscopy and its application to skeletal muscle research, J. Appl. Physiol., vol. 126, no. 5, pp. 1360–1376, 2019.

Author's Address

Nur Azah Hamzaid
Department of Biomedical Engineering, Faculty of Engineering, Universiti Malaya, 50603, Kuala Lumpur, Malaysia
azah.hamzaid@um.edu.my
umexpert.um.edu.my/azah-hamzaid

Title: Investigating Predictors of Recovery After Spinal Cord Injury: A Statistical Approach to Secondary Injury and Clinical Outcome Analysis

Authors: Ellen Huld Þórðardóttir[1,2], Katrín Rut Mar Þórðardóttir[2], Selma Gunnarsdóttir[2], Kára Dís Ólafsdóttir[2], Páll E. Ingvarsson[1], Ólöf Jóna Elíasdóttir[1], Þórður Helgason[1,2]
[1]Landspítali – The National University Hospital of Iceland, [2]Reykjavík University
ellenht@landspitali.is

Introduction: Spinal cord injuries (SCI) often lead to severe and lasting neurological impairment[1]. Increasing evidence suggests that a portion of the damage results from secondary injury mechanisms—such as ischemia, inflammation, and cellular apoptosis unfold after the initial trauma[2]. These processes may be modifiable through early interventions. Among the critical factors believed to influence outcomes are the timing of surgical decompression, maintenance of adequate mean arterial pressure (MAP)[3], and the potential neuroprotective effects of therapeutic hypothermia[4]. Our hypothesis is that optimized surgical timing, sustained MAP above recommended thresholds, and early-phase cooling can reduce the extent of secondary injury and improve functional recovery. This study uses national hospital data from Landspítali (2005–2023) to explore patterns in diagnosis, treatment timing, and physiological variables that may predict clinical outcomes following SCI.

Aim: To identify patterns in SCI diagnosis and treatment pathways in Iceland and analyze the relationship between prehospital care, surgical timing, and neurological outcomes using data from Landspítali between 2005 and 2023.

Methods: Patient records were analyzed based on ICD-10 diagnosis codes, NOMESCO procedure codes, and hospital admission data. Variables included age, gender, transport method, emergency department (ED) arrival time, blood pressure, and time to surgery. Surgeries were categorized as early (≤24h) or delayed (>24h). Chi-square tests evaluated associations between care variables and outcomes. An AI tool was developed to extract unstructured data from clinician notes, capturing qualitative indicators like spinal stabilization or mention of permanent neurological damage.

Results: Among 439 identified patients with spinal injuries, 35% received surgical intervention within 24 hours. Timing varied by spinal region: cervical injuries (e.g., S12, S14) were treated more promptly than thoracic and lumbar injuries (e.g., S22, S32), where the average surgical delay exceeded five days. Mean arterial pressure (MAP) at emergency department arrival was generally consistent across younger patients (~83–86 mmHg), while some patients presented with significantly lower values, including MAPs averaging 51.4 mmHg—below recommended clinical targets. Free-text analysis showed inconsistent documentation of prehospital interventions and neurological outcomes.

Conclusion: International guidelines—such as the 2013 AANS/CNS statement—recommend maintaining mean arterial pressure (MAP) between 85–90 mmHg for 5–7 days following acute spinal cord injury to support spinal cord perfusion[3]. Prior studies have demonstrated that maintaining MAP ≥85 mmHg correlates with significantly improved neurological outcomes[5]. Therapeutic hypothermia has also shown promise in both animal models and clinical studies, with meta-analyses reporting neurological improvement in over 50% of cooled SCI patients[4].
Our analysis reveals variation in treatment timing and MAP management across spinal injury locations, suggesting potential areas for better alignment with established care standards—particularly in thoracic and lumbar SCI. These findings support ongoing efforts to evaluate the role of early-phase cooling and MAP optimization in minimizing secondary injury. Future work will expand the dataset and integrate prehospital variables—such as MAP, oxygenation, stabilization methods, and timing of intervention—to clarify their combined influence on neurological recovery following SCI [2].

References

1. van Middendorp JJ et al. Diagnosis and prognosis of traumatic spinal cord injury. *Lancet Neurol*. 2011;10(1):75–86.
2. Khaing ZZ et al. Advances in understanding secondary injury after spinal cord trauma. *Int J Mol Sci*. 2023;24(4):3824.
3. Walters BC et al. Guidelines for the management of acute cervical spine and spinal cord injuries. *Neurosurgery*. 2013;72(Suppl 2):1–259.
4. Batchelor PE et al. Meta-analysis of therapeutic hypothermia in human spinal cord injury. *Lancet Neurol*. 2023;22(5):407–417.
5. Hawryluk GWJ et al. Elevated mean arterial pressure reduces disability after spinal cord injury. *Scientific Reports*. 2017;7(1):13430.

Respiration-Driven Closed-Loop Modulation of Binaural Beats

Dorfer S[1], Buccellato P[2], Schuh K[1], Chowdhury D[1], Rottondi C[2], Kaniusas E[1]

[1]Institute of Biomedical Electronics, Technical University Vienna, Austria
[2]Department of Electronics and Telecommunications, Politecnico di Torino, 10129 Turin, Italy

Abstract:
Binaural beats (BB) have gained attention for their potential to entertain brainwave activity to favor relaxation. Current research on BB typically employs a static frequency difference (Δf), which may limit their adaptability to individual physiological states. Furthermore, existing systems do not incorporate real-time biosignals, thereby missing the opportunity to align auditory stimulation with the body's own dynamic physiological rhythms. This work presents a closed-loop system for real-time modulation of binaural beats based on respiratory activity. Unlike conventional approaches, the proposed method continuously adjusts the Δf according to the user's real-time respiratory biosignal. This design is motivated by the established role of breath control in the sympathovagal balance, relevant for relaxation and meditative practices. The system aims to enhance the effectiveness of BB through physiological alignment. Respiratory activity is acquired via a chest belt sensor and linearly mapped to a Δf range of 4–10 Hz, corresponding to relaxation-related brainwave frequencies in electroencephalography. The system has been implemented on a custom embedded platform, enabling low-latency signal processing and stable audio output. 10-minute functional pre-tests were conducted involving five healthy participants, and the results validated the proposed operational concept.

Keywords: *Binaural Beats, Binaural pulse modulation, Respiration, closed-loop system*

Introduction

Relaxation has been associated with a wide range of health benefits, including improved cardiovascular function, reduced stress levels, and enhanced cognitive performance [1]. In recent years, there has been increasing interest in non-pharmacological techniques to facilitate relaxation through neurophysiological modulation [2]. Among these, auditory stimulation via binaural beats (BB) has gained attention for its potential to entertain brainwave activity in specific frequency bands associated with mental states such as focus, meditation, or relaxation [3, 4].

BB are perceived when two pure tones of slightly different frequencies are presented separately to each ear. The brain detects the frequency difference (Δf) and generates a third, perceived rhythmic beat, which can influence neural oscillations through a process known as auditory driving [3]. The effectiveness of BB in modulating cognitive and affective states has been explored in a range of studies, with particular emphasis on frequency ranges such as theta (4–8 Hz) and alpha (8–12 Hz), which are commonly linked to relaxed wakefulness and meditative states [3, 4, 5].

Despite their potential, most current implementations of BB systems rely on an open-loop principle with static parameters, typically applying a fixed Δf throughout the session, irrespective of the listener's physiological state. This lack of adaptivity may limit their efficacy, especially when used for individualized relaxation or therapeutic purposes. Integrating real-time physiological feedback into auditory stimulation systems may offer a more responsive and effective approach [6].

Respiration presents itself as a particularly suitable biosignal for this purpose, as its depth and period are strongly related to the sympathovagal balance of the autonomic nervous system [7], closely coupled with the mental state. Controlled breathing is a fundamental component of meditative and mindfulness practices, and variations in respiratory amplitude and rhythm are known to influence the autonomic nervous system. Previous work has demonstrated the role of breath regulation in increasing vagal tone, improving heart rate variability, and enhancing subjective relaxation [8]. These characteristics make respiration a strong candidate for driving adaptive modulation in auditory neurostimulation contexts [1, 8].

This paper introduces a closed-loop system that dynamically adjusts the Δf of BB in real-time according to the user's respiratory amplitude. The respiratory signal is mapped to a Δf range of 4–10 Hz. The system is implemented on a custom embedded platform, enabling real-time signal acquisition, processing, and audio synthesis with imperceptible latency. This approach leverages a closed-loop design to enhance the responsiveness of BB applications to the user's physiological state, aiming to induce a measurable relaxation response.

Material and Methods

This section describes the system components and methods for implementing the closed-loop BB prototype, covering the hardware and software architecture, including signal acquisition, processing, and audio output, as well as the functional test.

System Overview

The setup, illustrated as a block diagram in Fig. 1, shows the implementation of a closed-loop approach for modulating BB in real time based on the user's respiratory activity. It is composed of three main functional blocks: (a) a respiratory signal acquisition module, (b) a signal processing and mapping unit, and (c) a stereo signal generator.

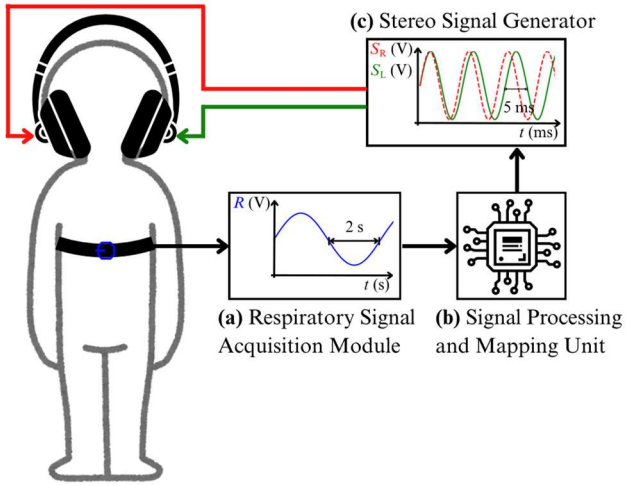

Figure 1: Setup Block Diagram.

Respiratory Signal Acquisition Module

Respiratory effort was measured using a Biopac SS5LB transducer connected to a Biopac MP36 acquisition system (Fig. 1a). The analog signal, proportional to thoracic expansion, was first conditioned by applying a DC offset of 0.75 mV to ensure positivity, and then amplified with a gain of 1000 to match the input range of the single-ended 12-bit Analog-to-Digital Converter (ADC) on the STM32 Nucleo H723ZG board. The resulting signal was well-centered and within a suitable voltage window for digitization, and was subsequently routed to the embedded unit for real-time processing.

Signal Processing and Mapping Unit

Signal acquisition and processing were managed by an STM32 Nucleo H723ZG evaluation module (Fig. 1b). The first operation performed by the processing unit was the sampling of the analog respiratory signal via the board's internal single-ended ADC. The signal was sampled at 80 Hz, a rate selected primarily to satisfy the system's low-latency requirement. Due to the low-frequency content of the respiratory signal, with dominant spectral content below 1 Hz [9], the chosen sampling rate easily meets the Shannon–Nyquist criterion, providing adequate temporal resolution for real-time control of BB without excessive computational load.

Upon system initialization, a 30-second calibration phase was performed to determine the minimum R_{min} and maximum R_{max} sample values of the respiratory signal. During the subsequent modulation phase, each new sample, denoted as R (i.e., the current sample representing the instantaneous respiratory effort), was normalized to the [0, 1] interval according to:

$$R_{\text{norm}} = \frac{R - R_{\text{min}}}{R_{\text{max}} - R_{\text{min}}} \qquad (1)$$

The normalized amplitude R_{norm} was then linearly mapped to a Δf range of 4–10 Hz, corresponding to the theta and low-alpha brainwave bands commonly associated with relaxation and meditative states, according to:

$$\Delta f = f_{\text{min}} + R_{\text{norm}} * (f_{\text{max}} - f_{\text{min}}) \qquad (2)$$

To simplify synthesis and enhance system stability, Δf was quantized with a resolution of 1 Hz, restricting values to discrete steps within the set {4, 5, ..., 10 Hz}. This choice of 1 Hz resolution also contributed to improved system robustness against signal noise.

Audio Signal Generation

The BB signal was generated in real time by producing two sinusoidal waveforms S_L (for left earphone) and S_R (for right earphone) sharing a joint base frequency f_0 of 110 Hz (Fig. 1c), with a variable Δf applied to only one channel as defined by Eq. 2.

These signals were converted to analog form using an external PCM5102 digital-to-analog converter, which provided high-resolution stereo output with low noise and minimal distortion. The analog audio was delivered to the user via over-ear stereo headphones. The sound pressure level was fixed at approximately 65 dB SPL, a value chosen to ensure perceptibility while minimizing auditory fatigue and avoiding amplitude-driven confounds [10]. To maintain a smooth listening experience, phase continuity was preserved during Δf transitions, preventing artifacts or abrupt perceptual shifts. An example of ideal Δf modulation is shown in Fig. 2.

Functional Testing

To evaluate perceptual latency, sound quality, and the continuity of the modulated audio signal, a 10-minute functional test was conducted involving five healthy participants. Each participant listened to the real-time audio output and was asked to report any noticeable delay, discontinuity, or discomfort associated with the auditory feedback. To introduce controlled variability, the test included both spontaneous breathing and guided phases with paced and alternating slow/fast respiratory rhythms.

Results

A fully functional prototype was developed, incorporating both auditory and visual feedback to monitor system behavior and validate real-time signal processing.

Fig. 3 shows a respiratory signal (blue) along with the current resulting value of Δf. User feedback from the functional testing confirmed that the system met real-time requirements under normal operating conditions. Participants consistently reported no noticeable latency and described the auditory output as continuous and free from discomfort. Notably, these results were consistent across different breathing conditions, indicating that the system provides perceptually seamless feedback in terms of responsiveness, signal continuity, and overall user comfort.

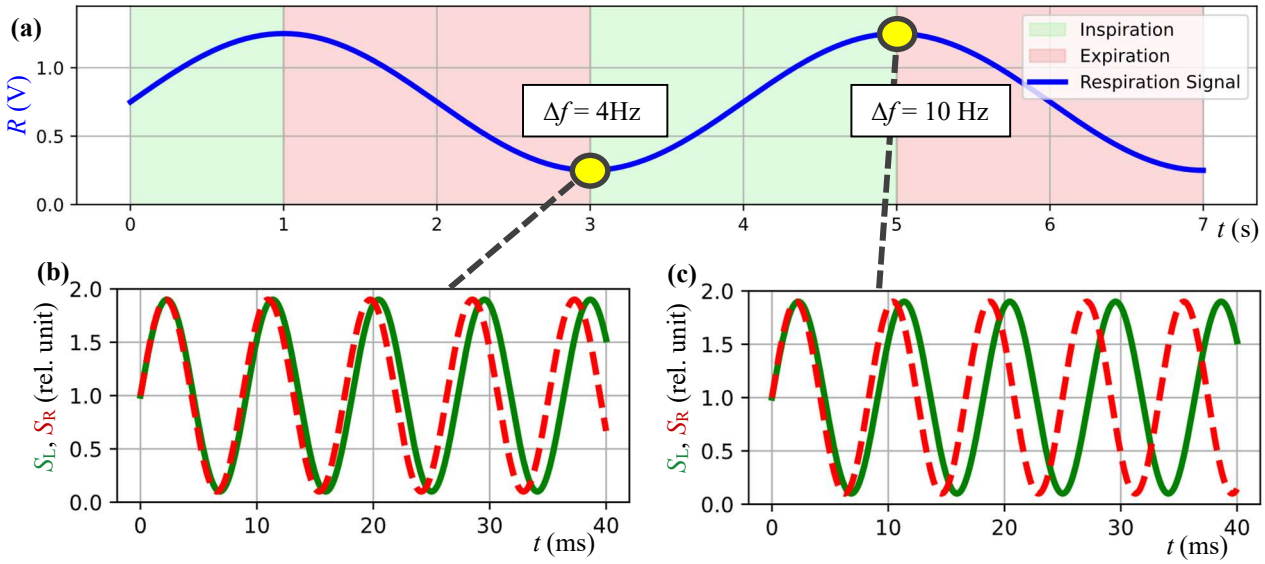

Figure 2: Example of BB modulation driven by respiratory signal amplitude. a) Respiratory waveform with inspiration and expiration phases. Two sample points indicate the smallest and highest amplitudes of the respiration signal R used to modulate the BB. b) BB corresponding to the smallest Δf. c) BB corresponding to the largest Δf.

Discussion

This work presents a closed-loop system for real-time modulation of BB based on respiratory activity. By dynamically adjusting the Δf in response to the user's breathing amplitude, the system aligns auditory stimulation with respiration patterns known to support relaxation.

Latency: To ensure a good user experience in a real-time feedback system, the latency is crucial. The delay between the respiration and the change of Δf is mainly determined by the sampling time of the respiratory signal, which is 12.5 ms according to the 80 Hz sampling frequency. Other factors like conversion and processing times have only a negligible impact (<0.5 ms). Increasing the sampling frequency could lead to a lower latency but also to the acquisition of higher-frequency components, which are more likely related to noise than to meaningful respiratory information. The current latency, as determined by the chosen sampling rate, has proven sufficient to ensure that feedback remains imperceptible to users.

Resolution of Δf: The current Δf resolution was sufficient to ensure robust system behavior and perceptually stable feedback during testing, but it may limit the smoothness of transitions in certain cases. Employing smaller step sizes could provide a finer modulation granularity, leading to more continuous auditory dynamics and potentially enhancing user immersion. However, this must be balanced against the risk of introducing increased sensitivity to noise in the respiratory signal.

Selection of the Biosignal: Respiration was selected due to its strong association with the autonomic nervous system and relaxation, with controlled breathing playing a key role in regulating physiological states. In addition, the respiratory signal is easily accessible, as its absolute value can be processed in real time without extensive preprocessing. This combination makes it a suitable choice for closed-loop biofeedback systems. Alternative biosignals such as electrocardiogram offer richer physiological information [9], but they typically require more advanced processing pipelines and may introduce additional latency and noise.

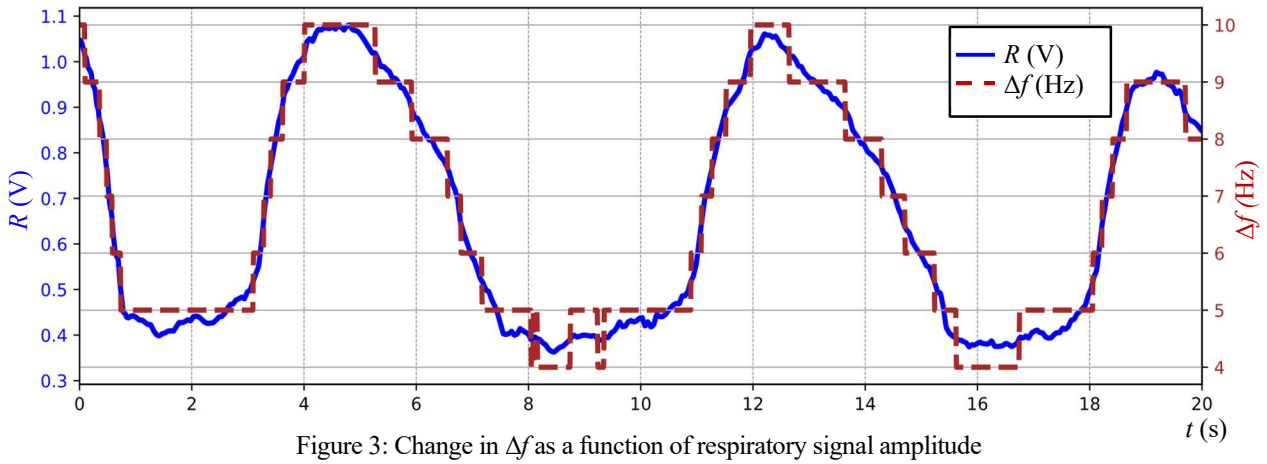

Figure 3: Change in Δf as a function of respiratory signal amplitude

Conclusions

The proposed implementation, based on a custom embedded platform, demonstrated low-latency performance and perceptually seamless feedback, as confirmed by preliminary user testing. Further research will focus on integrating heart rate variability measurements to evaluate the system's impact through statistical analysis. Signal modulation could also be expanded by varying the amplitude of S_L and S_R, as well as the base frequency f_0. Additionally, the system's flexibility opens avenues for incorporating alternative biosignals beyond respiration, potentially broadening its applicability across diverse neurophysiological contexts.

Acknowledgement

This publication is part of the project PNRR-NGEU which has received funding from the MUR- DM 118/2023.

References

[1] Selye, H. *The stress of life*. McGraw-Hill, 1956.

[2] El-Malahi O, Mohajeri D, Bäuerle A, et al. *The Effect of Stress-Reducing Interventions on Heart Rate Variability in Cardiovascular Disease: A Systematic Review and Meta-Analysis. Life*. 2024

[3] Kasprzak, Cezary. *Influence of Binaural Beats on EEG Signal*, Acta Physica Polonica A. 119. pp. 986-990, 2011

[4] *Foster, Dale S.. "EEG and Subjective Correlates of Alpha-Frequency Binaural-Beat Stimulation Combined with Alpha Biofeedback."* 2011

[5] McConnell, P.A., Froeliger, B., Garland, E. L., Ives, J.C., & Sforzo, G. A. *Auditory driving of the autonomic nervous system: Listening to theta-frequency binaural beats post-exercise increases parasympathetic activation and sympathetic withdrawal*. Frontiers in psychology, 5, 1248., 2014

[6] Merlin Kelly, Tom Carlson, Youngjun Cho. *Diving into Binaural Beat Meditation: An EEG-Based Evaluation of User Experience.* Authorea, 2025

[7] E. Kaniusas, Biomedical Signals and Sensors I, Berlin: Springer, 2012.

[8] Van Diest, I., Verstappen, K., Aubert, A.E. et al. *Inhalation/Exhalation Ratio Modulates the Effect of Slow Breathing on Heart Rate Variability and Relaxation.* Appl Psychophysiol Biofeedback 39, 171–180, 2014

[9] E. Kaniusas, Biomedical Signals and Sensors II, Berlin: Springer, 2015.

[10] M. Chockboondee, T. Jatupornpoonsub, K. Lertsukprasert and Y. Wongsawat, "Long and Short Durations of Binaural Beats Differently Affect Relaxation: A Study of HRV and BRUMS" in IEEE Access, vol. 11, pp. 84842-84851, 2023

Author's Address

Sandra Dorfer
TU Vienna
sandra.dorfer@tuwien.ac.at

Electrical Conditioning of Denervated Muscles in a Non-Human Primate Model of Nerve Transection and Repair

Krenn MJ[1,2,3,4], Armas-Salazar A[1], Upton SJ[1], Brooks A[1], Mandeville RM[1], Shah SB[5,6], Brown JM[1]

[1] Department of Neurosurgery, Harvard Medical School, Massachusetts General Hospital, Boston, MA, USA
[2] Department of Neurosurgery, University of Mississippi Medical Center, Jackson, MS, USA
[3] Center for Neuroscience and Neurological Recovery, Methodist Rehabilitation Center, Jackson, MS, USA
[4] Research Department, VA Medical Center, Jackson, MS, USA
[5] Departments of Orthopedic Surgery and Bioengineering, University of California-San Diego, CA, USA
[6] Research Division, VA San Diego Medical Center, San Diego, CA, USA.

Abstract: *Prolonged denervation after peripheral nerve injury causes severe muscle atrophy and fibrosis, which limit functional recovery following nerve repair or transfer. Long-pulse electrical muscle activation (LPMA) has been proposed as a method to directly activate muscle fibers and help preserve muscle viability during denervation. This study examined how muscle degeneration progresses and whether LPMA can maintain muscle excitability and improve recovery after nerve repair. Three non-human primates underwent bilateral radial nerve transection, with repair performed after 5–6 months. Muscle condition was monitored monthly through ultrasound imaging, histology, and force measurements. LPMA recruitment thresholds were assessed using long-duration electrical pulses (20 to 100 ms). In the intervention group, LPMA was applied during denervation and the early phase after nerve repair; the opposite limb served as a control. Denervation caused progressive muscle atrophy, fibrosis, and reduced electrically evoked forces, with a faster decline after 119 days. After nerve repair, wrist extension stimulated by electrical impulses recovered more in the LPMA-treated limb, indicating that direct muscle activation helped preserve muscle responsiveness without hindering reinnervation. These results demonstrate that LPMA can effectively preserve muscle health during prolonged denervation. LPMA-based activation thresholds could serve as useful biomarkers to guide surgical and rehabilitation decisions in patients with peripheral nerve injuries.*

Keywords: *Electrical Stimulation, Stimulation Parameters, Denervated Muscle, Neurotization, Upper Extremity*

Introduction

Following spinal cord injury or peripheral nerve injury, muscles innervated by lower motor neurons undergo rapid atrophy due to denervation, resulting in substantial loss of muscle mass and function [1–3]. Long-pulse electrical muscle activation (LPMA) has emerged as a promising therapeutic strategy to mitigate denervation-induced muscle degeneration, particularly as a preparatory intervention before nerve transfer procedures or during the reinnervation phase [4]. In contrast to conventional neuromuscular electrical stimulation, which relies on intact motor nerves, LPMA employs high-energy electrical pulses with extended pulse durations to directly depolarize muscle fibers [5], thereby bypassing the requirement for neural input. The resulting muscle contractions play a critical role in preserving muscle structure and function by reducing atrophy, maintaining tissue integrity, and enhancing local circulation [6, 7]. Clinical studies have demonstrated the potential of LPMA to promote muscle recovery in humans and address the challenges faced by patients who present late for nerve transfer surgery, when denervation-related muscle degeneration is already advanced [8].

This study aimed to characterize the progression of muscle denervation over time and to evaluate the safety and feasibility of LPMA as a strategy to prevent or reverse muscle degeneration, thereby improving functional outcomes following delayed nerve transfer surgery.

Materials and Methods

Three non-human primates (NHPs) underwent bilateral radial nerve transection, with nerve repair performed after a 5–6-month denervation period. The progression of denervation and subsequent reinnervation was assessed monthly using a multimodal approach. LPMA recruitment properties were evaluated in the wrist and finger extensor muscles using rectangular pulses (10, 20, 50, and 100 ms) across intensities up to 60 mA. The excitability threshold, defined as the minimum amplitude eliciting visible wrist extension, was determined through frame-by-frame video analysis. Tetanic muscle responses were further assessed using 1-second trains at 40 Hz with 10 ms pulses, and wrist extension forces were quantified using a dynamometer. Muscle status was monitored via serial B-mode ultrasound imaging of the extensor carpi radialis and histological analysis of brachioradialis biopsies. During the recovery phase, beginning two months post-repair, active extension was evaluated through behavioral reaching tasks. In the left arm, LPMA was applied as an intervention, using biphasic rectangular pulses delivered either at 2x20 ms/20 Hz or 2x50 ms/9 Hz (2 seconds on, 2 seconds off) for 30 minutes per session, five days per week. The duration of the intervention varied across NHPs, ranging from 3 to 7 months.

Results

The denervation process prior to nerve repair followed a consistent pattern across all non-human primates. Serial ultrasound imaging revealed a progressive reduction in total muscle diameter, indicating ongoing muscle atrophy over the denervation period (Fig. 1).

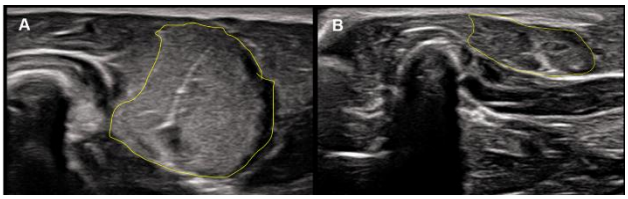

Figure 1. Ultrasound image of the extensor carpi radialis muscle (yellow line outlines the cross-sectional muscle area) before and after 12 months of denervation in NHP2.

Histological analysis confirmed these findings, demonstrating marked reductions in muscle fiber cross-sectional area accompanied by increased fibrosis and connective tissue infiltration (Fig. 2). Functionally, denervation was associated with a gradual decline in electrically evoked wrist extension forces. This decline became particularly pronounced after approximately 119 days of denervation, suggesting a critical threshold beyond which muscle degeneration accelerates (Fig. 3, top).

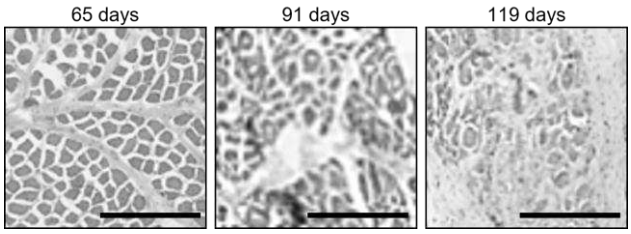

Figure 2. Representative histological image (hematoxylin and eosin-stained) of the brachioradialis muscle in NHP 2 at 65, 91, and 119 days post-denervation. The bars indicate 400 µm.

Following nerve repair, the first signs of functional reinnervation, evidenced by measurable voluntary wrist extension during behavioral reaching tasks and increased stimulated force output, were observed approximately 105 days post-repair (Fig. 3, bottom). Notably, the limb receiving LPMA intervention (left arm) demonstrated superior recovery of muscle force compared to the contralateral control arm, indicating a potential protective or restorative effect of the LPMA treatment during the denervation phase.

Discussion

This study demonstrates the feasibility of directly activating denervated muscles using long-pulse electrical muscle activation (LPMA), providing critical insights into muscle viability during prolonged denervation. The ability to elicit contractions in denervated muscles highlights that, despite significant atrophy and fibrotic changes, muscle fibers retain a degree of excitability that can be harnessed therapeutically. Importantly, the excitability thresholds obtained through LPMA offer a quantitative measure of muscle responsiveness in the absence of neural input, which may serve as a biomarker for assessing residual muscle health.

Our findings support the notion that electrical stimulation, when appropriately targeted and dosed, does not impede reinnervation following delayed nerve repair. The arm receiving LPMA intervention exhibited improved functional recovery, suggesting that direct muscle activation may help preserve the structural and functional integrity of denervated muscles during the critical waiting period before reinnervation occurs. This protective effect may be attributed to the prevention of irreversible muscle degeneration, maintenance of local circulation, and modulation of the extracellular environment.

Optimization of stimulation parameters remains a key challenge for clinical translation. Determining the ideal balance between sufficient stimulation to maintain muscle health and avoiding potential overstimulation or fatigue requires further investigation. Moreover, the translational relevance of these findings to human patients with chronic denervation warrants additional study, particularly regarding the time windows during which muscle viability can be maintained.

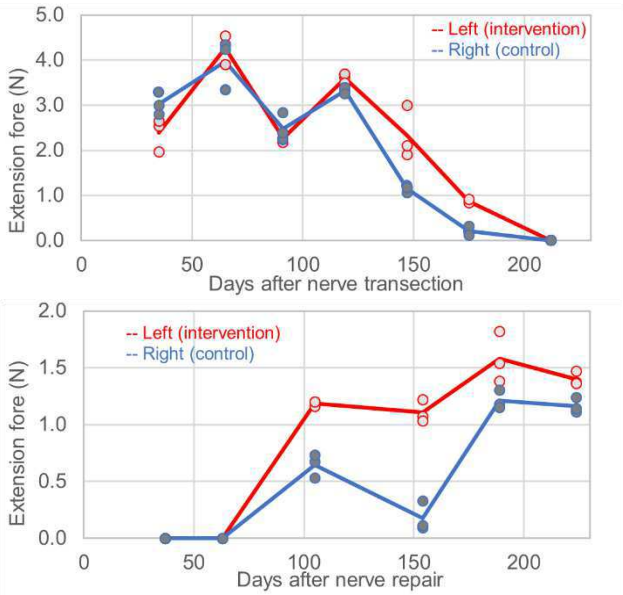

Figure 3. Extension force during the denervation (top) and recovery (bottom) phase in the left (intervention, red) and right (control, blue) arms. Following radial nerve transection, extension forces declined progressively in both arms, indicating loss of muscle activation capacity. Electrical stimulation intervention was initiated in the left arm starting 119 days after nerve transection and continued until 150 days post-nerve repair.

Conclusion

Our results suggest that LPMA is a possible strategy to preserve muscle excitability and support functional recovery after prolonged denervation. Measuring activation thresholds in denervated muscles may provide a valuable tool for guiding clinical decision-making, including identifying candidates for nerve transfer surgery and tailoring rehabilitation interventions.

References

1. Jejurikar SS, Marcelo CL, Kuzon WM (2002) Skeletal muscle denervation increases satellite cell susceptibility to apoptosis. Plast Reconstr Surg 110:160–168.
2. Boncompagni S, Kern H, Rossini K, et al (2007) Structural differentiation of skeletal muscle fibers in the absence of innervation in humans. Proc Natl Acad Sci U S A 104:19339–44.
3. Chandrasekaran S, Davis J, Bersch I, et al (2020) Electrical stimulation and denervated muscles after spinal cord injury. Neural Regen Res 15:1397–1407.
4. Bersch I, Fridén J (2020) Upper and lower motor neuron lesions in tetraplegia: implications for surgical nerve transfer to restore hand function. J Appl Physiol 129:1214–1219.
5. Woodcock AH, Taylor PN, Ewins DJ (1999) Long pulse biphasic electrical stimulation of denervated muscle. Artif Organs 23:457–459. https://doi.org/10.1046/j.1525-1594.1999.06366.x
6. Mödlin M, Forstner C, Hofer C, et al (2005) Electrical stimulation of denervated muscles: First results of a clinical study. Artif Organs 29:203–206.
7. Kern H, Carraro U (2020) Home-Based Functional Electrical Stimulation of Human Permanent Denervated Muscles: A Narrative Review on Diagnostics, Managements, Results and Byproducts Revisited 2020. Diagnostics (Basel) 10:529.
8. Castanov V, Berger M, Ritsma B, et al (2021) Optimizing the Timing of Peripheral Nerve Transfers for Functional Re-Animation in Cervical Spinal Cord Injury: A Conceptual Framework. J Neurotrauma 38:3365–3375.

Author's Address

Matthias Krenn
University of Mississippi Medical Center
Department of Neurosurgery
mkrenn@umc.edu

Coupling FES and dynamic surface electromyography: advancing neurorehabilitation

Namysl J, Neurorehabilitation Practice INNOMED, Poznań, Poland

Abstract

FES activate numerous neurotrophic factors that allow for remyelination, axon growth, and muscle strengthening, significantly surpassing the effectiveness of rehabilitation based solely on exercise. Muscle tension regulation centers in the brain and spinal cord respond to neuronal damage and the loss of functional motor units, by generating abnormal muscle tone. Dynamic surface electromyography (DsEMG) plays a crucial role in determining optimal FES parameters. This approach when combined with FES and EMG-biofeedback, enhances therapy effectiveness, shortens recovery time and reduces long-term healthcare costs by minimizing the need for other medical interventions.

Keywords: FES, electromyography, muscle tension, muscle stimulation, Emg-biofeedback

Introduction

Depending on electrical parameters and application methodology, FES activates VEGF[1] which facilitates revascularization and nerve regeneration[2], prevents muscle atrophy[3], allow for axon remyelination[4] and increases the expression of neurotrophic factors (BDNF, NGF, CNTF).[5] The loss of neurons or myelin alters the excitation patterns generated by muscle tension regulation centers in the brain and spinal cord. This leads to increased muscle tone at rest, unstable or reduced during contraction or to a complete inability to contract muscles. Cells exposed to abnormal muscle tension cannot respond properly to the body's demands, as their functional state is determined by membrane tension.[6] Therefore, muscle tension must be assessed using EMG. Typically, a diagnostician assesses the degree of nerve damage in a single body position and does not examine how changes in position, FES or biofeedback, affect the way muscle tension is generated. The result of such an examination offers little value for the rehabilitation process. Even a negative EMG result does not exclude the possibility of functional recovery.[7] A complete loss of the ability to generate muscle tension, indicates the need for FES using pulsed current. Triangular current should be avoided.[8] To determine the optimal stimulation parameters, electrode placement, exercise load, and monitoring therapy-related changes, noninvasive surface electromyography (sEMG) is essential. EMG biofeedback os an important tool in neuromotor re-education by improving neuromuscular coordination, reducing stress levels, and lowering neurotoxic cortisol.[9] I have developed and implemented dynamic surface EMG (DsEMG), as it has proven to be highly effective. This method enables the observation of how spinal structural degeneration, FES, EMS, and biofeedback exercises influence muscle tone at rest and during activity. DsEMG provides objective and valuable information that cannot be obtained in any other way, reduces the time to make a good diagnosis and apply effective therapy. Its advantages are illustrated by the electromyograms included in this text.

Method

DsEMG involves the registration of resting muscle tension in a semi-recumbent relaxed position with head and neck support, and tension recorded in a supine position, as well as after lumbar, thoracic, or cervical spine support, using a rehabilitation roller. It allows for the

identification of conflicts between spinal structures and the nervous system, which are often either the cause or consequence of motor disabilities and should be addressed therapeutically. These conflicts affect individuals following a stroke, as well as those with cerebral palsy, multiple sclerosis, spinal muscular atrophy, incontinence, chronic pain and many other neurological disorders.

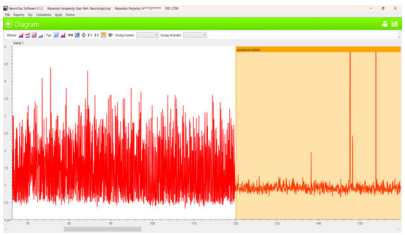

Fig.2. Resting tone of tibialis anterior muscle recorded in laying position before stretching of the lumbar area. Shaded side, result of 3 minutes stretching of paravertebral muscles on rehab roller. Authors archives.

Stretching of the paraspinal muscles reduces pressure exerted by spinal structures on the nerves, creating favorable conditions for the activation of regenerative mechanisms. Without appropriate therapy abnormal muscle tension persists, negatively affecting cell membrane potential, which can impair or completely prevent the recovery of motor function or sensation. The visualization of correlations between dorsal or cervical muscle tension and the resting tone of assessed muscles, provides significant diagnostic and educational value. Dynamic muscle tension changes, similar to those observed after paraspinal muscle stretching, occur following FES (Fig.2), EMS, EMG-biofeedback or ETS (Electromyographic Triggered Stimulation). (Fig.3)

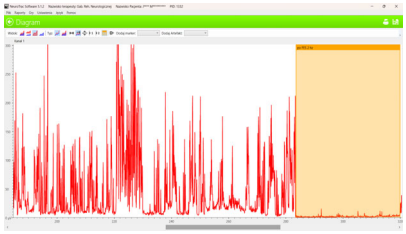

Fig.2. Resting tone of TA muscle in patient with spastic paresis after SCI. Left side before, right (shaded) side, highly improved muscle tone after only 3 minutes of mild 2 Hz stimulation. Authors archives.

An initial Work/Rest Assesment in a 14 years old patient with giggle incontinence, revealed that muscle tension increased in response to the "Rest" command, instead of the "Work" command. After just a few minutes of ETS, muscle coordination improved significantly (Fig.3). Home therapy with this method restored continence within four months.

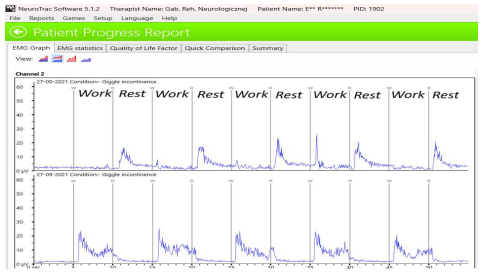

Fig. 3. Comparison of Work/Rest assessments of perineal muscle activity in a patient with giggle incontinence, demonstrating improved muscle coordination after a 5-minute ETS therapy session Authors archives.

One key advantage of low-level sEMG is its ability to record muscle tone even when movement is impossible. In a patient with flaccid paralysis following reconstruction of a transected radial nerve, no change in muscle tension was detected during the Contract/Relax test. After six months of daily home-based FES and EMS, the difference increased to 4.5µV, which was still too low to produce a noticeable contraction. Such low electrical activity is often referred to as electrical silence, which suggests a lack of progress and exacerbates stress. After 18 months therapy 3–4 hours per day, the difference reached an average of 19.6 µV, allowing for slight hand elevation. The ability to generate 100µV difference, the threshold for functional recovery, required almost four years of therapy. The comparison of electromyograms from follow-up examinations illustrates the gradual improvements. (Fig.4)

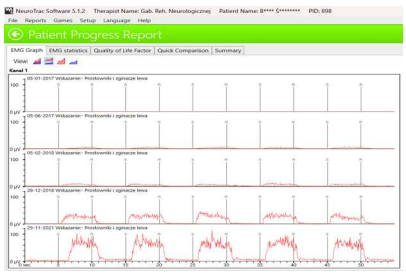

Fig.4. A progress report of a four-year history of improvement in wrist extensors activity in a patient with severed radial nerve injury. Author's archives

Discussion

There is much controversy surrounding the concept of muscle tone. Definitions such as "The ability of muscles to counteract passive contractions during stretching" or "A constant state of tension, minimal even during relaxation, and increasing in response to passive stretching", fail to account for many significant factors influencing muscle tone. Muscle electrical activity results from the continuous transmembrane movement of electrically charged ions. Its key characteristics are amplitude, frequency and stability. The aforementioned examples of muscle tension changes in response to stimulation, stretching or biofeedback exercises highlight the central nervous system's role in both generating and normalizing muscle tension. As a physical phenomenon, muscle tension requires evaluation using a recording device that measures and expresses the results in SI units, specifically microvolts. Additionally, sEMG testing reveals reaction time, relaxation ability and coordination between synergists and antagonists - factors that cannot be assessed by touch alone. These conclusions are based on observations from thousands of sEMG studies conducted over years on individuals with limb or pelvic floor muscle dysfunction.

I propose a more precise definition: *"Muscle tension is a time-varying value of action potentials recorded in muscles, expressed in microvolts and objectively measurable using electromyography. It depends on the functional state of the neural pathways, the method of activation of muscle tension regulation centers in the brain and spinal cord, environmental conditions, muscle physiology, and the psycho-emotional state of the person.*[10]

The rehabilitation model for individuals with flaccid or spastic muscle paralysis that relies solely on exercise is near 70 years old and deviates significantly from principles supported by modern scientific research. Muscle flaccidity, spasticity and reduced ability to generate force, arise from a deficiency of neurons responsible for stimulating or controlling muscle activity. To maintain tone or execute movement, remaining neurons must increase the activation frequency of the available motor units. A regularly activated neural circuit strengthens over time, leading to increased muscle resting tone. This negatively impacts adjacent tissues, leading to circulatory disturbances, degeneration of type S fibers, muscle fatigue, shortening of muscles and tendons and joint deformities associated with paralysis, following the principle that structure is determined by function. While exercises can improve range of motion and enhance tissue flexibility, they operate within the existing abnormal muscle tension and reinforce dysfunctional control patterns. Their impact on neuroregeneration and muscle tension normalization is insufficient and the results often fall short of expectations. In the assessment of muscle tension, palpation and observation predominate. Both methods are subjective and do not allow for the recording of clinically significant features of muscle tension. Ignoring muscle tension assessment via DsEMG and failing to normalize it with FES, ETS and EMG biofeedback, significantly reduces the effectiveness of neurorehabilitation. There is no method that works in every case. Therefore, different methods should be combined.

Conclusions

The systematic and sufficiently long-term use of FES, EMS, and DsEMG, are key methods for improving motor function in individuals with flaccid or spastic paralysis. Without these methods, many neuroregenerative processes and plastic changes within the nervous system have little chance to occur. Continuous tracking of

muscle tension changes and reinnervation progress in DsEMG examinations plays a crucial role in maintaining patient motivation and adherence to treatment. Assessing muscle tension by touch alone does not allow for recording, visualization or detection of dynamic tension changes, such as those presented above. It may also lead to diagnostic errors, as each touch alters muscle resting tone. Through early DsEMG diagnostics, FES, ETS and biofeedback therapy combined with motor exercises, many complications, medications and surgical interventions can be avoided. These techniques have high potential for muscle tension normalization and can improve the function of skeletal muscles, the diaphragm, the neurogenic bladder, the intestines and the sphincters. Visualization of muscles tension teaches the brain how to coordinate motor units, enables desired plasticity changes and strengthens positive patient engagement in therapy. The brain registers the impact of FES, biofeedback treatments and awareness on the body and in response to stimuli creates tension, the characteristics of which determine the functioning of cells. Stimulated with stable tension using an FES or EMS unit, and properly guided by conscious awareness through the visualization of muscle activity patterns via sEMG, the brain becomes the architect of recovery.

The renowned polish neurophysiologist, prof. Jerzy Vetulani, expressed this concept in the following words: *"The brain was not designed for thinking; it is the primary organ of survival."* FES, ETS, and the visualization of muscle tension using DsEMG enable it to fulfill this fundamental task.

References

[1]Theis V, Theiss C., VEGF - A Stimulus for Neuronal Development and Regeneration in the CNS and PNS. Curr Protein Pept Sci. 2018; 19(6):589-597.,

[2]Willand Michel P.,Electrostimulation enhances reinnervation after nerve injury, Eur. J. Transl Myol-Basic Appl Myol 2015;25(4):243-248]

[3] Crameri R.M et.al, Effects of electrical stimulation leg training during the acute phase of spinal cord injury. Eur.J.Appl.Physiol.2000 Nov;83(4-5):409-15.

[4] Boulanger JJ, Messier C (2014) From precursors to myelinating oligodendrocytes: contribution of intrinsic and extrinsic factors to white matter plasticity in the adult brain. Neurosc. 269:343–366

[5] Hurtado E., Cilleros V. et al., Muscle Contraction Regulates BDNF/TrkB Signaling to Modulate Synaptic Function through Presynaptic cPKCα and cPKCβI, Front Mol Neurosc 2017; 10:147,.

[6] Keren K., Membrane tension leads the way. Proc Natl Acad Sci USA.2011 Aug 30;108(35):14379-80.

[7] Feinberg J. „EMG: myths and facts",HSS journal: the musculoskeletal journal of Hospital for Special Surgery,vol. 2,1 (2006): 19-21.

[8]Terzis J.K.,Smith K.L.,The Peripheral Nerve, Structure, Function and Reconstruction, A Hampton Press Publication, Raven Press: New York, 1990

[9]Thabrew H., Ruppeldt P., Sollers J. J., III Systematic review of biofeedback interventions for addressing anxiety and depression in children and adolescents with long-term physical conditions. Applied Psychophysiology and Biofeedback. 2018;43(3):179–192.

[10]Namysl J., (in press) "Muscle tension: Objective Assessment and the importance of its normalization", p.7, Chapter in the book „Sparks of Life. Neuroregeneration after injuries and in diseases of the nervous system", 2025

Authors adress

Namysl Jan, Neurorehabilitation Practice INNOMED, Poznań, Poland
jan@innomed.pl
www.innomed.pl

Title: Effects of Internal and External Cooling on Temperature Regulation Following Spinal Cord Injury: A mathematical Simulation-Based Study

Authors: Ellen Huld Þórðardóttir[1,2], Katrín Rut Mar Þórðardóttir[2], Selma Gunnarsdóttir[2], Kára Dís Ólafsdóttir[2], Páll E. Ingvarsson[1], Ólöf Jóna Elíasdóttir[1], Þórður Helgason[1,2]
[1]Landspítali – The National University Hospital of Iceland, [2]Reykjavík University
ellenht@landspitali.is

Introduction: Traumatic spinal cord injury (SCI) frequently leads to secondary damage, including ischemia, inflammation, and progressive neurodegeneration[1,2]. Therapeutic hypothermia has been proposed as a neuroprotective intervention to mitigate these effects by lowering metabolic demand and inflammatory signaling[1,2]. However, the comparative effectiveness of internal cooling (e.g., epidural or intravenous infusion) versus external cooling (e.g., surface-based techniques) remains inadequately characterized[1,3].

Aim: To evaluate the thermal efficacy of external spinal cooling using numerical simulations and compare results with reported outcomes from internal cooling methods.

Methods: A transient one-dimensional heat conduction model was developed in Python to simulate temperature changes across four biological layers (skin, subcutaneous fat, muscle, bone), with the spinal cord positioned at a depth of 45 mm. Constant surface temperatures of 0°C, 2°C, and 7°C were applied over 60 minutes using Dirichlet boundary conditions. Thermal properties were assigned based on literature data[4,5]. The resulting temperature profiles were assessed at spinal depth and compared with published outcomes from internal cooling strategies, including epidural saline infusion and intravenous cold saline administration[1,6].

Results: External surface cooling resulted in limited temperature reductions at spinal cord depth. Specifically, surface temperatures of 0°C, 2°C, and 7°C yielded spinal temperatures of 34.92°C, 35.06°C, and 35.33°C, respectively. Heat transfer decreased with tissue depth, largely due to the insulating effects of fat and bone. These findings contrast with internal cooling approaches, which have demonstrated more rapid and uniform cooling to within the therapeutic range (32–34°C) under clinical and experimental conditions[1,6].

Conclusion: External cooling can achieve modest reductions in spinal cord temperature and may serve as a feasible, non-invasive option in prehospital or early hospital settings. However, its limited penetration to deeper tissues may constrain its neuroprotective potential. Further research using anatomically realistic models and transient 3D simulations is needed to explore optimized combined strategies for early therapeutic hypothermia in acute SCI.

References

1. Batchelor PE et al. Meta-analysis of therapeutic hypothermia in human spinal cord injury. *Lancet Neurol.* 2023;22(5):407–417.
2. Kim Y et al. The neuroprotective effects of hypothermia in spinal cord injury. *Int J Mol Sci.* 2019;20(19):5010.
3. Xu X, Werner J. A dynamic model of the human thermal system. *J Appl Physiol.* 1997;83(5):2043–2050.
4. Duck FA. *Physical Properties of Tissue: A Comprehensive Reference Book.* Academic Press; 1990.
5. Hasgall PA et al. IT'IS Foundation Database for Thermal and Electromagnetic Properties of Biological Tissues, Version 4.1. 2021.
6. Salzano MP et al. Systemic and epidural hypothermia after spinal cord injury. *J Neurosurg.* 1994;80(6):963–969.

Session 6: FES-Cycling

Real-Time Bayesian Optimization of FES Cycling

Baglikow S[1] and Schauer T[1,2]

[1]Control Systems Group, Technische Universität Berlin, Germany
[2]SensorStim Neurotechnology GmbH, Berlin, Germany

Abstract: *Stimulation patterns used within FES-cycling systems are often based on the crank angle, and the manufacture's default parameters require manual tuning for the individual cyclist. A novel approach uses one thigh's inclination angle, estimated by an inertial sensor, to auto-calibrate the cycle percentage concerning leg flexion and extension phases. While related stimulation patterns work out of the box for most cyclists, individual fine-tuning for different cadences might even improve the cycling performance due to the unknown muscle-specific electromechanical delay in muscle activation. This contribution proposes the usage of Bayesian optimization to temporally adapt the stimulation patterns for the quadriceps and hamstring, with the aim to maximize the cadence at a stationary ergometer when applying a constant stimulation intensity. The feasibility of this approach is demonstrated in computer simulations using a complex neuro-musculoskeletal model. The results show a fast convergence within three minutes of FES cycling, taking only twelve pattern updates. The approach also compensates effects of muscle fatigue.*

Keywords: *Functional Electrical Stimulation, Cycling, Optimization, Simulation, Biomechanical Model*

Introduction

FES cycling is an established excise modality for people with spinal cord injury [1], [2]. There are various cycling systems available for stationary or mobile cycling, which mostly rely on the crank angle to temporally control the stimulation [3]. However, the corresponding patterns depend on the geometry of the bike and the cyclist and change when the seating position is changed. Recent developments shift from crank-angle controlled patterns to limb-inclination controlled patterns in which body-worn sensors automatically determine flexion and extension phases of the legs and assign the muscle stimulation to these phases [4], [5], [6]. Typically, the percentage of the cycle from 0 to 50% is associated with the extension phase and from 50 to 100% with the flexion phase. Such novel systems require at least one rotation of the crank, which is performed either by a motor or by the cyclist using the residual functions of the legs or the hands. However, one remaining challenge is the adaptation of the stimulation patterns at different cadences to take account of the electromechanical delay in muscle activation. A simple, but probably suboptimal, method is to stimulate the faster one pedals, the earlier. Here, a common approach is to apply the same shift for all muscles, assuming a general valid time delay in muscle activation. Technically, this is established by determining the muscle stimulation with a static stimulation pattern for zero cadence, which is evaluated using a forecasted cycle percentage. The latter is the currently measured cycle percentage plus a term proportional to the current cadence.

As an alternative, this contribution investigates the usage of real-time optimization to determine cadence-specific stimulation patterns that are evaluated at the current cycle percentage. This approach should deliver patterns that deal better with muscle-specific electromechanical delays. The applied objective function maximizes the mean cadence for a given constant stimulation intensity chosen by the cyclist.

To prove the feasibility of such an approach, a computer simulation was established based on a FES cycling model with a motor-assisted stationary ergometer. Bayesian optimization has been employed, that has shown promising results in terms of convergence speed and performance outcome for the tuning of other neuro-prosthetic applications [7].

Figure 1: Considered setup for the creation of the computer simulation model used for optimization.

Material and Methods

Simulation model

The cyclist and the ergometer are modelled as five-bar linkage. As the ankle-joint angles are fixated, the system has a single mechanical degree of freedom. The kinematics and dynamics of the five-bar linkage model were modelled using the Open Dynamics Engine (ODE), which is an open source, high-performance library for simulating articulated rigid body dynamics, implemented in C++ [8]. The muscle models with artificial electrical stimulation from [9] were

used and implemented in C++, generating joint torques for the knee and hip joints. Stimulated are only the quadriceps and hamstring muscle groups. However, the model also includes other leg muscles that are not activated but are purely passive when cycling. Viscous and elastic joint moments, as described in [9], were also considered. Finally, the muscle models can emulate fatigue and recovery behavior. This function can be activated and deactivated. The muscle and five-bar linkage models have been incorporated into Matlab/Simulink (The Mathworks Inc., USA) using S-Functions. Inputs are the currently applied pulse widths (stimulation intensities) and stimulation frequencies to the muscles of the hamstrings and quadriceps muscle groups, as well as a motor torque that can be applied at the crank. Outputs are the crank angle, the cadence, joint angles, limb inclination angles, and pedal forces. The Simulink model further contains a motor controller and the pattern generator with Bayesian optimization as Matlab User Functions.

Pattern Generator

The pattern generator uses the right thigh inclination angle to determine the cycle percentage for both legs. The change from leg flexion to extension takes place at 0% and the change from extension to flexion at 50%. The default stimulation pattern activates the quadriceps in the range 0 to 50% and the hamstrings in the range 50% to 100%. Outside these ranges, the pulse width is set to zero. Inside the ranges, the pulse width ramps up within 10% of the cycle percentage until it reaches the set value *pw*. Ramping down is initiated 10% of cycle percentage before the activation range ends. The stimulation frequency was set to 40 Hz.

Motor Control

To initiate the cycling, an electric motor is emulated in the simulation model and controlled. The motor controls the cadence to a reference of 20 rpm with a PI controller. When muscle stimulation is activated, the user can exceed this cadence, and the motor-controller output will be saturated at a predefined resistance torque. Here, no additional motor resistance (i.e. zero torque) has been assumed.

The entire simulation model aims to replicate the setup shown in Figure 1, where a body-worn stimulator, Stim2Go (Pajunk GmbH Medizintechnologie, Germany), with integrated inertial sensor, is attached to the paraplegic cyclist's right thigh to control FES cycling. The user can adjust the stimulation intensity via the smartphone.

Real-time Bayesian Optimization

The Bayesian optimization updates the ranges of the muscle activation for the quadriceps and hamstrings every 15 seconds with the aim to maximize the mean cadence as objective function (OF) for a given common pulse width value *pw.* The average cadence is calculated from the ten seconds of steady-state cycling before the updates.

In Gaussian Process-based Bayesian Optimization (GPBO), Gaussian Processes (GP) are employed as the probabilistic model for predicting the OF [10], [11]. The fundamental idea of GPBO is to develop a probabilistic model of the OF instead of directly optimizing the function itself. This model is refined step by step by strategically evaluating the unknown function. By using GPBO, the potentially expensive and time-consuming comprehensive evaluation of the function can be avoided, as the method often provides a good prediction of the desired maximum after only a few optimization steps.

The procedure begins with predicting the OF for all points in the search space based on known sample points. GP regression, used for this prediction, provides not only an expected value for each point, but also a variance, which serves as a measure of uncertainty in the prediction. In a second step, this information is processed using an acquisition function (AF), which identifies the point in the search space where the OF should be evaluated next. This approach systematically improves the predictive model and iteratively narrows down the optimum.

In GPBO, the kernel (also known as the covariance function) is a core component of the GP model. It defines how the outputs (function values) are correlated based on their input locations. In essence, the kernel encodes prior beliefs about the smoothness, periodicity, and structure of the unknown function being optimized. We have used a Matérn-Kernel with the hyperparameters ν=1.5 and l=0.5. The first parameter defines how smooth the predicted objective function is, and the second parameters determines how far two sample points influence each other, i.e. how quickly this function can change. For the acquisition function, we used the Upper-Confidence Bound (UCB) approach, which represents a tradeoff between exploration and exploitation. The chosen trade-off parameter κ=0.3 favors exploitation (the mean of the prediction) more than the exploration (standard deviation (uncertainty) of the prediction). The discrete search space has been limited to –30% to +10% around the start and stop of the default ranges, with a step size of 2.5%.

Test Procedures

Two scenarios have been investigated. The first one applies a constant pulse width value *pw* of 250 µs. The fatigue model is disabled at first to see the optimization effect if the model remains time-invariant. Then the fatigue model is activated, and the behavior with and without optimization is studied.

In the second scenario, the effects of stepwise changes in the pulse width value *pw* are observed for the fatigable model with and without optimization. The GPBO is reset after each step in the pulse width, while taking the last best predicted pattern as the initial setting for the new optimization. Updates take place again every 15 seconds, except after the changes in the intensity, for which we wait 20 seconds before the next update to allow more time to establish steady state cycling.

Results

Figure 2 shows the cycling performance when maintaining a constant stimulation intensity. For the case with the disabled fatigue, the optimum is reached just after 12 updates within three minutes of cycling (blue lines). The average cadence increased by about 13%. The default, i.e. initial, and the optimized stimulation patterns are shown in

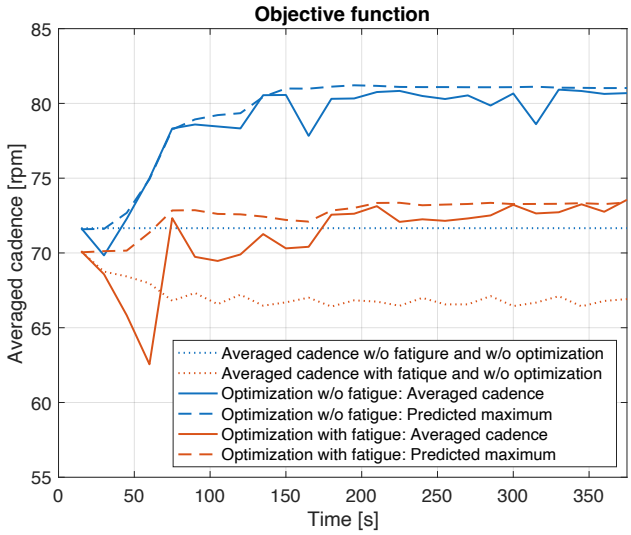

Figure 3: Average cadence for different model settings with and without GPBO.

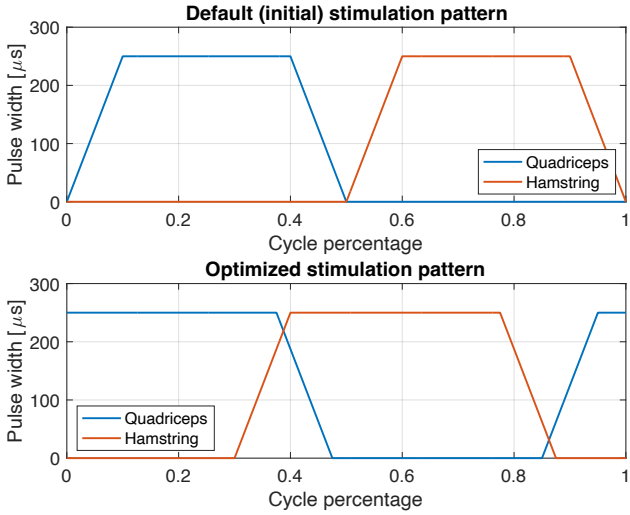

Figure 2: Default (initial) and optimized stimulation pattern.

Figure 3 for comparison. It is clearly visible, that the shift in the activation is different for both muscle groups, indicating the need for muscle-specific cadence adaptation. All updates to the stimulation pattern are illustrated in Figure 4. Shown are the differences compared to the initial default pattern. The green dots indicate the initial pattern change, and the black dots the last observed pattern change.

Figure 2 further displays the course of the average cadence for muscle fatigue without optimization (dotted red line). Performance decreases significantly in the first two minutes until fatigue and recovery are in balance. This cadence drop can be avoided by activating the GPBO (solid and dashed red lines).

The results of stepwise changes in the pulse width value *pw* are reported in Figure 5 with and without optimization. In both simulations, muscle fatigue is active. The cycling with optimization yields for all stimulation intensities higher cadences.

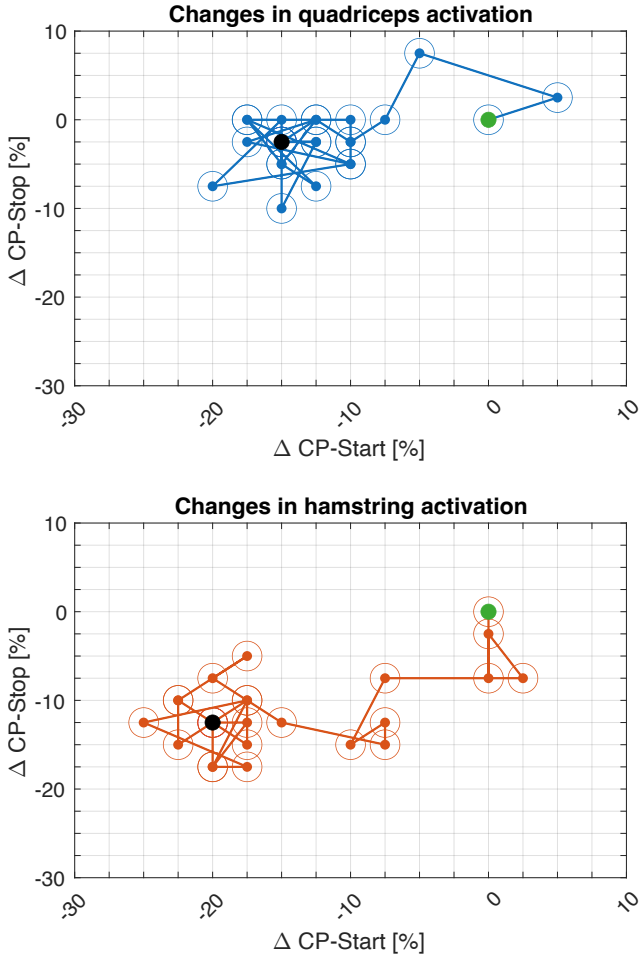

Figure 4: Changes in the activation ranges over time during optimization for the model with fatigue and pulse width pw=250µs. The differences relate to the initial default pattern. The start is shown as a green dot. The last applied pattern is marked with a black dot.

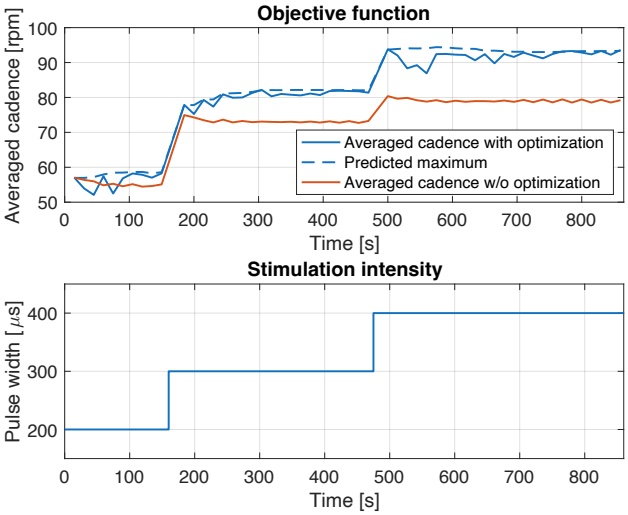

Figure 5: Effect of optimization on FES cycling with stepwise changes in the stimulation intensity. The muscle fatigue was activated in the model.

Discussion

The results demonstrate the usefulness of GPBO for tuning the stimulation pattern of FES cycling to maximize cadence for a user-set stimulation intensity. The observed convergence speed fast enough to apply this approach to real FES cycling exercises.

However, these findings are based on a computer simulation which certainly diverges from reality. For example, no time-varying spasticity or residual motor function have been considered, and the observed muscle fatigue in the simulation appears to be mild in comparison to observations in individuals with SCI. Furthermore, the assumption of identical muscle behaviour in both legs is not tenable in practice. In addition, reported results are only for one virtual subject, one sitting position, and a limited set of stimulated muscles.

Despite these limitations, the study strongly suggests that such real-time optimization is practically feasible, not requiring a digital twin of the cyclist. On modelling of the user or system is required for applying the GPBO. The simulation of 875 s cycling with optimization took only 176 s on a MacBook Pro (M1 Pro). A transfer of the GPBO to real FES cycling is technically feasible. With the setup shown in Figure 1, the GPBO could easily be executed on the smartphone. The communication load would be minimal, as only the average cadence and the updated stimulation patterns need to be exchanged between the stimulator and the smartphone at relatively long time intervals, e.g. every 15 to 20 seconds.

Conclusions

Bayesian optimization turned out to be a suitable method for the real-time adjustment of stimulation patterns in FES cycling. By adapting the stimulation timing to the specific muscle, it was possible to maximize the cadence and partially compensate for fatigue in a setup with user-controlled stimulation intensity.

The resulting patterns suggest that the muscle-specific electromechanical delays require approaches such as GPBO to customize the activation range for each muscle. The commonly used identical shift of all stimulation ranges proportional to the cadence may not be the best solution.

Further investigations, in simulations and with SCI individuals, must be carried out to develop and validate the GPBO approach further. More active muscles and leg-specific stimulation should be incorporated in the optimization problem.

References

[1] D. R. Dolbow, I. Bersch, A. S. Gorgey, and G. M. Davis, "The Clinical Management of Electrical Stimulation Therapies in the Rehabilitation of Individuals with Spinal Cord Injuries," *J Clin Med*, vol. 13, no. 10, p. 2995, May 2024, doi: 10.3390/jcm13102995.

[2] D. R. Dolbow, A. S. Gorgey, J. M. Ketchum, and D. R. Gater, "Home-based functional electrical stimulation cycling enhances quality of life in individuals with spinal cord injury," *Top Spinal Cord Inj Rehabil*, vol. 19, no. 4, pp. 324–329, 2013, doi: 10.1310/sci1904-324.

[3] C. Wiesener, "Inertial-sensor-based control of functional electrical stimulation for paraplegic cycling and swimming," Doctoral Thesis, Technische Universität Berlin, Berlin, 2021. Accessed: Feb. 27, 2025. [Online]. Available: https://depositonce.tu-berlin.de/handle/11303/13669

[4] C. Wiesener and T. Schauer, "The Cybathlon RehaBike: Inertial-Sensor-Driven Functional Electrical Stimulation Cycling by Team Hasomed," *IEEE Robotics & Automation Magazine*, vol. 24, no. 4, pp. 49–57, Dec. 2017, doi: 10.1109/MRA.2017.2749318.

[5] B. Sijobert, R. Le Guillou, C. Fattal, and C. Azevedo Coste, "FES-induced cycling in complete SCI: A simpler control method based on inertial sensors," *Sensors (Switzerland)*, vol. 19, no. 19, 2019, doi: 10.3390/s19194268.

[6] T. Schauer and C. Wiesener, "Generating smooth stimulation patterns in FES cycling with motor assistance based on a single body-worn inertial sensor – a simulation study," presented at the RehabWeek 2023, Singapore, Sep. 2023.

[7] M. Bonizzato *et al.*, "Autonomous optimization of neuroprosthetic stimulation parameters that drive the motor cortex and spinal cord outputs in rats and monkeys," *Cell Reports Medicine*, vol. 4, no. 4, p. 101008, Apr. 2023, doi: 10.1016/j.xcrm.2023.101008.

[8] R. Smith, *Open Dynamics Engine (ODE), User Guide, http://www.ode.org*. (2006).

[9] R. Riener and T. Fuhr, "Patient-driven control of FES-supported standing up: a simulation study," *IEEE Trans Rehabil Eng*, vol. 6, no. 2, pp. 113–124, 1998.

[10] E. Brochu, V. M. Cora, and N. de Freitas, "A Tutorial on Bayesian Optimization of Expensive Cost Functions, with Application to Active User Modeling and Hierarchical Reinforcement Learning," Dec. 12, 2010, *arXiv*: arXiv:1012.2599. doi: 10.48550/arXiv.1012.2599.

[11] B. Shahriari, K. Swersky, Z. Wang, R. P. Adams, and N. de Freitas, "Taking the Human Out of the Loop: A Review of Bayesian Optimization," *Proceedings of the IEEE*, vol. 104, no. 1, pp. 148–175, Jan. 2016, doi: 10.1109/JPROC.2015.2494218.

Author's Address

Thomas Schauer
Control Systems Group, Technische Universität Berlin
schauer@control.tu-berlin.de
https://tu.berlin/control

Adding imposed ankle motion to FES cycling

Donaldson N.[1] and Husseini H.[1]

[1]University College London, United Kingdom

Abstract: *We think that cycle ergometers for rehabilitation after spinal cord injury would be improved if ankle motion were imposed with the knee and hip motion. A mechanism to produce this motion is proposed which uses three gears, one non-circular. It is not possible, with this mechanism to get the same amplitude as shown by recreational able-bodied cyclists.*

Keywords: *FES Cycling, ankle motion, mechanism.*

Introduction

FES cycling is a popular exercise for people with spinal cord injury because of its health benefits. Several companies supply stationary ergometers which can be used in clinics, gyms or even at home. All these machines have footplates that are freely-pivoted on the cranks so that the plantarflexion angle of the ankle is undefined unless the rider also wears ankle-foot orthoses.

No doubt one reason why FES cycling is popular with clinicians is the simplicity of setting up the stimulator, which is probably done under the assumption (perhaps not usually noticed) that the ankle and foot can be disregarded. In that case, if the leg of the cyclist on the ergometer is considered as a linkage comprising thigh, shank and crank, with the hip joint and crankshaft fixed, then the position of the knee is determined by the position of the crank (Figure 1(a)), and stimulation of the knee and hip, flexors and extensors, can be set so that shortening muscles contract. These contractions produce forward torque in the crankshaft.

When a foot is added as an additional link between the shank and the crank, the position of the knee is no longer defined by the crank position. There is then a degree of freedom allowing some covariation of the hip, knee and ankle angles. In principle, this extra degree of freedom makes control of the motion much more complicated but in practice the complication is avoided by placing the pivot on the footplate close to the ankle joint (Fig 2).

In able-bodied cycling, the pedal is placed under the forefoot to allow the ankle muscles to contribute to extension and flexion of the leg. Placing the pivot for the footplate near the ankle reduces the effective length of the foot to about one half or third of its normal length.

When we started experimenting with FES cycling, we were concerned about this extra degree of freedom, and provided an ankle-foot orthosis to prevent ankle motion(1) (Perkins Vienna 2004?). Generally, this extra restraint does not seem to be necessary with current footplate designs.

There is increasing evidence that FES cycling causes neurological recovery (2); simultaneous voluntary effort and electrical stimulation strengthens the motor pathways. But in that case, should not the ankles be trained as well as the knees and hips? Having the pivots so close to the ankle joints means that the ankle muscles cannot contribute much to driving the crankshaft, and generally the plantarflexors and dorsiflexors are not stimulated, and yet they are important muscles. Able-bodied cyclists typically get 10% of the total power from the ankles (3). If FES-cycling is being used as

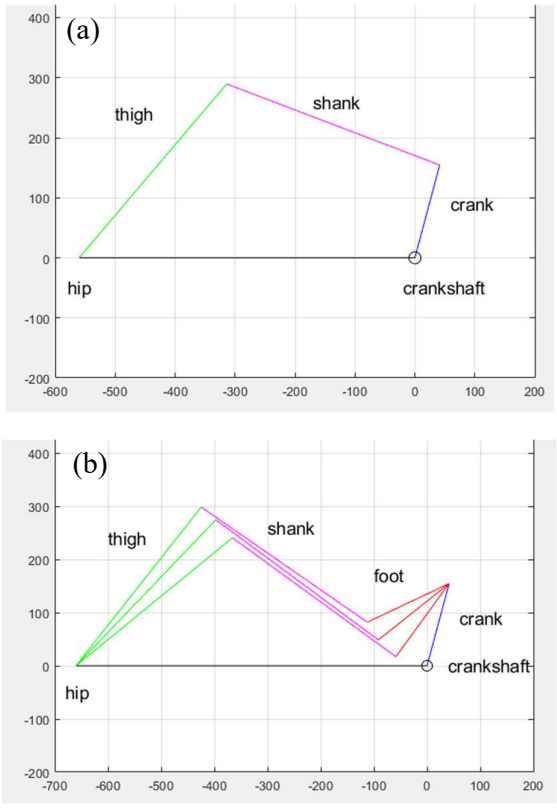

Figure 1 (a) If crank is pivoted at ankle joint, the position of the leg is determined by the crank angle. (b) With pivot under forefoot, the leg position is not defined by crank angle.

a therapy to enabling walking, the ankle muscles are important because of the impulse they provide at push-off, which propels the body forward (4).
In this paper, we propose that ergometers for FES cycling be improved by adding appropriate motion of the footplates so that as the crankshaft rotates, the hips, knees and ankles all move appropriately. What this requires is a mechanism to impose the footplate motion. We provide here a simulation of an appropriate mechanism that uses three gears between the crank shaft and the footplate pivot. One of these gears is non-circular. We have a program to optimise the gear sizes and the shape of the non-circular gear.

Figure 2. RT300 footplate from Restorative Therapies. The pivot is about 8 cm forward of the malleoli.

Finding the Footplate Motion

We start from Ericson's ankle motion function which was averaged from able bodied recreational cyclists (5). The peak-peak amplitude is 22°. We derived the angle of the footplate by geometrical calculation (Fig 3(a)), giving the footplate angle, which has a larger amplitude of ~44°. This β curve is the motion which we want the new mechanism to produce.

Gear Mechanism

The proposed mechanism is shown in Fig 4.
Seen as in Fig 3(a): as the crank rotates clockwise with the crankshaft, the foot and footplate rotate anticlockwise, relative to the crank, but not at the same rate. Considering the mechanism, it is easier to imagine the crank being fixed while the crankshaft and the pedal shaft rotate anticlockwise, the former at a constant rate and the latter not constant but still completing each revolution at the same time.
To investigate whether a non-circular gear could be found that gave the target footplate angle shown in Figure 3(b), a circular harmonic function was used to describe the shape of C.

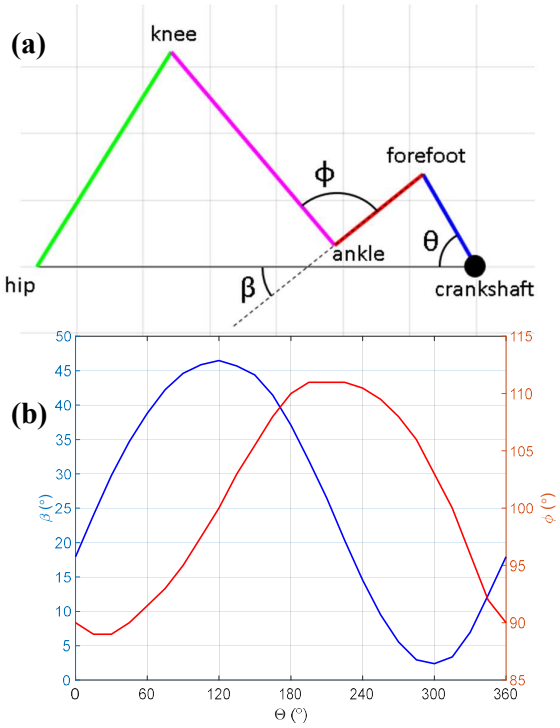

Figure 3. (a) Stick figure calculation of footplate angle β as a function of crank angle θ given the ankle angle (ϕ) function from Ericson. Lengths: thigh 38cm, shank 38cm, foot 17cm, crank 16cm, hip-crankshaft 66cm. (b) Ericson's ankle angle function (red) and corresponding footplate angle (blue).

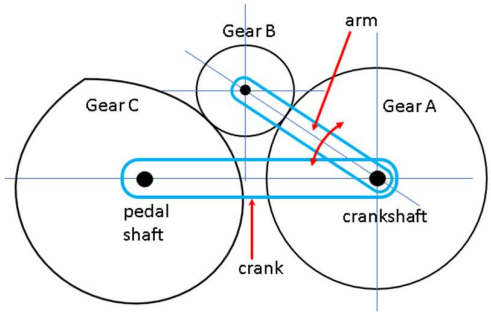

Figure 4. Concept of mechanism, seen with crank stationary. Gear A rotates about the crankshaft and Gear C is connected to the footplate. Gears A and B are circular. B is on an arm that holds it meshed with A. C is non-circular but has a perimeter that is equal to the circumference of A. B is held meshed against C.

$$p = \left(a + b.cos(\theta + \theta_1) + c.cos(2.\theta + \theta_2)\right)e^{j\theta}$$

p is the outline of the gear as a function of θ, the angle around the axis of the gear. The parameters were *a, b, c,* θ_1, θ_2, and the crank length. The radius of A was calculated so that its circumference is equal to the perimeter of C.A and C will have an equal number of teeth. The number of teeth on B is the seventh parameter which determines the radius of B and hence the arm length. Our program simulated the motion for each set of parameters, comparing the footplate motion the target function (Fig 3b) and showing faults, for example, A colliding with C.

Optimisation was performed by repeatedly running the Matlab script and comparing the footplate angle with the target motion. Figure 5 is near optimal. It is not possible to reach the amplitude of the target.

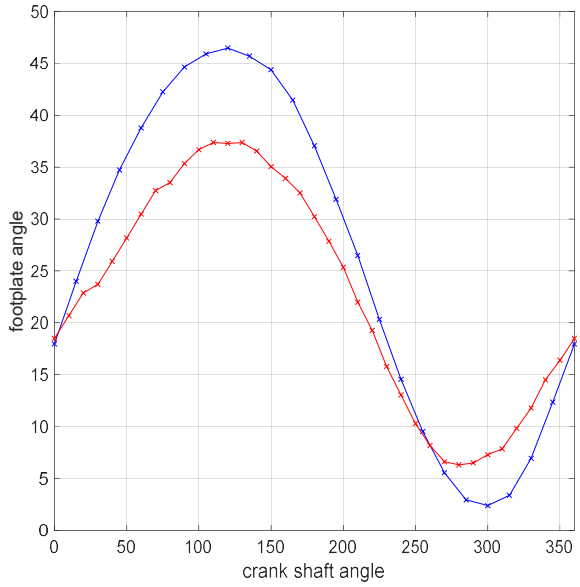

Figure 5. Target (blue) and optimal motion (red)

In Figure 6, rotation of the three gears is shown by the radial red lines.

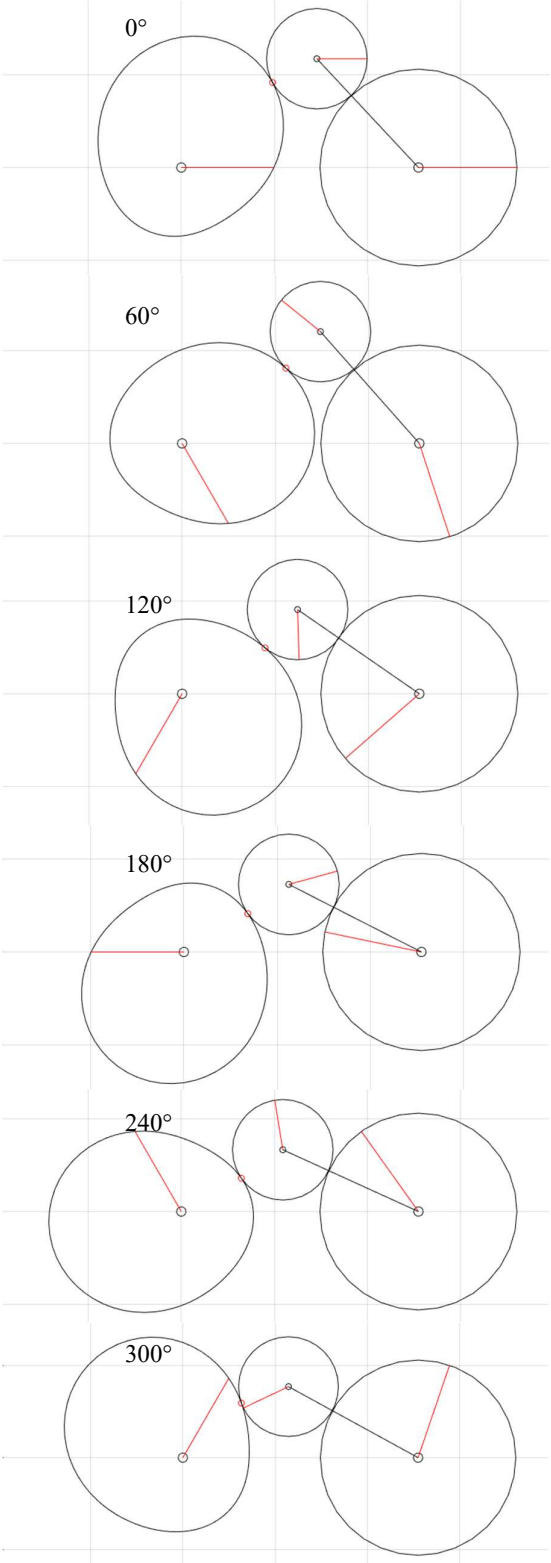

Figure 6. Optimal Motion. Rotation angles are Gear C

Discussion

It is disappointing that the optimal motion produces an amplitude of only 31°, less than the target amplitude of 41°. However, the mechanism should define the ankle motion. Of course, the target angle depends on both the ankle motion, which we took from Ericson (Fig 3(b)), but also the dimensions used in the stick figure (Fig 3(a)). It may be that some patients may need even less amplitude than the able-bodied cyclist, for example, if they are hypertonic. For them alternative gear sets may be needed.

To design a practical mechanism, involute teeth must be added to all three gears which must mesh during the motion and then the three-dimensional machine must be designed which is compact enough to be added to the ergometer but also strong enough to transmit the ankle plantarflexion moment.

Acknowledgement

We acknowledge contributions to this work by Hattie Palmer, Tomowo Owoseje and Antonia Xie.

References

1. Perkins TA, Donaldson N. de N., Fitzwater R., Phillips G.F. & Wood D.E., editor Leg powered paraplegic cycling system using surface functional electrical stimulation. 7th Vienna FES Workshop; 2001 2001; Vienna.
2. Duffell LD, Paddison S, Alahmary AF, Donaldson N, Burridge J. The effects of FES cycling combined with virtual reality racing biofeedback on voluntary function after incomplete SCI: a pilot study. J Neuroeng Rehabil. 2019;16(1):149.
3. Aasvold LO, Ettema G, Skovereng K. Joint specific power production in cycling: The effect of cadence and intensity. PLoS One. 2019;14(2):e0212781.
4. Winter DA. Energy generation and absorption at the ankle and knee during fast, natural, and slow cadences. Clin Orthop Relat Res. 1983(175):147-54.
5. Ericson M. NR, Nemeth G. Joint motions of the lower limb during ergometer cycling. Orthopaedic and Sports Physical Therapy. 1988:273-8.

Author's Address

Nick Donaldson
University College London
Dept. of Medical Physics and Biomedical Engineering
n.donaldson@ucl.ac.uk

FES-induced changes in excitability of denervated muscles in flaccid paraplegia – single case study

Mariann Mravcsik[1,3], Amelita Fodor[1,2,4], Lilla Botzheim[1,3], Melinda Feher[2], Balázs Radeleczki[1,4], Quang Nguyen[5], Martin Schmoll[5], Winfried Mayr[5], Jozsef Laczko[1,3,4]

[1]HUN-REN, Wigner Research Centre for Physics, Budapest, Hungary
[2]Semmelweis University, Rehabilitation Clinic, Budapest, Hungary
[3]University of Pécs, Hungary
[4]Pazmany Peter Catholic University, Faculty of Information Technology and Bionics, Budapest, Hungary
[5]Center for Medical Physics and Biomedical Engineering, Medical University of Vienna, Austria

Abstract:
A patient with flaccid paraplegia participated in muscle strengthening training using a Stimulette den2x stimulator which delivered a biphasic symmetrical rectangular current with 40 ms impulse durations (both phases) and 10 ms impulse pause administered with 2-seconds bursts and 4-seconds breaks. The maximal current amplitude was 180 mA for the quadriceps, 100 mA for the tibialis anterior, 75 mA for the hamstrings. The excitability of the quadriceps, gastrocnemius and tibialis anterior muscles was characterized by a threshold, defined as the smallest current amplitude that can induce a muscle twitch. This threshold was measured 86 times for the quadriceps, 40 times for the gastrocnemius and 30 times for the tibialis anterior over a period of three years. The threshold decreased over the course of the training sessions in both legs for the quadriceps and gastrocnemius. The linear trendline showed a decrease in the case of Q and GA, suggesting improved excitability during the training. The patient participated in weekly FES cycling training sessions during initial 20 months, and after a period 16 months with FES training without cycling, again 5 cycling sessions using a special tricycle equipped with a 4-channel electrical stimulator designed for denervated muscles. The quadriceps and hamstring muscles of both legs were activated. During the 30 minutes long training sessions, the average cycling speed was higher in the last third of the training session than in the first third. This case study demonstrates an improvement in the excitability of denervated leg muscles and the ability of a patient with flaccid paraplegia to successfully participate in FES cycling training.

Keywords: *Muscle excitability, Denervation, FES cycling, Quadriceps, Tibialis Anterior, Gastrocnemius*

Introduction

In Hungary, approximately 300-500 new spinal cord injuries (SCI) occur every year, and 10-12 thousand people live with SCI. Spasticity affects approximately 46-65% of SCI patients, and 35-44% have flaccid paraplegia. Patients with injuries below T10 or injury of the cauda equina region are characterized by peripheral muscle denervation[1].

After denervation a quick onset of the rapid muscle atrophy is observed that turns to degeneration in the second year, with infiltration of intramuscular fat and formation of fibrous tissue along with altered metabolic processes. The start of early rehabilitation is key for rescue the muscle mass. The long pulse width stimulation technique is well applicable in this condition [1], [2], [3].

Muscle excitability provides information about the functional condition of the muscle during the denervation. Thus, we can monitor muscle changes without frequent need of costly imaging technics such as MRI.

The long-term denervation causes the degeneration of the muscle fibres, replacement of muscle fibre mass by fat and fibrous connective tissue, the dramatic loss of capillaries and degenerative changes within intramuscular nerve trunks [2], [4], [5].

The functional electrical stimulation (FES) guided cycling is available for spastic SCI people. In spastic SCI cases, the nerves that innervate the muscles are electrically stimulated, whereas in denervated cases this innervation is lost. We used a special tricycle, the Reha Funtrike (OVG, Munich, Germany) which got equipped with a 4 channel custom-build stimulator from the Medical University of Vienna. This system is for patients with lower motoneuron lesions where the excitability via nerve is missing, but the system makes it possible to contract denervated muscles for cycling exercises [6], [7]. The muscle fibers are stimulated directly, for which the appropriate long impulse durations of 10 to even hundreds of ms, are crucial, different to spastic paralysis, where the motoneurons are activated by short pulses with durations below 1 ms. Consequently, the electrical charge transfer across the electrode-skin interface is substantially higher for direct muscle stimulation. Therefore, the leg cycling is hard to implement for these patients.

In our present study we tracked changes in muscle excitability of a SCI patient who has lower motoneuron lesion on his lower limbs over time of long-pulse FES application. Our aim was to increase the overall performance of the patient in cycling training, to preserve his muscles and to monitor the change in his condition.

Material and Methods

Our participant was 44 years old when his heart stopped, which led to severe peripheral circulatory failure and metabolic acidosis, resulting in ischemic spinal cord damage from the thoracic to the sacral region. Sensation below the Th8 level was completely lost, with no voluntary movement in the lower limbs and flaccid muscle tone. His ASIA score is A. He is cooperative, and motivated, and for the past three years, he has been attending FES cycling training at the Rehabilitation Clinic once or twice a week.
One month after his injury he started the cycling training with the Reha Funtrike (OVG, Munich, Germany) bike. It is a special FES tricycle, with a sliding seat that can be pushed backward and drives the bike by stimulated knee extension and pulled forward by the participant's voluntary arm movements, while decoupled from the propelling chain.

Figure 1: Special tricycle equipped with an electrical stimulator for SCI patients with denervated muscles

The tricycle was modified for FES-controlled operation at the Medical University of Vienna, we apply it once a week. Preliminary results have been presented previously ([6], [8]) with cycling distance before fatigue and cycling velocity. This device gives a great opportunity for the whole-body training – the pilot can support leg movements with his arms as option to achieve a higher performance. The cycling distances were followed with a cycling computer (Sigma, BC 16.16 STS). For monitoring heart rate, an automatic heart rate monitor (Omron) was used.
We identified two types of training: functional electrical stimulation (FES)-assisted tricycle training and long-duration pulse stimulation training using a Stimulette den2x (Schuhfried, Vienna, Austria) device. Initially, our pilot participated in the tricycle training sessions (March 2022 - October 2023), which were complemented by a warm-up stimulation phase (Stimulette sessions).
The cycling sessions always start with a warm-up on Stimulette stimulation (SS) for the quadriceps (Q). Later, from (February 2023) the gastrocnemius (GA) was also stimulated in the warm-up.
During the 3 years there was a period (October 2023-March 2025), when we continued only selective stimulation for the quadriceps (Q), gastrocnemius (GA) tibialis anterior (TA) muscles (in the time frames presented at Figure 2.), using Stimulette den2x device (Schuhfried Medizintechnik GmbH, Austria), with the participant in sedentary position. Stimulation parameters were the following: biphasic symmetrical rectangular current, 40 ms impulse durations (both phases) and 10 ms impulse pause administered with 2 s bursts and 4 s breaks. The maximal current amplitude was 180 mA of the quadriceps, 100 mA for the tibialis anterior, 75 mA for the hamstrings. The fused contraction and the maximal knee extension was the goal during the training sessions.
For electrophysiological assessments the motor thresholds of muscles (which means the minimal value of the current intensity, what makes the muscle twitch) were monitored during SS. We registered that minimum value of the current amplitude in every SS.
The hamstring muscle group was included in the FES assisted tricycle training 3 years after the initial tricycle training sessions (from April 2025). The stimulation is controlled manually by the participant using push buttons placed on the handlebar. To date of writing this report the participant had 5 training sessions since restart of the cycle training. In the beginning tricycling training sessions lasted 5-minutes before muscle fatigue. Now he can cycle 3x5 minutes (3 phases) in each training session. The limitation was the hamstrings fatigue, which had not received any stimulation training since his injury, for 3 years.

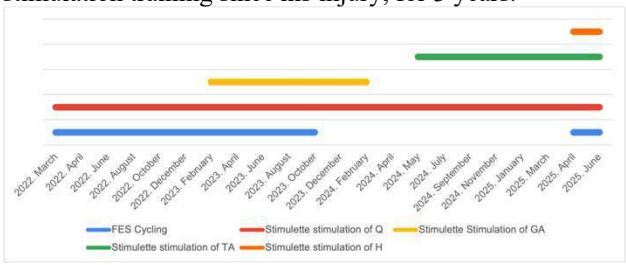

Figure 2: Timeline of the FES cycling and muscle strengthening training of leg muscles with Stimulette stimulators

For the tricycling training sessions and for Stimulette sessions we used conductive rubber electrodes with a 200cm^2 wet sponge pocket (Schuhfried, Medizintechnik GmbH, Austria), strapped to the anterior and posterior surface of the thighs in proximal and distal positions.

Results

FES cycling training with stimulated quadriceps and hamstring muscles.

During the five tricycling training session the cycled distance increased from 0,47 to 1,1 km. Fig 2. presents the average and maximal (across training sessions) speed in three phases of the sessions.

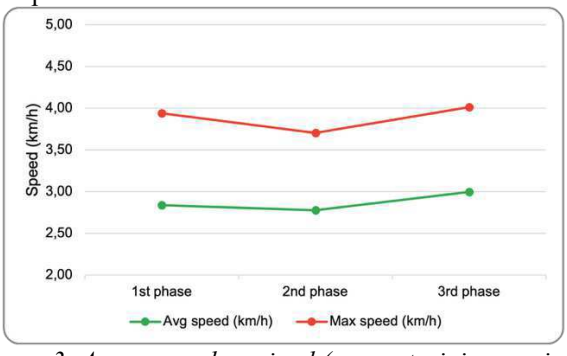

Figure 3: Average and maximal (across training sessions) speed of the cycling through three 5 minutes long phases

The average and maximal cycling speed decreased in the second and increased in the last phase.

Heart rate changes during the FES cycling

Figure 4 shows the average (across five training sessions) heart rates in five phases of the sessions. The resting HR was 101 bpm, then it rose from this level to 107. Five minutes after the end of the training session, it did not return to the baseline value.

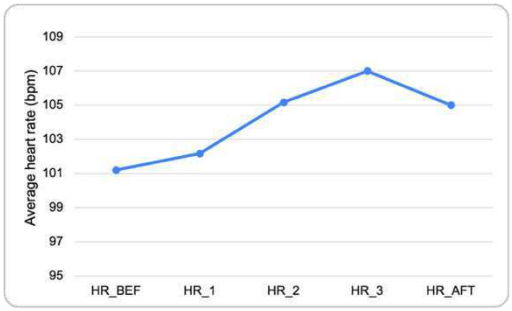

Figure 4: Average heart rate before (HR_BEF), during three phases (HR_1, HR_2, HR_3) and after (HR_AFT) the FES cycling training sessions (averaged across sessions)

Results of muscle excitability assessments with the Stimulette stimulator

Figure 5. shows the variation of the excitability threshold of the quadriceps muscles. The linear trendlines decrease (the slope of the trendline is -0.04 for the left and -0.08 for the right Q), what means that the excitability during the years increased. The mean and the standard deviations of the thresholds were 56.36 ± 9.9 for the left, and 54.09 ± 10.05 right side.

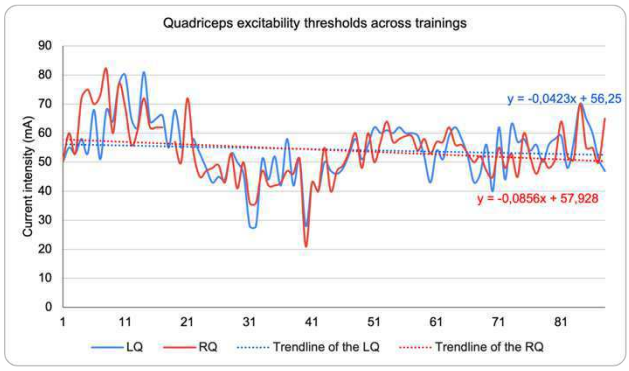

Figure 5: The quadriceps muscles excitability thresholds during the sequence of 86 training sessions (LQ-left quadriceps, RQ-right quadriceps)

Q thresholds were assessed 86 times. There is notable difference between the average of the first 20 training sessions and the average of the last 20 sessions. The standard deviation is higher in both side in the first 20 than in the last 20 training sessions (Table 1.)

Table 1: Average thresholds of the quadriceps muscles

86 trainings	Average thresholds and SDs (mA)	
	LQ	RQ
First 20 trainings	62.90 ± 9.27	64.37 ± 9.31
Last 20 trainings	55.50 ± 7.33	52.50 ± 6.33
Average	54.36 ± 9.90	54.09 ± 10.05

The GA muscles were assessed 40 times. The thresholds also show decreasing trends. The slope was -0,15 for the left and -0,13 for the right leg (Fig 6.), that show improved excitability.

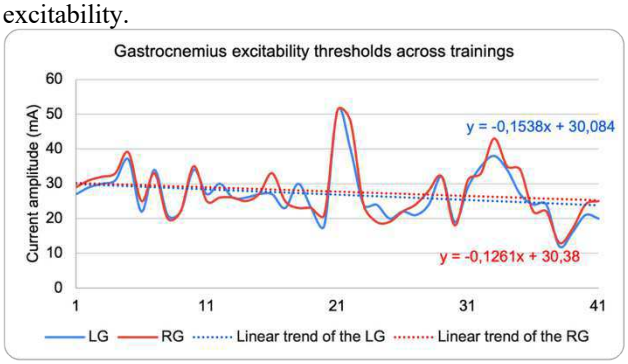

Figure 6: The gastrocnemius muscles excitability thresholds during the sequence of 40 training sessions (LG-left gastrocnemius, RG-right gastrocnemius)

The last 10 sessions' average thresholds were lower than that of the first 10. Standard deviations were a little bit higher (Table 2.).

Table 2: Average thresholds of the gastrocnemius muscles

40 trainings	Average thresholds and SDs (mA)	
	LG	RG
First 10 training	28.55 ± 5.35	29.45 ±5.84
Last 10 training	25.45 ± 8.13	27.18 ± 8.83
Average	26.85 ± 7.25	27.73 ± 8.02

TA stimulation started 2 years after the denervation. These muscles do not show improvement in excitability. The increase of the trend is 0.03 on the left and 0.35 on the right (Fig 7.).

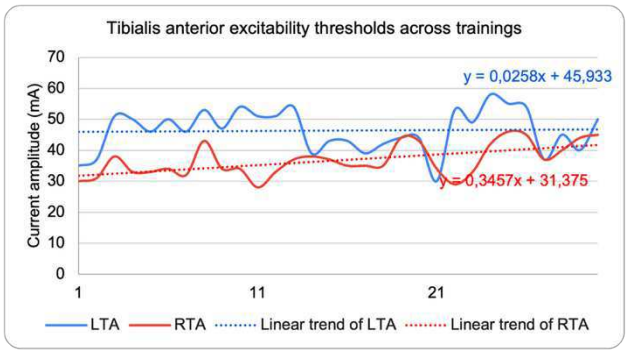

Figure 7: The tibialis anterior muscles excitability thresholds during the training sessions (LTA- left tibialis anterior, RTA – right tibialis anterior)

Table 3: Average threshold of the tibialis anterior muscles

30 trainings	Average thresholds and SDs (mA)	
	LTA	RTA
First 10 training	47.27 ± 6.17	33.64 ± 4.03
Last 10 training	46.82 ± 8.57	39.82 ± 5.74
Average	46.33 ±6.85	36.73 ± 5.19

Discussion and Conclusion

Our SCI participant had the opportunity and was able to participate in this research for a long period of time. It is difficult to maintain muscle after denervation, but rebuilding it is even more challenging than maintaining its existing condition. This is because after denervation, all physiological processes promote degradation. In this study, we showed how electrostimulation started early after the injury and continued for a long time (3 years), has affected the excitability of the quadriceps, tibialis anterior, and gastrocnemius muscles. We observed an improvement in excitability in the quadriceps and gastrocnemius, but not in the tibialis anterior. Further studies are needed to explore how to improve the condition of the TA. A limitation of our study is that we did not investigate whether changes in muscle morphology occurred.

The relatively high heart rate may be explained by the fact that, in addition to cycling controlled by FES, the arms were also involved in the training. The heart rate values are comparable to previously reported values, that were assessed during FES-controlled leg cycling combined with arm exercise of SCI patients[9].

While we had a high number of training sessions, generally once a week, the limitation of our work was that during this long period the frequency of training sessions depended on when the patient was able to come to the rehabilitation centre to attend a session. Nevertheless, we are the first who started to use a unique tricycle, which allowed FES cycling training by stimulating denervated flexor and extensor muscles. Here we described our preliminary results (after 5 training sessions) in terms of average and maximal cycling speed. The training should be continued to explore further effect of FES cycling on denervated muscles.

Acknowledgement

Supported by National Research, Development and Innovation Fund, Hungary Grants: TÉT-2023-00064 and RRF-2.3.1-21-2022-00004, and Austrian - Hungarian Action Foundation Grant: 115öu10.
We express our thanks for the devoted assistance of physiotherapists Anita Nagy and Orsolya Malczanek.

References

[1] S. Chandrasekaran, J. Davis, I. Bersch, G. Goldberg, and A. S. Gorgey, "Electrical stimulation and denervated muscles after spinal cord injury," *Neural Regen Res*, vol. 15, no. 8, pp. 1397–1407, 2020, doi: 10.4103/1673-5374.274326.

[2] B. M. Carlson, "The biology of long-term denervated skeletal muscle," *Eur J Trans Myol-Basic Appl Myol*, vol. 24, no. 1, pp. 5–11, 2014.

[3] I. Bersch and W. Mayr, "Electrical stimulation in lower motoneuron lesions, from scientific evidence to clinical practice: a successful transition," *Eur J Transl Myol*, vol. 33, no. 2, Jun. 2023, doi: 10.4081/ejtm.2023.11230.

[4] M. Alberty, W. Mayr, and I. Bersch, "Electrical Stimulation for Preventing Skin Injuries in Denervated Gluteal Muscles—Promising Perspectives from a Case Series and Narrative Review," *Diagnostics*, vol. 13, no. 2, Jan. 2023, doi: 10.3390/diagnostics13020219.

[5] B. Carlson, E. I. Dedkov, D. E. Dow, and T. Y. Kostrominova, "The biology and restorative capacity of long-term denervated skeletal Muscle," *Basic Appl Myol*, vol. 12, no. 6, pp. 247–254, 2002, [Online]. Available: https://www.researchgate.net/publication/231186226

[6] M. Mravcsik, A. Klauber, M. Putz, C. Kast, W. Mayr, and J. Laczko, "Tricycling by FES quadriceps muscles leads to increased cycling speed over series of trainings of persons with flaccid paraplegia," in *Proceedings of the 13th Vienna FES Workshop*, 2019, pp. 133–135.

[7] M. Mravcsik, C. Kast, S. Malik, W. Mayr, and J. LAczko, "Cycling speed increases through Functional Electrical Stimulation (FES) assisted tricycling trainings of spinal cord injured individuals," in *World Congress on Medical Physics & Biomedical Engineering*, 2018, p. Program Book p. 592.

[8] M. Mravcsik *et al.*, "FES driven cycling by denervated muscles," in *22th Anual Conference of the Functional Electrical Stimulation Society*, 2018, pp. 134–136.

[9] N. Hasnan *et al.*, "Exercise responses during functional electrical stimulation cycling in individuals with spinal cord injury," *Med Sci Sports Exerc*, vol. 45, no. 6, pp. 1131–1138, 2013, doi: 10.1249/MSS.0b013e3182805d5a.

Author's Address

Mariann Percze-Mravcsik
HUN-REN Wigner Research Centre for Physics
percze-mravcsik.mariann@wigner.hun-ren.hu

Development of Models to estimate realistic Key Performance Indicators on a FES-Cycling-Ergometer

Rösler I[1], Nguyen Q[1], Schmoll M[1],

[1]Center for Medical Physics and Biomedical Engineering, Medical University of Vienna, Austria

Abstract: *For individuals with spinal cord injury (SCI), access to independent physical activity and exercise is often limited, despite its strong contribution to quality of life and its potential to reduce secondary health complications (SHC). Cycling with functional electrical stimulation (FES) offers a promising approach: electrical impulses stimulate muscle contractions, enabling the reactivation of paralyzed muscles. This counters muscle atrophy and helps minimize SHC. The aim of this work is to enable people with paraplegia to independently perform FES-Cycling with real-time, realistic performance feedback. To this end, the BerkelBike Fitness ergocycle was equipped with a new interface. Based on two models—one for power estimation and one for speed calculation—performance metrics are computed in real time. These models are based on measuring cadence and resistance levels. Both models proved reliable in transferring feedback derived from outdoor measurements to indoor training sessions. The R^2 values for the power model ranged from 0.82 to 0.99, while the speed model achieved an R^2 of 0.91. Thus, the work successfully achieved its goal: performance indicators were displayed in real time via the interface. Data storage allows long-term tracking of training status. Participants can train independently and continuously analyse their performance data, gaining valuable insights into their progress and enabling individualized adjustments to their training regimen.*

Keywords: *Spinal Cord Injury, FES-Cycling, Neurorehabilitation, Cycling computer, Power estimation*

Introduction

Cycling with functional electrical stimulation (FES) enables individuals with spinal cord injury (SCI) to engage in physical activity by electrically stimulating paralyzed muscles to produce coordinated movements [1].

To support training motivation, it is essential to provide users with meaningful and realistic feedback. For athletes training with FES, interpreting their performance can be difficult, especially for beginners who may lack the context to understand raw metrics. Real-time tracking of key performance indicators (KPI) such as power, speed, cadence, and heart rate can offer valuable insight into the training load, physical effort, and overall progress [2]. When displayed in a comprehensible way, these values can help users better understand their training progress and make informed decisions about their further training strategies.

The goal of this work was to develop a system that provides FES-Cyclists with realistic real-time information to improve training motivation. A cycling computer was designed for the BerkelBike Fitness ergocycle, using only the system's built-in rotary encoder. Based on indoor and outdoor cycling power data, two performance models were developed to estimate KPIs. These models translate basic sensor input into realistic estimates of power and speed, offering visual feedback.

Material and Methods

Power Model:
Four able-bodied individuals were measured while cycling on the stationary BerkelBike Fitness (BerkelBike BV, Netherlands). They pedaled at cadences from 30 to 100 RPM in 10 RPM steps, each for 30 seconds. Power output was measured using Favero Assioma DUO pedals (FAVERO ELECTRONICS Srl, Italy) and recorded via the software Golden Cheetah. The pedals were temporarily mounted on the ergocycle for these measurements. Recordings were taken across all eight resistance levels of the ergocycle.

Data analysis was performed in Matlab R2022a (Math Works, Inc., USA), using a third-degree polynomial function with a fixed starting point (eq. 1). This resulted in eight polynomial curves, each representing one resistance level. The curves follow eq. 1, where *c* is cadence and *a, b, c* are regression coefficients. The fit quality was evaluated calculating the R^2-value and the root mean square error (RMSE) of power against cadence.

$$p(c) = a * (c) + b * (c)^2 + c * (c)^3 \qquad \text{(eq.1)}$$

Speed Model:
Outdoor data was collected from five able-bodied participants aged 16 to 41 years (avg. height: 172.8 ± 12.1 cm; weight: 69.0 ± 12.6 kg), using a recumbent ICE VTX trike (ICE Trikes, UK) equipped with a 2INPOWER crank power meter (Rotor, Spain). A preliminary test with one person covered all 11 gears to validate the setup. Due to the length of that run (>1.5 h), the main protocol focused on three representative gears: first (low), sixth (medium), and eleventh (high) gear. Participants received an introduction to the trike and completed a 5-minute self-paced warm-up.

Data was recorded with a Garmin Fenix 7 watch (Garmin Ltd, USA), which tracked speed and distance via GPS and connected to the power meter via Ant+ to log cadence, power, speed, and distance at 1 Hz. Files were exported in. fit format using Garmin Connect.

Table 1: Regression coefficients and quality measures for the eight resistance levels of the BerkelBike Fitness.

Resistance Level	a	b	c	R^2	RMSE W
1	-0.09886	0.00877	-4.4816e-5	0.8280	3.46
2	-0.09140	0.01357	-6.1283e-5	0.9355	4.38
3	0.03131	0.01400	-4.0702e-5	0.9501	5.67
4	0.06623	0.01848	4.8846e-5	0.9749	5.68
5	0.03390	0.02550	8.1999e-5	0.9751	7.05
6	0.01525	0.03527	-12.927e-5	0.9840	7.07
7	0.08092	0.04164	-15.928e-5	0.9902	6.91
8	0.08516	0.04835	-18.711e-5	0.9900	7.83

The cadence was increased stepwise from 25 RPM to 30 RPM and then in steps of 10 RPM to a maximum of 100 RPM, each time for 30 seconds. The tests were carried out on a standard tartan running track in an open-air stadium to ensure a flat and constant riding surface. All measurements were carried out in dry and windless conditions to minimize external influences. Participants followed pre-recorded audio instructions via headphones and used a metronome (2/4 time) to stay in rhythm with pedaling. Instructions also guided gear changes. An onboard display allowed cadence monitoring. Overall, most of the participants were able to maintain the required frequencies.

Data processing was done in MATLAB R2022a (MathWorks, USA). Cadences above 80 RPM were excluded due to excessive variations in the data. Speed was smoothed using a 10 s moving average filter. All data was fitted to a single global polynomial function with a fixed starting point (eq. 1), enabling comparison with the indoor Ergocycle setup. Model quality was assessed by calculating the R^2-value and RMSE of speed against power.

To validate the speed model each dataset from the outdoor measurement was compared to its calculated values. Therefore, the measured power values were fed into the speed model to calculate a modeled speed, which was then integrated over time to derive the modeled distance.
For each gear, the measured and modeled values were compared. Subsequently, the mean and standard deviation of both speed and distance were calculated, along with the absolute and relative deviations between modeled and measured values. For the speed these values were calculated on a point-wise difference whereas for the distance, these values were calculated for the total difference.

Results

The result of the measurements for power on the ergocycle resulted in eight individual third degree polynomial curves with a fixed starting point at 1 that represented each resistance level (Fig. 1). shows the regression coefficients and the quality measures.

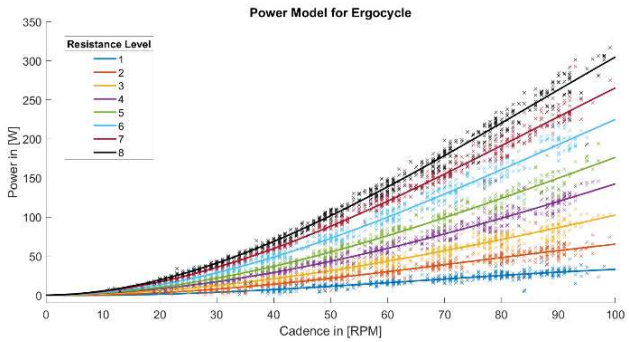

Figure 1: The result of the power model that is used to calculate the power calculation on the ergocycle. Data points are shown with x. Each color displays one resistance level of the ergocycle.

The speed model resulted in one polynomial equation shown in **Figure 2** that is eq. 2 with v being speed and p being power.

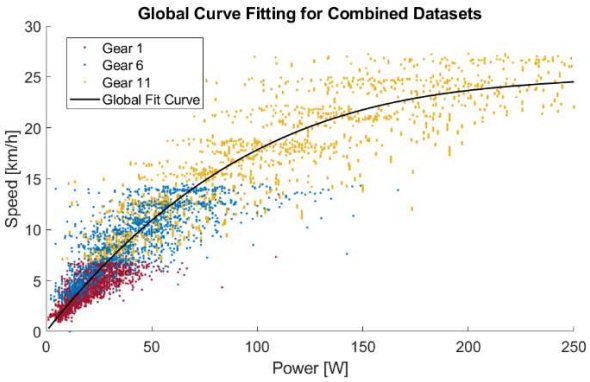

Figure 2: The data points of the speed model from the first gear are shown in red, from the sixth gear in blue, and from the eleventh gear in yellow. The global curve (black line) was fitted over all data points.

$$v\,(p) = 0.2555 * p - 9.104 * 10^{-4} * p^2 + 1.133 * 10^{-6} * p^3 \qquad \text{(eq. 2)}$$

The curve shows an almost linear increase in the range below 50 watts but then rises increasingly less. At 50 watts, the speed was estimated by the model as 10.64 km/h, whereas at 250 watts, the speed of the trike was estimated at 24.7 km/h.
The quality of the fit was assessed using the determination coefficient, R^2, which in this case is 0.9116. The root mean square error (RMSE) was 2.0377 km/h, representing the average deviation of predicted values from the actual speed measurements.

Table 2: Validation of Speed. Measured speed was used as reference and calculated speed based on the measured power was compared.

Gear	n	$v_{measured}$ (Ref) [km/h]	v_{model} (calculated) [km/h]	Δv [km/h]	Δv [%]
Gear 1	5	3.2 ± 0.1	3.7 ± 0.2	0.5 ± 1.0	14.2 ± 28.9
Gear 6	5	6.7 ± 0.3	6.6 ± 0.3	-0.3 ± 1.9	-5.2 ± 25.7
Gear 11	5	15.6 ± 0.6	15.1 ± 0.5	-0.5 ± 2.6	-3.1 ± 19.6

Table 3: Validation of Distance. Measured distance was used as reference and calculated distance based on the calculated speed was compared.

Gear	n	$v_{measured}$ (Ref) [km/h]	v_{model} (calculated) [km/h]	Δv [km/h]	Δv [%]
Gear 1	5	275.2 ± 9.1	325.1 ± 15.2	49.9 ± 6.2	18.1 ± 1.7
Gear 6	5	614.8 ± 30.1	592.6 ± 31.4	-22.2 ± 11.8	-3.6 ± 1.8
Gear 11	5	1322.8 ± 42.8	1327.7 ± 39.0	4.9 ± 17.6	0.4 ± 1.4

The calculated speed differences to validate the model can be found in Table 2. For gear 1, the model calculated higher values with 14.2 % more than the actual speed and a deviation of 28.9 %. For gear 6 and 11 the model calculates lower speeds than the actual speed with 5.2 ± 25.7 % difference in gear 6 and 3.1 ± 19.6% difference in gear 11. Distance was compared using the accumulated distance of each measurement and the calculation from the model. It shows a minimal difference of 0.4 ± 1.4 % in gear 11. For gear 6 the model calculated 3.6 ± 1.8 % less than was measured. For the first gear, the difference in the measured values was 49.9 ± 6.2 m, which is a relative difference of 18.1 ± 1.7%.

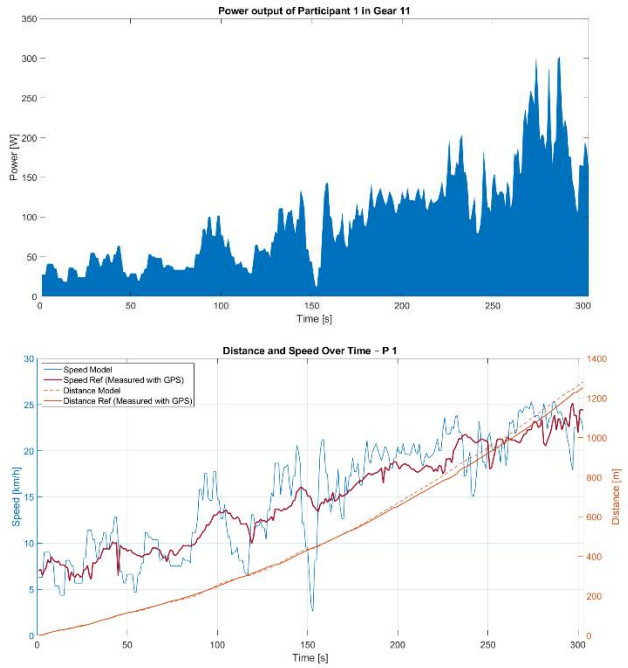

Figure 3: Validation of speed model. Representative example for the calculation for one measurement in gear 11. The upper graph shows power that is used to calculate the speed with the speed model in eq. 5. Below the calculated speed in blue, the measured speed in red and the distance in orange. The solid line is the measured distance, and the dashed line is the calculated distance with eq. 2 and 3 from the calculated speed.

A representation of one measurement in gear 11 is shown in Fig. 3. The measured and modeled distances are very similar up to 165 s, which corresponds to a speed of 15 km/h. After that, the modeled distance is slightly higher than the actual measured distance. After 5.5 min they differ by 28.3 m.

Both models have been integrated into a custom-built cycling computer for the BerkelBike Fitness (Figure 4). It enables the user to save the training, show statistical overviews of all trainings and the last training and provides visual feedback during training.

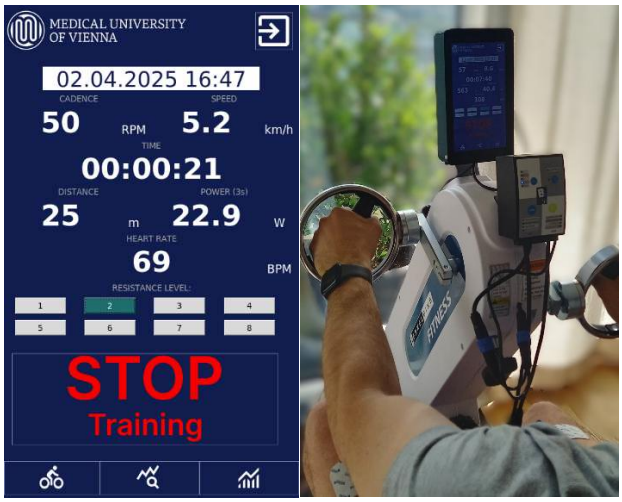

Figure 4: Left: Graphical User Interface to show realistic estimations of KPIs. It contains the current time with white background, the selection buttons for the resistance level, start and stop buttons to start and stop the training. KPI are cadence, speed, training time, distance, power and heart rate. **Right: Hardware** mounted onto the BerkelBike Fitness with the interface used during training.

Discussion

The aim of this work was to develop a cycling computer for indoor FES training with real-time display of power and speed estimations based on cadence. Since speed cannot be directly measured indoors and power is not measured by the BerkelBike Fitness, a model-based approach was necessary.

The first model calculates a power value derived from the athlete's cadence, with the resistance level being crucial for selecting the correct parameters. The model's reliability was evaluated across all resistance levels using regression analysis, yielding R^2-values between 0.83 and 0.99. The RMSE ranged from 3.5 W in the lowest gear to 7.8 W in the highest gear. This confirms that the chosen third-degree polynomial curve with a fixed starting point accurately describes the relationship between cadence and power.

The speed model was developed to calculate realistic key performance indicators for FES-Cyclists by establishing the relationship between power and speed. This model demonstrated a R^2-value of 0.91, indicating a strong correlation between the modeled values and the measured data. The validation of this model revealed that for the highest gear, the distance was accurately represented, with only a 0.4 ± 1.4 % difference between modeled and measured values. Similarly, the sixth gear also exhibited reliable results, showing a distance difference of 3.6 ± 19.6 %. However, the first gear displayed higher variances, with differences reaching up to 18.1 ± 1.7 %.

In terms of speed, the model was able to estimate measured speeds across all gears, with an absolute difference of less than 0.5 ± 1 km/h. In the lowest gear, this led to a relative difference of 14.2 ± 28.9 %, while in the highest gear, it was only 3.1 ± 19.6 %. The performance discrepancies, particularly in the first gear, were attributed to the difficulty of maintaining a smooth pedaling motion at low resistance. Cyclists often exerted more force than necessary, resulting in jerky movements instead of consistent power delivery. This disruption affected both speed and power data, contributing to the higher deviations observed in the first gear.
The model's accuracy improved significantly with higher gears, where maintaining a fluid circular motion was easier. Consequently, the deviations in speed and power data were lower, reflecting the model's better fit in these conditions. Despite the overall reliability of the speed model, its limitations in lower speeds highlight the need for more sensitive power measurements, as most power meters are designed for outputs above 50 W, leading to increased random errors.
It is important to note that the performance model is specifically calibrated for the ICE-VTX trike, which limits the validity of the data when applied to other ergocycles or tricycles. Despite these limitations, the tool demonstrates significant potential within its intended application.

Conclusions

The objective of this work was to develop a method for estimating indoor cycling speed based on outdoor performance data specifically for FES cycling, while also providing real-time KPIs during training. Our results demonstrate that the developed speed model effectively estimates speed based on power data, with strong performance in higher gears. However, challenges in lower gears and the influence of pedaling technique on accuracy suggest areas for further investigation and refinement.
Systematic recording of training data is able to empower users to track their progress, thereby increase motivation and engagement. Furthermore, it bridges the gap between home-based training and supervised rehabilitation by enabling users to share performance data with clinicians or therapists. In future this capability should fosters a more continuous and personalized rehabilitation process, ultimately supporting the users' health and recovery journey.

References

[1] S. Luo, H. Xu, Y. Zuo, X. Liu, and A. H. All, "A Review of Functional Electrical Stimulation Treatment in Spinal Cord Injury," *NeuroMolecular Medicine*, vol. 22, no. 4, pp. 447–463, 2020, doi: 10.1007/s12017-019-08589-9

[2] L. D. Duffell, N. D. N. Donaldson, and D. J. Newham, "Power Output During Functional Electrically Stimulated Cycling in Trained Spinal Cord Injured People," *Neuromodulation*, vol. 13, no. 1, pp. 50–57, 2010, doi: 10.1111/j.1525-1403.2009.00245.x

Author's Address

Isabelle Rösler, BSc
Center for Medical Physics and Biomedical Engineering, Medical University of Vienna, Austria
isabelle-roesler@web.de

Optimal Control Framework for Personalized FES-cycling in Individuals with Spinal Cord Injury

Coelho-Magalhães T[1], Azevedo-Coste C[1], Bailly F[1]

[1]CAMIN, Inria, University of Montpellier, Montpellier, France

Abstract: *Functional Electrical Stimulation (FES)-cycling is employed to facilitate pedalling in individuals with spinal cord injury (SCI), with the aim of promoting physical activity and enhancing overall health. However, the efficiency of FES-cycling remains limited due to the challenge of optimally timing muscle contractions to maximise power output while minimizing muscle fatigue. This study aims to explore the use of an optimal control framework to improve FES-cycling performance in simulation. We use a muscle model that accounts for the effects of electrical stimulation on muscle contraction dynamics and identify its parameters using experimental data collected from 1 individual with SCI. Isometric evoked contractions were measured using the crankset power meter of our tricycle instead of an isokinetic dynamometer. We then demonstrate the feasibility of using trajectory optimization to track a 4.4 rad/s (42 rpm) pedalling cadence and a 20 W crank power output by optimizing the electrical stimulation pulse duration applied on six muscles. Results show the power achieved is 17.53 ± 7.87 W and velocity 4.09 ± 0.36 rad/s. This study presents a first step towards improving the realism of FES-driven simulations, showcases the use of physiological model-based control of FES-cycling, and highlights the potential of predictive modelling and optimal control to personalize FES protocols.*

Keywords: *Biomechanics, Functional Electrical Stimulation, numerical optimal control, FES-cycling, musculoskeletal model*

Introduction

Functional Electrical Stimulation (FES) assisted cycling employs electrical stimulation pulses to evoke coordinated contractions of paretic or paralyzed muscles of the lower limbs to reproduce a pedaling movement, usually on an adapted tricycle [1]. It is a widely investigated rehabilitation strategy for people with neurological conditions, such as spinal cord injury (SCI), and has demonstrated to be efficient in improving muscle, bone and cardiovascular health, fitness, feelings of well-being, and motor functions [2]. Despite its benefits, effectively controlling evoked cycling movement through FES remains a major challenge due to the resulting rapid onset of muscle fatigue [3], and the non-selective activation of muscle groups that results in poor synergistic coordination of agonist and antagonist muscles around a joint [4]. To minimize these drawbacks, researchers aim to optimize the stimulation patterns (i.e., the pulse parameters and their activation timing within the pedalling cycle) and the control laws that dynamically adjust it to the activity goals. Yet, the solution is frequently sub-optimal and often obtained through trial and error or time-consuming procedures [1].

Numerical simulation can be used to explore stimulation patterns or advanced control strategies that generate optimized muscle forces and joint kinematics. In particular, trajectory optimization is an efficient method to explore novel control strategies, guided by the system's dynamics and task-related constraints. Recent advances in musculoskeletal modeling and numerical optimal control provide tools to simulate and optimize such movements [5]. In [6], a framework combining numerical optimal control and FES cycling to track different crank velocities and resistances is presented. The model in this study uses pure torques at the joints, avoiding muscle modeling, thus lacking physiological accuracy related to muscle contraction dynamics. In a previous work [7], we adapted a physiological muscle model that predicts electrically-evoked muscular force to be used with gradient-based optimization, in particular with numerical optimal control/estimation problems. Experimental data obtained from individuals with SCI were used to identify the model's parameters and the feasibility of employing this adapted model in numerical optimal control problems was demonstrated.

In the following, this specific muscle formulation is used in a personalized FES-cycling model containing three different muscle groups in each leg. Their parameters are identified using experimental data from one individual with SCI. We then formulate a trajectory optimization problem to achieve a target pedaling cadence and crank power output, and simulate the FES-cycling activity to obtain optimal stimulation patterns.

Material and Methods

Subject: One male participant with spinal cord injury (SCI) for over 14 years (J.S.M., 66 kg, 42 years, male) and a body mass index of 26.6 (±2.9) was included in the study. Written consent was obtained from the participant for the study procedures. The research was approved by a local Ethical Committee (CAAE: 30989620.6.0000.5149, Ethical Approval number 4.190.128) in agreement with the Declaration of Helsinki. The participant exhibited unrestricted joint mobility and did not present any lower limb fractures within the 12 months preceding the start of the protocol. The individual had previously undergone neuromuscular electrical stimulation (NMES) muscle strengthening and FES-cycling sessions for about four years prior to the commencement of the study.

Experimental Setup: A commercially recumbent tadpole trike (ICE Adventure, ICE, Falmouth, Cornwall, UK) was fixed on an instrumented cycling stationary trainer (KICKR Smart Trainer, Wahoo, Atlanta, Georgia, US). The original crankset was replaced by a power-meter crank (2INPOWER, Rotor Bike Components, Madrid, Spain) to quantify torque and pedaling power, with the resultant data transmitted via ANT+ communication protocol to a personal computer at a sample rate of 50 Hz, as detailed in [8]. Orthotic calf support (HASE Bikes, Waltrop, Germany) was fixed to the pedals to keep the ankle joint at 90° and restrict the leg movement to the sagittal plane. A personal electrical stimulator system with eight channels (detailed in [1]) was employed in the experiments. The stimulation interval and the stimulation parameters were adjusted via a mobile application.

Measurements for parameter identification: electrical stimulation pulse were applied to the following muscles: *rectus femoris* and *vastus lateralis* muscles; *vastus medialis*; and *hamstrings* muscle group (see [1] for electrode positioning). A warming-up phase preceded the isometric measurements phase, which are detailed below:

a) Warm-up phase: the volunteer was seated on the tricycle and hydrogel electrodes were attached to the legs over the motor points previously identified. The experimenter propels the participant legs passively (no FES) for 3 min at a maximum speed of 30 rpm.

b) Static measurement: the maximum evoked torque was first measured with the pedal at 90º (right crank arm in the vertical top position). Balanced biphasic pulses were delivered over the quadriceps muscle group with pulse amplitude of 50 mA, frequency of 35 Hz, and pulse duration varying from 500 to 1200 µs in 50 µs steps, for a stimulation duration of 500 ms. We then measured the range of motion (ROM) of the volunteer's knee while seated on the tricycle using a goniometer, which varied from 70° to 120°, and performed six isometric evoked contractions within this range, with knee angle varying in 10° steps, for both knee extension (quadriceps) and flexion (hamstrings). At this point, we set the pulse duration to ~40% of the value that elicited the strongest evoked contraction in the previous step (resulting in 800 µs). The experimenter moved the crank to the designated position, locked it in place by holding the pedal opposite the leg being measured, and provided a minimum of 5-second settling period before the stimulation began. A subsequently resting time of 2 s was then given. For each knee angle, two stimulations were performed before the crank was moved to the next position. This novel procedure allowed for the evaluation of evoked muscle contractions at different knee angles as an alternative to conventional dynamometers. Finally, 20 s of passive pedalling at 20 rpm was performed by the researcher.

Musculoskeletal Model: We adapted the musculoskeletal model of the lower limbs from the OpenSim core models Leg6Dof9Musc to be used with Bioptim [5]. The rotational movement was kept limited to the sagittal plane. The model has seven degrees of freedom (DOF) (gear, pedal right, pedal left, knee right, knee left, hip right, hip left). The ankles were kept at 90° and the feet were fixed to the pedals. In addition, muscles in the model are *biceps femoris long head* for knee flexion, *vastus medialis* for knee extension and *rectus femoris* for both knee extension and hip flexion (Fig. 1).

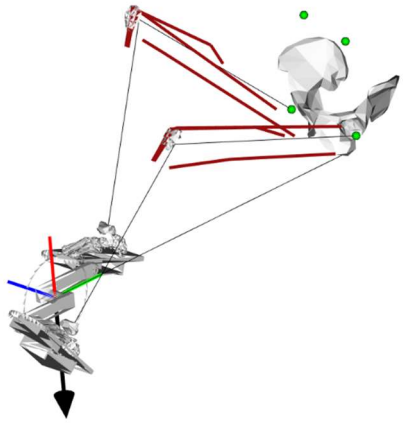

Figure 1: FES-cycling musculoskeletal model

The dynamics of our adapted muscle model captures the temporal influence of consecutive electrical pulses on the formation of the calcium-troponin complex and the regulation of muscle contraction leading to force development. The activation dynamics is given by:

$$\frac{dc_N}{dt} = \frac{1}{\tau_c}\sum_{i}^{n(t)} \alpha_i R_i \exp\left(-\frac{t-t_i}{\tau_c}\right) - \frac{c_N(t)}{\tau_c}, \quad (1)$$

where T represents a constant pulse period and $n(t) = \lfloor t/T \rfloor$ is the largest integer n, such that $n \leq t/T$, and $i = \max(1,\ n(t)-p)$ is within a limited window train of pulses containing the history of the last $p \in \mathbb{N}^*$ pulses. The activate or deactivate states of each pulse is given by $\alpha_i = 0{,}1$ during the i^{th} pulse $t_i = iT$. The parameter R_i accounts for the nonlinear summation of the cN transient upon the time response τ_c (ms) –a constant controlling the rise and decay of c_N –, which is given by:

$$R_i = \begin{cases} 1 & if\ i = 1, \\ 1 + (R_0 - 1)\exp\left(-\frac{t-t_i}{\tau_c}\right) & if\ i > 1, \end{cases} \quad (2)$$

with R_0 (unitless) representing the magnitude of enhancement in c_N [9]. The activation dynamics is then related to the muscle force dynamics defined by:

$$\frac{dF}{dt} = A(p_d,\theta)\frac{c_N(t)}{K_m + c_N(t)} - \frac{F(t)}{\tau_1 + \tau_2\frac{c_N(t)}{K_m + c_N(t)}}, \quad (3)$$

where K_m is the sensitivity parameter of strongly bound cross bridges to c_N, τ_1 (ms) is the time constant of force decline in the absence of strongly bound cross-bridges and τ_2 (ms) is the time constant of force decline due to friction between actin and myosin [9]. The resulting force F (N) is parameterized by five parameters (τ_1, τ_2, τ_c, K_m, and R_0) and one function (A) that accounts for the influence of the stimulation pulse duration and the knee angle. It is defined by:

$$A(p_d(t),\theta) = a(\theta)(1 - \exp(-(p_d(t) - p_{d_0})/p_{d_t})), \quad (4)$$

where $a(\theta)$ represents a force scaling factor that is dependent on the knee joint angle θ. The parameter $p_d(t)$ (µs) is the pulse duration, p_{d_0}(µs) is a constant threshold offset characterizing the muscle sensibility to the pulse intensity, and p_{d_t}(µs) describes how the scaling parameter varies with the increasing of pulse duration [9].

Optimal Control Problem Formulation: a multiple shooting trajectory optimization problem was formulated to both identify the model parameters (estimation) and to control the model in simulation. The resulting nonlinear programs are then solved using the IPOPT, with CasADi used for algorithmic differentiation. For a system whose dynamics is governed by an ordinary differential equation of the form $\dot{x} = f(\mathbf{x}(t), \mathbf{u}(t))$, with $\mathbf{x}$ and $\mathbf{u}$ the state and control vectors, a generic trajectory optimization problem can be written as:

$$\min_{\mathbf{x}(t),\mathbf{u}(t),\mathbf{p}} \quad = \quad J(\mathbf{x}(t),\mathbf{u}(t),\mathbf{p}) \tag{5a}$$

$$\text{s.t.} \quad \forall t, \quad \dot{\mathbf{x}} = \mathbf{f}(\mathbf{x}(t),\mathbf{u}(t),\mathbf{p}) \tag{5b}$$

$$\forall t, \quad \mathbf{g}(\mathbf{x}(t),\mathbf{u}(t)) \leq 0 \tag{5c}$$

$$\mathbf{x}(0) = \mathbf{x_0} \tag{5d}$$

with J the cost function, $\mathbf{p}$ a vector of model parameters and $\mathbf{x_0}$ the initial state. The inequality constraints are gathered in function $\mathbf{g}$. The objective is to find the control input $\mathbf{u}(t)$, the states $\mathbf{x}(t)$, and the parameters $\mathbf{p}$ that minimize the cost function while satisfying the dynamic and boundary constraints. The control input $\mathbf{u}$(t) contains the pulse duration and the resistive torque. The latter needed only for the parameter identification (see **Model Personalization** steps 1 and 2) process; the states $\mathbf{x}$(t) includes $c_N(t)$ and force $F(t)$ for each muscle, the joint positions $\mathbf{q}(t)$ and velocities $\dot{\mathbf{q}}(t)$, and pulse state $\alpha_i(t)$.

Model Personalization: the model is described with one function $A(p_d, \theta)$ and five parameters: τ_1, τ_2, τ_c, K_m, and R_0. In Eq. 4, we defined A as a function of θ and as function of pulse duration $p_d(t)$. Parameters p_{d_0} and p_{d_t} are the average values presented in [9]. The parameters R_0 and τ_c are fixed at 5 and 11 ms, respectively, as suggested in [9] for the quadriceps femoris muscles of individuals with SCI. Thus, only three parameters and one function remain to be identified for each subject and leg: τ_1, τ_2, K_m and $a(\theta)$. Finally, the following steps were used to identify the model's parameters and obtain predicted torques.

Step 1: Identification of τ1, τ2, and Km. For each muscle, we gathered six torque trajectories containing the first evoked contraction (see **Static measurements**) in an experimental torque vector $\boldsymbol{\tau^{ex}}$. An optimal estimation problem was formulated to track these experimental torque data by optimizing τ_1, τ_2, K_m and A (Eq. 6), while satisfying the system's dynamics. Hence, a problem of the form of (Eq. 5) was solved with the following equation as a transcription of (Eq. 5a):

$$\min_{\mathbf{x}(t),\mathbf{u}(t),\mathbf{p}=[\tau_1,\tau_2,K_m,A]} = \frac{1}{N}\sum_{k=0}^{N-1}(\boldsymbol{\tau}_k^{\boldsymbol{pr}}(A,\tau_1,\tau_2,K_m) - \boldsymbol{\tau}_k^{\boldsymbol{ex}})^2, \tag{6}$$

where $\boldsymbol{\tau^{pr}}$ is the torque trajectory predicted by the model and N is the total number of shooting nodes (35 per second). To enforce isometric contractions during the optimization, the crank was locked by applying an opposite resistive torque through a null velocity constraint. We defined a constant $p_d(t) = 400 + p_{d_0}$ (µs) when stimulation was on, or p_{d_0} otherwise. The control bounds were set according to the stimulation state (i.e., *on* or *off*) of the experimental data. As the parameters τ_1, τ_2, K_m are not dependent on θ, the resulting identified values for these parameters were kept fixed in the next steps.

Step 2: Determination of the a(θ) polynomial. In this step, we defined a to be an optimization parameter and used six contractions from the dataset at θ = [70°, 80°, 90°, 100°, 110°, 120°] to identify $a(\theta)$. Similarly to the previous step, for each θ value, 6 separate problems were formulated to track the experimental torque data by optimizing a, while satisfying the system's dynamics. As a result, a problem of the form of Eq. 5 was solved with the following equation (Eq. 6) as a transcription of Eq. 5a:

$$\min_{\mathbf{x}(t),\mathbf{u}(t),\mathbf{p}=\hat{\boldsymbol{a}}_\theta} J_\theta = \frac{1}{N}\sum_{k=0}^{N-1}(\boldsymbol{\tau}_k^{\boldsymbol{pr}}(\hat{\boldsymbol{a}}_\theta) - \boldsymbol{\tau}_k^{\boldsymbol{ex}})^2, \tag{6}$$

with $\hat{\boldsymbol{a}}_\theta$ the optimized value of a at angle θ. Finally, the values of $\hat{\boldsymbol{a}}_\theta$ were fitted with a 5th-degree polynomial, yielding an analytical expression for $a(\theta)$.

FES-cycling optimal Stimulation pattern: to synthesize the optimal stimulation pattern, pulse duration was optimized as a piecewise constant control variable within 86-1200 µs at a constant frequency of 35 Hz. In Eq. 4, the

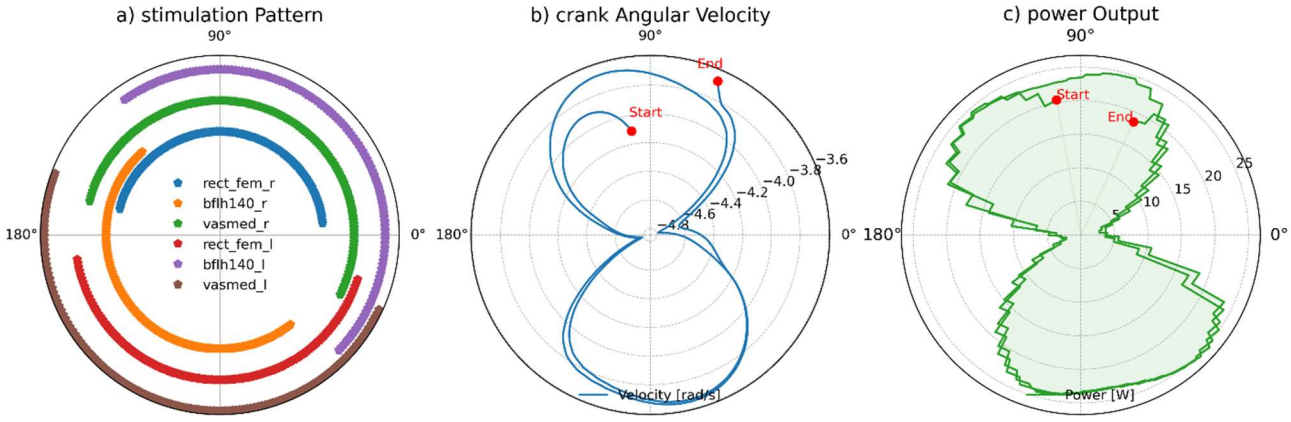

Figure 2: Solutions for the FES-cycling simulation: a) resulting stimulation pattern and the corresponding range of activation for each muscle; b) the crank angular velocity obtained while tracking ~4.4 rad/s. Due to the counter clockwise pedalling motion, the velocity appears to be negative; c) the power output produced at the crank axis of rotation while tracking 20 W.

values of p_{d_0} and p_{d_t} were considered as the average values presented by [9]. The parameters for each muscle obtained in the previous steps were used. An optimal control problem was formulated to track a desired pedaling cadence (42 rpm or ~4.4 rad/s) by optimizing $p_d(t)$, while satisfying the system's dynamics (Eq. 5). A constant Coulomb friction torque ($-\mu_0 \cdot sign(\dot{q}_0)$, with $\mu_0 = 0.2$ Nm) and a viscous friction torque ($-B \cdot \dot{q}_0$, with $B = 1.0378\,\mathrm{Nm \cdot s/rad}$) were applied at the crank axis to simulate the resistive environment opposing the bike's forward motion, where $\dot{q}_0$ is the crank velocity. The value of μ_0 was set manually, while B was computed based on the desired cadence and power. Hence, a problem of the form of Eq. 5 was solved with the following equation (Eq. 7) as a transcription of Eq. 5a:

$$\min_{\mathbf{x}(t),\mathbf{u}(t)} \sum_{k=0}^{N-1} [\omega_1 (\dot{q}_{0_k}^{\ sim} - \dot{q}_{0_k}^{\ target})^2 + \omega_2 \, \boldsymbol{p}_{\boldsymbol{d}_k}^2 + \omega_3 (\boldsymbol{c}(\mathbf{u}(\boldsymbol{t}))_k^2], \quad (7)$$

where $\omega_1 = 5e2$, $\omega_2 = 1e3$, $\omega_3 = 1e3$, and $\boldsymbol{c}$ is a function that penalizes co-activation of homologous muscles across both legs.

Results

Figure 2.a presents the stimulation pattern, highlighting the intervals of the pedaling cycle in which each muscle is activated over a 3 s simulation, featuring coordinated agonist and antagonist activations. The resulting pedaling cadence was 4.09 ± 0.36 rad/s (Fig. 2.b), and the corresponding power output was 17.53 ± 7.87 (Fig. 2.c).

Discussion

The proposed methodology demonstrates its ability in generating coordinated muscle activations to achieve specific target power output and pedaling cadence. As shown in Figure 2a, the stimulation pattern exhibits coherent phase-specific recruitment of agonist and antagonist muscles, closely aligned with the manually-tuned stimulation pattern obtained in [1]. Although the achieved cadence and power fall slightly below the target values defined, the results are encouraging given that it advances in the definition of the stimulation pattern relying entirely on muscle models that predict muscular force in response to electrical stimulation [8]. Our approach contrasts with prior FES-cycling simulation works [6], which are lacking muscle modeling.

Although significant nonlinearities and physiological constraints are introduced into the system, making the control problem more challenging, it offers the possibility of addressing realistic and personalized protocols needed for the generation of optimized muscle forces and joint kinematics. The ability of our model to produce near- target outputs under these constraints highlights the potential of personalized predictive simulations to support the design of FES protocols for individuals with SCI.

Despite the lack of experimental validation with the final stimulation pattern, this methodology can be further explored to improve FES-assisted activities performances, paving the way for more efficient rehabilitation strategies for people with SCI and other neurological conditions.

Conclusions

This study presents a first step towards improving the realism of FES-driven simulations and showcases the possibility of using model-based control of FES-cycling, with possible application in other FES-assisted tasks.

Acknowledgement

We thank the volunteer for his dedication and availability. This work was supported by *Défi Clé Robotique centrée sur l'Humain* funded by Région Occitanie, France.

References

1. Coelho-Magalhães T., Fachin-Martins E., Silva A., Azevedo-Coste C., Resende-Martins H.. Development of a High-Power Capacity Open Source Electrical Stimulation System to Enhance Research into FES-Assisted Devices: Validation of FES Cycling. *Sensors*. 2022; no. 2:531.
2. van der Scheer, J.W., Goosey-Tolfrey, V.L., Valentino, S. E., Davis, G. M., & Ho, C. H.. Functional electrical stimulation cycling exercise after spinal cord injury: a systematic review of health and fitness-related outcomes. *J NeuroEngineering Rehabil*. 2021; 18(1),99
3. Maffiuletti, N.A. Physiological and methodological considerations for the use of neuromuscular electrical stimulation. *Eur J Appl Physiol* 110, 223–234 (2010).
4. Szecsi J, Straube A, Fornusek C. A biomechanical cause of low power production during FES cycling of subjects with SCI. *J Neuroeng Rehabil*. 2014 Aug 16;11:123.
5. B. Michaud, F. Bailly, E. Charbonneau, A. Ceglia, L. Sanchez, and M. Begon, "Bioptim, a Python framework for musculoskeletal optimal control in biomechanics," *IEEE Transactions on Systems, Man, and Cybernetics: Systems*, vol. 53, no.1, pp. 321–332, Jun. 2022.
6. de Sousa, A. C. C., Font-Llagunes, J. M.. Predictive Framework for Electrical Stimulation Cycling in Spinal Cord Injury. *IFAC-PapersOnLine*. 2024. Vol. 58, Issue 24, Pages 332-337.
7. T. Coelho-Magalhães, C. Azevedo-Coste and F. Bailly, "Numerical-Optimal-Control-Compliant Muscle Model for Electrically Evoked Contractions," in *IEEE Transactions on Medical Robotics and Bionics*, doi: 10.1109/TMRB.2025.3590453.
8. Schmoll Martin, Le Guillou Ronan, Fattal Charles, Coste Christine Azevedo. OIDA: An optimal interval detection algorithm for automatized determination of stimulation patterns for FES-Cycling in individuals with SCI. *J NeuroEngineering Rehabil*. 2022;19:39.
9. J. Ding, Li-Wei Chou, T. M. Kesar, S. C. K. Lee, T. E. Johnston, and A. S. Wexler, and S. A. Binder-Macleod, "Mathematical model that predicts the force–intensity and force–frequency relationships after spinal cord injuries," *Muscle Nerve*, vol. 36, no. 2, pp. 214–222, Aug. 2007.

Author's Address

T. Coelho-Magalhães; tiago.coelho-magalhaes@inria.fr

Assessing accuracy of power-pedals for low power output in FES-Cycling – preliminary results

Schmoll M[1], Pataraia A[2,3], Nguyen Q[1], Rosenauer B[1], Kornfellner E[1], Mayr W[1,2], Crevenna R[2,3]
[1]Center for Medical Physics and Biomedical Engineering, Medical University of Vienna, Austria
[2]Department of Physical Medicine, Rehabilitation and Occupational Medicine, Medical University of Vienna, Austria
[3]Comprehensive Center for Musculoskeletal Disorders, Medical University of Vienna, Austria

Abstract: *Functional Electrical Stimulation (FES) Cycling enables individuals with complete spinal cord injury (SCI) to perform cycling by activating paralyzed leg muscles via surface electrical stimulation. At the Cybathlon 2024, an FES-Cycling race was conducted on a stationary setup using power-based scoring, requiring reliable power measurement at low power output levels. This work aimed to assess the accuracy of a dual-sided pedal power meter (used during the competition) compared to a crank-based reference system, with particular focus on mounting torque and orthosis positioning. Power and cadence were recorded simultaneously from both systems under varying conditions: four different pedal mounting torques (15 – 40 Nm) and three orthosis configurations (original, narrow and wide foot position). Data were modelled using polynomial fitting to predict power output across cadences from 0 – 100 RPM, and compared using average power and root-mean-square error (RMSE). Results showed that low pedal mounting torque, particularly at 15 Nm, led to power overestimations of over 20 % and substantially increased RMSE. Similarly, altered orthosis positions significantly affected the accuracy of the pedal power meter, with deviations up to 34.8 %. In contrast, the crank-based power meter showed more consistent results across all conditions. These findings highlight the importance of proper mechanical setup and adherence to manufacturer specifications when using pedal-based power meters in FES-Cycling.*

Keywords: *Power measurement, Cybathlon, FES, FES-Cycling,*

Introduction

Functional Electrical Stimulation (FES) Cycling is a competitive rehabilitative discipline that enables individuals with complete spinal cord injury (SCI) to cycle using surface electrical stimulation to activate their paralyzed leg muscles [1].

A prominent platform for FES-Cycling competition is the Cybathlon [2], an international championship where pilots with physical disabilities compete using state-of-the-art assistive technologies. Within the Cybathlon, the FES-Cycling Race is a timed event in which pilots aim to complete a fixed-distance track using only their stimulated leg muscles for propulsion. Over the past editions of the Cybathlon, required distances have continuously increased, aiming to trigger innovation and drive advancements in stimulation strategies, training protocols, and mechanical optimization of recumbent trikes.

Besides the main objective of FES-Cycling being to increase mobility in the SCI population, it was decided to conduct the latest edition, the Cybathlon 2024, on a stationary home trainer. In contrast to the edition in 2020, the competition took place in a virtual race environment called IndieVelo (TrainingPeaks, Louisville, USA) which was based on the measurement of power generated by the athletes. Due to the low power output in FES-Cycling, most teams were not able to use the stationary home trainer as power source, which is why the participating teams were allowed to use pedal power meters supplied by the organizing committee.

However, although the pedals were providing power readings also at lower power outputs, challenges remained – especially in the mechanical setup and measurement accuracy during FES-Cycling. One critical issue concerned the use of calf supports and ankle orthoses, which are required to stabilize the paralyzed lower limbs. These supports, while essential for safety and positioning, may alter force transmission and interfere with the accuracy and reliability of the power measurements.

To better understand these effects, we assessed different pedal configurations such as: mounting torques, and orthosis positions on a recumbent trike typically used in FES-Cycling. A calibrated crank-based power meter was used as a reference to evaluate the accuracy of a dual-sided pedal-based power meter. Both systems were mounted on a stationary setup to allow controlled comparisons.

Material and Methods

Power measurements were performed using a Garmin sport watch (Fenix 7, Garmin Ltd. Olathe, USA) with an additional data field [3] to record power from two separate devices. The raw data with a sample frequency of 1 S/s was exported as .fit-file via Garmin Connect.

A crank arm power meter (2INPOWER, ROTOR Bike Components, Madrid, Spain) served as a reference, to evaluate the accuracy of a dual-sided pedal power meter (PowrLink Zero Dual, Wahoo Fitness, Atlanta, USA). Both power meters were calibrated as recommended by the manufacturer, having set the correct crank-length of 170 mm.

Both power meters were installed on a recumbent trike (model VTX, ICE Trikes, Cornwall, UK), which was mounted on a standard home trainer (In'Ride 100, Van Rysel, Lille, France).

According to the manufacturer of the power pedals, a mounting torque of 30 Nm is required to achieve correct readings. As a torque wrench is needed to correctly mount the pedals, cyclists often ignore this requirement. Thus, we investigated the influence of the pedal mounting torque at 15, 20, 30, 40 Nm.
Further, it is important to note that power pedals are generally designed to be used with dedicated cycling shoes, defining the position of force application and thus the corresponding active levers used by the power meter to calculate the power. In FES-Cycling, the paralysed legs require stabilization via an ankle orthosis. To assess the influence of an ankle orthosis and its position, we performed measurements using the original pedals (POS ORIG) in contrast to measurements using an ankle orthosis (ergopedals with calf support, HP-Velotechnik GmbH, Kriftel, Germany). To attach the orthosis to the calibrated power pedals, a custom-built adapter plate (Fig. 1) was used, allowing to adjust the orthosis to a narrow (POS 0) or wide (POS 1) leg position. The midline of the foot was shifted by +6 cm and +12 cm in contrast to the original position, respectively for POS 0 and POS 1.

Figure 1: Mounting positions. Illustration of the different mounting positions. An adapter plate was used for mounting the ankle orthosis to the power pedals at different positions.

Measurement protocol
A healthy participant (38 years, 85 kg, 195 cm) was cycling without FES at different target cadences of 25, 30, 40, 50, 60, 70, 80, 90 and 100 RPM. Each cadence level was maintained for approximately 30 s, paced via a metronome app. As in FES-Cycling, a rather low power output is to be expected, a transmission from a chain ring at the front of 26T to a rear sprocket of 51T was chosen, while setting the home trainer to its lowest resistance.

Data analysis
The .fit-files were converted into .csv-files using the official software package FitSDK (release 21.141.00, Garmin Ltd. Olathe, USA). Data was analysed using Matlab (R2017b, MathWorks, Natick, USA). For each measurement condition a direct graphical comparison of the power and cadence was made between both power meters.

Further, all power values were sorted by the corresponding cadence to calculate a model (eq. 1) to predict power (p) values by the generated cadence (c). The model represents a 3rd degree polynomial curve with k_0 set to 0 W and k_1, k_2, k_3 fitted to minimise the overall error. To compare both power meters, the average power predicted by the model from 0 to 100 RPM was calculated.

$$p(c) = k_1 * c + k_2 * c^2 + k_3 * c^3 \qquad \text{(eq. 1)}$$

Based on the power model the variation of the data can be described by the root-mean-square-error (RMSE) of all measured values. The RMSE is calculated for the recorded data of each power meter for its own model.

$$RSME = \frac{1}{n}\sum_{n}^{1}\sqrt{(p_n - p\_fit_n)^2} \qquad \text{(eq. 2)}$$

Results

This work is assessing the accuracy of a dual sided pedal power meter in comparison to a crank arm power meter (reference), for different mounting torques and mounting positions of an ankle orthosis required for FES-Cycling.

Different mounting torques of 15, 20, 30 and 40 Nm were investigated, along with a narrow (POS 0) and wide (POS 1) mounting position of the orthosis.

For each recorded measurement, data points were sorted by cadence, to create a model to predict the power output for a particular cadence. A representative example of the recorded raw data, for the case of 15 Nm mounting torque, can be found in Fig. 2 with its corresponding power models presented in Fig. 3.

An overview of the all power models for the different torques is illustrated in Fig. 4, along with the different mounting positions illustrated in Fig. 5. For each power model the average power has been calculated for a range of 0 to 100 RPM, along with the RMSE obtained from the raw data (Tabl. 1).

Table 1: Comparison of the power readings between two independent power meters (reference: crank arm against pedals)

Condition	*Average Power* Crank PM	*Average Power* Pedal PM	Δ relative	*RMSE* Crank PM	*RMSE* Pedal PM
	W	W	%	W	W
Torque 15 Nm	12.4	14.9	20.2%	0.39	2.57
Torque 20 Nm	14.0	14.3	2.1%	0.48	1.32
Torque 30 Nm	12.6	13.1	4.0%	0.39	0.89
Torque 40 Nm	10.3	10.3	0.0%	0.41	1.50
POS ORIG	12.0	12.4	3.3%	0.47	0.83
POS 0	12.5	14.5	16.0%	0.45	2.20
POS 1	13.8	18.6	34.8%	0.43	4.60

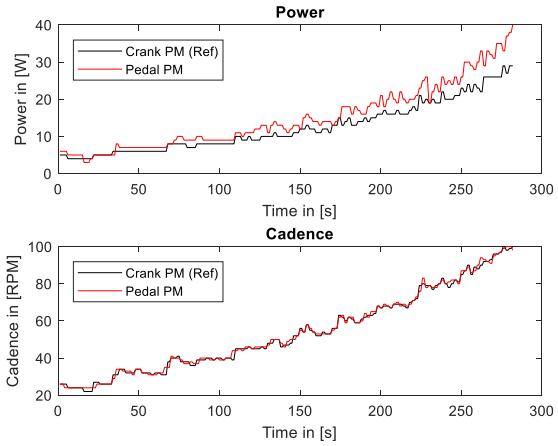

Figure 2: Power measurement. Illustration of a representative example for a power measurement at different cadences (case: Mounting torque 15 Nm). The crank arm power meter (black trace, reference) is displayed in comparison to the pedal power meter (red trace).

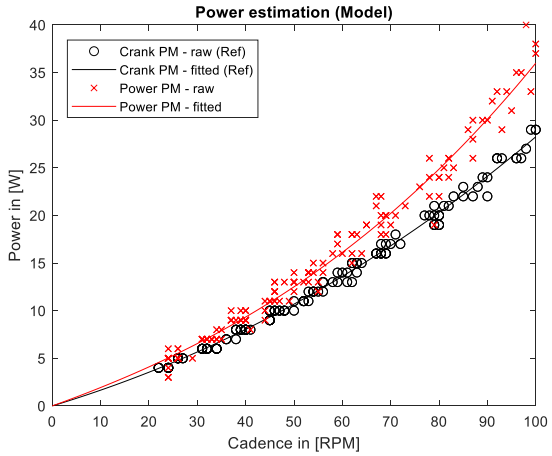

Figure 3: Power estimation model. Illustration of a representative example for the fitting of a power model based on the power measurements (case: Mounting torque 15 Nm). The crank arm power meter (black trace, reference) is displayed in comparison to the pedal power meter (red trace).

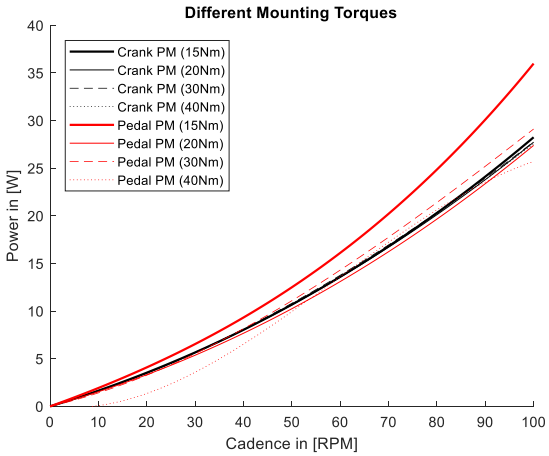

Figure 4: Influence of mounting torque. Comparison of the power models for different mounting torques. Models of the crank arm power meter (black traces, reference) are displayed in contrast to the models of the pedal power meter (red traces).

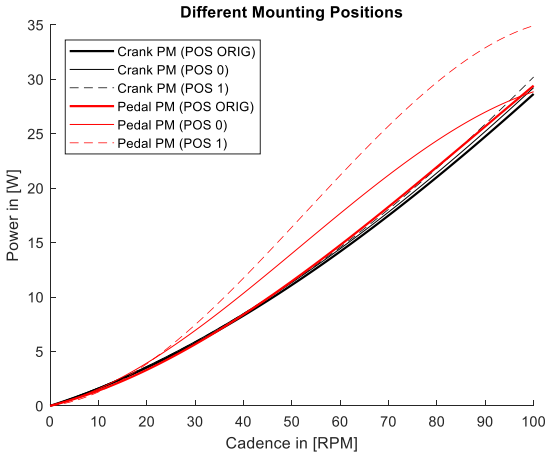

Figure 5: Influence of mounting position. Comparison of the power models for different mounting positions. Models of the crank arm power meter (black traces, reference) are displayed in contrast to the models of the pedal power meter (red traces).

Discussion

The aim of this work was to evaluate the accuracy of a dual-sided pedal power meter, which was used in the FES-Cycling race at the Cybathlon 2024. It was evaluated against a crank-arm-based reference system, particularly for low power outputs, which are typical in FES-Cycling. Special attention was given to variations in pedal mounting torque and the use of ankle orthoses for leg stabilization.

Our results show that mounting torque had a substantial influence on power readings, especially at lower mounting torques. At 15 Nm, the pedal power meter overestimated power output by 20.2% compared to the crank-arm-based reference, with a markedly higher RMSE (2.57 W vs. 0.39 W for the crank). As the mounting torque increased, the accuracy of the pedal system improved, showing minimal deviation (≤ 4 %) at torques of 20 – 40 Nm. The lowest RMSE was observed at 30 Nm, aligning with the manufacturer's specifications.

In addition to mounting torque, the mounting position of the orthosis had a pronounced influence on measurement accuracy. When using the original pedal configuration (POS ORIG), the power meter showed only a minor deviation of 3.3 %, with an acceptable RMSE of 0.83 W. However, when the ankle orthosis was mounted in a narrow (POS 0) or wide (POS 1) position, the pedal power meter overestimated the output by 16.0 % and 34.8 %, respectively. RMSE also increased significantly in these configurations, especially at POS 1 (4.60 W), indicating that changes in the point of force application, resulting from altered foot positioning and mechanical constraints, can compromise the internal force calculation of the power meter.

Pedal-based power meters are typically designed for use with rigid cycling shoes that generate predictable force vectors. In contrast, FES-Cycling often requires ankle orthoses to stabilize the paralyzed legs during stimulation. The adapter plate used in this work enabled orthosis mounting but likely shifted the location and angle of applied force, negatively impacting sensor accuracy. Although this influence was more pronounced for the pedal power meter, the crank-based reference system also showed a slight overestimation of power, as illustrated in Fig. 4. Based on these findings, it is advisable to mount the ankle orthosis as close to the crank arm as possible, minimizing the lateral deviation of the foot's midline from its standard position.

Limitations of this study include the use of a single participant, which restricts generalizability. Moreover, each condition was measured only once. Future work should include multiple participants and repeated trials per condition to better capture variability. However, it is important to note that the magnitude of discrepancies between the two power measurement devices remains highly relevant in the context of a competition such as the Cybathlon, where a reliable power measurement is essential for a fair ranking.

To account for the overestimation observed, the Cybathlon committee implemented a compensation procedure by adjusting the crank arm length setting on the pedal power meter. All participating teams were required to perform calibration trials, with their trikes mounted on a Wahoo Kickr 5 home trainer, at a target power output of 40 W (i.e. minimum power output reliably measurable with the home trainer). Power data from both the pedal power meter and the home trainer were recorded via the IndieVelo software and analysed by the Cybathlon committee, which then communicated a crank length setting to be used during the competition. While this approach may help to compensate for overestimation at 40 W, it remains unclear whether the same correction applies to lower power outputs, which are more typical in FES-Cycling. Additionally, the drivetrain of the trike introduces mechanical resistance between the two systems, which may have further influenced the calibration results. More detailed validation is needed to assess the effectiveness and generalizability of this compensation method.

Conclusions

This work highlights mechanical factors influencing the accuracy of pedal-based power meters in FES-Cycling. While dual-sided pedal power meters can deliver acceptable results under ideal conditions (i.e. proper mounting torque and standard foot position), their accuracy is compromised by the use of ankle orthosis typically required in FES-Cycling. Crank-based power meters demonstrated more reliable and consistent results across varying setups, making them the preferred option for precise power monitoring. However, practical limitations, such as trike compatibility and race regulations, may necessitate the use of pedal-based systems. In such cases, careful calibration and standardization are essential to ensure valid and fair performance evaluation.

References

[1] D. J. Newham and N. de N. Donaldson, 'FES cycling', *Acta Neurochir Suppl*, vol. 97, no. Pt 1, pp. 395–402, 2007, doi: 10.1007/978-3-211-33079-1_52.

[2] 'Cybathlon Description and Rules 2024'. [Online]. Available: https://cybathlon.ethz.ch/documents/races-and-rules/CYBATHLON%202024/CYBATHLON_RacesAndRules_2024.pdf

[3] takura87, 'ANT+ Power Meter data field'. [Online]. Available: https://apps.garmin.com/apps/70f1aea3-f1d3-47f6-b7aa-23f029a75e3b

Author's Address

Martin Schmoll
Center for Medical Physics and Biomedical Engineering, Medical University of Vienna, Austria
martin.schmoll@meduniwien.ac.at
https://mpbmt.meduniwien.ac.at/en/research/neuroprosthetics-and-rehabilitation-engineering/

Session 7:
Movement Restoration

Towards Electrophysiological and Histological Mapping of Upper Limb Nerves in Pigs Using Epineural Stimulation

Baum J[1], Chamot-Nonin M[2], Oppelt V[3], Guiraud D[2], Azevedo Coste C[1], Guiho T[1]

[1]INRIA, University of Montpellier, France
[2]NEURINNOV company, Montpellier, France
[3]CorTec company, Freiburg, Germany

Abstract: *Understanding the relationship between nerve anatomy and the functional outcomes of electrical stimulation is critical for optimizing neural interface design. In this study, we conducted acute experiments on four pigs in which epineural cuff electrodes with multiple contacts were placed around upper limb nerves. A subset of electrical stimulation configurations - previously identified via computational study - was applied, and the resulting evoked electromyographic (EMG) responses were recorded from target muscles. Muscle recruitment curves were extracted and analysed offline to quantify activation patterns. Following the electrophysiological experiments, the stimulated nerves were harvested and processed for histological analysis to visualize fascicular organization and distribution. This work presents preliminary results from the combined analysis of muscle activation profiles and fascicle anatomy in one animal. Our findings aim to inform the design of stimulation strategies by linking electrode configuration to selective muscle recruitment, ultimately contributing to more effective neuromodulation and neuroprosthetic applications.*

Keywords: *epineural stimulation, swine, needle EMG, histology, selectivity*

Introduction

Implanted peripheral nerve stimulation has shown promise in restoring impaired motor functions of the upper limb—particularly hand and wrist movements—in individuals with complete spinal cord injury [1]. Compared to epimysial or intraneural electrodes, the use of multicontact epineural electrodes offers a less invasive alternative while maintaining access to multiple motor pathways [2]. However, achieving selective activation of specific muscle subgroups to produce functional movements remains a significant challenge. Currently, stimulation parameters and electrode configuration are typically adjusted empirically, based on observed motor responses, which limits reproducibility and precision. This approach is further complicated by inter- and intraindividual variability in nerve morphology, particularly regarding the complex fascicular organization and plexiform architecture of the human brachial plexus [3]. Understanding how these anatomical factors influence stimulation outcomes is essential for optimizing electrode design and stimulation strategies.

To partially address this scientific challenge, equivalent electrical models of axons were developed to enable the in-silico identification of the most selective and efficient current configurations. Cuff epineural electrodes were considered in the model due to their moderately invasive characteristics and widespread commercial availability - in contrast to other architectures such as TIME intraneural electrodes which might be less suitable for clinical trials due to mechanical constraints associated with their transversal positioning through the nerves. Previously, subset of stimulation configurations identified as selective by the model [4] was evaluated in 28-days clinical trials investigating peripheral nerve stimulation for hand and wrist rehabilitation [5]. These configurations were further refined empirically using evoked electromyography (eEMG) and observation of evoked movements to elicit specific functional gestures. However, this empirical approach is time-consuming, and only a limited portion of the extensive parameter space can be explored clinically for the refinement of epineural functional electrical stimulation (FES). Optimization of stimulation parameters and electrode configurations should be more comprehensive and objective, while remaining time-realistic. The development of automated tools capable of correlating epineural current patterns with evoked electromyographic (eEMG) responses is essential to systematically explore the extensive parameter space and enhance individualized epineural stimulation. However, existing models are either based on stereotypical assumptions of nerve structure [6], or on histological observations that lack electrophysiological validation [7]. A recent study attempted to bridge this gap by combining anatomical and electrophysiological data using a specific epineural electrode [8], but the stimulation paradigm was limited to bipolar configurations. While this work highlights the value of building subject-specific models, it remains constrained in selectivity. This challenge is then compounded by inter-individual variability, which further complicates the development of accurate and generalizable models. With these considerations in mind, we designed a preclinical study that aimed at elucidating the relationship between upper limb nerve architecture and electrophysiologically evoked responses. To enhance the translational relevance of the findings, priority was given to a large animal species. In particular, the selected species – the domestic pig (*sus scrofa domesticus*) - exhibits anatomical similarities to humans, notably in the distribution of the brachial plexus, including the median, radial, and ulnar nerves, which are functionally conserved in controlling wrist and finger flexion and extension. [9].

In this article, on top of confirming the relevance of swine for electrophysiological studies of upper limbs functions, we exploited eEMGs to draw a parallel between evoked muscular activities elicited by a subset of presumably selective multipolar stimulation configuration/parameters and actual nerve anatomy - obtained via histological analyses of stimulated nerves.

Material and Method

After approval by the animal ethics committee of Languedoc-Roussillon (France, Agreement number #47593-2024021614231926v2), acute pre-clinical trials were conducted on four neurotypical juvenal swine (2-3 months age, 30-40 kg).

Surgery protocol

After premedication, anaesthesia was induced with propofol and maintained via intravenous infusion of propofol mixed with sufentanil for analgesia. Swine condition was then monitored throughout the procedure (body temperature; heart rate; blood saturation; breathing rate with air and oxygen mechanically assisted ventilation).

After ensuring proper anaesthesia, swine axillary fossa was incised to expose the brachial plexus. After anatomical prospection, the median nerve was further identified with a bipolar stimulation stick inducing contraction of predefined forelimb muscles, namely “Flexor carpi radialis” (FCR), “Flexor digitorum superficialis” (FDS), "Pronator teres" (PT). “Extensor carpi radialis” (ECR) muscle was also identified to enable monitoring of antagonist contractions. A multichannel cuff electrode (CorTec™, Germany) with two plain contacts on distal and proximal extremities and six individual contacts distributed along the central circumference (Fig. 1, see [2] for further details) was then wrapped around the nerve before connection to a 16 channels bench-top neural stimulator (SimENS, Neurinnov’s®, France) for electrophysiological measurements. Armpit incision was then filled with saline to enable moisturization of the nerve and electrical continuity between the electrode contacts and the nerve.

Stimulation and Electrophysiological recordings protocol

Epineural stimulation was delivered using asymmetric biphasic pulses - 150 µs phase width - at a frequency of 35 Hz. Model-based preidentified stimulation configurations were investigated, ie. rings and “steering current” (STR). The STR configuration is characterized by the distribution of current between one cathode and three anodes leading to anodic current repartition of 1/3 on each ring and on the inner contact opposite to the cathodic one. STR are numbered from 1 to 6 according to cathodic central contact position around nerve circumference (Fig. 1, [2]).

For each configuration (7 in total), stimulation intensity was initially set at a low value (few tens of µV) before gradually increasing - step of 9 µA - until estimation of saturation of the muscle recruitment. Each step duration was 4.5 s long leading to trains of 19 stimulation pulses and 19 M-waves per intensity.

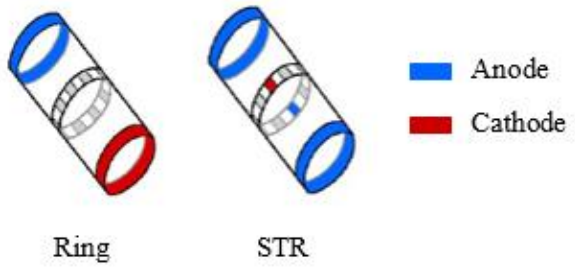

Figure 1: Schematic representation of ring and STR configurations. Adapted from [2]

Targeted muscles were localized via skin palpation further confirmed through stimulation-evoked contractions and movements. Pairs of Teflon-insulated stainless-steel wires were inserted percutaneously to record evoked EMGs (eEMGs). The signals were then amplified with a gain of 5000, band pass filtered between 1 Hz and 5 kHz (Butterworth filter of 4th order) et notch filtered at 50 Hz using a g.Bsamp GT201 amplifier (g.tec medical engineering, Austria) before sampling at 20 Khz (PowerLab 16/35, AD Instrument, New Zealand). The associated LabChart software (LabChart 7, AD Instrument, New Zealand) was used throughout the experiments to record and also stream signals in real time

Histological protocol

Following euthanasia of the swines, both the stimulated and control nerves were harvested and immediately immersed in saline solution. The positions of the electrode contacts were marked on the epineurium using tattoo ink prior to nerve sectioning. Nerve fragments were fixed in 10% paraformaldehyde (PFA) for 48 hours, followed by dehydration through a graded ethanol series prior to paraffin embedding. The paraffin-embedded nerve fragments were sectioned at a thickness of 3 µm and subsequently stained with hematoxylin-eosin-saffron (HES) to visualize intraneural structures, or processed for choline acetyltransferase (ChAT) immunohistochemistry to specifically evaluate the distribution of motor fibers within the fascicles.

eEMGs processing

Raw recorded eEMGs were further band pass filtered between 10 and 500 Hz (Butterworth filter of 4th order). For each muscle and each stimulation intensity, repeated M-waves were averaged before peak-to-peak calculation. The obtained data were then normalized using maximum eEMG peak-to-peak values (obtained over all recordings) before plotting recruitment curves.

Results

In this section only preliminary results from pig #2 (P#2) are presented.

Relevance of swine’s nerve model for an electrophysiological study of upper limbs innervation.

As shown in Fig. 2, swine's eEMGs provided recruitment curves indicating selective stimulation of forelimb muscles Recruitments show selectivity for FCR; PT; and ECR for STR2 configuration- ie. with the second central active site as cathode - at 225µA, whereas opposite contact (STR5) shows selectivity for FDS muscle at 200µA.

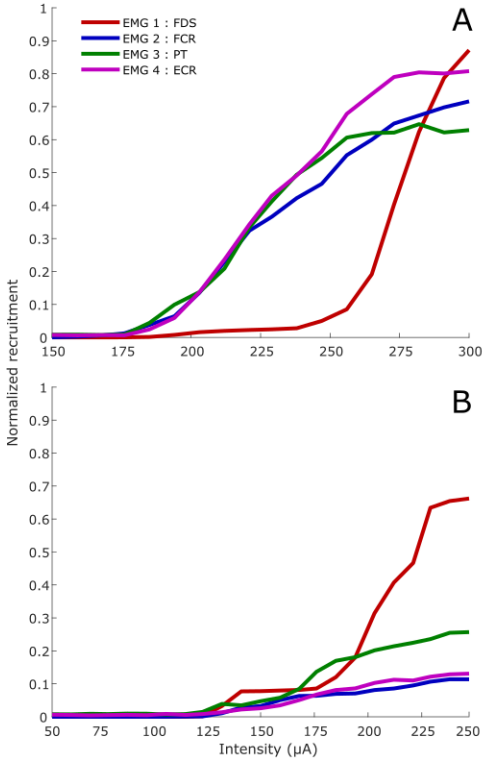

Figure 2: Normalized recruitment curves from P#2's eEMGs in STR2 (A) and STR5 (B) stimulation configurations.

Histological sections of the median nerve reveal its fascicular organization and show slight variations of fascicle number and position over short distances - ie 100 µm (distance between two successive histological cross-sections). On top of that, fascicle's size also varies between sections. In Fig. 3, section A shows 18 fascicles against 19 in section B. This last has two fascicles resulting from division of the fascicle observed in the previous section (phenomenon highlighted by frames C).

Recruitment compared with nerve's histology

Polar representation relative to each STR configuration provides information about recruitment evolution against increases in stimulation intensity. As shown in Fig. 4, FCR, PT, and ECR muscles were recruited preferably by STR 2 and 3, with maximum values obtained for STR 3. Concerning FDS, recruitment was only achievable with STR 3, 4, and 5. STR 4 seems to be the best configuration for early recruitments, whereas STR 3 generates the highest recruitment values for FDS.

Regarding histological analysis, anti-ChAT immunohistochemistry revealed motor fiber distribution among fascicles; suggesting that some fascicles are more likely to participate to motor control than others due to their higher concentration of motor fibers (Fig. 5)

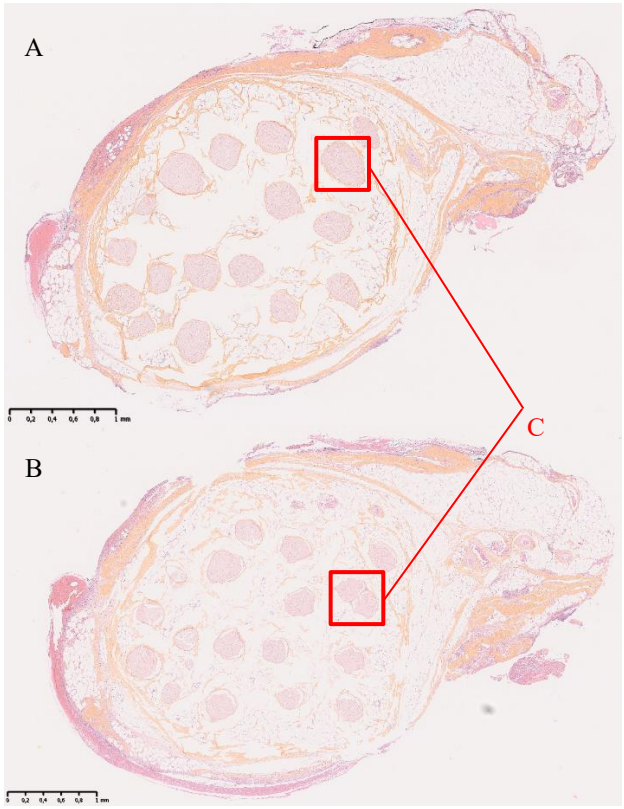

Figure 3: P#2 median nerve transversal sections stained with HES. A (the most proximal) and B sections are taken from the same nerve and are 400µm apart. C frames indicate the same fascicle (dividing in section B).

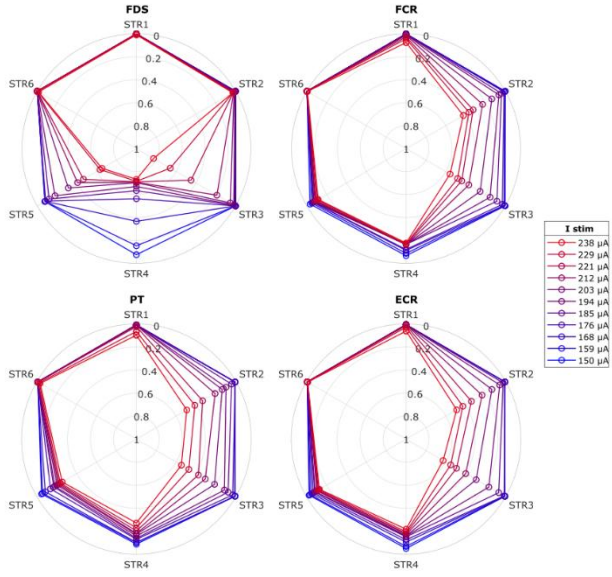

Figure 4: Polar representation of muscle recruitments from P#2 depending on STR configuration selected. Stimulation intensities are increasing from 150 to 238µA (blue to red colour lines) for each muscle. Recruitment values are normalized, from 0 on circumference of polar plot to 1 on the centre.

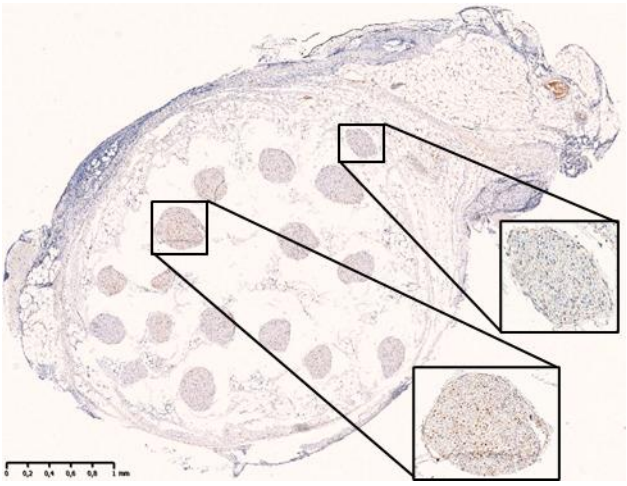

Figure 5: Anti-ChAT immunochemistry staining on P#2 median nerve transversal section. Motor fibres appear coloured in brown. Blue stains are cell nucleus of conjunctive tissues in nerve.

Discussion

Recruitment curves are an efficient way to assess stimulation selectivity. Their analysis allows for refinement of stimulation configuration supposedly resulting in a wider range of functional movements. Plexiform organisation of brachial nerves observed in pigs – and somewhat similar to humans - has still to be confirmed on more individuals and longer transversal distance. This gap will be filled in the next few weeks after receipt and analysis of new histological sections from additional nerve samples.

On the other hand, anti-ChAT immunochemistry revealed the location of the fascicles containing most of the motor fibers. Combining those physiological parameters to polar representation could provide a better understanding of optimized stimulation configurations although this will require further analysis - especially regarding correlation of recruitment and location of motor axons within the nerve.

This work contributes to a better understanding of how stimulation parameters influence recruitment. It also raises the question of whether EMG-based recruitment data alone can reliably infer internal nerve architecture. Ultimately, the integration of anatomical and functional data may enhance computational models and guide the design of more selective and efficient neuroprosthetic systems.

Conclusions

Regarding the obtained recruitment curves, electrical stimulation configurations determined through computational models appear to elicit selective muscle activation in swine upper-limb. Moreover, histological analysis reveals the actual distribution of motor fibers within the nerve, information that should ultimately contribute to the validation/improvement of the current computational models of peripheral nerve stimulation. We are planning to consolidate these preliminary results by pursuing the analyses of recruitment curves and histological data from the remaining animals. Results will be presented at the conference.

Acknowledgement

The authors thank the RAM-PTNIM (Nîmes, France,) facilities for supporting with animal caring and surgical logistic and the RHEM (Montpellier, France) for advices on nerve sampling and, histological analysis and scanning of microscope slides.

Funded by AI-Hand European project (EIC Pathfinder – Grant No. 101099916) and Plasticistim (EMERGENCE program - No #23004566, Région Occitanie, France).

References

[1] K. L. Kilgore et al., « Evolution of Neuroprosthetic Approaches to Restoration of Upper Extremity Function in Spinal Cord Injury », Top Spinal Cord Inj Rehabil, vol. 24, no 3, p. 252-264, 2018, doi: 10.1310/sci2403-252.

[2] C. A. Coste et al., « Activating effective functional hand movements in individuals with complete tetraplegia through neural stimulation », Sci Rep, vol. 12, no 1, p. 16189, oct. 2022, doi: 10.1038/s41598-022-19906-x.

[3] I. Delgado-Martínez, J. Badia, A. Pascual-Font, A. Rodríguez-Baeza, et X. Navarro, « Fascicular Topography of the Human Median Nerve for Neuroprosthetic Surgery », Front. Neurosci., vol. 10, juill. 2016, doi: 10.3389/fnins.2016.00286.

[4] M. Dali et al., « Relevance of selective neural stimulation with a multicontact cuff electrode using multicriteria analysis », PLOS ONE, vol. 14, no 7, p. e0219079, juill. 2019, doi: 10.1371/journal.pone.0219079.

[5] C. Fattal et al., « Restoring Hand Functions in People with Tetraplegia through Multi-Contact, Fascicular, and Auto-Pilot Stimulation: A Proof-of-Concept Demonstration », J Neurotrauma, vol. 39, no 9-10, p. 627-638, mai 2022, doi: 10.1089/neu.2021.0381.

[6] K. E. I. Deurloo, J. Holsheimer, et P. Bergveld, « Fascicular Selectivity in Transverse Stimulation with a Nerve Cuff Electrode: A Theoretical Approach », Neuromodulation: Technology at the Neural Interface, doi: 10.1046/j.1525-1403.2003.03034.x.

[7] D. K. Leventhal et D. M. Durand, « Subfascicle stimulation selectivity with the flat interface nerve electrode », Ann Biomed Eng, vol. 31, no 6, p. 643-652, juin 2003, doi: 10.1114/1.1569266.

[8] S. L. Blanz et al., « Spatially selective stimulation of the pig vagus nerve to modulate target effect versus side effect », J. Neural Eng., vol. 20, no 1, p. 016051, févr. 2023, doi: 10.1088/1741-2552/acb3fd.

[9] A. S. Hanna et al., « Brachial plexus anatomy in the miniature swine as compared to human », J Anat, vol. 240, no 1, p. 172-181, janv. 2022, doi: 10.1111/joa.13525.

Author's Address

BAUM Jonathan - jonathan.baum@inria.fr

Interferential or middle-frequency stimulation of peripheral nerve

Edmondson J[1], Osorio R[2], Andrews B[3] , Fitzgerald J[3], Jarvis JC[1]

[1] Liverpool John Moores University UK

[2] Universidad de Concepción Chile

[3] Nuffield Dept. of Surgery Oxford UK

- ***Abstract:*** *interferential stimulation involves injecting current, usually across the skin, from two or more sets of electrodes at medium frequencies (around 1-5 KHz is typical) whose* ***difference*** *in frequency matches a desired physiological rate of activation. The voltage field within the tissue resulting from* ***interference*** *of the currents activates neural tissue at appropriate physiological rates. The lower impedance of skin to higher frequencies is exploited. There have been recent virtual and actual experiments designed to demonstrate a focused effect of interferential stimulation beneath the skin. We have made some relevant observations activating the adductor pollicis muscle in the human hand via the ulnar nerve at the wrist.*

Keywords: *interferential stimulation, middle frequency, peripheral nerve,*

Introduction

Interferential stimulation is the use of two or more pairs of electrodes, each of which delivers current at slightly different typically kilohertz frequencies. Because axons have a maximum firing rate of less than 1 kHz they cannot follow directly such high frequency oscillation of the electric field, but may follow the oscillation represented by the summed waveforms whose frequency is the difference between the higher primary currents.
A theoretical advantage of such currents is that the volume within which the currents interfere may be arranged to be some distance below the surface of the skin.

Another theoretical advantage may be relatively poor activation or even blocking of pain fibres.

Material and Methods

We have tried to test some of these assumptions as they apply to typical FES activation, that is stimulation of a peripheral nerve in the wrist. In this case, the (ulnar) nerve is only a few mm under the skin, but the model we have used has the advantage that we can make an unbiased estimation of the degree of activation by means of the force response of the adductor pollicis muscle.

We used a matrix of electrodes formed from 6mm stainless steel rod radiused to a hemispherical shape at the skin contact so that the contact area was about 0.5 cm^2 with approximately 10mm spacing between centres. We prepared the skin beforehand with an application of moisturising cream (Cerave, L'Oreal (UK) Ltd.)

In all of our studies we have examined the response to stimulation via each pair of electrodes separately before comparing the response to simultaneous activation via both pairs of electrodes.

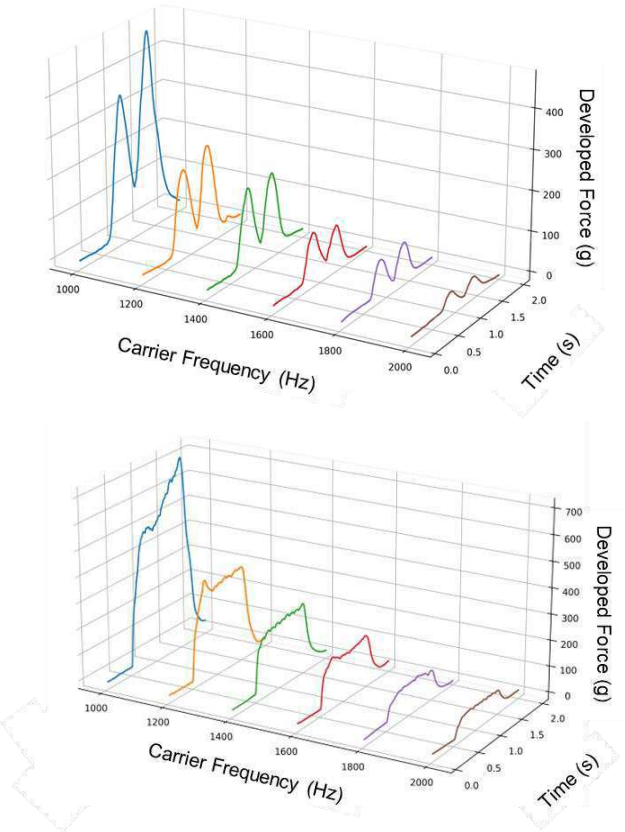

Figure 1: effect of carrier frequency

Results

Interferential stimulation can be demonstrated in this preparation but with quite severe pre-requisites in terms of

electrode position relative to the nerve and the characteristics of the middle frequency currents. The results shown here come from experiments in which pairs of electrodes are aligned in the long axis of the ulnar nerve and in which the anode of one pair lies between the anode and cathode of the other pair (a so-called nested arrangement) [1]. Figure 1 shows examples of interferential activation with a difference frequency of 2Hz (upper panel) or 20 Hz (lower panel) using carrier frequencies of between 1kHz and 2kHz in steps of 200Hz. The carrier frequency has a large impact on the muscle force elicited and this could be because of a difference in the degree of activation or possibly the ratio of activation to blocking. Frequencies above 1 kHz provide significantly less activation, which falls away sharply between 1 and 3Khz. Thus experiments that use a common difference frequency but different carrier frequencies should be compared with caution.

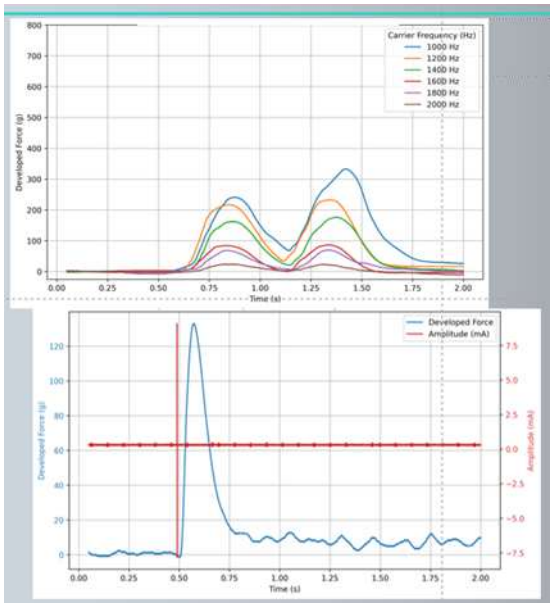

Figure 2: shape of force responses

Figure 2 shows the shape of force responses generated by single pulses (lower panel) or with a low difference frequency between two interfering kHz frequencies (upper panel). We interpret these responses to suggest that interferential stimulation does not cause synchronised activation of axons at the beat frequency. The force response with interferential stimulation always has a longer duration than with pulse stimulation and is therefore suggestive of somewhat asynchronous activation of multiple motor units.

Figure 3 shows that the relationship between the timing of the summation of the activating currents and the force response is consistent across different carrier frequencies but the relationship of the envelope to the force response is to our knowledge so far unexplained by the current concepts for activation [2].

With interferential stimulation, the force response has the same period as the summed envelope, but the peak of the envelope and the peak of the force response are shifted by about 90º

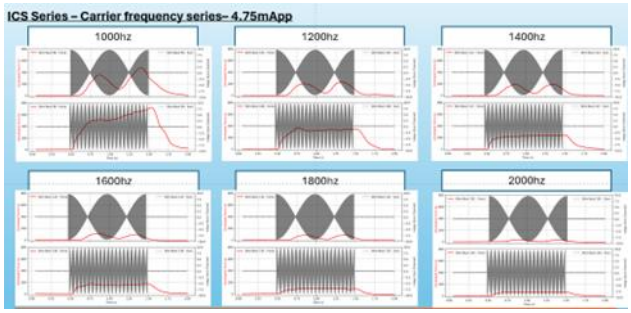

Figure 3: the force response at different carrier frequencies shows a consistent temporal relationship to the interfering envelope

Discussion

Recent publications suggest complex arrays of electrodes for transcutaneous stimulation [3, 4] and complex combinations of frequencies [4], some of which are subject to protection of intellectual property.

All assume some form of summation of the component waveforms within the tissues.
We will probably need to apply machine learning techniques to synthesise optimal waveforms and to select best electrode combinations. Our preparation in which such combinations can be explored may have an important role in such projects.

We still need basic testing of these assumptions and further testing of numerical models as attempts are made to predict the likely effect of complex activation patterns. The goal to probe the activation space to find efficient and effective targeted activation is competitive and potentially rewarding.

Bibliography:

1. Characterization and Evaluation of Interferential Current Stimulation for Functional Electrical Stimulation

Rodrigo Osorio, Jack Edmondson, Siobhan Mackenzie Hall, Francisco Saavedra, Javier Sáez, Adrian Poulton, James FitzGerald, Pablo Aqueveque, Brian Andrews, Jonathan Jarvis

Artificial Organs First published: 26 May 2025
https://doi.org/10.1111/aor.15027

2. The Mechanics of Temporal Interference Stimulation bioRxiv doi:https://doi.org/10.1101/2020.04.23.051870;

Jiaming Cao, Brent Doiron, Chaitanya Goswami, Pulkit Grover

3. Salchow-Hömmen C, Schauer T, Müller P, Kühn AA, Hofstoetter US, Wenger N. Algorithms for Automated Calibration of Transcutaneous Spinal Cord Stimulation to Facilitate Clinical Applications. J Clin Med. 2021 Nov 22;10(22):5464. doi:10.3390/jcm10225464. PMID: 34830746; PMCID: PMC8623351.

4. Improved Temporal and Spatial Focality of Non-invasive Deep-brain Stimulation using Multipolar Single-pulse Temporal Interference with Applications in Epilepsy

Emma Acerbo, Boris Botzanowski, Damian Dellavale, Matthew A. Stern, Eric R. Cole, Claire-Anne Gutekunst, Miller L. Gantt, Melanie Steiner, Florian Missey, Antonino Cassara, Esra Neufeld, Ken Berglund, Viktor Jirsa, Robert E. Gross, Daniel L. Drane, Eric Daniel Glowacki, Andrei G. Pakhomov, Adam Williamson

doi: https://doi.org/10.1101/2024.01.11.575301

Author's Address

Name JC Jarvis
Affiliation Lverpool John Moores University
eMail J.C.Jarvis@ljmu.ac.uk
homepage https://profiles.ljmu.ac.uk/7219-jonathan-jarvis

Study Protocol: Efficacy of EMG-triggered four-channel functional electrical stimulation in arm-hand paresis following stroke

Riegler M[1], Hohenwarter C[1], Pucks-Faes E[2], Mittermaier C[3], Tevnan B[3], Wanner M[4], Fheodoroff K[5]

[1]Gailtal-Klinik Hermagor, Department for Neurorehabilitation, Austria
[2]ö. Landeskrankenhaus Hochzirl-Natters, Department for Neurorehabilitation, Austria
[3]Kepler Universitätsklinikum Linz, Institute for Physical Medicine and Rehabilitation, Austria
[4]MED-EL Medical Electronics, Business Unit STIWELL, Austria
[5]Dr. Fheodoroff Klemens Andreas, Forschung und Entwicklung im Bereich Medizin, Austria

Abstract: *This randomized, controlled, single-blinded, multicenter study aims at evaluating the efficacy of EMG-triggered four-channel functional electrical stimulation (FES) compared to cyclic one-channel neuromuscular electrical stimulation (NMES) in arm-hand paresis in stroke patients. Planned sample size is 44 participants with a first ischemic stroke and moderate arm-hand paresis. Participants will receive 15 interventions over the course of three weeks either with EMG-triggered four-channel FES (group 1) or cyclic one-channel NMES (group 2) in addition to standard care. Primary endpoint is the Subscale Recovery of the Stroke Impact Scale. Secondary endpoints are changes in motor control, arm-hand-activities and health-related quality of life. Outcomes will be evaluated before and after intervention and in a twelve week follow up. A subgroup of participants (n = 15) will participate in a home-based exercise program. The study aims at demonstrating the efficacy of EMG-triggered four-channel FES compared to cyclic one-channel NMES in moderate arm-hand paresis following stroke, presenting a standardized procedure for task-oriented training and exploring the feasibility of a supervised home-based training.*

Keywords: *EMG-triggered multichannel electrical stimulation, Functional electrical stimulation, stroke, arm-hand paresis, home-based training*

Introduction

Approximately 50-80 % of stroke survivors experience arm-hand paresis, leading to limitations in daily activities, participation, and quality of life [1, 2]. Substantial evidence supports the efficacy of electrical stimulation (ES) in the rehabilitation of arm-hand paresis after stroke, especially when combined with task-oriented training, as supported by international guidelines and meta-analyses [3, 4, 5].

Despite sufficient evidence for the efficacy of different types of ES, there remains no standardized approach in clinical practice regarding the choice of methods and parameters [6]. While functional electrical stimulation (FES) shows greater benefits than other modalities like neuromuscular electrical stimulation (NMES) or transcutaneous electrical nerve stimulation (TENS), findings remain inconsistent regarding the optimal form of stimulation for enhancing motor function and daily activities post-stroke [7].

FES operates by providing electrical assistance precisely when an individual initiates movement, requiring active participation for optimal therapeutic effect. This contrasts with NMES, which primarily induces passive muscle contractions, targeting both structural and functional deficits [8].

Results from a pilot study conducted in 2022 [9] demonstrated positive effects of electromyography (EMG)-triggered four-channel FES and cyclic one-channel NMES on improving motor control (Fugl-Meyer Assessment) as well as arm-hand use and stroke recovery (in subscales of the Stroke Impact Scale). Participants in the EMG-triggered four-channel group achieved, on average, greater gains compared to the control group. However, due to the small sample size, no statistically significant differences could be established.

EMG-triggered stimulation appears promising, particularly in subacute stroke, but more research is needed. Integrating ES into home-based, task-oriented programs may further support recovery.

Study Objectives

The planned study aims at evaluating the superiority of EMG-triggered four-channel FES in moderate arm-hand paresis following stroke compared to cyclic one-channel NMES. The primary endpoint is the recovery of arm-hand paresis, assessed by the subscale Recovery of the Stroke Impact Scale (SIS). Secondary endpoints include changes in motor control (Fugl-Meyer Assessment), arm-hand-activities (Action Research Arm Test), and health-related quality of life (subscales of the SIS) at the beginning and end of the intervention as well as at a twelve-week follow-up.

Additionally, the feasibility of a home exercise program with ES through adherence rate, satisfaction rate and usability rate will be explored.

The net treatment duration of the stimulation between the two groups will be compared. Safety will be continuously monitored.

Material and Methods

This randomized, controlled, single-blinded, multicenter study (conducted at three Austrian clinical institutions, Gailtal-Klinik Hermagor, ö. Landeskrankenhaus Hochzirl-Natters, Kepler Universitätsklinikum Linz) aims at verifying the research questions. This study will include 44 participants which have to meet the following inclusion and exclusion criteria (Tab. 1):

Table 1: Inclusion and exclusion criteria

Inclusion criteria
• First-time ischemic stroke with moderate arm paresis (Motricity Index – Upper Extremity Sum-Score ≥ 40 ≤ 77 points) • Early to late subacute phase (7 days - 6 months) • Existing activity of daily living (ADL) ability before the event • Age ≥18 • Signed and dated informed consent form before the start
Exclusion criteria
• Lack of compliance with any inclusion criteria • Implanted defibrillators, brain stimulators, pacemakers, medication pumps • Therapy-resistant epilepsy • Fever or infectious diseases • Inflammatory or tumorous skin diseases in the stimulation area • Thromboses or vein inflammations • Severe contractures of the affected extremity • Wounds in the stimulation area • Pregnancy • Known allergic reactions to components of the investigational medical device • Unstable psychological status • Participation in other pharmacological clinical investigations within four weeks prior to enrolment • Anything that, in the opinion of the investigator, would place the subject at increased risk or preclude the subject's full compliance with or completion of the study

In phase one, participants receive a task-oriented EMG-triggered four-channel FES (5x / week, 30 minutes per intervention) over three weeks in addition to standard care. Figure 1 shows the electrode placement of the four stimulated muscle groups: M. extensor carpi radialis longus / brevis (EMG trigger channel), M. flexor digitorum superficialis, M. infraspinatus, M. triceps brachii.

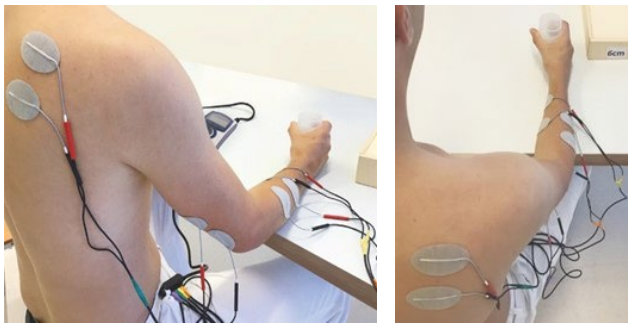

Figure 1: Electrode placement of the task-oriented EMG-triggered four-channel FES

The contraction pattern (Fig. 2) for the activity - to grasp an object, move it from the middle sagittal plane to the laterally outward and release the object - as well as the difficulty level of the activity can be adapted.

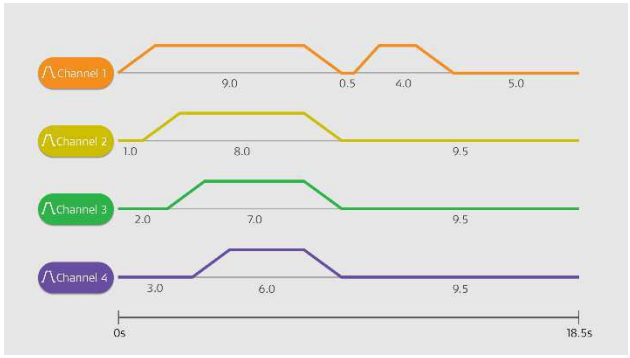

Figure 2: Contraction pattern of the task-oriented EMG-triggered four-channel FES. Pulse width: 200-300 µs, frequency: 25-35 Hz, intensity (mA): visible muscle contractions

The comparison group will receive cyclic one-channel NMES of the wrist and finger extensors (Fig. 3).

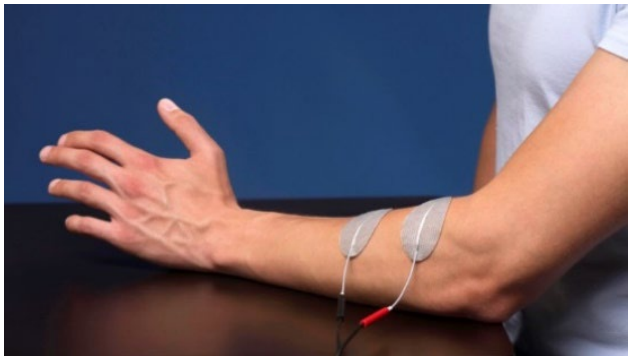

Figure 3: Electrode placement of the cyclic one-channel NMES

For phase two, a subset of participants (n = 15) will engage in an additional supervised home-based exercise program with the two different ES types for twelve weeks post-intervention. Patients in the EMG-triggered four-channel group train at home for twelve weeks using two or three individualized task-oriented FES programs, selected from a predefined set, with 30 minutes of daily stimulation.

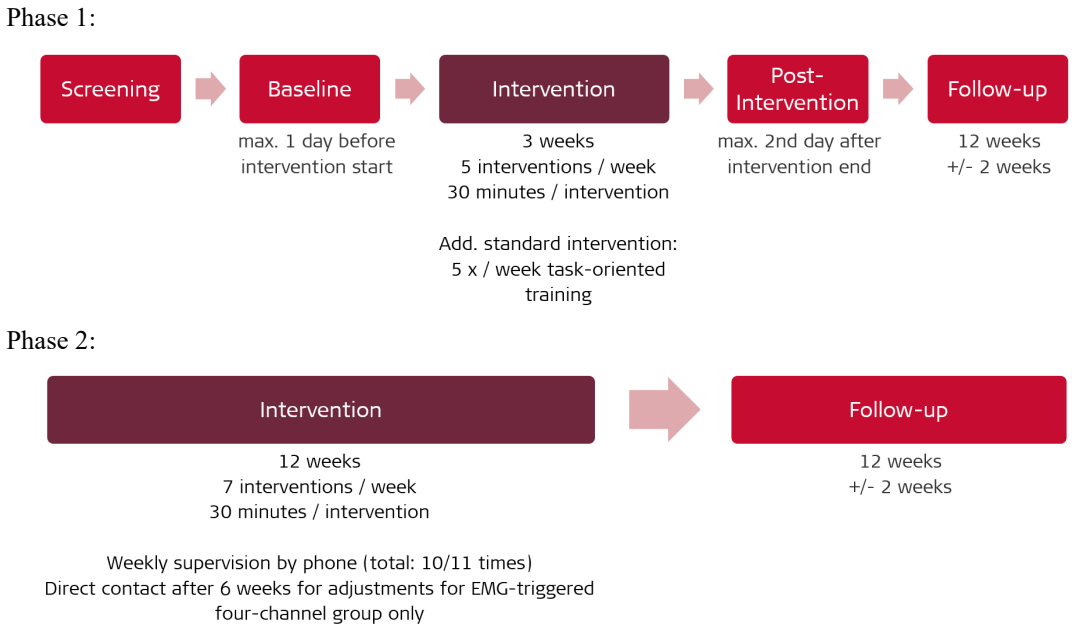

Figure 4: Overview of phase one, phase two and assessment time points

The cyclic one-channel group receives the same intervention than in phase one. All participants document training duration in a logbook, supplemented by device-based data Supervision includes weekly phone calls and one in-person visit of the EMG-triggered four-channel group only at week six for adjustments. Figure 4 gives an overview of the timepoints of the study procedure.

Data analysis will include descriptive statistics for quantitative (mean, standard deviation, median, quartiles) and qualitative data (absolute and relative frequencies) as well as z-statistics. Inferential statistics will employ non-parametric tests (Mann-Whitney U-Test) and parametric tests (t-test). Exploratory questions will be addressed through Principal Component Analysis (PCA).

Sample size calculations using G*Power 3.1 [10] with an alpha of 5% and a power of 95% indicated a total of 44 participants (22 per group) with a 20% dropout rate.

Expected Outcomes

This study aims at demonstrating the superiority of EMG-triggered four-channel FES over cyclic one-channel NMES in moderate arm-hand paresis following subacute stroke. It will explore a standardized FES approach in combination with task-oriented training and assess feasibility in an outpatient home-based setting as supervised home training. The ultimate goal is to provide evidence-based recommendations for clinical and outpatient practice.

Further research and clinical trials are needed to determine the most effective forms of ES and their integration into comprehensive rehabilitation strategies for clinical and outpatient practice. Consistent implementation of home-based exercise programs with ES remains a key component of post-stroke care to enhance intensity of training and better outcomes.

References

[1] Persson, H. C., Parziali, M., Danielsson, A. & Sunnerhagen, K. S. Outcome and upper extremity function within 72 hours after first occasion of stroke in an unselected population at a stroke unit. A part of the SALGOT study. *BMC Neurol.* 12, p. 162, 2012.

[2] Nichols-Larsen, D. S., Clark, P. C., Zeringue, A., Greenspan, A. & Blanton, S. Factors Influencing Stroke Survivors' Quality of Life During Subacute Recovery. *Stroke* 36, pp. 1480–1484, 2005.

[3] Teasell, R. et al. Canadian Stroke Best Practice Recommendations: Rehabilitation, Recovery, and Community Participation following Stroke. Part One: Rehabilitation and Recovery Following Stroke; 6th Edition Update 2019. *Int J Stroke* 15, pp. 763–788, 2020.

[4] Winstein, C. J. et al. Guidelines for Adult Stroke Rehabilitation and Recovery: A Guideline for Healthcare Professionals from the American Heart Association/American Stroke Association. *Stroke* 47, pp. e98–e169, 2016.

[5] Tenberg, S. et al. Comparative Effectiveness of Upper Limb Exercise Interventions in Individuals With Stroke: A Network Meta-Analysis. *Stroke* 54, pp. 1839–1853, 2023.

[6] Yang, J. D. et al. Effectiveness of electrical stimulation therapy in improving arm function after stroke: a systematic review and a meta-analysis of randomised controlled trials. *Clin Rehabil* 33, pp. 1286–1297, 2019.

[7] Tang, Y. et al. Optimal Method of Electrical Stimulation for the Treatment of Upper Limb Dysfunction After Stroke: A Systematic Review and

Bayesian Network Meta-Analysis of Randomized Controlled Trials. *Neuropsychiatric Disease and Treatment* 17, pp. 2937–2954, 2021.
[8] Popovic, M. R. et al. Functional electrical stimulation therapy of voluntary grasping versus only conventional rehabilitation for patients with subacute incomplete tetraplegia: a randomized clinical trial. *Neurorehabil Neural Repair* 25, pp. 433–42, 2011.
[9] Schick, T. et al. Efficacy of Four-Channel Functional Electrical Stimulation on Moderate Arm Paresis in Subacute Stroke Patients - Results from a Randomized Controlled Trial. *Healthcare* 10, 704, 2022.
[10] Faul, F., Erdfelder, E., Lang, A. G. & Buchner, A. G*Power 3: a flexible statistical power analysis program for the social, behavioral, and biomedical sciences. *Behav Res Methods* 39, pp. 175–191, 2007.

Ethical approval was received from the Ethics Committee of the Medical University of Innsbruck, Austria (1096/2025), the Ethics Committee of the Medical Faculty of the Kepler University Linz, Austria (1126/2025) and the Ethics Committee of the State of Carinthia (M2025-08). Before study start, the trial will be registered.

Author's Address

Manuela Riegler, MSc
Gailtal-Klinik Hermagor, Department of Neurorehabilitation, Austria
Manuela.riegler@kabeg.at

Epineural Electrical Stimulation for Grasp Recovery: 28-Day Study in 4 Tetraplegic Participants

Christine Azevedo Coste[1], Thomas Guiho[1], François Bailly[1], Fernanda Ferreira[2], Benjamin Degeorge[4], Antoine Geffrier[5], Valentin Maggioni[1], Jonathan Baum[1,2], David Andreu[2], Jacques Teissier[4], David Guiraud[2], Charles Fattal[3]

[1]INRIA, University of Montpellier, France
[2]NEURINNOV company, Montpellier, France
[3]Centre Bouffard-Vercelli USSAP, Perpignan, France
[4]Clinique Saint Jean ORTHOSUD, France
[5]CHU Rennes, France

Abstract: *Two epineural multicontact cuff electrodes were implanted around the median and radial nerves in four individuals with complete tetraplegia for a duration of 28 days. The electrodes were connected via percutaneous leads to an external, computer-controlled stimulator. Stimulation parameters and electrode configurations were empirically optimi□ed to evoke functional hand gestures. Comprehensive technical and functional assessments were conducted throughout the study period. This work reports on the functional outcomes achieved across the four participants.*

Keywords: *functional electrical stimulation (FES), epineural cuff electrodes, upper limb, tetraplegia*

Introduction

Orthopaedic surgical interventions, such as tendon transfers and joint stabilization procedures, are generally effective in individuals with tetraplegia whose upper limbs are classified as International Classification for Surgery of the Hand in Tetraplegia (ICSHT) group 3 or higher. This classification system quantifies, below the elbow, the number of active residual muscles available for transfer to restore specific functions, such as finger opening and closing or key grip. In individuals below group 3, traditional surgical interventions have demonstrated limited effectiveness in restoring even basic functional capabilities, particularly in achieving adequate grip strength for object manipulation. In such cases, functional electrical stimulation (FES) presents a viable alternative. Prior research has primarily focused on intramuscular and epimysial stimulation approaches [1]. In contrast, our study proposed a neural stimulation strategy aimed at minimizing the number of implanted cables and electrodes. We hypothesized that multi-contact epineural stimulation of the median and radial nerves could selectively activate distinct muscle subgroups, thereby enabling individuals with complete tetraplegia to perform functional grasping tasks.

Material and Methods

Four male participants were enrolled in this preliminary study. All presented a complete tetraplegia (AIS A, C4 or C5), demonstrated neurological stability, and were deemed ineligible for tendon transfer surgery. Based on the ICSHT classification, three participants were categorized as group 0 (P0, P1 and P3) and one as group 1 (P4). All participants received comprehensive written and oral information regarding the study at least 30 days prior to enrolment.

Two multi-contact epineural cuff electrodes (CorTec GmbH Freiburg Germany) were surgically implanted around the median and radial nerves proximal to the elbow. The electrode leads were tunneled subcutaneously toward the shoulder and connected to two external percutaneous connectors. Each electrode was connected to a multi-source external stimulator (STIMEP, INRIA, Montpellier). Electrode removal was carried out between days 28 and 30 post-implantation. The stimulation was delivered to each electrode using a rectangular balanced stimulus with a fixed cathodic phase of 100µs (low threshold muscles) or 150µs, 24 Hz stimulation frequency and a varying intensity (lowest step 5µA). The current spreading over contacts is based on preliminary studies [2-3].

Several piloting interfaces were tested with the participants, including: voluntary movements of the contralateral shoulder detected via a single inertial measurement unit (IMU), voluntary muscle contractions recorded using electromyography (EMG), and head-activated push buttons [3]. Participant P1 was using EMG modality, P2 the push-button interface, P3 and P4 were using the IMU-based interface.

Two successive protocols were conducted including two participants each (ClinicalTrials.gov NCT04306328 and NCT05555914). Both protocols were approved by Ethical Committees and the national competent authority (ANSM). Some results from the first protocol were previously published [4-5].

A longitudinal analysis was carried over the implantation period to analyse electrode stability and performances as well as functional progress.

An analytical evaluation was conducted using the Motor Capacities Scale (MCS) and execution times on two tasks performed by all participants: (1) grasping a 250 ml bottle, bringing it to the mouth, and returning it to the table; and (2) picking up a fork, raising it to mouth level, and placing it back on the plate.
The second protocol was slightly modified based on insights gained from the first one. Evaluation for P3 and P4 focused on functional outcomes from a user-centered perspective, assessing perceived usefulness, usability, performance, satisfaction, and acceptability. This phase was guided by the Canadian Occupational Performance Measure (COPM), in which participants identified and rated five self-selected tasks in terms of performance and satisfaction. Consequently, both five predefined tasks and five self-selected tasks were evaluated. Additionally, system usability was assessed using the System Usability Scale (SUS). Grasping performance was also evaluated using dynamometry (Commander Echo Grip JTECH USA) and instrumented objects. Hand kinematics was assessed using a markerless approach based on 4 webcam video recordings [6]. Evoked-surface EMG (Delsys, Natick, MA) was offline processed through wavelet analysis and synthetic wave detection. Every identified muscle response was then normalized by its own maximum response within all stimulation configurations to establish recruitment curves [7].

Results

All four participants were able to perform the two common predefined grasping tasks (Figure 1 and table 1). P1, P2 and P3 required a wrist orthosis to stabilize the joint and prevent wrist flexion associated with finger grasping movements. P2 required an assistive adaptation to hold the bottle, compensating for limited elbow and shoulder mobility.

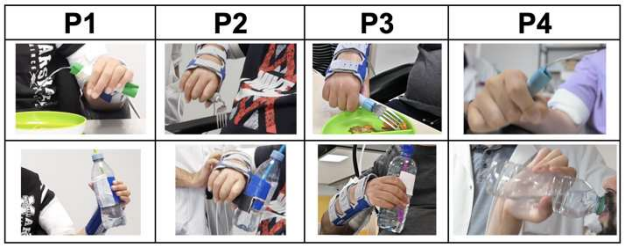

Figure 1- Video snapshots of the two common preselected tasks achieved by the 4 participants

Table 1: MCS scores and execution times.

Task		P1 MCS	P1 EXECUTION TIME (sec)	P2 MCS	P2 EXECUTION TIME (sec)	P3 MCS	P3 EXECUTION TIME (sec)	P4 MCS	P4 EXECUTION TIME (sec)
Grab a bottle, bring it up to mouth level, then place it back on the table.	A :GRAB	3	40	2	31	3	14	3	9
	B :HOLD	3		2		3		3	
	C :RELEASE	3		2		3		3	
	Total score: A+B+C	9		6		9		9	
Grab a fork from a plate, bring it up to mouth level and place it back on the table.	A :GRAB	3	25	2	28	3	16	3	7
	B :HOLD	3		2		3		3	
	C :RELEASE	3		2		3		3	
	Total score: A+B+C	9		6		9		9	

Different electrode configurations and stimulation parameters induced different hand movements. The relationship between kinematics (derived from video data) and evoked EMG was analyzed. Detailed results will be presented, including impedance and stimulation thresholds evolution along the implant period. Grasping performance will also be expanded.

Conclusions

This study presents comprehensive results on object grasping performance following the implantation of two epineural electrodes around the median and radial nerves, maintained for a period of one month. Longitudinal monitoring of certain parameters is also provided and offers valuable insights on the stability of the electrodes and stimulation parameters. The assessment of grasp quality raises both technical and theoretical questions, which we will explore further.

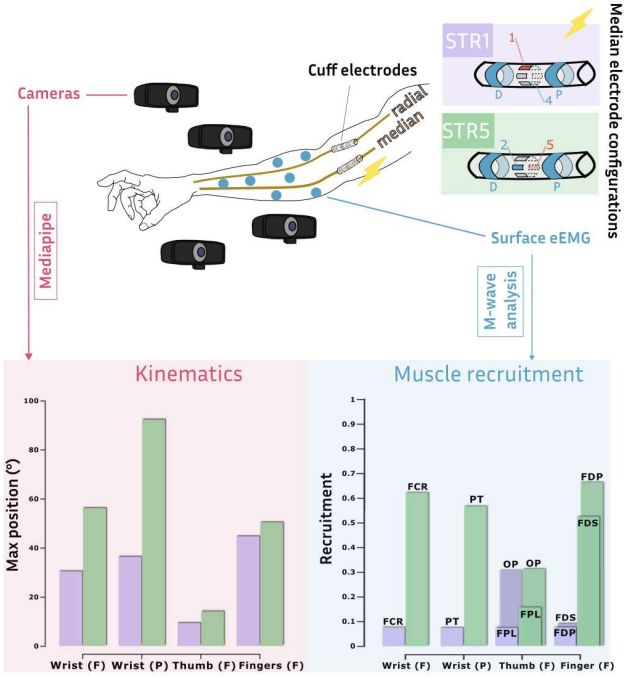

Figure 2- Example of one trial from P4. Maximum flexion of the joints are compared to muscle recruitment induced Here, we analyze data from the fourth participant through two specific median electrode configurations: steering current + ring with cathodes on contact 1 (STR1) or 5 (STR5) and anodes on the 2 peripheral rings and the contact opposite to cathode contact [2].

Acknowledgement

We thank the participants of this study for their invaluable contribution, as well as the clinical teams for their daily monitoring and support. We also acknowledge the work of the engineers and researchers from the INRIA and NEURINNOV teams, who developed the methods and tools essential for conducting these trials.
Funding: EIT Health, ISITE Muse, EIC Pathfinder, Région Occitanie

References

[1] M. Keith, P.H. Peckham, G.B. Thrope, K.C. Stroh, B. Smith, J.R. Buckett, K.L. Kilgore, J.W. Jatich.

Implantable functional neuromuscular stimulation in the tetraplegic hand. *J Hand Surg Am*. 1989.
[2] Dali et al. Model based optimal multipolar stimulation without a priori knowledge of nerve structure: application to vagus nerve stimulation, JNE, 2018
[3] Tigra et al. Selective neural electrical stimulation restores hand and forearm movements in individuals with complete tetraplegia, JNER, 2020
[4] C. Azevedo, L. William, L. Fonseca, A. Hiairrassary, D. Andreu, A. Geffrier, J Teissier, C Fattal, D Guiraud Activating effective functional hand movements in individuals with complete tetraplegia through neural stimulation *Scientific Reports*. 2022.
[5] C. Fattal, J. Teissier, A Geffrier, L. Fonseca, L. William, D. Andreu, D. Guiraud, C. Azevedo Restoring Hand Functions in People with Tetraplegia through Multi-Contact, Fascicular, and Auto-Pilot Stimulation: A Proof-of-Concept Demonstration. *J Neurotrauma*. 2022.
[6] V. Maggioni, C. Azevedo-Coste, S. Durand, F. Bailly. Optimisation and Comparison of Markerless and Marker-Based Motion Capture Methods for Hand and Finger Movement Analysis. *Sensors* (Basel). 2025.
[7] L. William, M. Dali, C. Azevedo Coste, D. Guiraud. A method based on wavelets to analyse overlapped and dependent M-Waves. *Journal of Electromyography and Kinesiology*, 2022.

Author□s Address

Christine Azevedo
INRIA
christine.azevedo@inria.fr

Real-time gait event detection using motion capture to control an electrical stimulator: Proof-of-concept

Graffagnino G[1], Gasq D[2,3], Patte K[4], Sijobert B[4], Azevedo-Coste C[1]

[1]Inria, University of Montpellier, France
[2]Toulouse NeuroImaging Center, University of Toulouse, France
[3]Service des Explorations Fonctionnelles Physiologiques, Clinique Universitaire du Mouvement, Centre Hospitalo-Universitaire de Toulouse, France
[4]Institut St Pierre, Palavas-les-Flots, France

Abstract: *Cerebral palsy (CP) is the most prevalent motor disorder in childhood and often results in gait abnormalities that hinder mobility and diminish quality of life. Functional electrical stimulation (FES) has demonstrated potential in enhancing gait in individuals in this population, however, its practical implementation remains complex, as it requires monitoring various gait parameters and delivering personalized stimulation to different muscles in order to correct various gait impairments. Recent advancements in real-time motion capture (MOCAP) and wearable sensors now enable the development of closed-loop, multi-channel FES systems. This study will assess the feasibility and responsiveness of a real-time, event-triggered multi-channel stimulation protocol during treadmill walking. The stimulation is triggered by specific gait events (heel strike, knee flexion, ankle dorsiflexion) detected through the MOCAP system and administered via a multichannel electrical stimulator. Conducted on healthy adults, this preliminary study focuses on assessing technical feasibility. We report different technical outcomes including the latency between gait event detection and the appearance of stimulation artifacts in EMG signals. The results confirm the viability of the system, laying the groundwork for future clinical application in the rehabilitation of children with CP.*

Keywords: *Electrical Stimulation, Gait analysis, Motion Capture, Artificial walking technologies*

Introduction

Cerebral palsy (CP) is the most prevalent motor disorder in childhood, affecting approximately 1 in every 500 live births worldwide. It involves a spectrum of motor impairments - such as increased muscle tone, muscle weakness, and poor coordination - that significantly limits functional mobility and reduce quality of life [1]. Gait abnormalities are among the most common functional limitations observed in individuals with CP, often resulting in reduced walking efficiency, impaired balance, and limited independence [2]. Recent advances in wearable sensors and real-time motion analysis have opened new avenues for the development of closed-loop electrical stimulation techniques, which adapt stimulation in response to specific biomechanical events. In this context, functional electrical stimulation (FES) has emerged as a promising method to support motor function by enhancing muscle activation in a task-specific manner [3]. Over the past two decades, single-channel gait-specific FES has been shown to improve ankle motion during the swing phase but remains insufficient for addressing more complex gait impairments, such as flexed-knee or stiff-knee gait, commonly observed in CP [4]. Emerging evidence suggests that multi-channel gait-specific FES may provide more comprehensive gait correction, though further research is needed to validate its effectiveness [5]. On the other hand, real-time detection of gait events and real-time feedback emerge as a potential new way of improving rehabilitation of children with cerebral palsy, using motion capture [6]. As motion capture can visualize various kinematic parameters, we aimed to combine real-time detection of multiple specific gait events using motion capture to control multi-channel gait-specific FES to address a new functional tool of gait correction of children with cerebral palsy. Our approach would be to determine, in a gait analysis laboratory, the most relevant events to detect in order to trigger stimulation of various muscles, to test different stimulation strategies, and then to transfer the selected one to a personalized wearable system [7]. To advance this line of research, it is essential to first evaluate the feasibility and reliability of such systems in a controlled environment.

The present study aims to evaluate from a technical perspective, a real-time, event-triggered electrical stimulation protocol during treadmill walking in healthy individuals, as a first step toward validating its feasibility and effectiveness for future applications in children with CP.

Material and Methods

The objective of this study is to compute the latency between the detection of various gait events and the reception of a stimulation on the muscles of interest. The study design is schematized in figure 1.

Participants: 10 participants: from 18 to 60 years old, without any neurologic disorder, able to walk on a treadmill without any assistance.

Electrical Stimulation: Electrical stimulation is delivered by the 8 channel Motimove stimulator (3F Company, Belgrade, Serbia), operated in research mode via

hexadecimal command signals. Stimulation frequency and phase width were set to 30Hz and 150us respectively.

Data collection: Kinematic and electromyographic (EMG) data were collected using the Gait Real-time Analysis Interactive Lab (GRAIL, Motek Medical, Houten, Netherlands) and processed through the D-Flow software, in which a custom interactive task was developed in accordance with the study design. Twenty-two reflective markers were placed on anatomical landmarks of both legs and tracked at 100 Hz using a 10-camera optoelectronic motion capture system (Vicon Motion Systems Ltd., Oxford, UK), employing the Human Body Model (HBM) for real-time gait analysis, as described by Van den Bogert et al. [8]. Stimulation artifacts were recorded using a multi-channel acquisition system (Cometa Systems, Bareggio, Italy) at a sampling rate of 1000 Hz.

Study design: Participants were instructed to walk normally on a treadmill across three separate sessions. In the first session, the focus was on detecting the heel strike event; each time a heel strike is identified, electrical stimulation is triggered. The second session involved real-time monitoring of knee flexion for each leg. When the knee angle exceeds a predefined threshold, stimulation is triggered. The third session followed a similar protocol, but based on ankle dorsiflexion to trigger stimulation.

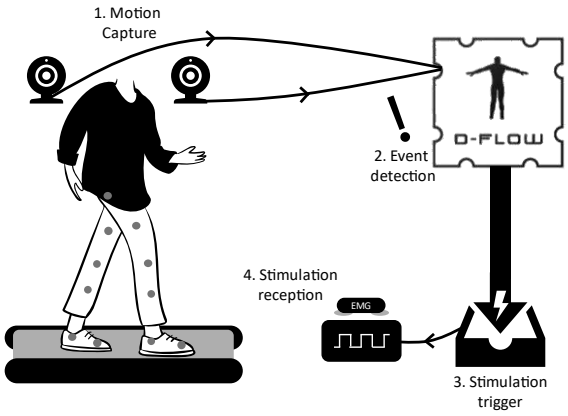

Figure 1: Schema of study design

Data processing: All data collected using the D-Flow software were imported and processed in MATLAB (v2020b, The MathWorks Inc., Natick, USA). The timestamps of specific gait events (heel strike, knee flexion, ankle dorsiflexion) were extracted and compared to the timestamps of the first appearance of stimulation artifacts and the stimulation duration in the EMG signals. This analysis allows for the determination of the delay between event detection and the actual delivery of stimulation to the body. The measured latency was then compared to the duration of each corresponding gait event to assess whether the delay is acceptable for real-time gait correction, or if an anticipatory stimulation offset is required to ensure effective intervention.

Results

The results demonstrate the feasibility of triggering electrical stimulation with a latency of less than 100 ms using the motion capture system integrated within the GRAIL platform. Details will be presented during the conference.

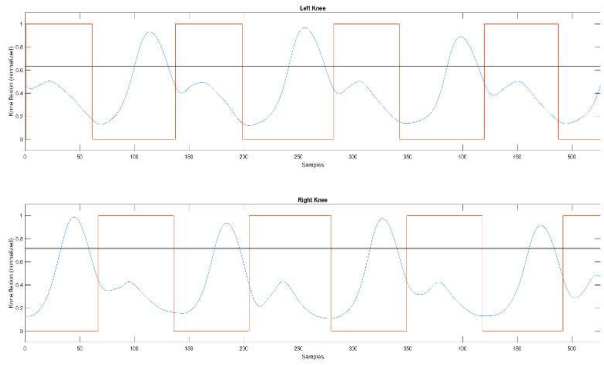

Figure 2: Example of the experiment on the knee flexion. In blue knee flexion normalized to maximal knee flexion. In orange, stimulation activation (on/off). In black, knee flexion threshold (stimulation is on when flexion is below this threshold).

Discussion

The primary objective of this study was to assess the latency of stimulation delivery based on gait events, these results were combined with previously published electromechanical delay values [10] to estimate the total latency of our corrective application.
Healthy participants exhibit typical gait patterns, which may not pose the same challenges to the stimulation system as pathological gait. This limits the generalizability of latency and responsiveness outcomes in more variable or unpredictable gait conditions. The stimulation was applied below the motor threshold, and we will need to verify the adaptation to an FES-assisted gait. In parallel to this work, we have assessed the event detection approach on retrospective data acquired on the GRAIL platform with children with CP.

Conclusions

This study proposed to evaluate a real-time, event-triggered electrical stimulation protocol during treadmill walking in healthy adults, as a preliminary step towards gait correction in children with cerebral palsy. The system leverages motion capture technology to detect biomechanical events and trigger multi-channel stimulation with minimal latency. While stimulation was delivered below the motor threshold, the recorded delay—combined with known electromechanical response times—offers insight into the feasibility of timely muscle activation for gait modulation. Although conducted in a controlled environment and limited to a healthy population, the results provide a foundational understanding of the system's responsiveness and technical

reliability. This work lays the groundwork for developing adaptive, sensor-based neurorehabilitation strategies tailored to the complex motor impairments characteristic of cerebral palsy.

Acknowledgement

This work was funded by an INRIA-INSERM grant. We gratefully acknowledge the Physiotherapy Department and the management of the St Pierre Institute for granting access to the GRAIL system and supporting the data acquisition for this protocol.

References

[1] P. Rosenbaum *et al.*, "A report: the definition and classification of cerebral palsy April 2006," *Dev. Med. Child Neurol. Suppl.*, vol. 109, pp. 8–14, Feb. 2007.

[2] J. Zhou, E. E. Butler, and J. Rose, "Neurologic Correlates of Gait Abnormalities in Cerebral Palsy: Implications for Treatment," *Front. Hum. Neurosci.*, vol. 11, 2017, Accessed: Nov. 21, 2023. [Online]. Available: https://www.frontiersin.org/articles/10.3389/fnhum.2017.00103

[3] S. C. K. Lee, A. Behboodi, J. F. Alesi, and H. Wright, "Functional Electrical Stimulation Interventions for Children and Youth with Cerebral Palsy," in *Cerebral Palsy*, F. Miller, S. Bachrach, N. Lennon, and M. E. O'Neil, Eds., Cham: Springer International Publishing, 2020, pp. 2661–2686. doi: 10.1007/978-3-319-74558-9_166.

[4] J. A. Mooney and J. Rose, "A Scoping Review of Neuromuscular Electrical Stimulation to Improve Gait in Cerebral Palsy: The Arc of Progress and Future Strategies," *Front. Neurol.*, vol. 10, p. 887, Aug. 2019, doi: 10.3389/fneur.2019.00887.

[5] J. Rose, K. Cahill-Rowley, and E. E. Butler, "Artificial Walking Technologies to Improve Gait in Cerebral Palsy: Multichannel Neuromuscular Stimulation," *Artif. Organs*, vol. 41, no. 11, pp. E233–E239, 2017, doi: 10.1111/aor.13058.

[6] L. van Gelder, A. T. C. Booth, I. van de Port, A. I. Buizer, J. Harlaar, and M. M. van der Krogt, "Real-time feedback to improve gait in children with cerebral palsy," *Gait Posture*, vol. 52, pp. 76–82, Feb. 2017, doi: 10.1016/j.gaitpost.2016.11.021.

[7] Sijobert B, Azevedo C, Pontier J, Graf S, Fattal C. A Sensor-Based Multichannel FES System to Control Knee Joint and Reduce Stance Phase Asymmetry in Post-Stroke Gait. Sensors (Basel). 2021 Mar 18;21(6):2134. doi: 10.3390/s21062134.

[8] A. J. van den Bogert, T. Geijtenbeek, O. Even-Zohar, F. Steenbrink, and E. C. Hardin, "A real-time system for biomechanical analysis of human movement and muscle function," *Med. Biol. Eng. Comput.*, vol. 51, no. 10, pp. 1069–1077, 2013, doi: 10.1007/s11517-013-1076-z.

[9] H. J. Hermens *et al.*, "European Recommendations for Surface ElectroMyoGraphy," pp. 13–54, 1999.

[10] S. Zhou, D. L. Lawson, W. E. Morrison, and I. Fairweather, "Electromechanical delay in isometric muscle contractions evoked by voluntary, reflex and electrical stimulation," *Eur. J. Appl. Physiol.*, vol. 70, no. 2, pp. 138–145, Mar. 1995, doi: 10.1007/BF00361541.

Author's Address

GRAFFAGNINO Gabriel
CAMIN Team, Inria, University of Montpellier, France
gabriel.graffagnino@inria.fr

Session 8:
Current Challenges and Future Directives of FES 1

Development of toolkits as an implementation strategy for functional electrical stimulation (FES) in neurorehabilitation practice

Musselman KE[1-3], Jervis-Rademeyer H[4]

[1]Department of Physical Therapy, University of Toronto, Canada
[2]Rehabilitation Sciences Institute, University of Toronto, Canada
[3]KITE Research Institute, Toronto Rehabilitation Institute-University Health Network, Canada
[4]School of Rehabilitation Science, University of Saskatchewan, Canada

Abstract: *Functional electrical stimulation (FES) is an evidence-based tool that can augment the movement and function of children and adults living with damage to the central nervous system. Despite recommendations to use FES in neurorehabilitation, it is underutilized. One of the most commonly cited barriers to FES use by physical and occupational therapists is a lack of knowledge and skill in FES application. One low-cost, but far-reaching, implementation strategy used in healthcare settings is a toolkit. Toolkits are a collection of knowledge translation products (e.g., manual, videos, case studies) combined into a single, easily accessible format. Recently, two FES-related toolkits were created to address knowledge gaps in Canadian neurorehabilitation practice: the FES Toolkit and the FES Cycling Toolkit. The aim of this article is to describe the development of the FES Toolkit and the FES Cycling Toolkit. The development process included: 1) selecting a framework to guide the overall research and development process (i.e., the Knowledge-to-Action Framework), 2) identifying guiding principles to follow in the creation of the toolkits (i.e., user-centred design and evidence-based content), and 3) considering factors that would influence toolkit design (i.e., format, timeline, resources and sustainability). Adopting a framework, guiding principles and design considerations facilitated decision-making during toolkit development. The process described here may serve as a guide for future FES- and technology-related toolkit creation.*

Keywords: *functional electrical stimulation, knowledge translation, implementation, cycling*

Introduction

More than 3.6 million Canadian children and adults live with a neurological condition, such as stroke, cerebral palsy, multiple sclerosis and spinal cord injury (SCI) [1]. These individuals access privately- and publicly-funded rehabilitation (e.g., physical and occupational therapy) to improve their ability to move, function and participate in daily activities. One rehabilitation technology that is recommended in clinical practice guidelines for several neurological conditions is functional electrical stimulation (FES) [2,3]. With non-invasive FES, an electrical current is applied to a peripheral nerve or paralyzed muscle through electrodes placed on the skin. The resulting electrically generated muscle contractions are incorporated into functional movement training with the aim or supporting and/or restoring movement proficiency.

Although there is strong evidence to support the use of FES in neurorehabilitation practice, FES and technology use in clinical practice remains low [4,5]. In Canada, FES is rarely implemented by rehabilitation teams in both private and public healthcare settings [5,6]. A key implementation barrier specific to FES is a lack of knowledge and skill in FES [5,7]. Physical and occupational therapists seek guidance on *how* to apply FES; for example, how to set stimulation parameters, position electrodes and select dosage parameters. This knowledge may be gained through a continuing education course, with courses leading to increased therapist confidence in applying FES [5]. However, the cost, location and time required for continuing education courses prevent therapist access [8,9]. Moreover, with a limited number of educators offering FES training, it is difficult to provide this education on a large scale.

Toolkits may be an effective alternative to continuing education courses. A toolkit is a self-directed resource that packages a variety of knowledge translation products, such as a manual, instructional videos, illustrations, case studies, knowledge quizzes and practical activities [10]. Toolkits are considered a low-cost implementation strategy that can facilitate widespread use of evidence-based interventions and clinical practice guidelines [10]. From 2023-2024, two toolkits related to FES were created to address clinical gaps in FES use in Canada. First, the FES Toolkit was created to provide rehabilitation professionals with foundational knowledge and practical skill in neuromuscular electrical stimulation to support FES implementation in pediatric and adult neurorehabilitation settings [11]. Second, the FES Cycling Toolkit was created to support physical therapists with the implementation of FES cycling for adults with SCI into acute care environments [12,13]. In this article, we describe the development of the FES Toolkit and the FES Cycling Toolkit, including the guiding framework, principles and design considerations. The development process described here may serve as a guide for future FES- and technology-related toolkit creation.

Material and Methods

The **Knowledge-to-Action Framework** [14] was used to guide the overall research process related to FES implementation. This framework outlines the steps required for the creation and implementation knowledge or products, and consists of two interacting components: the action cycle and the knowledge creation funnel [14]. The development of the FES Toolkit and the FES Cycling Toolkit resulted from steps of both components, beginning with three steps of the action cycle and ending with the creation of the toolkits through the knowledge creation funnel (Fig. 1).

Step 1: Identify Clinical Gaps Although there was strong evidence supporting the efficacy and safety of FES and FES cycling in rehabilitation [2,3] and acute care settings [15], respectively, these technologies were not adopted by rehabilitation professionals [5,6].

Step 2: Assess Barriers and Facilitators The barriers and facilitators of FES use in acute care and rehabilitation settings were identified from previous research [5,16-18]. Limited FES knowledge and low confidence in its application were the most frequently identified implementation barriers.

Step 3: Adapt Knowledge to Context The barriers to FES implementation suggested a need for educational resources. Interviews and focus groups with physical and occupational therapists were conducted to identify their learning needs and preferences to inform the creation of toolkits on FES [19]. This work identified that learning needs were influenced by internal factors (e.g., baseline knowledge, learning style) and external factors (e.g., collaborative learning, practice setting) [19]. The toolkits were created with these factors in mind.

Step 4: Knowledge Creation Two **guiding principles** were followed during toolkit creation.

1) *User-centred design*: Co-design teams were formed for both toolkits since including end-users in the design process was expected to increase toolkit adoption [20]. The co-design team for the FES Toolkit (n=15) included people with SCI, physical therapists, occupational therapists, exercise physiologists and researchers with expertise in biomedical engineering, neurorehabilitation, implementation science and adult education. The FES Cycling Toolkit engaged a co-design team (n=12) of people with SCI, acute care physical and occupational therapists, a physiatrist, hospital administrator and researchers with expertise in knowledge translation, FES cycling and SCI rehabilitation. In addition, one PT from each participating acute care hospital was identified as the local FES cycling champion, serving as a liaison between the co-design team and the therapists at their site.

2) *Evidence-based content*: The toolkits' content was based on current scientific evidence. For the FES Toolkit, systematic reviews and randomized clinical trials were prioritized for review, and the validated FES Clinical Decision Making Tool [7] was used to guide learning on how to apply FES. For the FES Cycling Toolkit, a recently complete systematic review completed by the team was used to inform content [21]. The team also consulted the manufacturer's website that was specific to the FES cycle model used at the participating acute care hospitals.

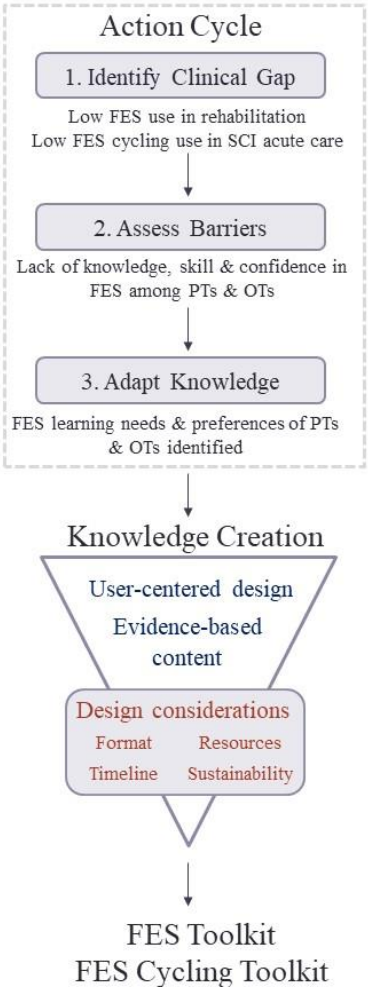

Figure 1: Steps in the development of the FES Toolkit and FES Cycling Toolkit. The Knowledge-to-Action Framework guided the process [14]. Three steps of the Action Cycle were followed by Knowledge (i.e. toolkit) Creation, which was informed by two guiding principles (blue text) and four design considerations (orange text).

Additionally, four **design considerations** guided toolkit development: format, timeline, resources and sustainability.

1) *Format*: When formatting the toolkits, we considered cost, available funding, end-users' technical needs, and diversity and inclusion. We used design features known to facilitate the use of implementation tools, such as hyperlinks, PDF formats, and diverse and realistic case studies [22]. We also followed guiding principles for sex and gender considerations recommended for implementation interventions [23].

2) *Timeline*: When estimating the time required to create the toolkits, preparatory activities (e.g., applying for funding and completing the research ethics submission) were considered, as was the time required to disseminate the final products.

3) *Resources*: The content and format of the toolkits influenced the resources and personnel required for development. The co-design team members, who had subject matter expertise, generated the toolkit content. Graphic designers, videographers, a website developer and English to French translators were hired to improve the toolkits' accessibility and aesthetics. Individuals living with neurological conditions were hired as models for video and photo shoots. Our institutions' legal services were consulted for front matter content (e.g., disclaimers).

4) *Sustainability*: When creating a knowledge translation tool, such as a toolkit, it is important to consider the resource's sustainability. Questions we considered included who holds the copyright for the resource (e.g., the project lead, the co-design team, the funding body, or the institution), and who would assume responsibility for resource updates and ongoing costs (e.g., website hosting)?

Results

The **FES Toolkit** took 2.5 years to create, from writing grant applications to creating and revising the toolkit content to disseminating the final version. Educational grants were received from the Paralyzed Veterans of American and the Canadian Institutes of Health Research to fund the project. The FES Toolkit is a 98-page manual available in PDF and EPUB formats. It includes 27 instructional videos, 9 case studies, 9 hands-on activities, 6 quizzes and 6 group learning sessions. It has a flexible design, enabling users to navigate between 11 modules (Tab. 1) depending on their baseline knowledge and learning goals. The hands-on activities can be completed individually or in groups to support collaborative learning.

Table 1: FES Toolkit Modules

Module Title
Introductory content: Why it the toolkit needed?
1. The Who, What, When & How of FES
2. What Should Clinicians Know about Currents?
3. Electrical Stimulation Parameters Explained!
4. What Does FES do to Muscles and Nerves?
5. How to Prepare Patients for FES
6. How to Position Electrodes
7. How to Plan a FES Application
8. A How-to Guide: Common Lower Limb Applications
9. A How-to Guide: Common Upper Limb Applications
10. How Can Electrical Stimulation Reduce Spasticity?
11. Strategies to Successfully Implement FES in Practice

The **FES Cycling Toolkit** took 2 years to produce, from research ethics submission to dissemination and manuscript submission [13]. Funding for the project was secured through a provincial grant (i.e., Campus Alberta Neuroscience) in partnership with the Alberta Paraplegic Association and the University of Alberta. Two FES Cycling Toolkits were created; one for clinicians and one for patients and caregivers. The toolkits exist in two forms: website and PDF. These toolkits contain information written in both scientific and lay language about FES cycling benefits and risks, patient screening, parameters, muscle selection, outcome measures, patient preparation, technical setup, transitions in care, and sustainability. The FES Cycling Toolkit is supplemented with practice resources, including checklists, glossaries and a logbook. Personal experiences from individuals living with SCI about FES cycling during acute care were documented through a video and quotes were distributed throughout the toolkits.

Discussion

In this article, we outlined the process for developing toolkits on FES. Identifying a guiding framework, principles and design considerations facilitated decision-making about the development process. The FES Toolkit and FES Cycling Toolkit were designed with the Canadian healthcare context in mind; however, these toolkits could be adapted to other contexts for use in countries or healthcare settings (i.e., step 3 of the Knowledge-to-Action Framework).

The Knowledge-to-Action Framework outlines the next steps for the toolkits in the knowledge translation process [14]. Monitoring toolkit use (e.g., reach and adoption) and evaluating the clinical and service outcomes as a result of that use (e.g., impact of the toolkits on therapist knowledge, FES provision, patient outcomes) are important next steps in the process. The FES Toolkit and FES Cycling Toolkit are being investigated as implementation interventions that may impact therapist decision-making and behaviour.

A greater emphasis on implementation science is needed in the FES field in order to bridge the gap between FES research and neurorehabilitation practice. Toolkits are one implementation strategy that may help bridge that gap.

Conclusions

We described the processes used to create the FES Toolkit and FES Cycling Toolkit and demonstrated the value of following a guiding framework, principles and design considerations. This article is a resource for how to create a toolkit to increase the adoption of FES or other technology for neurorehabilitation.

Acknowledgement

Funding was provided by the Paralyzed Veterans of America, Canadian Institutes of Health Research and the

Canada Research Chairs Program to KEM. HJR received funding from Campus Alberta Neuroscience, Alberta Paraplegic Association and the University of Alberta. We appreciate the involvement of the co-design teams in creating the toolkits.

References

[1] Government of Canada. *Introduction: Mapping Connections: An understanding of neurological conditions in Canada.* 2014.

[2] Teasell, R., Salbach, NM. et. al.: Canadian stroke best practice recommendations: rehabilitation, recovery and community participation following stroke. Part one: rehabilitation and recovery following stroke; 6th edition update 2019, *Int. J. Stroke.,* vol. 15, pp. 763-788, October 2020

[3] SCIRE Professional-Spinal Cord Injury Research Evidence. *Spinal Cord Injury Research Evidence.* 2021.

[4] Alt Murphy, M., Pradhan, S. et. al.: Uptake of technology for neurorehabilitation in clinical practice: a scoping review, *Phys. Ther.,* vol. 104, pp. pzad140, February 2024

[5] Auchstaetter, N., Luc, J. et al.: Physical therapists' use of functional electrical stimulation for clients with stroke: frequency, barriers, and facilitators, *Phys. Ther.,* vol. 96, pp. 995-1005, July 2016

[6] Salbach, NM., Wood-Dauphinee, S. et al.: Facilitated interprofessional implementation of a physical rehabilitation guideline for stroke in inpatient settings: process evaluation of a cluster randomization trial, *Implement. Sci.,* vol. 12, pp. 100, August 2017

[7] Abouzakhm, N., Choy, S. et al.: Evaluating the validity of a functional electrical stimulation clinical decision making tool: a qualitative study, *Front. Neurol.,* vol. 13, pp. 1001123, November 2022

[8] Austin, TM., Graber, KC. et al.: Variables influencing physical therapists' perceptions of continuing education, *Phys. Ther.,* vol. 87, pp. 1023-1036, August 2007

[9] Reeves, S., Fletcher, S. et al.: Interprofessional online learning for primary healthcare: findings from a scoping review, *B. M. J. Open.,* vol. 7, pp. e016872, August 2017

[10] Yamada, J., Shorkey, A. et al.: The effectiveness of toolkits as knowledge translation strategies for integrating evidence into clinical care: a systematic review, *B. M. J. Open.,* vol. 5, pp. e006808, April 2015

[11] Musselman, KE., Marquez Chin, C. et al.: *Functional Electrical Stimulation (FES) Toolkit, first ed.* 2024.

[12] Jervis-Rademeyer, H., Gautam, S. et al.: *FES Cycling Toolkit.* 2024.

[13] Jervis-Rademeyer, H., Gautam, S. et al.: Development of a functional electrical stimulation cycling toolkit for spinal cord injury rehabilitation in acute care hospitals: a participatory action approach, *PLOS. One.,* vol. 20, pp. e0316296, February 2025

[14] Graham, ID., Logan, J. et al.: Lost in knowledge translation: time for a map?, *J. Contin. Educ. Health. Prof.,* vol. 26, pp. 13-24, Winter 2006

[15] Lai, CH., Chang WH-S. et al.: Effects of functional electrical stimulation cycling exercise on bone mineral density loss in the early stages of spinal cord injury, *J. Rehabil. Med.,* vol. 42, pp. 150-154, February 2010

[16] Tedesco Triccas, L., Donovan-Hall, M. et al.: A nation-wide survey exploring the views of current and future use of functional electrical stimulation in spinal cord injury, *Disabil. Rehabil.,* vol. 18, pp. 752-762, August 2023

[17] Walker, DM., Fletcher-Smith, J. et al.: Designing a trial of early electrical stimulation to the stroke-affected arm: qualitative findings on the barriers and facilitators, *Br. J. Occup. Ther.,* vol. 85, pp. 181-186, September 2021

[18] Bulley, C., Meagher, C. et al.: Development of clinical guidelines for service provision of functional electrical stimulation to support walkin: mixed methods exploration of stakeholder views, *B. M. C. Neurol.,* vol. 21, pp. 263, July 2021

[19] Musselman, KE., Mayhew, M. et al.: Physical and occupational therapists' learning needs and preferences for education on functional electrical stimulation: a qualitative descriptive study, *Artif. Organs.,* vol. 48, pp. 1018-1030, September 2024

[20] Katsulis, Z., Ergai, A. et al.: Iterative user centered design for development of a patient-centered fall prevention toolkit, *Appl. Ergon.,* vol. 45, pp. 117-126, September 2016

[21] Van der Scheer, JW., Goosey-Tolfrey, VL. Functional electrical stimulation cycling exercise after spinal cord injury: a systematic review of health and fitness-related outcomes, *J. Neuroeng. Rehabil.,* vol. 18, pp. 99, June 2021

[22] Salbach, NM., Solomon, P. et al.: Design features of a guideline implementation tool designed to increase awareness of a clinical practice guide to HIV rehabilitation: a qualitative process evaluation, *J. Eval. Clin. Pract.,* vol. 25, pp. 648, August 2019

[23] Adisso, EL., Zomahoun, HTV. et al.: Sex and gender considerations in implementation interventions to promote shared decision making: a secondary analysis of a Cochrane systematic review, *PLOS. One.,* vol. 15, pp. e0240371, October 2020

Author's Address

Kristin Musselman PT, PhD
Department of Physical Therapy and Rehabilitation Sciences Institute, University of Toronto
KITE Research Institute-University Health Network
kristin.musselman@utoronto.ca
https://www.physicaltherapy.utoronto.ca/kristin-musselman

Strategies to Improve Use, Knowledge, and Confidence of Functional Electrical Stimulation in Cerebral Palsy Rehabilitation

Nezon E[1,2], Ho ES[3,4], Munce S[1,2,5,6], Marquez-Chin C[2,7], Musselman KE[1,2,8]

[1]Rehabilitation Sciences Institute, University of Toronto, Toronto, ON, Canada

[2]KITE Research Institute, University Health Network, Toronto, ON, Canada

[3]Department of Occupational Science and Occupational Therapy, University of Toronto, Toronto, ON, Canada

[4]Division of Plastic and Reconstructive Surgery, The Hospital for Sick Children, Toronto, ON, Canada

[5]Holland Bloorview Kids Rehabilitation Hospital, Bloorview Research Institute, Toronto, ON, Canada

[6]Institute of Health Policy, Management and Evaluation, University of Toronto, Toronto, ON, Canada

[7]Institute of Biomedical Engineering, University of Toronto, Toronto, ON, Canada

[8]Physical Therapy Department, University of Toronto, Toronto, ON, Canada

Abstract: *Functional Electrical Stimulation (FES) is underutilized by Canadian physical and occupational therapists (PTs, OTs) in pediatric neurorehabilitation. Despite the demonstrated feasibility, effectiveness, and safety of pediatric FES, there are mixed clinician perspectives on suitability, a lack of access to FES equipment, and a lack of knowledge and confidence cited among PTs and OTs. We aimed to increase PTs' and OTs' knowledge and confidence in using FES through a six-week online course that included lectures, mentoring, and provision of FES devices. Seventeen PTs and one OT working in public or private cerebral palsy (CP) rehabilitation participated. Valid questionnaires of FES knowledge, confidence and use, as well as the Technology Acceptance Model 2 (TAM2) Questionnaire, were administered before and immediately after the course. Significant increases in participants' knowledge, confidence, and use of FES, as well as in the TAM2 Results Demonstrability domain, were found, while other factors related to technology acceptance remained unchanged. The findings suggest that implementation strategies targeting FES knowledge and confidence can help bridge the knowledge-practice gap in CP rehabilitation.*

Keywords: *Implementation intervention, cerebral palsy, functional electrical stimulation, physical and occupational therapists*

Introduction

Cerebral palsy (CP), resulting from a brain injury that occurs during pregnancy or birth, is one of the most common childhood motor disorders worldwide and represents the most prevalent lifelong physical disability globally. Research on functional electrical stimulation (FES) in individuals with cerebral palsy is growing. In rehabilitation practices for children and teens with CP, there is increasing evidence supporting the effectiveness of FES. Studies have demonstrated its feasibility and efficacy in addressing impairments and activity limitations across the upper and lower limbs as well as the trunk [1], [2], [3]. Despite evidence highlighting the effectiveness and safety of FES in the rehabilitation of children with CP, its application in Canadian clinical pediatric settings remains limited [4]. Similarly, parents whose children participated in FES studies echoed a lack of access to FES treatments in Canadian rehabilitation services; however, they reported notable benefits in physical, functional, and psychological domains in their children following FES treatment [5].

A survey and qualitative interviews with clinicians and parents of children with CP have identified various barriers and facilitators influencing the adoption of FES [4], [5], [6]. From the perspective of physiotherapists (PTs) and occupational therapists (OTs), several obstacles hinder the use of FES, including insufficient access to necessary equipment, a lack of knowledge and skills related to FES, and the time demands required to become proficient in its use [6]. Although clinician FES confidence in pediatrics has not been well researched, therapist factors such as preference for alternative interventions, clinician skill level, and lack of confidence have been reported by clinicians who work in adult neurological populations [7]. Additionally, some clinicians perceive that FES may not be suitable for young patients [4]. However, they also noted several facilitating factors to implementation, including educational resources, peer collaboration, and equipment availability [6]. There is a need to address existing barriers and leverage facilitators to promote the implementation of FES; PTs and OTs also report that there is a need to improve educational initiatives of FES for healthcare providers.

The barriers to FES use in pediatric rehabilitation can be addressed using tailored, evidence-based implementation strategies. Additionally, facilitators can be leveraged to improve the implementation of an intervention. The Expert Recommendations for Implementing Change (ERIC) framework [8], integrated with behaviour change

strategies, such as those found in the Behaviour Change Techniques (BCT) Taxonomy [9], can provide a more tailored approach to implementation [10]. These strategies and behaviour change actions are tailored in this study to address the previously mentioned barriers to implementation of FES in pediatric clinical practice. Informed by the ERIC framework and BCT Taxonomy, we designed an FES implementation intervention targeting PTs and OTs who work in CP rehabilitation. As a result of the needs identified and the importance of using an implementation framework, the objective of this study was to evaluate the immediate effect of the six-week FES implementation intervention on pediatric PTs' and OTs' FES knowledge, confidence, acceptance and use in CP rehabilitation. We hypothesized that FES knowledge and confidence will increase immediately following the intervention, while FES use will be increased at the 6-month follow-up.

Material and Methods

Study design: This study is part of a larger clinical trial investigating FES implementation in pediatric rehabilitation (ClinicalTrials.gov NCT06689007). The present study follows a pre-post design with repeated measures at baseline and immediately after the six-week implementation intervention. Ethical approval was obtained from the Research Ethics Board of the University of Toronto (REB#46640).

Implementation intervention: The implementation intervention integrated four established strategies from the ERIC framework: (1) educational meetings, (2) ongoing consultation, (3) technical assistance, and (4) modifications to physical structures and equipment [8]. This was coupled with the BCT Taxonomy to outline specific actions related to each strategy [9], [10]. For example, the ERIC strategy of conducting educational meetings was linked to the behaviour change actions of a) instruction on how to perform a behaviour, b) demonstration of the behaviour, c) verbal persuasion to boost self-efficacy, and d) feedback on behaviour. The intervention consisted of a six-week online course facilitated by Senior Author KEM, which included weekly pre-recorded lectures, interactive sessions, group mentoring, and a reflective assignment. Participants also received an FES Toolkit [11], which outlined theoretical and practical information to support them in using FES in their clinical practice, and an FES device to keep if their place of work did not have one.

Study participants: Participants were recruited via convenience sampling. A target sample size of 11 participants was calculated using G*Power software based on the expected change in FES confidence [12]. Accounting for a 40% dropout rate, 18 PTs or OTS were recruited. Participants were included if they were a licensed PT or OT in Canada, with at least 20% of their caseload consisting of clients with CP over the past year and reported minimal or no use of neuromuscular electrical stimulation (NMES) or FES in their practice and no prior participation in a FES continuing education course. Participants were also required to be available for a six-week online FES course in English that ran from October 18, 2024, to November 28, 2024.

Data collection: Data collection prior to the intervention and immediately following the intervention occurred via individual virtual meetings with Zoom videoconferencing. Four quantitative questionnaires were administered by a researcher (EN). These questionnaires were:
(1) An FES Knowledge Quiz that evaluated participants' understanding of course content. The quiz consisted of 18 multiple-choice questions that queried clinical application of FES (e.g., To stimulate thumb abduction, which of the following combination of parameters would be most appropriate?). Participants chose one of four possible multiple-choice responses (i.e., A, B, C or D), with only one pre-determined correct response.
(2) An FES Confidence Questionnaire, which followed standardized instructions for participants to rate their confidence in using FES on an 11-point ordinal scale (0 = not at all confident, 10 = completely confident). Twelve questions about decision-making for FES application were posed (e.g., "As of now, how confident are you that you can select the appropriate waveform for a FES application?)
(3) A pre-existing survey of FES use [4] was adapted to be used in the context of CP rehabilitation. This questionnaire asked participants to rate their FES use on a 6-point Likert scale that spanned 'Never (0%)' to 'Most of the time (>80%)'. Nineteen possible therapeutic or orthotic uses of FES were queried (e.g., How frequently do you use motor level stimulation (NMES or FES) for the therapeutic goal of improving standing function, for your patients with CP).
(4) An adapted Technology Acceptance Model 2 (TAM2) questionnaire [13] that asked 33 questions regarding participants' acceptance of FES technology and intentions to use FES. The questions covered the following TAM2 domains: Perceived Ease of Use, Perceived Usefulness, Subjective Norm, Voluntariness, Job Relevance, Image, Output Quality, Intention to Use, Results Demonstrability and Proposed Facilitating Conditions.

Data analysis: Questionnaire scores were determined according to each questionnaire's instructions. For Questionnaire (1), participants received a score of 1 for each correct response and 0 for each incorrect response. Scores were summed for a total score out of 18. For Questionnaire (2), the total score was calculated by summing the responses on the 11-point ordinal scale, resulting in a total score out of 120. Each participant's total score was then divided by 12. Index scoring was used to convert the Likert scale of the Survey of FES Use to numerical values. Scores on the TAM2 were calculated for each domain and normalized according to the number of questions contributing to each domain. Mean scores (± standard deviation) were calculated for each questionnaire. The Shapiro-Wilk test was used to assess the normality of each data set. A paired t-test or a Wilcoxon Signed-Rank

Test was used to compare pre- and post-intervention scores, as appropriate. All statistical analyses were performed using SPSS® Statistics 27 (IBM) and alpha was set to 0.05.

Results

Seventeen PTs and one OT were recruited for this study from five practice locations (three private and two public healthcare settings).

Following the FES implementation intervention, participants' scores on the **FES Knowledge Quiz and FES Confidence Questionnaire** increased significantly ($p<0.001$) (see Figures 1A and 1B, respectively). **Survey of FES Use:** Pre-intervention, participants reported between 'never' or 'most of the time' using FES to address a variety of therapeutic and orthotic goals for clients with CP. Post-intervention, 9/18 participants reported greater use of FES for at least one therapeutic or orthotic goal. This amounted to a small, but significant ($p<0.001$), increase in the mean FES use score (i.e. 4.3±9.5 increase in score). **TAM2:** With respect to FES technology acceptance, only the Results Demonstrability domain of the TAM2 Questionnaire showed a significant increase from pre- to post-intervention (pre-score: 1.3±0.8, post-score: 1.9±0.8, $p=0.012$). All other domains showed no change immediately post-intervention: Perceived Ease of Use ($p=0.600$), Perceived Usefulness ($p=0.265$), Subjective Norm ($p=0.449$), Voluntariness ($p=0.253$), job Relevance ($p=0.111$), Image ($p=0.820$), Output Quality ($p=0.253$), Intention to Use ($p=0.127$), and Proposed Facilitating Conditions ($p=0.944$).

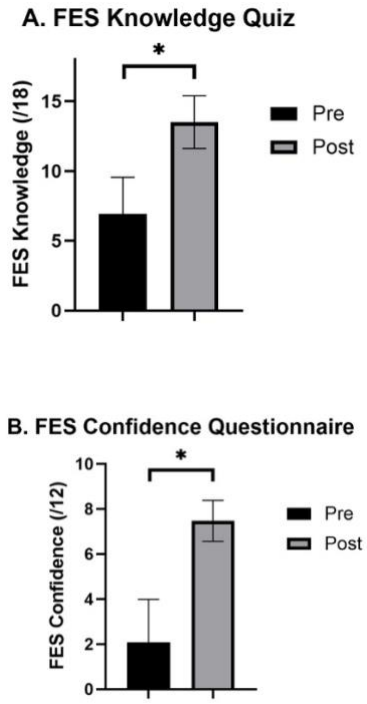

Figure 1: Mean (±1 standard deviation) scores on the FES Knowledge Quiz (1A) and the FES Confidence Questionnaire (1B). *$p<0.05$

Discussion

The results suggest the implementation intervention led to an immediate increase in participants' knowledge and confidence of FES, as well as a small increase in their reported use of FES in clinical practice. Overall, participants' acceptance of FES technology did not change with the implementation intervention. However, a significant change was seen in the Results Demonstrability domain, which suggests that participants acquired a more positive attitude about the usefulness of FES technology through the implementation intervention. Altogether, the findings highlight the potential for tailored implementation strategies to facilitate FES use in clinical practice and bridge the research to practice gap.

The increase in FES confidence with the implementation intervention was not surprising as we have reported this finding previously in PTs and OTs working in adult neurorehabilitation [12]. An increase in confidence in applying FES is likely key for therapists to implement FES in their clinical practice. Belief in one's ability to execute a behaviour (i.e., self-efficacy) greatly impacts one's motivation to engage in the behaviour and one's actual performance of the behaviour [14]. While we expected FES use to increase with the intervention, in large part due to increased self-efficacy in FES application, the increase was small. Change in clinical practice behaviour takes time; it is possible that a greater change will be observed six-months post-intervention, which is the final data collection point for the larger clinical trial.

Although FES knowledge and confidence increased post-intervention, participants' perceptions regarding aspects of FES technology use, such as perceived ease of use and job relevance, did not change. This finding may reflect the persistence of attitudes that could prevent the clinical adoption of FES. However, this finding likely also reflects the positive attitudes about FES that participants possessed at study outset. PTs and OTs who were not interested in using FES in their clinical practice would likely not have volunteered for this study.

Conclusions

The implemented intervention resulted in an increase in therapists' knowledge, confidence, and use of FES. Participants' acceptance of FES technology remained unchanged, except in the Results Demonstrability domain. Future FES implementation interventions should incorporate tailored implementation strategies based on the known barriers and facilitators to FES use.

Acknowledgement

The authors acknowledge funding to KEM from the Cass Family Grant for Catalyzing Access and Change, Coriat Family Research Fund, and Canada Research Chairs Program. EN was supported by scholarships from the Branch Out Neurological Foundation, Peterborough K.M. Hunter Charitable Foundation Graduate Award, Toronto Rehabilitation Institute Student Scholarship, Diane Gasner Graduate Scholarship, and Ruth Bradshaw Graduate Award. We would also like to express our gratitude to the study participants.

References

[1] K. E. Musselman, P. Manns, J. Dawe, R. Delgado, and J. F. Yang, "The Feasibility of Functional Electrical Stimulation to Improve Upper Extremity Function in a Two-year-old Child with Perinatal Stroke: A Case Report," *Physical & Occupational Therapy In Pediatrics*, vol. 38, no. 1, pp. 97–112, Jan. 2018, doi: 10.1080/01942638.2016.1255291.

[2] E. S. Park, C. I. Park, H. J. Lee, and Y. S. Cho, "The effect of electrical stimulation on the trunk control in young children with spastic diplegic cerebral palsy," *J Korean Med Sci*, vol. 16, no. 3, p. 347, 2001, doi: 10.3346/jkms.2001.16.3.347.

[3] I. Moll *et al.*, "Functional electrical stimulation of the ankle dorsiflexors during walking in spastic cerebral palsy: a systematic review," *Develop Med Child Neuro*, vol. 59, no. 12, pp. 1230–1236, Dec. 2017, doi: 10.1111/dmcn.13501.

[4] N. Auchstaetter *et al.*, "Physical Therapists' Use of Functional Electrical Stimulation for Clients With Stroke: Frequency, Barriers, and Facilitators," *Physical Therapy*, vol. 96, no. 7, pp. 995–1005, Jul. 2016, doi: 10.2522/ptj.20150464.

[5] E. Swaffield, J. F. Yang, P. Manns, K. Chan, and K. E. Musselman, "Parents' perceptions of functional electrical stimulation as an upper limb intervention for young children with hemiparesis: qualitative interviews with mothers," *BMC Pediatr*, vol. 22, no. 1, p. 346, Dec. 2022, doi: 10.1186/s12887-022-03403-1.

[6] K. E. Musselman, E. Provad, A. Djuric, D. Bercovitch, I. Yuen, and K. J. Kane, "Exploring the Experiences and Perceptions of Pediatric Therapists who use Functional Electrical Stimulation in their Clinical Practice," *Physical & Occupational Therapy In Pediatrics*, pp. 1–21, Apr. 2023, doi: 10.1080/01942638.2023.2197053.

[7] L. Tedesco Triccas, M. Donovan-Hall, B. Dibb, and J. H. Burridge, "A nation-wide survey exploring the views of current and future use of functional electrical stimulation in spinal cord injury," *Disability and Rehabilitation: Assistive Technology*, vol. 18, no. 6, pp. 752–762, Aug. 2023, doi: 10.1080/17483107.2021.1916631.

[8] B. J. Powell *et al.*, "A refined compilation of implementation strategies: results from the Expert Recommendations for Implementing Change (ERIC) project," *Implementation Sci*, vol. 10, no. 1, p. 21, Dec. 2015, doi: 10.1186/s13012-015-0209-1.

[9] S. Michie *et al.*, "The Behavior Change Technique Taxonomy (v1) of 93 Hierarchically Clustered Techniques: Building an International Consensus for the Reporting of Behavior Change Interventions," *ann. behav. med.*, vol. 46, no. 1, pp. 81–95, Aug. 2013, doi: 10.1007/s12160-013-9486-6.

[10] S. McHugh, J. Presseau, C. T. Luecking, and B. J. Powell, "Examining the complementarity between the ERIC compilation of implementation strategies and the behaviour change technique taxonomy: a qualitative analysis," *Implementation Sci*, vol. 17, no. 1, p. 56, Aug. 2022, doi: 10.1186/s13012-022-01227-2.

[11] Musselman KE *et al.*, "Functional Electrical Stimulation (FES) Toolkit," 2024.

[12] K. E. Musselman, M. Mayhew, H. Somal, N. L. Benn, N. M. Salbach, and S. Switzer-McIntyre, "Physical and occupational therapists' learning needs and preferences for education on functional electrical stimulation: A qualitative descriptive study," *Artificial Organs*, vol. 48, no. 9, pp. 1018–1030, Sep. 2024, doi: 10.1111/aor.14756.

[13] V. Venkatesh and F. D. Davis, "A Theoretical Extension of the Technology Acceptance Model: Four Longitudinal Field Studies," *Management Science*, vol. 46, no. 2, pp. 186–204, Feb. 2000, doi: 10.1287/mnsc.46.2.186.11926.

[14] A. Bandura, *Self-efficacy: the exercise of control*. New York: W.H. Freeman, 1997.

Author's Address

Elina Nezon
Rehabilitation Sciences Institute, University of Toronto, and KITE Research Institute, University Health Network,
Toronto, ON, Canada
Elina.provad@mail.utoronto.ca
https://sites.google.com/view/scimoblab/home

Session 9:
Current Challenges and Future Directives of FES 2

From innovative ideas to clinical trials - opportunities and obstacles in translational research on neural implants

Stieglitz T[1,2,3], Martens J[1,2], Baslan Y[1,2], Čvančara P[1,2]

[1]Lab. for Biomedical Microtechnology, Dept. Microsystems Eng.-IMTEK, University of Freiburg, Germany
[2]BrainLinks-BrainTools Center, University of Freiburg, Germany
[3]Bernstein Center Freiburg, University of Freiburg, Germany

Abstract: *Progress in rehabilitation goes hand in hand with the development of assistive devices. While a plethora of new tools are presented in the context of engineering and fundamental neuroscience research, only a few approaches proceed to first-in-human clinical trials. The authors share their experience in translational research using the example of the transverse intrafascicular multichannel electrode (TIME). While the initial ideas and evaluations in translational research are identical compared to fundamental neuroscientific studies, the following steps vary significantly. These stages include verification and validation measures and experiments, which focus more on engineering practices over traditional scientific knowledge generation. Large animal models are a necessary intermediate step towards clinical trials, along with rigorous tests to prove effective cleaning and efficient sterilization of the devices. The European Medical Device Regulation poses organizational challenges that need to be addressed from the beginning of any translational research. If engineers, fundamental and clinical neuroscientists and surgeons closely collaborate and share responsibility, first-in-human clinical trials can also be conducted in Europe and can set standards for innovative treatment developments using neural implants.*

Keywords: *clinical trial, essential requirements, validation, microsystems, materials*

Introduction

New and innovative devices quite often do not come from a large unmet need of society but emerge as a business idea as has been the case in cars, personal computers and smartphones. The needs come later with the arrival of the devices. In the case of medicine and medical devices, the desire is to develop new treatments and devices to cure diseases, alleviate harm and to improve quality of life. Engineers implement their expertise in technology and material development to make important contributions and are advised to include medical expertise from the start. This helps prevent the creation of solutions for non-existing problems.

In the case of neural implants, neural engineers, clinical neuroscientists, surgeons and various healthcare professionals from rehabilitation collaborate to develop and evaluate new and innovative approaches to improve the quality of life in subjects who got paralysed after spinal cord injury or stroke, who lost limbs after amputation, or in treatments in which electrical stimulation shall substitute pharmaceutical treatments [1]. In contrast to fundamental research, in which the primary focus is the generation of knowledge, translational research begins with a working hypothesis of novel methods that are ultimately to be evaluated in humans.

Over the last two decades, the use of neural implants to deliver sensory feedback after amputation [2] and improve performance and acceptance of both hand and artificial leg prostheses [3] has been the focus of intense translational research. Scientific results are convincing in clinical trials on selected subjects, but they are not yet ready to be transferred into clinical practice [4].

When analyzing the process of translational research, which progresses from initial ideas to the design of treatment scenarios with accompanying devices, through animal experiments, and into clinical trials, it becomes clear that the scientific aspect is just one of many factors that determine success. Various other elements can act as insurmountable hurdles on the way to developing a novel treatment or bringing a medical product to market [5,6]. Overcoming these challenges requires a mindset with complementary expertise distinct from that of pure fundamental research. This includes the ability to convince collaborators, acquire funding, identify regulatory boundary conditions, select the right components and collect all the needed expertise to successfully conduct translational research (Fig. 1).

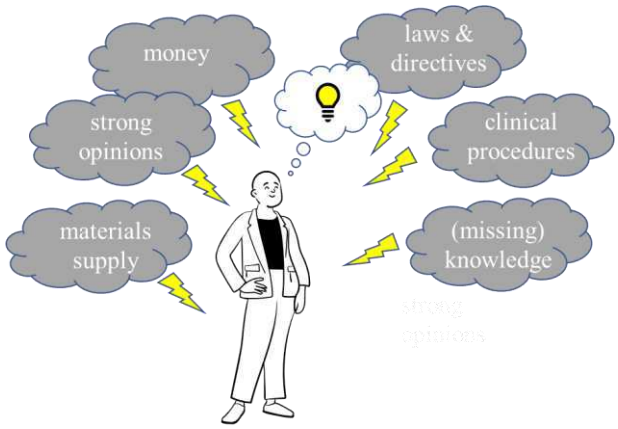

Figure 1: Potential obstacles in translational research.

The authors wish to share their experience in advancing from an initial idea to conducting first-in-human clinical trials. The experience has been gained under the regulations of the European Union, where an "investigational device exemption" status, as established in

the approval process of the U.S. Food and Drug Administration (FDA), does not yet exist. The "Medical Device Regulation" (MDR; 2017/745/EU), applicable to all member states of the European Union, addresses any "hypothesis-driven, investigator-initiated clinical trial" not intended for market placement under the term "other clinical trial" (Art. 82, MDR). The procedural details of such a study are delegated to the relevant national authority of the country where the study is conducted.

Material and Methods

Delivery of sensory feedback to alleviate phantom limb pain after amputation of the hand was a research objective in the TIME project [7]. The hypothesis was that spatially selective electrical stimulation of the remaining sensory nerves in the stump would provide an intuitive perception of the missing limb and alleviate phantom limb pain more effectively than existing non-invasive and invasive approaches. This new neural micro-implant was termed the "transverse intrafascicular multichannel electrode" (TIME) to indicate its implantation method within its name. While the goal of a first-in-human clinical trial was clear from the beginning, expertise was not yet sufficiently established to recognize that documentation should already start in the "idea phase" to comply with quality management system (QMS) requirements to develop medical devices (ISO 13485 - Medical devices - Quality management systems - Requirements for regulatory purposes). However, different stages were already carefully scheduled (Table 1). The design and development of the TIME were done in an academic microsystems cleanroom. First TIME devices [8] showed superior spatial selectivity compared to cuff electrodes and longitudinal intrafascicular electrode arrays (LIFEs) [9]. Cytotoxicity and foreign body reactions were evaluated in the laboratories of the research partners in the consortium to identify and assess potential biological side effects. The selectivity of TIMEs was successfully evaluated in a pig model to meet the dimensions of human nerves in acute studies [10].

Table 1: Example of tests of neural implants at different stages in translational research. V&V: verification and validation

Stage	**Setting**	**Research focus**	**Tests**				
First device proto-type	engineering laboratory	technology	mechanical strength	electrical insulation	optical inspection	electro-chemical impedance	charge injection
Acute small animal model	neuroscience/ physiology laboratory	basic functionality	nerve signal recording	electrical stimulation thresholds	spatial selectivity	recruit-ment/activat ion properties	
Chronic small animal model	neuroscience/ physiology laboratory	performance over time	foreign body reaction	device stability	changes in device functionality	connection to "outside" electronics	
Second device prototype	engineering laboratory	system assembly and final size	system integrity with cables and connectors	mechanical	repeatable connection and connector stability	electrochem ical impedance	charge injection
Acute large animal model	neuroscience/ physiology laboratory	functionality in large nerve	electrical stimulation thresholds	spatial selectivity	recruitment/ac tivation properties	cable and connector handling	
Chronic large animal model	neuroscience/ physiology laboratory	performance over time	foreign body reaction	device stability	changes in device functionality	connection to "outside" electronics	connector stability
Device for clinical trials	engineering laboratory	manufacturing, verification and validation according to regulatory requirements	design dossier	risk analysis and usability	standard operating procedures for V&V	process validations (including cleansing and steriliza-tion)	
First-in-human clinical trials	(university) hospital	evaluation of the research hypothesis (new treatment paradigm)	surgical procedure	function	stability	patient feedback	post-explanta-tion assessment (patient and device)

Chronic studies lasting up to 30 days were then conducted [11] to demonstrate stability over the intended implantation period for the first-in-human clinical trial. The device for these studies needed to have the final dimensions intended for the human clinical trial, along with a robust and reliable assembly of cables and connectors for the planned percutaneous implantation in humans. However, for chronic pig experiments, fully implantable cables were preferred. The pig model posed serious challenges since their behaviours of rolling on the floor and scratching at walls required particular measures to protect the cables from damage that would not occur in humans. Experiments on human cadavers turned out to be extremely valuable in determining cable lengths and defining the standard operating procedures for human implantation [12]. Documentation, including standard operating procedures, lists of parts and components, and form sheets, was completed before manufacturing TIMEs for human implantation began. Procedures of our ISO 13485 quality management systems were fulfilled. Since the microsystems cleanroom was outside of this QMS, test structures were added to the manufacturing wafers to allow for the qualification of these components upon integration into the QMS. The final dossier with the documentation of all previous knowledge of the design phase, any technical investigation in the laboratory and all results from animal studies in rodents and pigs was assembled, and the series for clinical trials was manufactured and packaged in the medical device cleanroom (Fig. 2).

Figure 2: Cleanroom as infrastructure within an ISO 13485 quality management system in an academic research environment.

Medical devices' cleanroom status, processes which cannot undergo a final inspection, cleanliness of the devices after cleansing, and sterilization efficacy needed to be validated via accredited test laboratories. All documentation needed to be handed in via the clinical partner to the national legal authority for assessment. In this study, the TIME was not intended to be placed on the market as a medical device but a scientific hypothesis was to be investigated in the clinical trial. In such a “hypothesis-driven investigator-initiated clinical trial”, the manufacturer of the TIME is responsible for fulfilling the “essential requirements” to prove safety, but does not take the role of a “sponsor”, which a manufacturing company usually does. The clinical partner has to overtake this sponsor role and with it the full responsibility of this clinical study. Since the implantation took place in Rome, Italy, the Italian Ministry of Health was the responsible authority. After approval and clearance, the clinical study with a duration of 30 days was conducted as a “safety study” according to international regulations. The devices were explanted after the end of the study to evaluate device stability from the engineering perspective.

Results

A series of TIMEs was manufactured, packaged and sterilized (Fig. 3), and transferred to the clinical partners.

Figure 3: TIME implant manufactured, packaged and sterilized for an investigator-initiated clinical trial under ISO 13485 QMS. Labels contain required information according to regulatory needs. Transport and holding frame needed to be codeveloped for deployment.

The clinical trial was completed, demonstrating a reduction of phantom limb pain during the implantation and stimulation period, as well as the capability to detect object shape and compliance through sensory feedback from a sensorized hand prosthesis [13].
Post-explantation analysis of TIMEs after the 30-day study revealed serious adhesion loss in the metallization [14]. As a result, changes in process technology details were implemented to improve stability and functionality over six months of studies [15].
While percutaneous cables worked well for the scheduled implantation times, they remain a weak point for further

transfer and translation towards chronic implants in which a fully implantable solution is essential.

Discussion

Translational and collaborative research in an academic environment is able to conduct first-in-human clinical trials if boundary conditions [5,6] and requirements of regulatory affairs are addressed from the outset of the project. To meet timelines, ethics committees and legal authorities need to be engaged early in the process. Underestimated challenges include supply chains in materials and components. Some companies are hesitant to comply with medical device regulation requirements and might prefer to stop supplying materials and components when they realize that their orders might be used in devices for clinical trials, even if the MDR poses no additional requirements on them. If commercialization through a start-up is pursued, it may become necessary to manufacture these materials and components independently. For all these reasons, creating an ecosystem that enables the development of active implantable devices under quality management system conditions within an academic environment enhances translational research efforts and strengthens both science and the economy in Europe.

Conclusions

Translational research can thrive in an academic environment when documentation and regulatory requirements are viewed not as burdens but as opportunities to improve quality, using standardized measurements with calibrated devices even for fundamental research questions. Education in quality management for medical devices equips young researchers for industry positions and contributes to the creation of an ecosystem to increase successful first-in-human clinical trials with new and innovative devices. This is important, particularly in the European research area, in which an investigational device exemption is still absent.

Acknowledgement

The development, preclinical and clinical evaluation of the TIME electrodes work has been done under the European projects TIME (FP 7, CP-FP-INFSO 224012), EPIONE (FP7-HEALTH-2013-INNOVATIO-1602547) and NEBIAS (FP7, CP-FP-INFSO 318478). We thank all the partners for their fruitful collaboration. Other parts of this work were partly supported by BrainLinks-BrainTools which is funded by the Federal Ministry of Economics, Science and Arts of Baden-Württemberg within the sustainability program for projects of the excellence initiative II.

References

[1] Olofsson, P.S., Bouton, C.: Bioelectronic medicine: an unexpected path to new therapies. *J Intern Med*., vol. 286(3), pp.237-239, Sep 2019

[2] Graczyk, E., et al.: Clinical Applications and Future Translation of Somatosensory Neuroprostheses, J Neurosci., vol. 44(40), e1237242024, Oct 2024

[3] Farina, D., et al.: Toward higher-performance bionic limbs for wider clinical use. Nat Biomed Eng., vol. 7(4), pp. 473-485

[4] Malešević, N., Antfolk, C.: Sensory feedback in upper limb prosthetics: advances and challenges. Nat Rev Neurol., vol. 20(8), pp. 449-450, Aug. 2024

[5] Borton, D.A. et al.: Developing Collaborative Platforms to Advance Neurotechnology and Its Translation. *Neuron*, vol. 108(2), pp. 286-301 Oct. 2020

[6] Stieglitz, T. Of Man and Mice: Translational Research in Neurotechnology. Neuron, vol. 105(1), pp.12-15. Jan 2020

[7] Stieglitz, T. et al.: Development of a neurotechnological system for relieving phantom limb pain using transverse intrafascicular electrodes (TIME), Biomed Tech (Berl), vol. 57(6), pp. 457-465, Dec 2012

[8] Boretius, T., et al.: A transverse intrafascicular multichannel electrode (TIME) to interface with the peripheral nerve. Biosens Bioelectron., vol. 26(1), pp. 62-69, Sept 2010

[9] Badia, J., et al.: Comparative analysis of transverse intrafascicular multichannel, longitudinal intrafascicular and multipolar cuff electrodes for the selective stimulation of nerve fascicles. *J Neural Eng*., vol. 8(3), 036023, Jun 2011

[10]Kundu, A., et al.: Stimulation selectivity of the "thin-film longitudinal intrafascicular electrode" (tfLIFE) and the "transverse intrafascicular multi-channel electrode" (TIME) in the large nerve animal model, IEEE Trans Neural Syst Rehabil Eng., vol. 22(2), pp. 400-410, Mar 2014

[11]Harreby, K.R., et al.: Subchronic stimulation performance of transverse intrafascicular multichannel electrodes in the median nerve of the Göttingen minipig, Artif Organs, vol. 39(2), pp. E36-48, Feb 2015

[12]Krähenbühl, S.M., Čvančara, P., et al.: Return of the cadaver: Key role of anatomic dissection for plastic surgery resident training. Medicine (Baltimore), vol. 96(29), e7528, Jul 2017

[13]Raspopovic, S., et al.: Restoring natural sensory feedback in real-time bidirectional hand prostheses, Sci Transl Med., vol. 6(222):222ra19, Feb 2014

[14]Čvančara, P., et al.: Stability of flexible thin-film metallization stimulation electrodes: analysis of explants after first-in-human study and improvement of in vivo performance. J Neural Eng. vol. 17(4), 046006, Jul 2020

[15]Čvančara, P., et al.: Bringing sensation to prosthetic hands—chronic assessment of implanted thin-film electrodes in humans. npj Flex Electron., vol. 7, 51, Nov. 2023

Author's Address

Thomas Stieglitz
Laboratory for Biomedical Microtechnology, Department of Microsystems Engineering-IMTEK & BrainLinks-BrainTools Center, Albert-Ludwig-University Freiburg, Georges-Koehler-Allee 201, 79110 Freiburg, Germany
thomas.stieglitz@imtek.uni.freiburg.de
https://www.imtek.de/bmt

Overview: Providing functional electrical stimulation to people with walking disabilities in Austria

Ullrich, C.

Paul Bständig GmbH, Vienna, Austria

Abstract: *Functional electrical stimulation (FES) is an innovative, rehabilitative and increasingly recognized healthcare measure for improving mobility in people with neurologically induced walking disabilities. In Austria, this technology is gaining in importance - especially for patients with impaired walking motor functions - like foot drop - following diseases such as multiple sclerosis, incomplete paraplegia or stroke. The presentation provides an overview of the use of FES in Austria using the example of peroneal nerve stimulation during walking and highlights the current care structures and challenges in the Austrian healthcare system. Current data and case examples will be used to illustrate both the medical and socio-legal aspects of supply with this kind of technical devices. The aim is to identify existing gaps in healthcare and provide impetus for more comprehensive, interdisciplinary coordinated care practice.*

Keywords: *Functional electrical Stimulation, foot drop, healthcare, medical supply*

SCHUHFRIED
MEDIZINTECHNIK

UNIQUE WORLDWIDE

STIMULATOR RISE

The **Stimulator RISE** represents a breakthrough in the electrotherapy of limp paralysed muscles. This is done with broad biphasic rectangular pulses and, if necessary, very high intensities. It also offers an impulse test to check the progress of training.

New trend: For combining and preparing exoskeleton units and FES sports.

For the treatment of

- Muscle weakness with innervated muscles
- Flaccid paralysis in denervated muscles and muscle degeneration in peripheral pareses
- Treatment of peripheral and central paralysis

Effects of electrostimulation in peripheral paresis

- Maintenance and development of muscle mass and muscle function
- Improved blood circulation
- Better skin condition
- Faster wound healing
- Thicker muscle padding
- Pressure ulcer prevention
- Improved visual appearance and increased self-esteem

Effects of electrostimulation in central paresis

- Muscle building and strength improvement
- Reduction of spasticity
- Promotion of neuroplasticity
- Improved function of the affected extremity
- Improvement of gait pattern, mobility and arm function

Other technical advantages

- Biphasic rectangular pulses
- Biphasic triangular impulses for sensitive skin
- Biphasic triangular pulses for selective stimulation
- Frequency readable on display
- Wide current pulses
- Patented safety electrodes for stimulation of limp paralysed muscles
- Patient switch for self-control during functional use when standing up or walking on the walking bar
- Individual limitation of the maximum current intensity
- For home therapy the device can be password protected

STIMULATOR RISE

Easy to use – constant current output – stimulation without direct current component – programmable.

For individual storys see our videolog.

SCAN ME!

+43 1 405 42 06
info@schuhfriedmed.at
www.schuhfriedmed.at

MED EL

STIWELL® PROFES

Functional Electrical Stimulation by MED-EL

- functional programs & focused stimulation for complex movement disorders
- intuitive & effective therapy through easy handling & usability
- EMG-triggered multichannel electrical stimulation
- biofeedback activities & 4-channel EMG analysis
- stimulation of denervated muscles
- help functions directly on the device

Find out more.

stiwell.com

Distribution in Österreich

Streifeneder ortho production

Für mehr Lebensqualität im Alltag

Streifeneder ortho.production: Ihr Partner für Fesia Walk und Fesia Grasp in Österreich

Fesia Produkte zum Ausgleich einer Behinderung **verbessern die Lebensqualität** durch funktionelle Elektrostimulation: Fesia Walk erleichtert das Gehen, Fesia Grasp unterstützt das Greifen. Die funktionelle Elektrostimulation ermöglicht dabei nicht nur die Funktionen Gehen und Greifen, sondern zeigt auch positive Effekte auf **Muskelkraft**, **Durchblutung**, **Reduktion von Schmerz und Spastik**, **Bewegungsumfang**, **motorisches Lernen** und **Neuroplastizität**.

Funktionen und Features

Geräte von Fesia kombinieren eine **Mehrfeldelektrode** mit einer einfach zu bedienenden Schnittstelle: Durch die sehr dünnen Elektroden, welche auf der Innenseite der Manschette eingesetzt werden, wird ein großer Bereich an der Muskulatur angeregt. Die funktionelle Elektrostimulation, welche kleine, elektrische Impulse aussendet, aktiviert die entsprechende Muskulatur.


Fesia Walk

Fesia Walk begleitet Patient:innen bei allen täglichen Aktivitäten.

- Stimulation der Plantarflexion und Dorsalextension, Inversion und Eversion
- einfaches Einrichten: Gehen innerhalb weniger Minuten möglich
- Erkennung der Gangphasen in Echtzeit dank Sensorik
- individuelle Konfiguration
- steuerbar mit Fesia Pro-App für Android: 6 Programme zur gezielten Alltagsunterstützung (zur externen Einstellung im Sanitätshaus)
- optionale App MyFesia für Android: ideal für die häusliche Fortschrittsverfolgung

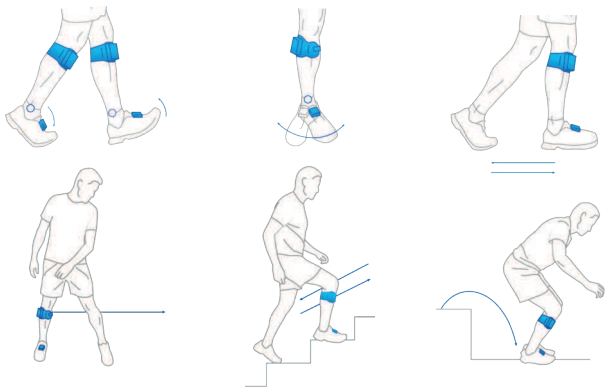



Fesia Grasp

Patient:innen können mit **Fesia Grasp** ihre täglichen **Greifaufgaben** problemlos und sicher erledigen.

- 10 individuelle und 6 kombinierte Bewegungen
- Entfaltung des funktionellen Potenzials im freien Handflächentraining
- maßgeschneiderte Konfiguration
- steuerbar mit der Fesia Pro-App: 5 Programme zur gezielten Alltagsunterstützung (zur externen Einstellung im Sanitätshaus)
- Öffnen und Schließen der Hand mit einer einzigen Berührung auf den Stimulator oder einer ruckartigen Bewegung

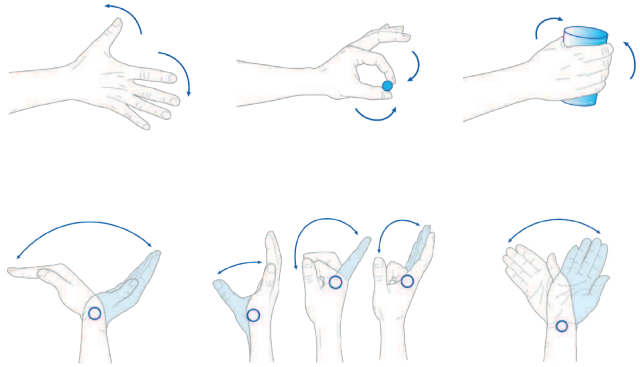

Bildquelle: Fesia

Moosfeldstr. 10 · 82275 Emmering · T +49 8141 6106-0 · F +49 8141 6106-50 · office@streifeneder.de · streifeneder.de/op/

Neurology

Stim2Go

Next Gen Neurostimulation

Stim2Go is a powerful non-invasive and App-controlled neurorehabilitation system. It comes along with ground-breaking features:

- Hybrid Assistance: device-independent for use with different cyclical movement trainers.
- Biofeedback: built-in inertial sensor captures patient's motion in real time and can be triggered to support movement.
- Rich Set of Programs: electrical stimulation methods and preset standard programs with customizable parameters in the field of NMES, FES, TENS and tSCS*.
- Cloud-Based Data Storage: synchronization between different smart devices and telemedicine.

Request your free demo now: **marketing@pajunk.com**

**tSCS only available for use in European Union*

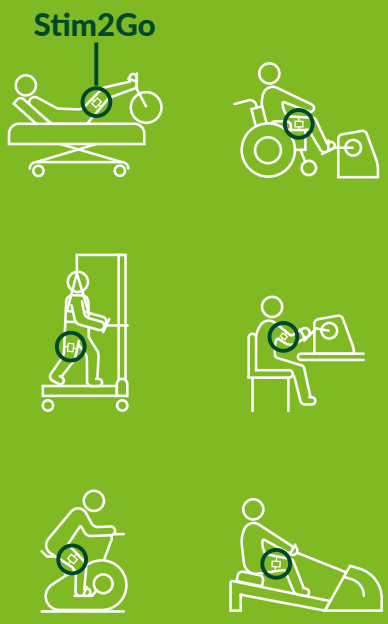

FOR FURTHER INFORMATION

PAJUNK®

Real People. Real Care.

- Suitable for Children
- Clinically Proven
- Track Your Symptoms
- Non-Invasive
- Made in Germany

tVNS®

The Only EU-MDR Approved Non-Invasive Vagus Nerve stimulation Device!

BETTER DAYS ARE AHEAD

Partners of the Vienna FES Workshop:

MEDICAL UNIVERSITY OF VIENNA

https://meduniwien.ac.at

AUSTRIAN SOCIETY FOR BIOMEDICAL ENGINEERING

https://www.oegbmt.at

IFESS International Functional Electrical Stimulation Society

https://ifess.org/

Artificial Organs

Edited by: Vakhtang Tchantchaleishvili, MD

https://onlinelibrary.wiley.com/journal/15251594

Sponsors and Exhibitors (in alphabetic order):

PAJUNK® Real People. Real Care.

Pajunk Medical Produkte GmbH
Pajunkstrasse 2
78187 Geisingen,Germany
https://pajunk.com

SCHUHFRIED MEDIZINTECHNIK

Dr. Schuhfried Medizintechnik GmbH
Van Swieten-Gasse 10
A-1090 Wien, Austria
https://schuhfriedmed.at

MED-EL

STIWELL® Neurorehabilitation

MED–EL Elektromedizinische Geräte GmbH
Fürstenweg 77a
6020 Innsbruck, Austria
https://stiwell.medel.com

Streifeneder ortho production

Friedrich Georg Streifeneder KG
Moosfeldstr. 10
82275 Emmering, Germany
https://streifeneder.de

tVNS®

tVNS Technologies GmbH
Wetterkreuz 5
91058 Erlangen, Germany
https://t-vns.com/